January 2013

A Modeling Investigation of Human Exposure to Select Traffic-Related Air Pollutants in the Tampa Area: Spatiotemporal Distributions of Concentrations, Social Distributions of Exposures, and Impacts of Urban Design on Both

Haofei Yu
University of South Florida, haofeiyu@live.com

A Modeling Investigation of Human Exposure to Select Traffic-Related Air Pollutants in the Tampa Area: Spatiotemporal Distributions of Concentrations, Social Distributions of Exposures, and Impacts of Urban Design on Both

by

Haofei Yu

A dissertation submitted in partial fulfillment
of the requirements for the degree of
Doctor of Philosophy
Department of Environmental and Occupational Health
College of Public Health
University of South Florida

Major Professor: Amy L. Stuart, Ph.D.
Yehia Hammad, Sc.D.
Foday Jaward, Ph.D.
Jayajit Chakraborty, Ph.D.
Abdul Pinjari, Ph.D.

Date of Approval:
June 19, 2013

Keywords: dispersion modeling, exposure, inequality, urban form, environmental justice

ACKNOWLEDGMENTS

I would like to express my sincerest gratitude to my advisor: Professor Amy L. Stuart, for her support, dedication, consideration, patience and all the thoughtful guidance and suggestions. I consider myself fortunate to have her as my major professor. I also would like to express my deepest thanks to Professor Yehia Hammad, Professor Foday Jaward, Professor Jayajit Chakraborty and Professor Abdul Pinjari for their kindly help on my research while being a member of my advisory committee. I would also like to extend my gratitude to Professor Getachew Dagne for chairing my dissertation defense.

Many thanks to Professor Nanhua Zhang, Kent Pan, Jill Sears, Ryan Michael, Sarah Burns, Daniel Mendoza Lebrun and many other friends for their help during the preparation of my dissertation. A special thanks to my girlfriend Xiao Liu, for her constant support and encouragement.

This material is based upon work supported by the National Science Foundation under Grant No. 0846342. Any opinions, findings, and conclusions or recommendations expressed in this material are those of the author(s) and do not necessarily reflect the views of the National Science Foundation. Funding is also in part provided by the National Center for Transit Research, USF and College of Public Health fellowships, 2011 and 2012 Graduate Student Challenge Grants. The authors also would like to acknowledge the use of the services provided by Research Computing, University of South Florida. Data were in part provided by the Tampa Bay Regional Planning Council.

TABLE OF CONTENTS

LIST OF TABLES

LIST OF FIGURES

ABSTRACT

Increasing vehicle dependence in the United States has resulted in substantial emissions of traffic-related air pollutants that contribute to the deterioration of urban air quality. Exposure to urban air pollutants trigger a number of public health concerns, including the potential of inequality of exposures and health effects among population subgroups. To better understand the impact of traffic-related pollutants on air quality, exposure, and exposure inequality, modeling methods that can appropriately characterize the spatiotemporally resolved concentration distributions of traffic-related pollutants need to be improved. These modeling methods can then be used to investigate the impacts of urban design and transportation management choices on air quality, pollution exposures, and related inequality.

This work will address these needs with three objectives: 1) to improve modeling methods for investigating interactions between city and transportation design choices and air pollution exposures, 2) to characterize current exposures and the social distribution of exposures to traffic-related air pollutants for the case study area of Hillsborough County, Florida, and 3) to determine expected impacts of urban design and transportation management choices on air quality, air pollution exposures, and exposure inequality.

To achieve these objectives, the impacts of a small-scale transportation management project, specifically the '95 Express' high occupancy toll lane project, on pollutant emissions and nearby air quality was investigated. Next, a modeling method

capable of characterizing spatiotemporally resolved pollutant emissions, concentrations, and exposures was developed and applied to estimate the impact of traffic-related pollutants on exposure and exposure inequalities among several population subgroups in Hillsborough County, Florida. Finally, using these results as baseline, the impacts of sprawl and compact urban forms, as well as vehicle fleet electrification, on air quality, pollution exposure, and exposure inequality were explored.

Major findings include slightly higher pollutant emissions, with the exception of hydrocarbons, due to the managed lane project. Results also show that ambient concentration contributions from on-road mobile sources are disproportionate to their emissions. Additionally, processes not captured by the CALPUFF model, such as atmospheric formation, contribute substantially to ambient concentration levels of the secondary pollutants such as acetaldehyde and formaldehyde. Exposure inequalities for NOx, 1,3-butadiene, and benzene air pollution were found for black, Hispanic, and low income (annual household income less than $20,000) subgroups at both short-term and long-term temporal scales, which is consistent with previous findings. Exposure disparities among the subgroups are complex, and sometimes reversed for acetaldehyde and formaldehyde, due primarily to their distinct concentration distributions. Compact urban form was found to result in lower average NOx and benzene concentrations, but higher exposure for all pollutants except for NOx when compared to sprawl urban form. Evidence suggests that exposure inequalities differ between sprawl and compact urban forms, and also differ by pollutants, but are generally consistent at both short and long-term temporal scales. In addition, vehicle fleet electrification was found to result in generally lower average pollutant concentrations and exposures, except for NOx.

However, the elimination of on-road mobile source emissions does not substantially reduce exposure inequality.

Results and findings from this work can be applied to assist transportation infrastructure and urban planning. In addition, method developed here can be applied elsewhere for better characterization of air pollution concentrations, exposure and related inequalities.

CHAPTER 1

PROBLEM STATEMENT

Rapid urban growth has been observed around the world (Cohen, 2004). After 2020, all world population growth is predicted to occur exclusively in urban areas (United Nations, 2008). The United States is no exception to this global phenomenon. From 1980 to 2010, the US urban population increased by 49%, the area of urbanized land increased by 108%, but the total US population increased by only 36%. In fact, 98% of US population growth from 2000-2010 occurred in an urban area (U.S. Census Bureau, 1983, 2013).

Urban growth has resulted in increasing dependency on motor-vehicles, and drastically increased distance travelled by motor-vehicles, quantified by Vehicle Mileage Travelled (VMT). Figure 1.1 shows the trend of US population, number of registered vehicles, and total vehicle mileage travelled from 1980 to 2010. In 30 years, the number of registered motor-vehicles increased by 55%, while the US population increased by only 36%. Additionally, total vehicle mileage travelled increased by 108%, three times the population increase.

The substantial increase of vehicle mileage travelled has led to significant emissions of traffic-related pollutants, which are major contributors to total air pollutant emissions (Colvile et al., 2001; Mage et al., 1996). Data from US Environmental Protection Agency (USEPA)'s 2008 National Emission Inventory (NEI) show that 62%

of Nitrogen Oxides (NOx), 86% of Carbon Monoxide (CO), and 46% of Volatile Organic Compounds (VOC) emissions came from mobile sources (U.S. Environmental Protection Agency, 2013).

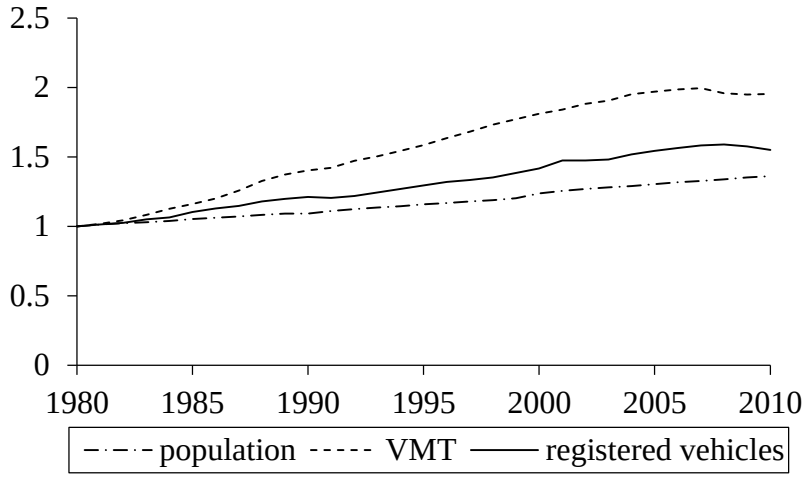

Figure 1.1. Trend of US population, number of registered vehicles and total VMT from 1980 to 2010 (Federal Highway Administration, 2013). For comparison purposes, data were normalized to 1980 values.

Traffic-related pollutants significantly contribute to the deterioration of air quality in urban areas and the associated adverse health outcomes due to exposure to urban air pollution. The Health Effects Institute (HEI) estimated that over 50% of the cancer cases resulting from air pollution exposure can be attributed to mobile source Hazardous Air Pollutants (HAPs) (HEI Panel on the Health Effects of Traffic-Related Air Pollution, 2010). Some sensitive groups, such as children and the elderly, are especially at risk to urban air pollution (Andersen et al., 2012; Brook et al., 2010; Morgenstern et al., 2008; Schultz et al., 2012).

The environmental inequalities of exposure to air pollution has been well documented (National Research Council, 2004; O'Neill et al., 2003; U.S. Department of Transportation, 1997; US Department of Health and Human Services, 2000). More specifically, minority population subgroups such as black, Hispanic, and low income

groups have been found to be disproportionately exposed to air pollution, and consequently suffer from more adverse health outcomes due to this exposure (Keating, 2004; The American Lung Association, 2001). This increased exposure could be attributed to the tendency for minorities to reside closer to major roadways with the largest traffic volume (Chakraborty, 2009). This issue has been well recognized, and taking actions to reduce environmental inequalities related to air pollution exposure were deemed necessary by a number of governing agencies (National Research Council, 2004; O'Neill et al., 2003; U.S. Department of Transportation, 1997; U.S. Department of Health and Human Services, 2000).

To understand the impact of traffic-related pollutants on air quality, pollution exposure, and exposure inequalities, spatially and temporally resolved pollutant concentrations must be appropriately estimated (Denby et al., 2011; Isakov et al., 2007). Air quality monitoring activities could provide accurate ambient concentration levels for pollutant of interest. However, it can be cost-prohibitive when spatiotemporally resolved data are needed. In addition, monitoring techniques cannot be applied to hypothetical scenarios, given their diagnostic nature. Mechanism based air quality modeling methods are cost-effective, and can be readily applied to answer 'what-if' questions (Jerrett et al., 2005). Currently, these preferred modeling approaches for on-road mobile sources are limited, due to the inadequate characterization of important parameters affecting emissions, such as vehicle speed (Bai et al., 2007). A lack of balance between detailed emission representation and practical computational burdens also hinders current modeling approaches (Hatzopoulou, 2008).

Transportation infrastructure expectedly impacts traffic characteristics on roadways, and consequently emissions of traffic-related pollutants. Past studies have suggested that small scale transportation management, such as managed lane projects that encourage ride sharing, could help reduce pollutant emissions from on-road mobile sources (Boriboonsomsin & Barth, 2008; Shewmake, 2012; U.S. Environmental Protection Agency, 1998). However, studies on this subject have been limited, and the results are still inconsistent (Dowling et al., 2005; Lee et al., 2009; You et al., 2010). The mechanisms of how small scale transportation management impacts the emissions of traffic-related pollutants and air quality are still unclear.

At larger scale, the replacement of gasoline/diesel powered vehicles with electric vehicles, known as "vehicle fleet electrification", is known to reduce pollutant emissions from on-road mobile sources, while increasing emissions from power generation units (Electric Power Research Institute, 2007; Huo et al., 2010; Stephan & Sullivan, 2008). Evidence suggests potential air quality benefits from vehicle fleet electrification (Alhajeri et al., 2011), despite the shift in emissions. However, studies regarding the impact of vehicle fleet electrification on air quality and exposures are limited.

In addition, past studies have suggested that urban form could have a significant impact on on-road mobile source emissions and resulting air quality (Geurs & Wee, 2006; Kahyaoğlu-Koračin et al., 2009; Stone et al., 2007, 2009). While recognizing accurate characterization of urban form involves the consideration of many factors, such as morphology of the city, design of transportation infrastructure, and land use policy (Miranda et al., 2008), many studies have utilized simplified representations, such as the sprawl and compact urban forms. Characterized by scattered, stripped development and

extensive development of low density residential units (Ewing, 1997), the sprawl urban form is generally believed to encourage the usage of private motor-vehicles, while discouraging the use of public transit. Therefore, an increase in vehicle miles travelled and related mobile source emissions is associated with sprawl urban forms (Song et al., 2008). On the contrary, compact urban growth, which can be characterized by high density development in or near current urban centers with the implementation of mixed land use policies (Ewing et al., 2002), has been advocated by many urban planners to reduce travel distances and motor-vehicle dependency, encourage public transit, and therefore decrease mobile source air pollution emissions (Stone et al., 2007). However, findings on whether compact growth form could lead to improved air quality in urban areas have been inconsistent (Hixson. et al., 2012). The mechanisms of how urban form impacts air pollution concentrations, and consequently human exposures to pollution, are still largely unclear. Evidence suggests that population subgroups experience different types of impacts resulting from urban growth (Frumkin et al., 2004), but studies have not examined how urban growth may impact air pollution exposure inequalities among subgroups, especially those who are currently experiencing disproportionate exposures.

Here, the overarching goal of this work was to improve understanding of how to design sustainable cities that both reduce exposures to traffic-related air pollutants and distribute the burden of remaining exposures equitably. The specific objectives of this dissertation were to:

1. Improve modeling methods for investigating interactions between city and transportation design choices and air pollution exposures. A particular focus

was on improving methods for estimating spatiotemporal resolved emissions, concentrations, and exposures.

2. Characterize current exposures and the social distribution of exposures to traffic-related air pollutants for the case study area of Hillsborough County, Florida. The scientific questions included are as follows: Are historical disadvantaged race/ethnicity groups disproportionately exposure in the Tampa area? Are groups know to be susceptible to air pollution health outcomes disproportionately exposed? Are inequalities in the Tampa area consistent with those in previous case study areas? Do the inequalities differ substantially between specific pollutants? Do they change substantially with temporal scale (e.g. acute versus chronic exposures)? Which emission sources contribute the most the exposure and exposure inequalities?
3. Determine expected impacts of urban design and transportation management choices on air quality, air pollution exposures, and exposure inequality. The scientific questions included are as follows: Is compact growth expected to reduce concentrations and exposures to traffic-related pollutants? Is the impact expected to be similar for all pollutants and time scales? How may compact growth versus sprawl growth affect exposure inequality? Are small scale transportation management options, such as managed lanes, potential mitigating options? How may large-scale transportation management option, such as vehicle fleet electrification, impact air quality and exposures?

The research presented here is divided into three components, attempting to address the scientific questions mentioned above. First, the impact of a small-scale

transportation management project on pollutant emissions and nearby air quality was investigated using the "95 Express" managed high occupancy toll lane project as an example. Second, spatiotemporally resolved pollutant concentrations were estimated for the Tampa area by applying a developed air quality modeling method that is capable of characterizing detailed on-road mobile source emissions. Air pollution exposure and exposure inequality among chosen population subgroups were estimated using the modeled concentrations. Third, the impact of sprawl, compact urban forms, and vehicle fleet electrification, on emissions, pollutant concentrations, air pollution exposure and exposure inequalities were explored by using results from the second component of this research as a baseline. Details of each component are presented in the following chapters.

CHAPTER 2

LITERATURE REVIEW

2.1. Introduction

With increasingly stringent regulations on point source emissions and increasing motor-vehicles dependency, on-road mobile source emissions have become one of the major contributors to urban air pollution and its consequent adverse health effects (HEI Panel on the Health Effects of Traffic-Related Air Pollution, 2010). Urban areas, due to their high population and motor-vehicle density, are focal points for on-road mobile source emissions and pollution exposure.

Another issue associated with air pollution exposure in urban areas is environmental inequalities related to air pollution exposure among different population subgroups (O'Neill et al., 2003). Some subgroups were found to have greater health risks due to exposure to higher pollution concentrations (Keating, 2004; The American Lung Association, 2001). This issue has been well recognized by both academia and governmental agencies (National Research Council, 2004; U.S. Department of Transportation, 1997; US Department of Health and Human Services, 2000).

Recently, an increasing amount of research have focused on the impact on the impact of urban form on air quality, and have shown that urban planning toward certain urban forms, such as compact and sprawl urban form, could significantly impact urban air quality and human exposure to air pollution (Geurs & Wee, 2006; Kahyaoğlu-Koračin

et al., 2009; Stone et al., 2007, 2009). Evidences from previous studies also suggest that different population subgroups may be impacted differently (Grineski et al., 2007).

Although many definitions exist, compact urban form is usually characterized by concentrated, high density and continuous development on already developed areas, combined with implementation of mixed land use policies. On the contrary, sprawl urban form is usually associated with extensive developments on raw lands, low density, and scattered and highly segregated developments (Bechle et al., 2011; Ewing, 1997). Compact urban form is popular among urban planners as it has been shown to pose less impacts on agricultural lands, wetlands, and conserve green spaces (Westerink et al., 2012), reduce energy and water use (Chang et al., 2010; Ewing & Rong, 2008). Previous studies suggest that compact and sprawl urban forms indirectly impact urban air quality, pollution exposure, and exposure inequalities by affecting urban inhabitants' relocation (Grineski et al., 2007), travel behavior, motor-vehicle dependency, public transit usage, and the adoption of non-motor-vehicle based travel modes such as walking and biking (Boarnet & Crane, 2001).

This chapter provides a synthesis of previous literature regarding the impact of compact and sprawl urban forms on urban air quality, air pollution exposure and environmental inequalities related to exposure, with an emphasis on public health impacts. Future research needs are identified and discussed. Further, air quality modeling tools that could be used to improve our understandings on this topic are critically reviewed, and the needs for model improvements are discussed.

2.2. Impact of Urban Form on Air Quality and Exposure

Figure 2.1 illustrates the pathway for human exposure to pollutants as influenced by compact and sprawl urban development forms. Pollutant emissions, especially on-road mobile source emissions, are directly impacted by urban forms. After being released into the air, pollutants may undergo physical and chemical processes, and the amount of pollutant that is airborne is characterized by concentrations. Human exposure to atmospheric pollutants may result in a myriad of health effects. Meanwhile, each step of the pathway is impacted by human activities. For better understanding, the impact of urban forms on urban air quality and exposures are discussed at each step along the pathway.

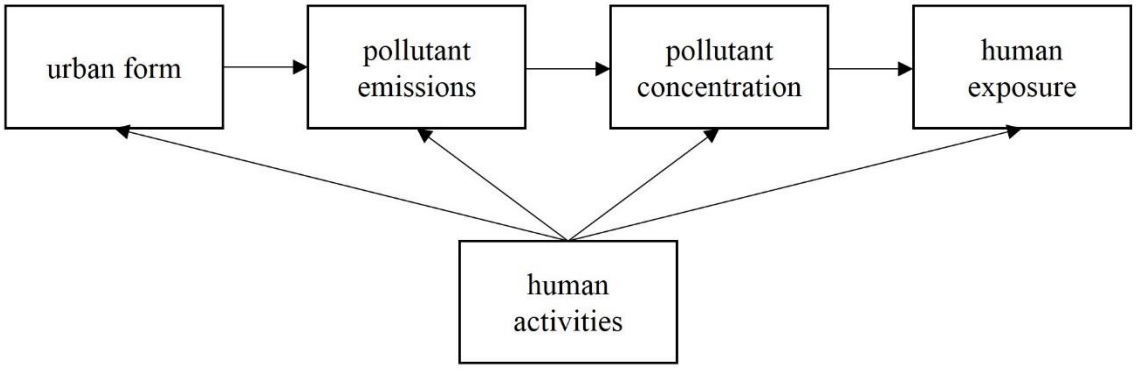

Figure 2.1 Pathway of how urban form impact human exposures

2.2.1. Impact of Urban Form on Pollutant Emissions

Previous studies have shown that urban forms have direct impacts on air pollutant emissions. Findings from previous studies regarding the relationships between urban form and air pollutant emissions are rather consistent: compact urban forms were generally found to have less total and on-road mobile source emissions than sprawl (Borrego et al., 2006; Ridder et al., 2008; Frank et al., 2000; Kahyaoğlu-Koračin et al., 2009; Liu, 2003; McDonald-Buller et al., 2010; Niemeier et al., 2011; Song et al., 2008;

Stone et al., 2007, 2009). Stone et al. (2009) suggested that the effect of aggressive compact policy on reducing on-road mobile source emissions is even comparable with replacing all light duty vehicles with hybrid-electric vehicles.

The reduction of on-road mobile source emissions associated with compact urban form may be explained by reduced vehicle mileage travelled. Briefly, due to the "compactness" of urban area and mixed land uses, vehicle usage and average length of vehicle trips are expected to be lower and smaller than in sprawl urban form (Ewing & Cervero, 2001, 2010; Frank & Engelke, 2005; Handy, 2005; Salon et al., 2012; Williams & Wright, 2007). In addition, some studies also pointed out that compact urban form impacts transportation infrastructure not only by expanding the capacity of roadway network, but also by promoting the usage of public transit systems, and encouraging non-motor-vehicle based travel behaviors, such as walking and biking (Schwanen et al., 2001; Schwanen et al., 2004), which also lead to reduced vehicle mileage travelled. However, these effects were seldom considered in past literatures regarding the impact of urban forms on pollutant emissions.

One interesting finding is that the majority of studies focused on a few pollutants: PMs (PM_{10} or $PM_{2.5}$), ozone and its pre-cursors (NO_x, NO_2 and VOC). While these pollutants are certainly important, there are other important pollutants as well, such as the Urban Air Toxics (UAT). USEPA (Environmental Protection Agency) has pointed out that urban air toxics are the "greatest threats to public health in urban areas" in the US (U.S. Environmental Protection Agency, 2008b). Exposure to urban air toxics have been shown to be associated with many severe health effects including cancer (Agency for Toxic Substances and Disease Registry, 2007; National Toxicological Program, 2010,

2011), with mobile source air toxics being associated with greater the 50% of cancer cases resulting from air pollution (HEI Panel on the Health Effects of Traffic-Related Air Pollution, 2010). The importance of urban air toxics warrants more attention.

Compact urban form has been found to alter the spatial distribution of emissions (Borrego et al., 2006). In compact urban form, anthropogenic air pollution emissions, including on-road mobile source emissions, were found to be concentrated in populated urban areas. Borrego et al. (2006) estimated that compact urban form would have less "per person" emissions of NO_x and VOC than sprawl, but the maximum emission per area values were in fact much higher. The spatially re-distributed emissions could have significant effect on subsequent steps along the pathway (Figure 2.1).

Many studies focused specifically on estimating air pollutant emissions under sprawl and urban forms have concluded that compact urban form lead to better air quality due to lower pollutant emissions. However such conclusions may be pre-mature, and more investigations on the subsequent steps of the pathway may be needed.

2.2.2. Impact of Urban Form on Air Pollution Concentrations

Many studies have examined how compact and sprawl urban form impact air pollutant concentrations (Borrego et al., 2006; Ridder et al., 2008; Hixson et al., 2010, 2012; Kahyaoğlu-Koračin et al., 2009; Martins, 2012; McDonald-Buller et al., 2010; Song et al., 2008). The findings, however, are complex and mixed.

Compared to sprawl, compact urban form was generally found to have overall lower pollutant concentrations in the study domain, due primarily to lower pollutant emissions. This finding applies for primary pollutants such as PM_{10}, secondary pollutants such as ozone, and pollutants that have both significant primary and secondary

contributions (herein referred as “intermediate pollutants”), such as NO_2 and $PM_{2.5}$ (Bechle et al., 2011; Ridder et al., 2008; Hixson et al., 2012; Kahyaoğlu-Koračin et al., 2009; Martins, 2012; Schweitzer & Zhou, 2010). However, spatial distribution of pollutant concentrations, are different for each pollutants.

For primary pollutants, which were mainly released into the atmosphere rather than formed through reactions, urban centers tend to have higher pollutant concentrations in compact urban form (Hixson et al., 2010; Martins, 2012). This observation is expected as concentrations of primary pollutants are expected to be higher near emissions sources, whereas in compact urban form, pollutant emissions are concentrated in urban centers due to concentrated human activities. In sprawl urban form, since emissions are scattered distributed, such spatial pattern will not be as apparent, although pollutant concentrations are also elevated near sources.

For secondary pollutants such as ozone, which are mainly formed in the atmosphere, urban centers do not always have the highest pollutant concentrations. For example, Martins (2012) found the highest ozone concentration areas are located downwind of emissions. Song et al. (2008) found higher ozone concentrations in suburban areas in compact urban form, but not urban cores. Such observations are due to the nature of secondary pollutants, whose concentrations levels are mainly determined by atmospheric reactions and meteorological conditions.

In addition, due to the non-linear relationships between concentrations of secondary pollutants and emissions, emission reduction of pre-cursor species does not guarantee reduction of pollutant concentrations. For example, Grabow et al. (2012) found reducing on-road mobile source emissions in urban areas could help to reduce ozone

concentrations in downwind rural areas, but not in all urban areas. The relationships between concentrations of ozone, VOC, and NO_x may help explain this finding (Godish, 2004). In VOC limited regime, where VOC concentrations are relatively low and NO_x concentrations are high, reduction of NO_x emissions alone could decrease NO_x concentrations, but may lead to higher ozone concentrations.

For intermediate pollutants, such as $PM_{2.5}$, near source impact and atmospheric formations are both important. Due to contributions from primary emissions, pollutant concentrations are expected to be higher near sources with substantial emissions, for example, urban centers in compact urban form. When transported away from emissions sources, pollutant concentrations are then determined by its fate in the atmosphere. Hixson et al. (2010) found $PM_{2.5}$ concentrations at urban centers are higher in compact than sprawl urban form, mainly due to increased emissions of primary PM components, such as elemental carbon (EC) and organic carbon (OC). Areas other than urban centers have higher $PM_{2.5}$ concentrations in sprawl urban form than compact, secondary PM components such as nitrate and ammonium ion, contribute to this pattern.

Overall, compact urban form are consistently found to have lower domain averaged pollutant concentrations, but the impact of urban forms on the spatial distribution of pollutant concentrations are complex and differ by pollutants. No generalizable mechanisms regarding how urban form impact pollutant concentration distributions are available.

Further, transportation infrastructure may also impact the complex relationship between urban form and pollutant concentrations. Clark et al. (2011) found that public transit supplies are associated with lower population weighted $PM_{2.5}$ concentrations. The

observed association is plausible as public transit has been commonly associated with reduce vehicle trips and vehicle mileage travelled (Litman, 2013), which in turn lead to lower on-road mobile source emissions.

2.2.3. Impact of Urban Forms on Air Pollution Exposures

Exposure is a consequence of the colocation of humans and pollutants. Even the highest pollutant concentrations would be harmless unless exposed to human. A lower domain averaged pollutant concentration cannot be translated directly into lower population exposure, and the spatial distribution of populations have to be considered jointly.

As discussed in previous sections, concentrations of primary and intermediate pollutants are expected to be higher in urban centers in compact urban form. Unfortunately, urban centers also have densely distributed populations. The colocation of population and increased pollutant concentration may lead to higher human exposure to these pollutants for compact urban form. For example, Hixson et al., (2010) found higher population weighted exposure for primary components of $PM_{2.5}$ in compact urban form. In addition, Martins (2012) found higher human exposure to PM_{10} in compact urban form, despite domain averaged concentrations being actually lower.

For secondary pollutants, human exposures to air pollution may potentially be lower in compact urban form, as higher concentrations are not expected near sources with substantial emissions of pre-cursor species (i.e. populated urban centers in compact urban form). This assumption is supported by the findings from Hixson. et al. (2012) and Song et al. (2008). In Borrego et al. (2006), the results clearly shows more people are exposed to higher concentrations of ozone in sprawl urban form. However, results from other

studies did not suggest significantly lower human exposure to secondary pollutants in compact urban forms, or even the opposite. Ridder et al., (2008) and Martins, (2012), found that human exposure to ozone in compact and sprawl urban forms differs by little. Additionally, McDonald-Buller et al. (2010), Schweitzer and Zhou, (2010), found that human exposure to ozone are actually higher in compact urban form.

Although seemingly contradictory, both findings are plausible. As discussed in previous section, the spatial distributions of secondary pollutants are mainly determined by local meteorological conditions and the fate of the selected pollutant in the atmosphere. The non-linear relationships between emissions and pollutant concentrations of secondary pollutants, combined with distinct meteorological conditions at different study areas, allow for these different findings. It seems that the impact of compact or sprawl urban forms on human exposure to secondary pollutants differs case by case, which suggest our lack of understanding regarding the mechanisms behind such observations.

Human exposures to intermediate pollutants in compact and sprawl urban forms are even more complex, and it is again not surprising to see different findings. Hixson et al., (2010) found similar $PM_{2.5}$ exposures for compact and sprawl urban forms. In a follow up study, Hixson et al., (2012) showed that although domain averaged $PM_{2.5}$ concentrations are lower in compact urban forms than sprawl, population weighted $PM_{2.5}$ concentrations are higher in compact urban form. Similar findings are also found by Clark et al., (2011) and Schweitzer & Zhou (2010).

Although many studies have suggested potentially aggravated air quality in different urban forms, few studies have attempted to explore potential strategies to

alleviate air pollution exposures in compact urban forms. Hixson. et al. (2012) showed that mid-density compact development could lead to better air quality than high density. However findings from this study are rather restricted to the study area (San Joaquin Valley, CA) and study pollutant ($PM_{2.5}$), and may not be generalizable to other areas and other pollutants. Similarly, Marshall et al., (2005) suggested that compact urban development form could have decreased human exposure (inhalation to pollution) when the rate of emission increase is much smaller than the rate of population density increase (as represented by density-emissions elasticity factor). This finding may apply only for primary pollutants but may not be valid for secondary or intermediate pollutants.

Overall, compact urban form has the potential to increase human exposure to primary air pollutants, due to the colocation of increased pollutant emissions and high population density in urban centers. However findings for secondary and intermediate pollutants are mixed and may even be contradictory. Further studies are needed to better understand how urban forms impact air pollution exposure, as well as potential strategies to alleviate air pollution exposures.

Further, it was noted that virtually all of the studies did not investigate air pollution exposures at multiple temporal scales, although it is well known that the spatial distribution of short term air pollution concentrations may be distinct from long term concentrations. The importance of spatiotemporal variation of air pollution concentrations in exposure assessment have been noted in many studies (Ghosh et al., 2012; Li et al., 2013; Wu et al., 2011). More studies on this subject are needed.

2.2.4. Impact of Urban Form on Exposure Inequalities

Environmental inequalities regarding air pollution exposure is another well recognized issue related to urban air pollution (National Research Council, 2004; O'Neill et al., 2003; U.S. Department of Transportation, 1997; US Department of Health and Human Services, 2000). Inequalities, including inequalities related to air pollution exposure, need to be recognized and treated with caution during development. However, only a few studies have investigated how compact or sprawl urban form impact exposure inequalities (Ridder et al., 2008; Fan & Song, 2009; Schweitzer & Zhou, 2010).

Evidence from previous studies suggest that urban growth may impact the relocation of different population subgroups, and hence may change the distribution of exposures among different subgroups (Grineski et al., 2007). Historically, Caucasians and people with high socioeconomic status have tended to relocate to suburban areas during urban development, whereas minority and poor people have tended to stay closer to urban centers (Frumkin et al., 2004). Ridder et al., (2008) found that people moving to suburban areas during urban growth may experience decreased air pollution exposure, and people staying in urban centers may be exposed to higher pollutant concentrations. In addition, Fan and Song (2009) found sprawl urban form lead to larger mortality gaps between urban and suburban areas. These findings suggests potentially aggravated inequalities during urban growth.

Schweitzer and Zhou (2010) combined Smart Growth American (SGA) indices, which was developed to quantify the degree of compact growth, with measured ozone and $PM_{2.5}$ concentrations at regulatory monitors to investigate the associations among urban form, pollution exposure and exposure inequalities. African Americans, Asian

ethnic minorities, and poor households were found to be exposed to higher pollutant concentrations. However no conclusive evidences were found for the associations between smart growth American indices and inequalities. One possible explanation maybe that air pollution exposures among subgroups were not well captured by regulatory monitoring activities (Stuart et al., 2009).

Much of studies mentioned above are focused on one or two pollutants, and are based upon statistical regression method or modeled pollutant concentrations at coarse spatial resolution. The limited literature on this topic, as well as the importance of environmental inequalities regarding air pollution, warrants more studies in this area.

2.2.5. Summary of Literature Review Findings and Research Needs

Overall, the number of studies attempting to understand the impact of transportation infrastructure and urban form on air quality, exposure and exposure inequalities are still limited. Much of these studies suggest compact and sprawl urban forms could have significant effect on air pollution emissions, pollutant concentrations and human exposures. Specifically: a) Compact urban form was found to reduce pollutant emissions, which may result in lowered domain average pollutant concentrations than sprawl. However compact urban form also altered the spatial distribution of emissions toward populated urban centers; b) Due to the altered emission distributions in compact urban form, concentrations of primary and intermediate pollutants may increase in urban centers, leading to potentially higher population exposure to these pollutants than sprawl urban form, although domain averaged concentrations could be lower; c) The impact of altered emission distributions on secondary pollutants are more complex and may differ by pollutants. Generally, higher concentrations of secondary pollutants are expected away

from sources with substantial emissions; d) Findings regarding the impact of urban forms on concentration distributions and exposures to secondary and intermediate pollutants are inconsistent. Mechanism and magnitude of the impacts are still unclear; e) Studies on the impact of compact and sprawl urban form on inequalities related to air pollution exposure are limited and preliminary, but evidences suggest potentially aggravated inequalities during urban growth.

To better understand the impact of urban forms on air quality, the following research needs are identified: a) Studies are needed to investigate how transportation infrastructure impact pollutant emissions and concentrations; b) Further studies are needed regarding how urban forms impact air pollution exposure, and inequalities related to exposure; c) Potential strategies to alleviate air pollution exposures needs to be developed; d) More pollutants, especially urban air toxics, needs to be assessed. In addition, multiple temporal scales need to be considered to appropriately characterize air pollution exposure.

2.3. Review of Urban Scale Exposure Estimation Models

Numerous methods have been developed to characterize pollutant concentrations and human exposures to air pollution in past literatures. Some of them were briefly reviewed previously (Kingham & Dorset, 2011; Steinle et al., 2013; Zou et al., 2009). Ideally, measurement of pollutant concentrations that an individual is exposed to (Steinle et al., 2013), or the individual biological outcomes due to pollution exposure (Vineis & Husgafvel-Pursiainen, 2005), would provide the most accurate information regarding personal exposures to air pollution. However, it is cost-prohibitive to do so when an entire urban area is the study area and exposure metrics are needed at varying temporal

scales. In addition, hypothesized development strategies cannot be tested and compared with measurement technique. Hence, exposure estimation models are used.

The purpose of this section is to review and identify appropriate exposure estimation models for the investigation of the impact of urban forms on urban air quality, human exposure and exposure inequalities. Jerrett et al. (2005) reviewed some of the models that could be used to estimate pollution exposures at urban scale. This following sections builds upon Jerrett et al. (2005), incorporated emerging models and categorize air quality models into five categories: empirical/statistic based models, chemical transport models, computational fluid dynamics models, street canyon models and hybrid models. Each category is briefly described, corresponding advantages and disadvantages of each type of model are discussed and evaluated using the established criteria. Needs for model improvements are also presented.

2.3.1. Empirical/Statistic Based Models

In empirical/statistic based models, exposures (or associations between exposure and outcomes) are either estimated empirically, or derived from statistical methods including regression, interpolation or extrapolation. There are mainly three types of models that falls under this category: a) land use regression; b) proximity based model; and c) spatiotemporal data interpolation or extrapolation.

2.3.1.1. Land Use Regression

Land Use Regression (LUR) models estimate pollutant concentrations by assuming concentrations at chosen locations are statistically associated with “predictor” attributes (variable) of surrounding areas. As indicated by the name, the predictor variables are mostly land use type, nearby roadway, and traffic characteristics. However,

other attributes not related to land use can also be used, such as wind field (Arain et al., 2007). Pollutant concentration data can be used in model development as well as model evaluation. The concentration data can be obtained from regulatory monitoring network (Saori et al., 2009), special sampling campaigns (Henderson et al., 2007), or even estimation from other models (Mölter et al., 2010; Wilton, 2011) (which will form a hybrid model, as discussed in section 2.3.5). Studies where land use regression models were applied were reviewed previously (Hoek et al., 2008; Ryan & LeMasters, 2007).

Generally, land use regression models could provide highly spatially resolved pollutant concentration distributions for exposure estimation purposes. However, as pointed out in Hoek et al. (2008), due to its empirical nature and lack of mechanisms, the generalizability of land use regression model is limited: a model that is developed for one area may not be suitable for estimating pollutant concentrations in another area (Jerrett et al., 2005; Wu et al., 2011). Applying land use regression model on alternative development scenarios with distinct spatial land use type distributions may also trigger concerns regarding its validity. Further, land use regression models lack the capability of resolving pollutant concentrations at various temporal scales (Hoek et al., 2008). Some studies attempted to improve the prediction capability of temporal pollutant concentrations variations for land use regression models by applying temporal profiles (Ghosh et al., 2012; Rose et al., 2010) or Bayesian maximum entropy methods (Jerrett et al., 2012), but such applications are rather preliminary. Therefore, land use regression model alone may not be suitable for investigating the impact of different urban forms on air quality and human exposure.

2.3.1.2. Proximity Based Model

Proximity based models generally do not estimate pollutant concentrations. Instead, proximities of the study subject to emission sources, and the outcomes of interest (concentrations, health outcomes etc.), are analyzed to investigate their statistical associations. Conclusions may be drawn from the results of statistical analysis. Examples of proximity based models could be found in the work of Allen et al., (2009), where the associations between residential proximity to major roads and the incidence of aortic atherosclerosis were evaluated.

Generally, proximity based models assume the outcome measures are associated with the proximity to emissions sources, which may not hold for secondary pollutants such as ozone. In addition, due to lack of mechanisms and distinct characteristics of different emission sources, the generalizability of proximity based models are questionable. Hence it may not be appropriate to apply proximity based models alone for investigating the impact of different urban forms on air quality and human exposure.

2.3.1.3. Spatiotemporal Data Interpolation or Extrapolation

In this method, pollutant concentrations at desired locations or time periods are estimated by interpolation or extrapolation of available sparse concentration data. Popular spatial interpolation or extrapolation methods including kriging (Mercer et al., 2011; Whitworth et al., 2011), splines and inverse distance weighting (Brauer, 2008). Temporal concentration interpolation or extrapolation, however, are less well studied. Historically, preliminary models, such as stochastic models (Milionis & Davies, 1994), were used. However, new, sophisticated models have emerged with the capability to account for both spatial and temporal pollutant concentration variations, such as those base on

Bayesian maximum entropy, two-stage models, and hierarchical models (Li et al., 2013; Yu et al., 2009).

Spatiotemporal data interpolation or extrapolation models could provide highly spatially and temporally resolved pollutant concentration distributions, which are desired for exposure estimation. However, the interpolated (or extrapolated) concentration field could be substantially different depending on the method used (Wong et al., 2003), and accuracy of the concentration field are somewhat questionable (Whitworth et al., 2011). Further, no pollutant concentration data are readily available in alternative future scenarios, which limit the usage of spatiotemporal data interpolation or extrapolation models for investigating impacts of urban forms on air quality and human exposure.

2.3.2. Chemical Transport Models

Differencing from empirical/statistic based models, which are essentially diagnostic and lack prognostic capabilities, chemical transport models are developed based upon atmospheric physics and chemistry, and pollutant concentrations are estimated at desired locations using both emission and meteorological data in the study domain. Chemical transport models do not attempt to solve for meteorological fields, the data are usually obtained from meteorological observations or other models such as weather forecasting models. There are mainly three types of models that fall under this category: a) steady-state Gaussian plume models; b) non-steady state Lagrangian models; and c) Eulerian grid chemical transport models. Details of each type of model are discussed below.

2.3.2.1. Steady-State Gaussian Plume Models

Steady-state Gaussian plume models have the longest history in regulatory air quality modeling, and are still extensively used in source-specific regulatory modeling practices. These models are normally characterized by: a) Assumption of homogeneous distributions of meteorological conditions (such as wind speed, wind directions etc.) in the study domain; b) No memory effect. Spatial distribution of pollutant concentrations in previous time step has no effect on concentrations in the next time step; and most importantly, d) Pollutant concentrations are estimated by Gaussian plume formulations. Within the pollutant plume, vertical and horizontal pollutant concentration profiles are characterized by Gaussian distributions.

Many steady-state Gaussian plume models are available and numerous studies have utilized these models to estimate pollutant concentration distributions (Batterman et al., 2010; McConnell et al., 2010; Bin Zou et al., 2009). Examples of steady-state Gaussian plume models are AERMOD (and its predecessor ISC) (U.S. Environmental Protection Agency, 2004b), CALINE (Benson et al., 1989) and ADMS-URBAN (Cambridge Environmental Research Consultants, 2010).

Steady-state Gaussian plume models could provide concentration estimates at very fine spatial resolutions down to several tens of meters. Geometry of emission sources, can be accurately represented in the model. This configuration is ideal for characterizing pollutant concentration near roadways, which is important as substantially higher concentrations can be found near roadways (Cook et al., 2008).

However, due to its homogeneous meteorological field assumption and Gaussian plume formulation, steady-state Gaussian plume models may not be suitable for areas

with complex meteorological conditions (such as coastal areas with land sea breeze) or complex terrain features. In addition, since these models generally incorporates very simple chemical reaction formulas such as zero or first order decay, the lack of adequate chemistry algorithms could be problematic for secondary or intermediate pollutants.

2.3.2.2. Non-Steady State Lagrangian Chemical Transport Models

In non-steady state Lagrangian chemical transport models, pollutants are represented as either air parcels (puff) or particles. The model tracks the movements of the pollutants both spatially and temporally, using gridded 3-dimensional meteorological datasets. Examples of non-steady state Lagrangian models are CALPUFF (pollutants are represented as puff) (Scire et al., 2000), HYSPLIT (Draxler et al., 2012) and FLEXPART (pollutants are represented as particle) (Stohl et al., 2011). Many studies have used non-steady state Lagrangian models to estimate pollutant concentration distributions (Ghannam & El-Fadel, 2013; Halse et al., 2013; MacIntosh et al., 2010; Yim et al., 2010). Sometimes, non-steady state Lagrangian models and steady-state Gaussian models are collectively called dispersion models.

Non-steady state Lagrangian models can also provide pollutant concentration estimates at very fine spatial resolutions and accurately represent the geometry of emission sources. In addition, they have the capability to characterize the impact of spatially varying meteorological fields and complex terrain features on pollutant concentration distributions. Although atmospheric chemistry is still not comprehensively characterized by non-steady state Lagrangian models, these models generally contain simplified reaction algorithms. Hence these models can not only be applied on pollutants that are largely inert, but also on pollutants whose reactions can be appropriately

represented by simplified chemistry. For investigating the impact of urban forms on air quality and human exposure, non-steady state Lagrangian models are reasonable candidate models.

2.3.2.3. Eulerian Grid Chemical Transport Models

Instead of tracking the movement of pollutants spatially and temporally (Lagrangian approach), Eulerian grid chemical transport models discretize the study area into grid cells, solving for pollutant concentrations in each cell from groups of mass balance equations. Within each grid, concentrations are represented as homogeneously distributed. Many Eulerian grid models that focused specifically on air pollution modeling have been developed, including CMAQ (Community Modeling and Analysis System, 2010), CAMx (ENVIRON International Corporation, 2011) and UCD (Held et al., 2005).

Studies that used Eulerian grid chemical transport models are generally focused on a large areas, such as regional (Hixson et al., 2010), national (Davidson et al., 2007), or even global scales (Lin et al., 2012). Eulerian grid chemical transport models are designed to handle complicated atmospheric chemical reactions and long range pollutant transportations, and are used by the majority of studies regarding impacts of urban forms on air quality and human exposures, mainly due to the nature of the study pollutants. As a tradeoff, Eulerian grid models are usually very data and computationally expensive, and the spatial resolution of the estimated pollutant concentrations are rather limited, mostly rangeing from 4 km to 25 km (Ridder et al., 2008; Hixson et al., 2010, 2012; Martins, 2012). The relatively coarse spatial resolution of the concentrations may trigger concerns regarding exposure misclassification.

For pollutants with complex chemistries, Eulerian grid chemical transport models are desired, but for pollutants that are largely inert, and pollutants with rather simple chemistries, other models such as non-steady state Lagrangian models are also suitable. In addition, non-steady state Lagrangian models are able to provide spatially resolved pollutant concentration distributions, which are desired for exposure estimations.

2.3.3. Computational Fluid Dynamics Models

Chemical transport models only solve for continuity (mass balance) equations, and rely on observations or numerical weather forecasting models for meteorological data. Computational fluid dynamics models take steps further, deriving meteorological fields within the model itself by solving additional equations such as momentum and energy equations. Naturally, computational fluid dynamics are even more computational expensive than chemical transport models. GEOS-CHEM (Yantosca et al., 2012), WRF/CHEM (Peckham et al., 2011) and GATOR-GCMOM (Jacobson, 2012) are examples of computational fluid dynamics models. These models are normally applied at very large scales from regional to global.

Recently, a few new studies have started to apply computational fluid dynamic models to model urban air pollution at neighborhood scales (down to a few kilometers) (Tong et al., 2011; Wang et al., 2013; Wang & Zhang, 2009), and new models were developed, such as the Comprehensive Turbulent Aerosol Dynamics and Gas Chemistry (CTAG, formally named CFD-VIT-RIT (computational fluid dynamic-vehicle induced turbulence-road induced turbulence)). Pollutant concentration distributions at extremely high spatial and temporal scales can be estimated by this model. However, field

applications of such models are preliminary and the size of the modeling domain is very limited, mainly due to the complexity involved and excessive computational burden.

2.3.4. Street canyon models

Street canyon models is a special model category that cannot be simply categorized into any of the three categorizes discussed above. These models are designed to estimate pollutant concentration distributions in street canyons, which refers to urban street with buildings at each side. Vardoulakis et al. (2003) provides a review on some of the street canyon models used previously. Examples of street canyons models include OSPM (Berkowicz, 2000), SEP-SCAM (Papathanassiou et al., 2008) and STREET-BOX (Mensink & Lewyckyj, 2001).

A wide range of methods were used to characterize the distribution of pollutant concentrations in street canyons, ranging from empirical expressions (Weber et al., 2013) to complicated computational fluid dynamics modeling (Kwak & Baik, 2012). Although street canyon models are normally applied at spatial scale of street block levels, they can be extended to larger scale to estimate pollutant concentrations and human exposures (Jensen et al., 2009; Mensink & Cosemans, 2008; Pénard-Morand et al., 2010).

Street canyon models are suitable for small urban areas that are highly developed and have many high-rise buildings. However, the applications of street canyon models in air pollution exposure estimation are still limited. No applications have been found where street canyon models are applied for a relatively large urban areas.

2.3.5. Hybrid models

When a single model is insufficient, two or more air quality models can be combined to form a hybrid model to fulfill the needs. Note that here the term “hybrid” is

defined differently from Jerrett et al. (2005), where "hybrid" refers to the combination of air quality models with concentration measurement data, which were used to evaluate or calibrate air quality models. Here, hybrid model specifically refers to the integration of two or more air quality models. The integrated models could be any of the air quality models discussed above. Some of the hybrid models were briefly described in Touma et al. (2006).

The purpose of model integration, and the role the integrated model serves, varies from case to case. For example, Hoek et al. (2002) applied inverse distance weighting on measurement data obtained from regulatory monitoring network to derive regional background of pollutant concentrations. A simple LUR model was then used to provide urban background pollutant concentrations, and finally a proximity based approach was applied to determine exposure status. Mölter et al. (2010) and Wilton (2011) incorporated concentration estimates from chemical transport models to calibrate land use regression models. Kassteele et al. (2009) applied spatial interpolation model on outputs from chemical transport models and found that application of the hybrid models could substantially improve the prediction of spatial concentration distributions.

Many studies have incorporated Eulerian grid chemical transport models with either steady-state Gaussian plume models or non-steady-state Lagrangian chemical transport models (two of the latter are collectively called dispersion models) (Beevers et al., 2012; Cook et al., 2008; Isakov et al., 2007; Isakov et al., 2009; Stein et al., 2007). As discussed previously, Eulerian grid models contains detailed chemistry algorithms which are critical for pollutants with complex chemistry and significant secondary contributions, however spatial resolutions of the concentration estimates from these

models are usually limited. Dispersion models, although generally lacking detailed chemistry, have the capability to estimate spatially resolved concentration data.

To appropriately characterize pollutant concentrations and air pollution exposures for different pollutants, atmospheric chemistry is needed, especially for pollutants with substantial atmosphere formations such as acetaldehyde and formaldehyde. In addition, concentration estimates have to be spatially resolved to avoid potential exposure misclassification bias (Denby et al., 2011; Isakov et al., 2007). The hybrid model formed by Eulerian grid chemical transport models with dispersion models combines the advantages of the two types of models, and could appropriately address these needs.

Two approaches have been used to combine Eulerian grid chemical transport models with dispersion models (Touma et al., 2006): a) Direct coupling of two models; and b) Blend concentration estimates from two models. These two approaches are discussed briefly below:

2.3.5.1. Direct Coupling of Two Models

In this type of model, Eulerian grid chemical transport models are directly coupled with dispersion models. In each time step, the dispersion model estimates pollutant concentration distributions within each Eulerian model grid. The coupled dispersion models could be based on steady-state Gaussian models such as ADMS (Beevers et al., 2012), or non-steady-state Lagrangian models such as SCICHEM (Karamchandani et al., 2012) or the plume-in-grid module in CMAQ (Community Modeling and Analysis System, 2010).

Benefits of such configurations are: a) Outputs from both models are combined at every time step, no post-processing are needed; b) Eulerian grid model could directly

provide concentrations of the reactant species and chemical reaction parameters to dispersion models, which can then be used by dispersion models to characterize pollutant reactions within grid. Technically, this approach could improve the performance of dispersion models, especially for reactive pollutants. However, one major tradeoff of such hybrid models is the intensive computational requirement, which may restrict the temporal coverage of the hybrid model.

Human exposure to air pollution may be distinct at different temporal scales, hence exposure estimation needs to be performed at multiple temporal scales. For this purpose, concentration estimates obtained from air quality models should cover a relatively large time period. Due to the restricted temporal coverage, direct couple of Eulerian chemical transport models with dispersion models may not be suitable for investigating the impact of urban forms on air quality and human exposure.

2.3.5.2. Blend Concentration Estimates From Two Models

In this configuration, Eulerian grid chemical transport models and dispersion models are executed individually, and their concentration estimates are blended together afterward. Example applications including combine modeling results from CMAQ model and AERMOD model (Cook et al., 2008; Lobdell et al., 2011), or extended to HYSPLIT model (Stein et al., 2007). The blending methods includes simple adding up (Cook et al., 2008; Lobdell et al., 2011), and combining background concentration from Eulerian grid models with local concentration variability derived from dispersion models (Isakov et al., 2007).

This approach is relatively easier to implement when compared with coupled models. However there are issues with the blending process. First, double counting may

occur when emissions from the same area were included in both Eulerian grid models and dispersion models. Stein et al. (2007) estimated that the effect of double-counting accounts for approximately 10% of the total pollutant concentrations using benzene as an example. However this percentage may be highly depended on the characteristics of the pollutant of interest. A zero-out approach could be applied to avoid double-counting. In this approach, Eulerian models are executed twice, with and without the emissions included in dispersion models, and the true background concentrations can then be derived. However this approach is apparently computational intensive. Second, similar with coupled models, Eulerian grid models and dispersion models are fundamentally different at every aspect including model design and model formulation. Hence mismatching spatial concentration variability may occur, and this issue has not been adequately addressed in the scientific literature.

2.3.6. Summary of Model Review Findings

Air quality models that can be applied to estimate pollutant concentration distributions at urban scale were categorized into five categories: empirical/statistic based models, chemical transport models, computational fluid dynamics models, street canyon models and hybrid models, and each of the categories were critically reviewed regarding their applicability for the investigation of the impacts of urban forms on air quality and human exposures.

Overall, empirical/statistic based models are found to be less suitable, mainly due to their diagnostic nature and lack of generalizability. Computational fluid dynamics models are prognostic, but may be too data and computational intensive to use. Street

canyon models are also excluded since it is designed for small urban areas with many high-rise buildings.

Among chemical transport models, steady-state Gaussian plume models and non-steady-state Lagrangian chemical transport models could provide spatially resolved pollutant concentrations, which are desirable for exposure estimation purposes, but they generally lack adequate chemistry when applying for secondary pollutants. Eulerian grid chemical transport models have the capability of characterizing detailed atmospheric chemistry but usually estimate pollutant concentrations at coarse spatial resolutions. Hybrid models that combine Eulerian grid chemical transport models with either steady-state Gaussian plume models or non-steady-state Lagrangian chemical transport models could combine the advantages of these models and hence are preferred. In addition, blending concentration estimates from two model during post-processing is technically feasible for the purpose of exposure estimation at multiple temporal scales, and hence is the preferred method for combining Eulerian grid chemical transport models with dispersion models. However, there are still technical issues regarding the data blending process and further studies may be needed.

2.4. Summary of Literature Review

Overall, the number of studies focused on impacts of urban design forms on air quality, exposure, and especially inequality regarding pollution exposures are still limited. Evidences suggest compact urban form could lead to less pollutant emissions than sprawl urban form. However the impacts of different urban forms on air pollution exposure seem to differ by pollutants and sometimes contradictory findings were found.

The mechanisms of how urban forms (as well as transportation managements) impact air quality, related exposure and inequalities are still largely unclear.

Additionally, to better understand the impact of urban design forms and transportation managements on air quality, exposure and inequality, a method that is capable of capturing high spatial and temporal resolution distribution of pollutant concentrations are needed. In addition, the method should be able to appropriately combine non-steady-state Lagrangian and Eulerian grid chemical transport models at multiple scales to incorporate the advantages of both models.

CHAPTER 3

AIR QUALITY IMPACT OF HIGH-OCCUPANCY TOLL LANE PROJECT

Note: Much of the ideas and displays in this chapter have been published as a research project report for the National Center for Transit Research on which the author of this dissertation is a co-author (Stuart et al., 2010). Here, the components that I performed that contribute to the dissertation objectives are compiled and discussed.

3.1. Introduction

Due to rapid urban growth and increasing motor-vehicle dependency, vehicle mileage travelled in the US has increased dramatically. This in turn has led to a substantial increase in emissions from mobile sources, which are now a major contributor to total air pollutant emissions (Mage et al., 1996). In addition, mobile source emissions pose significant threats to human health. Previous studies have shown that over 50% of cancer cases due to exposure to air pollution are attributable to mobile source Hazardous Air Pollutants (HAPs) (HEI Panel on the Health Effects of Traffic-Related Air Pollution, 2010).

Transportation infrastructure directly affects traffic characteristics on roadways which will consequently impact on-road mobile source emissions. Past studies suggest that changes in transportation infrastructure such as construction of high-occupancy vehicle lanes encourage ride sharing, which would ultimately reduce the total vehicle

mileage travelled and help to reduce on-road mobile source emissions (Boriboonsomsin & Barth, 2008; Shewmake, 2012; U.S. Environmental Protection Agency, 1998). These findings suggest the possibility of alleviating the issue of on-road mobile source emissions by changing current transportation infrastructure, however studies on this topic have been sparse and the results are rather inconsistent (Dowling et al., 2005; Lee et al., 2009; You et al., 2010).

Similarly to high-occupancy vehicle lanes, managed high occupancy/toll (HOT) lanes also encourage carpooling. High occupancy/toll lanes also generate revenue; hence they are of significant interest around the US. Despite this, studies regarding the air quality impact of high occupancy/toll projects are again scarce (Kall et al., 2009). Further studies are needed to better understand how pollutant emissions and air quality in surrounding areas were impacted by such transportation infrastructure changes.

Here, we assessed the air quality impact of a high-occupancy toll lane project which was implemented by the Florida Department of Transportation in 2009, known as the '95 Express' project. The project is located on the I-95 corridor between Miami and Fort Lauderdale (Figure 3.1) and consisted of three phases. Air quality impacts of phases 1A and 1B were studied. One existing high-occupancy vehicle lane was converted to two high-occupancy toll lanes and the number of general purpose lanes was kept the same. Public transit services including regular buses and Bus Rapid Transit (BRT) were also provided on the new high-occupancy lanes.

Baseline air quality before implementation of the high-occupancy toll lane project was first assessed by analyzing the trend of pollutant concentrations and the Air Quality Index (AQI) in two counties where the project was located: Broward and Miami-Dade

County. Emissions of the chosen pollutants, including carbon monoxide (CO), nitrogen oxides (NO_x), particulate matter (PM), hydrocarbons (HC), and selected mobile source air toxics were estimated. Dispersion modeling was then performed to evaluate the impact of the project on pollutant concentrations near the corridor. Details of each step are presented in following sections.

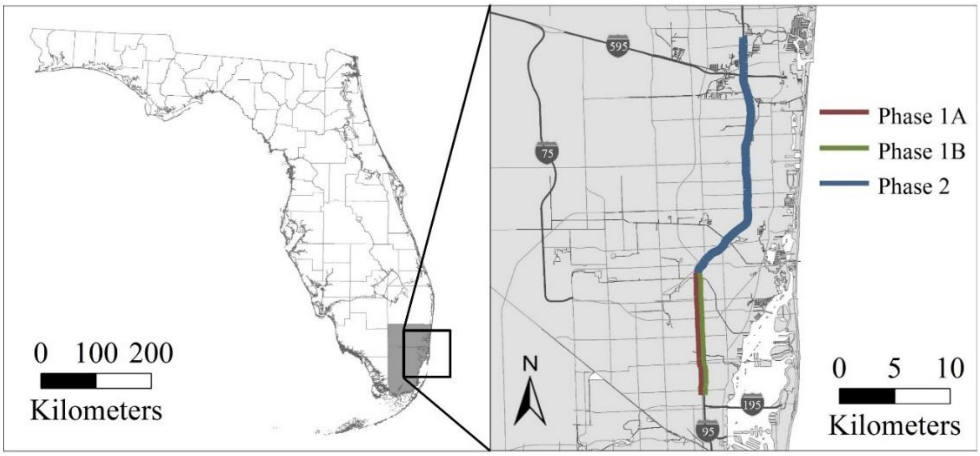

Figure 3.1 Location and three phases of the managed high-occupancy toll lane project

3.2. Baseline Air Quality Based on Measurement Data

Baseline air quality prior to the implementation of the high-occupancy toll lanes was evaluated for air pollutants including CO, nitrogen dioxide (NO_2), ozone (O_3) and particulate matter (PM) and selected mobile source air toxics including benzene, acetaldehyde, and 1,3-butadiene, alongside the air quality index. Pollutant concentration data from January 2000 to June 2009 and air quality index values for the same time period were collected from air quality monitoring reports (Table 3.2) and the AQS (air quality system) database from the U.S. Environmental Protection Agency (EPA). The collected data were cross-validated and compiled. Regulatory monitoring stations where pollutant concentration data were collected are listed in Table 3.1. Distances of these

monitors to Interstate-95 are also listed. Trends found in the compiled pollutant concentrations and index values are discussed in the following sections.

3.2.1. Criteria Air Pollutants

Six common air pollutants including CO, lead (Pb), NO_2, O_3, PM (specifically $PM_{2.5}$: PMs that have diameters less than 2.5 μm, and PM_{10}: PMs that have diameters less than 10 μm) and sulfur dioxide (SO_2), are collectively called Criteria Air Pollutants (CAP). These Criteria Air Pollutants are ubiquitously found across the continental US and are considered to pose a threat to human health and public welfare. Concentration threshold standards of these pollutants were specified in the National Ambient Air Quality Standards (NAAQS) (U.S. Environmental Protection Agency, 2012b). Four of these pollutants: CO, NO2, O3 and PM (including both PM10 and PM2.5), were selected in this study. Lead and SO2 were not included as they are not considered significant pollutants in the study area.

3.2.1.1. Carbon monoxide

Carbon monoxide (CO) is a gaseous pollutant that is both odorless and colorless. Once entering the human body, CO will bind to hemoglobin and consequently diminish the oxygen delivering capability of the blood. This effect can be fatal when concentrations of CO are high. Some population subgroups including children and people who suffer from cardiovascular disease are at greater risk (Allred et al., 1989). In the US, 86% of CO emissions in the US come from mobile sources and its concentration is expected to be higher near major roadways (U.S. Environmental Protection Agency, 2013). The current regulatory concentration standard for CO is 35 ppmv (maximum 1 hour) and 9 ppmv (8 hour average), with no exceedance allowed.

Table 3.1 List of regulatory monitoring stations where pollutant concentration data were collected

county	station ID	address	abbreviation	distance to I-95	CO	NO_2	O_3	PM_{10}	$PM_{2.5}$	Other
Broward	12-011-0010	Lincoln Park Elementary Sch. (Nw Corner)	Lincoln Park	0.1 mile	00-09			00-09		
Broward	12-011-0011	1800 Sw 4th Avenue, Fort Lauderdale	SW 4th Ave	1.4 miles				00-07		
Broward	12-011-0031	12600 West Sample Road	W Sample	9.9 miles		00-09	00-09			
Broward	12-011-0033	3211 College Ave, Vista View Park	Vista	10.6 miles			09		09	
Broward	12-011-1002	3205 Sw 70th Avenue	SW 70th Ave	4.3 miles				00-09	00-09	00-09
Broward	12-011-1201	2900 S. University Dr.	S Univ	5.1 miles	00-06					
Broward	12-011-2003	1951 Ne 48th St	NE 48th St	1.6 miles			00-09			
Broward	12-011-2004	851 Sw 3 Avenue Pompano Beach	SW 3 Ave	0.5 mile	00-09			00-09	00-09	00-08
Broward	12-011-3002	2701 Plunkett Street Hollywood	Plunkett St	0.4 mile	00-09			00-09	00-09	00-08
Broward	12-011-5001	3701 North State Road 207	N State RD	2.6 miles	00-04					
Broward	12-011-5002	11251 Taft Street Pembroke Pines	Taft St	8.2 miles				00-02		
Broward	12-011-5005	4010 Winston Park Blvd	Winston	3.3 miles				00-09		00,02-09
Broward	12-011-6002	1200 Nw 72 Avenue Plantation	NW 72 Ave	4.6 miles				00-01		
Broward	12-011-7002	301 Ne 12th Street	NE 12th St	0.9 mile				00		
Broward	12-011-8002	7000 N. Ocean Drive	Ocean Dr	3.5 miles		00-09	00-09			
Miami-Dade	12-086-0020	7100 Nw 36th St.	NW 36th St	6.0 miles				00-03		02-05
Miami-Dade	12-086-0021	Krome Ave Thompson Pk	Krome Ave	14.8 miles			00-03			
Miami-Dade	12-086-0027	Rosenstiel School	Rosenstiel	2.9 miles		00-09	00-09			
Miami-Dade	12-086-0029	19590 Old Cutler Rd-Perdue Med. Center	Perdue Med	13.5 miles			00-09			02-05
Miami-Dade	12-086-0030	Everglades NP	Everglades	38.8 miles			00-04			
Miami-Dade	12-086-0031	16000 South Dixie Highway	S Dixie Hw	12.1 miles	00-09					
Miami-Dade	12-086-0033	7700 Nw 186 Street	PF	7.3 miles					05-09	
Miami-Dade	12-086-0034	Nw Corner Of Intersection Of Sw 88 St & N Kendall Dr	SW 88 St	12.7 miles	05-09					
Miami-Dade	12-086-1016	Nw 20 St And 12 Ave,Fire Station	MF	0.1 mile				00-09	00-09	
Miami-Dade	12-086-1019	2201 Sw 4 St	SW 4 St	2.1 miles	00-09					
Miami-Dade	12-086-3001	6400 Nw 27th Ave.	NW 27th Ave	2.3 miles				00-03		
Miami-Dade	12-086-4002	Metro Annex 864 Nw 3rd Street	Annex	0.3 mile	00-09	00-09				02-03
Miami-Dade	12-086-6001	Fire Station 325 Nw 2nd St	HF	25.6 miles				00-03	00-09	

Hourly concentrations of CO were collected from five monitoring stations, one located in Broward County and four in Miami-Dade County (Figure 3.2). Two stations in Broward County, namely S Univ and N State RD, and one station in Miami-Dade County, namely SW 88 St, discontinued CO monitoring activities in 2006, 2004 and 2005 respectively. Thermo Electron/Thermo Environmental instruments model 48 series gas filter correlation ambient CO analyzers were used by all monitoring stations to measure hourly CO concentrations continuously. Three stations in Broward County (SW 3 Ave, Lincoln Park, and Plunkett St) and one station in Miami-Dade County (Annex) are located in close proximity to I-95. Among them, Annex station is located close to where the high-occupancy lane project was implemented.

Table 3.2 List of collected air quality monitoring reports and data availability

agency	report	availability
Florida Department of Environmental Protection (FDEP)	Annual Air Monitoring Report	2000-2006
	Quick Look Report	2000-2009
Broward County Environmental Protection and Growth Management Department (EPGMD)	Environmental Benchmarks Report	2000-2008
Miami-Dade County Department of Environmental Resources Management (DERM)	Ambient Air Monitoring Report	2000-2007

Figure 3.3 provides trends of the highest 1 hour and highest 8 hour CO concentrations in the two counties. For comparison purposes, regulatory standards of CO are also shown in the figure. The measured highest CO concentration is 7.5 ppmv (Lincoln Park site, 2000) in Broward and 11.9 ppmv (Annex site, 2004) in Miami-Dade County. Both of the concentration values are well below the previously mentioned corresponding standards.

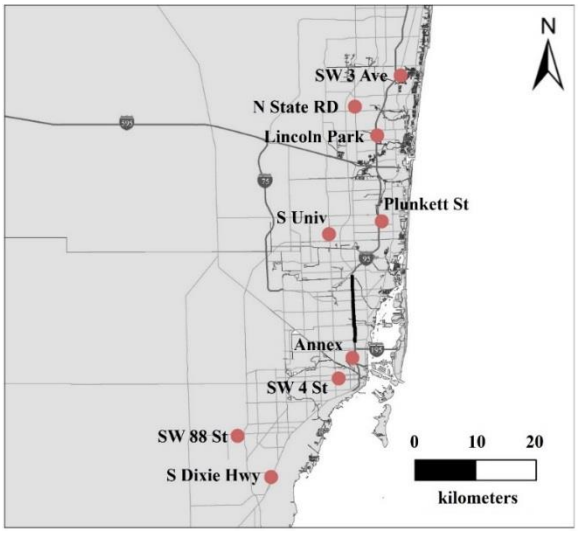

Figure 3.2 CO monitoring stations in Broward and Miami-Dade County. Location of the high-occupancy toll lane project (phase 1A and 1B) are bolded.

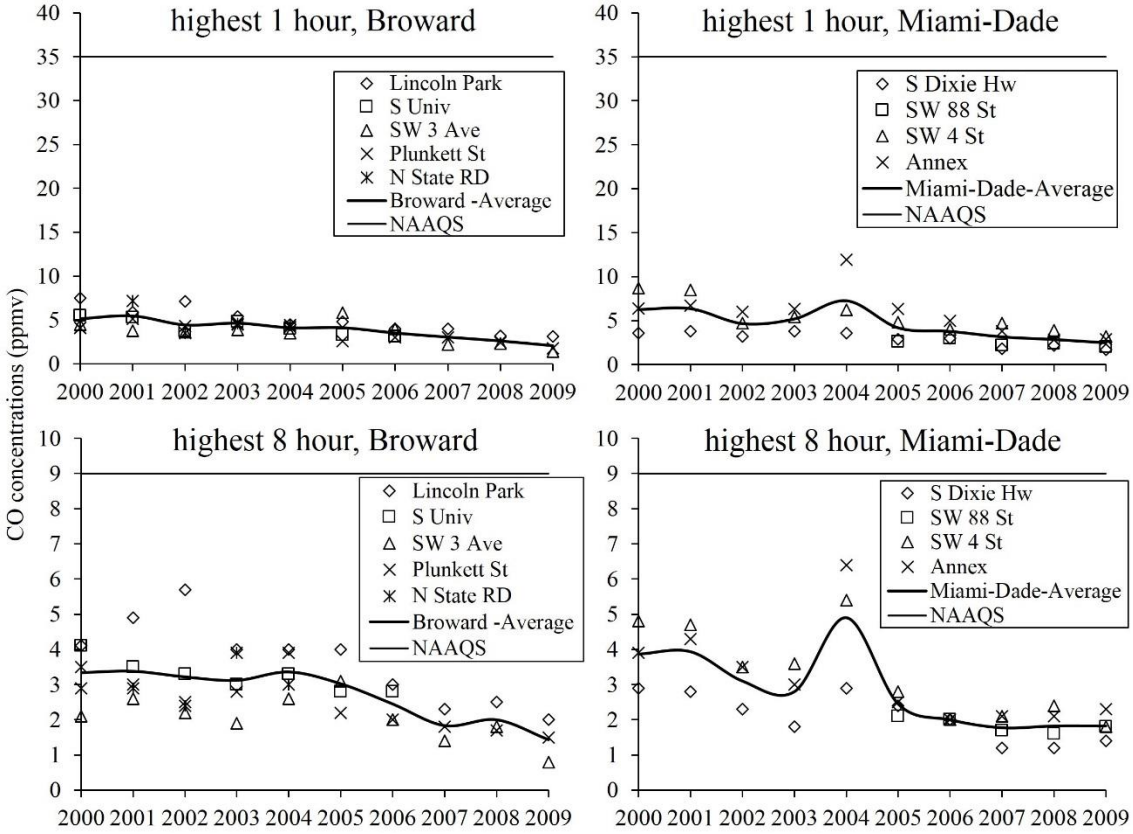

Figure 3.3 Trend of the highest 1 hour and highest 8 hour CO concentrations in Broward and Miami-Dade County. Trend of county average concentrations are shown in solid lines.

From 2000 to 2009, a declining trend can be observed for the highest 1 hour CO concentrations in both counties. County average CO concentrations dropped from 5.14 ppmv (2000) to 2.1 ppmv (2009) in Broward County, and from 6.23 ppmv (2000) to 2.45 ppmv (2009) in Miami-Dade County. Regarding the highest 8 hour concentrations, a similar declining trend can be observed although in this case with more fluctuations. The county average highest 8 hour CO concentrations decreased from 3.34 ppmv (2000) to 1.43 ppmv (2009) in Broward and from 3.86 ppmv (2000) to 1.83 ppmv (2009) in Miami-Dade County.

3.2.1.2. Nitrogen dioxide

Nitrogen Dioxide (NO_2) is light brown in color. It is highly reactive in the atmosphere and contributes to the formation of ground level ozone which is detrimental to human health. Adverse health effects associated with NO_2 exposure include irritation to the respiratory tract and increased incidents of acute respiratory diseases in susceptible groups (Denison, 2000). A significant proportion of NO_2 is formed through quick oxidization of nitrogen oxide (NO) primarily emitted during fuel combustion. Hence higher NO_2 concentrations are expected to be found not directly adjacent to major roadways, but a short distance away. The current regulatory standard for NO_2 is 0.053 ppmv (annual average) and 0.1 ppmv (98th percentile of 1 hour concentrations, averaged over 3 years).

NO_2 concentrations were measured at two monitoring stations in Broward and two stations in Miami-Dade County (Figure 3.4). Thermo Environmental Instruments model 42 series chemiluminescence NO-NO_2-NO_x analyzers were used at these stations

to collect hourly ambient NO_2 concentrations. In addition, Figure 3.5 shows the trend of the highest 1 hour and annual average NO_2 concentrations for the two counties.

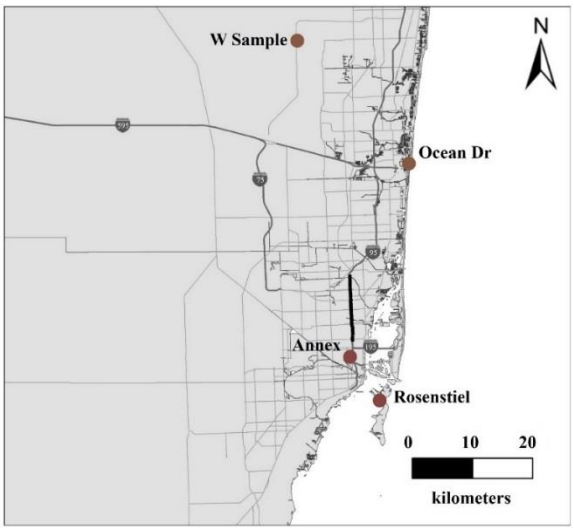

Figure 3.4 NO_2 monitoring stations in Broward and Miami-Dade County. Location of the high-occupancy toll lane project (phase 1A and 1B) are bolded.

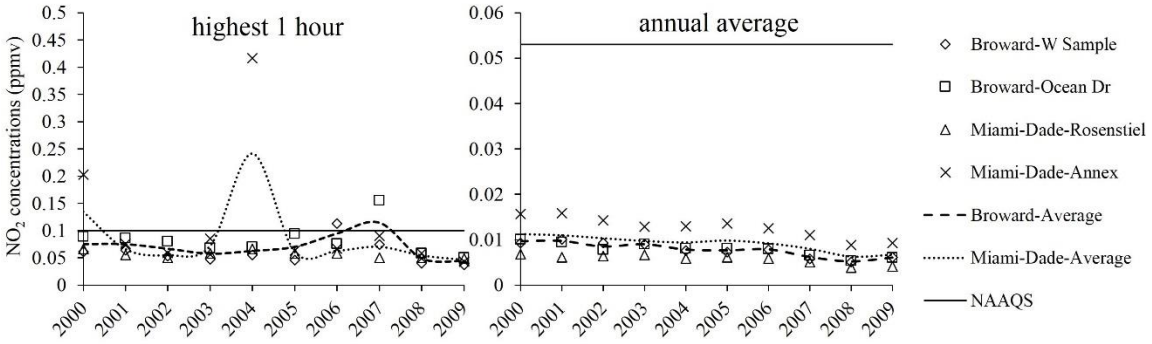

Figure 3.5 Trend of the highest 1 hour and annual average NO_2 concentrations in Broward and Miami-Dade County. Note that for the highest 1 hour NO_2 concentrations plot, concentrations shown are the highest 1 hour NO_2 concentrations, but NAAQS levels shown are referring to 3 year average of the highest 1 hour NO_2 concentrations. Hence they are not directly comparable.

The highest measured annual average NO_2 concentration was 0.01 ppmv (Ocean Dr site, 2000) in Broward and 0.016 ppmv (Annex site, 2001) in Miami-Dade County, both of the values are below regulatory standard (0.053 ppmv). From 2000 to 2009 the annual average NO_2 concentrations in both counties were declining with minor fluctuations. A similar magnitude of decrease was observed in both counties: a 36%

decrease from 0.0097 ppmv (2000) to 0.0061 ppmv (2009) in Broward, and a 39% decrease from 0.011 ppmv (2000) to 0.0067 ppmv (2009) in Miami-Dade.

There are measured concentration values that are larger than 0.1 ppmv for the highest 1 hour NO_2 concentrations. Specifically, the highest values are 0.16 ppmv (Ocean Dr site, 2007) in Broward and 0.42 ppmv (Annex site, 2004) in Miami-Dade. However, the observed exceedance does not necessarily imply regulatory non-attainment, as the highest 1 hour NO_2 concentration standard established in NAAQS is the 98^{th} percentile of hourly concentrations and averaged over three years. Regarding the trend of highest 1 hour NO_2 concentrations, no apparent tendency can be observed.

3.2.1.3. Ozone

Ozone is a gaseous pollutant that is colorless but with a strong odor. When present in the stratosphere, ozone absorbs a significant portion of the incoming high frequency ultraviolet light from the sun, which may be harmful to human health under direct exposure. Ground level ozone however is a secondary pollutant formed in the atmosphere from complex reactions involving nitrogen oxides (NOx) and volatile organic compounds (VOCs) with the presence of sunlight. Ground level ozone is the main component of urban smog, and repeated exposure may increase the risk of illnesses of the respiratory system including lung damage and permanent scar on lung tissues (Denison, 2000).

As of April 24, 2009, NAAQS set the highest 1 hour and the 4^{th} highest 8 hour concentration standards for ozone. The number of days with the highest 1 hour ozone concentrations over 0.12 ppmv may not exceed 1 in one year, the 3-year average of the 4^{th} highest daily maximum 8 hour average ozone concentrations measured at each

monitor over each year may not exceed 0.075 ppmv. The 1 hour ozone standard was revoked by the EPA on April 25, 2009. Standards for 8 hour ozone concentrations were also revised, changing from 0.08 ppmv to 0.075 ppmv since May 27, 2008.

Figure 3.6 provides locations of ozone monitoring stations in Broward and Miami-Dade County. As of 2009, there are four active stations in Broward County: W Sample, Vista, NE 48th St and Ocean Dr, among which Vista station was established in 2009. Miami-Dade County has two stations still under operation: Rosenstiel and Perdue Med station. Ozone monitoring activities have been discontinued at Krome Ave and Everglades stations since 2003 and 2004, respectively. Thermo Electron/Thermo Environmental instruments 49 series photometric ambient ozone analyzer (Method 047) was used to collect hourly ozone concentration data by all stations except Everglades station in Miami-Dade County, where Monitor Labs/Lear Siegler model 8810 photometric ozone analyzer was used.

Trends of the highest 1 hour and the 4^{th} highest 8 hour ozone concentrations in Broward and Miami-Dade County are shown in Figure 3.7. There are substantial fluctuations and no apparent trend can be observed. In Broward County, the measured highest 1 hour and 8 hour ozone concentrations are 0.11 ppmv (Ocean Dr site, 2001, 2006 and 2008) and 0.077 ppmv (Ocean Dr site, 2006), respectively. Both of the concentration values are below NAAQS standards. In Miami-Dade County, the measured highest 1 hour ozone concentration is 0.119 ppmv (Rosenstiel and Perdue Med sites, 2001), only slightly below the standard (0.12 ppmv). Regarding the highest 8 hour ozone concentrations in Miami-Dade, some of the measured values exceed 0.08 ppmv (0.084 ppmv, Krome Ave, 2001 and 0.081 ppmv, Rosenstiel, 2006). The observed exceedance

does not necessarily imply regulatory non-attainment as the metric used in the standard is the 4th highest daily maximum 8-hour average ozone concentrations averaged over three years.

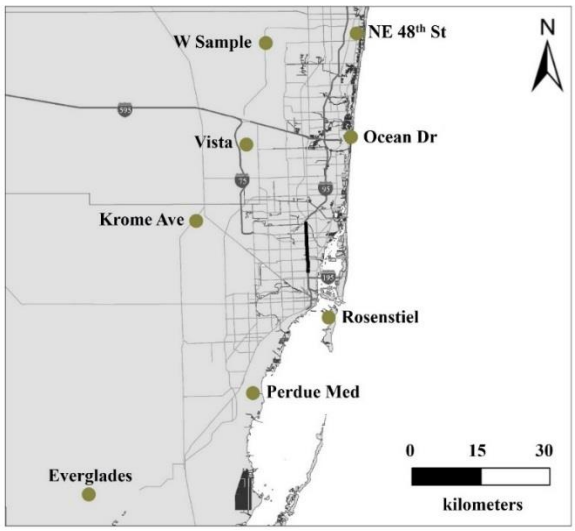

Figure 3.6 Ozone monitoring stations in Broward and Miami-Dade County. Location of the high-occupancy toll lane project (phase 1A and 1B) are bolded.

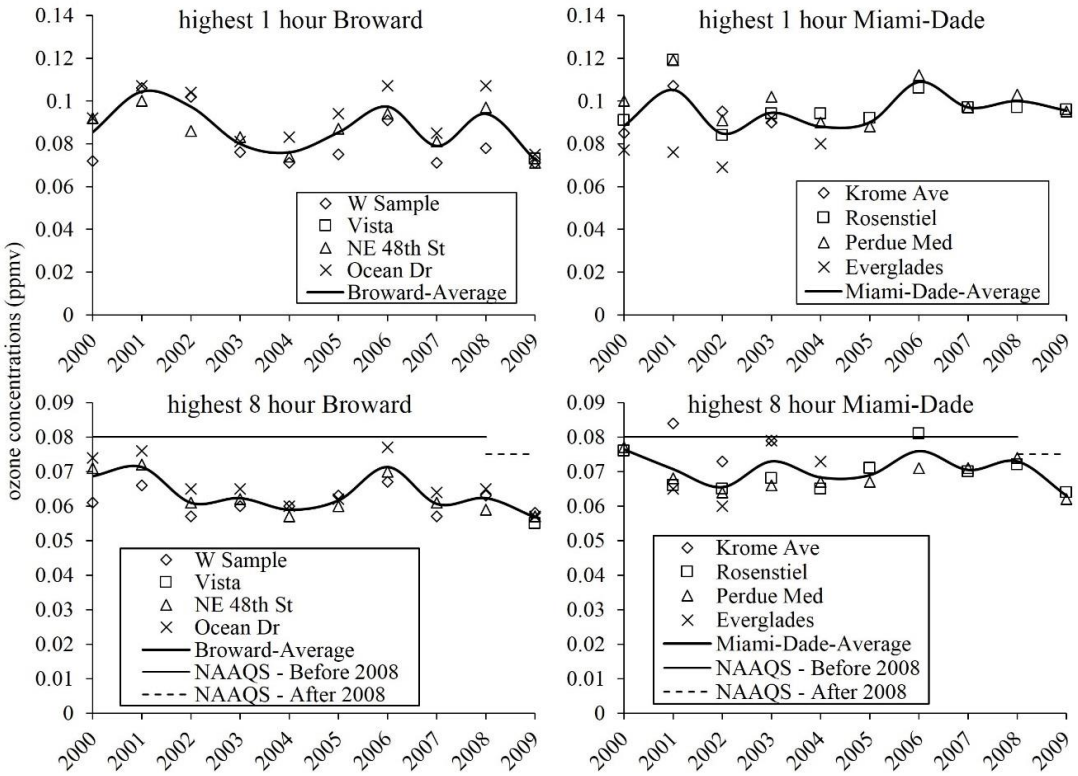

Figure 3.7 Trend of the highest 1 hour and 4th highest 8 hour ozone concentrations in Broward and Miami-Dade County.

3.2.1.4. Particulate matter

Particulate matter (PM) generally refers to very small solid particles or liquid droplets which are suspended in the air and vary greatly in diameter, shape and constitutive components. Particulate matter is usually categorized into PM_{10} and $PM_{2.5}$, the former referring to particulate matter with aerodynamic diameter larger than 2.5 μm and smaller than 10 μm, and the latter referring those with aerodynamic diameter smaller than 2.5 μm. Particulate matter with a diameter larger than 10 μm may be largely filtered in the nasal region of the human respiratory tract. $PM_{2.5}$ and smaller particles may penetrate into the lung (Hinds, 1999). Particulate matter has been found to be associated with various negative health effects ranging from increased symptoms of respiratory ailments to premature death for susceptible populations such as those with pre-existing cardiovascular or lung diseases (Denison, 2000). Particulate matter has both significant primary and secondary contributions; concentrations of PM_{10} are generally higher near emission sources (such as roadways), but concentrations of $PM_{2.5}$ are generally higher at downwind locations. As of 2009, the regulatory standard for PM_{10} is 150 $\mu g/m^3$ (24 hour average). The standard may not be exceeded more than once per year based upon a 3 year average. The standard for $PM_{2.5}$ is 15 $\mu g/m^3$ (annual average) and 35 $\mu g/m^3$ (24 hour average). The former refers to the 3 year average of annual $PM_{2.5}$ concentrations and the latter refers to the 3 year average of the 98^{th} percentile of 24 hour $PM_{2.5}$ concentrations. The primary standard for annual average $PM_{2.5}$ concentrations was revised in 2012 and lowered to 12 $\mu g/m^3$.

As of 2009 there were ten monitoring stations collecting concentrations of particulate matters in Broward County (Figure 3.8), among them six are still under

operation: Lincoln Park, SW 70th, SW 3rd Ave, Plunkett St, Winston and Vistas. In Miami-Dade County, there are currently three active particulate matter monitoring stations: PF, MF, and HF. Monitoring activities have been discontinued since 2003 at NW 27th Ave and NW 36th St stations.

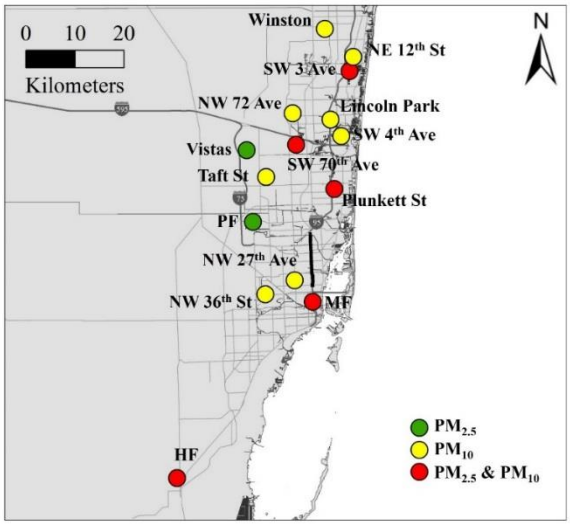

Figure 3.8 Particulate matter monitoring stations in Broward and Miami-Dade County. Location of the high-occupancy toll lane project (phase 1A and 1B) are shown in bolded.

For particulate matters, different samplers were established for various purposes (Table 3.3 and Table 3.4) and different sampling techniques may also be used. For regulatory purposes, samplers that use federal reference manual filter methods, such as method 062 and 063 for PM_{10}; and method 118 for $PM_{2.5}$, were established. Collected concentration data from these samplers were used to justify regulatory attainment decisions. For quality assurance purposes, co-located samplers were established which may be located within the same monitoring station as the regulatory samplers and use the same equipment and sampling techniques.

Manual sampling methods normally require the particulate matter to be filtered and collected for 24 hours. To obtain more temporally resolved concentration data samplers that use continuous monitoring methods were established, such as method 079

for PM_{10} and method 702 for $PM_{2.5}$. In addition, speciation samplers were created to provide detailed speciation data for particulate matters.

Table 3.3 List of particulate matter monitoring stations in Broward and Miami-Dade County, and corresponding sampling techniques

county & pollutant	ID	abbreviation	sampling method	technique
Broward (PM_{10})	12-011-0010	Lincoln Park	062	Manual
	12-011-0011	SW 4th Ave	062	Manual
	12-011-1002	SW 70th Ave	N/A	Manual-2
			062	Manual
	12-011-2004	SW 3 Ave	062	Manual
			079	Continuous
	12-011-3002	Plunkett St	062	Manual
			079	Continuous
	12-011-5002	Taft St	062	Manual
	12-011-5005	Winston	062	Manual
	12-011-6002	NW 72 Ave	062	Manual
	12-011-7002	NE 12th St	062	Manual
Miami-Dade (PM_{10})	12-086-0020	NW 36th St	063	Manual
	12-086-1016	MF	063	Manual-2
			063	Manual
	12-086-3001	NW 27th Ave	063	Manual
	12-086-6001	HF	063	Manual
Broward ($PM_{2.5}$)	12-011-0033	Vista	702	Continuous
	12-011-1002	SW 70th Ave	118	Manual-2
			118	Manual
			810	Speciation
			702	Continuous
	12-011-2004	SW 3 Ave	118	Manual
	12-011-3002	Plunkett St	118	Manual
Miami-Dade ($PM_{2.5}$)	12-086-0033	PF	118	Manual
	12-086-1016	MF	118	Manual-2
			118	Manual
			702	Continuous
			810	Speciation
	12-086-6001	HF	118	Manual
			702	Continuous

Figure 3.9 shows the trends of the highest 24 hour PM_{10} concentrations in the two counties from 2000 to 2009. The highest measured concentration is 122 $\mu g/m^3$ (Plunkett

St, 2007) in Broward County and 64.5 $\mu g/m^3$ (NW 27th Ave, 2003 and MF, 2009) in Miami-Dade County. Both of the values are below the regulatory standard (135 $\mu g/m^3$). No apparent temporal trend can be observed for the highest 24 hour PM_{10} concentrations in the two counties due to substantial fluctuations.

Table 3.4 Equipment and methods used in particulate matter sampling

	sampling method	type of method	equipment used
PM_{10}	062	Reference	Wedding & Associates/Thermo Environmental Instruments Inc. Model 600 PM_{10} Critical Flow High-Volume Sampler
	063	Reference	Sierra-Andersen/General Metal Works Model 1200 PM_{10} High-Volume Air Sampler System
	079	Equivalent	Thermo Scientific TEOM® 1400AB PM_{10} Ambient Particulate Monitor or Rupprecht & Patashnick TEOM® Series 1400 and Series 1400a PM_{10} Monitors
$PM_{2.5}$	118	Reference	Rupprecht & Patashnick Partisol®-Plus Model 2025 Sequential Air Sampler or Thermo Scientific Partisol-Plus 2025 Sequential Air Sampler
	702	Non-Reference	TEOM Gravimetric $PM_{2.5}$ Sharp Cut Cyclone (SCC) monitor with correction factor
	810	Non-Reference	Met-One speciation samplers (SASS) with Teflon filters

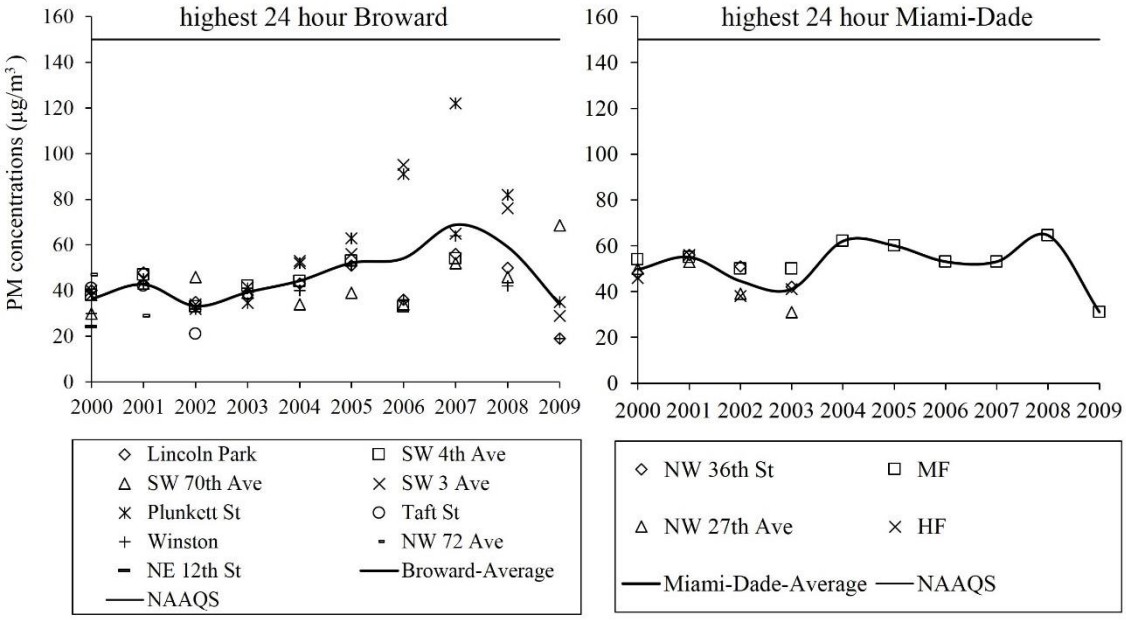

Figure 3.9 Trends of the highest 24 hour PM_{10} concentrations in Broward and Miami-Dade County. County averaged data are shown in solid lines.

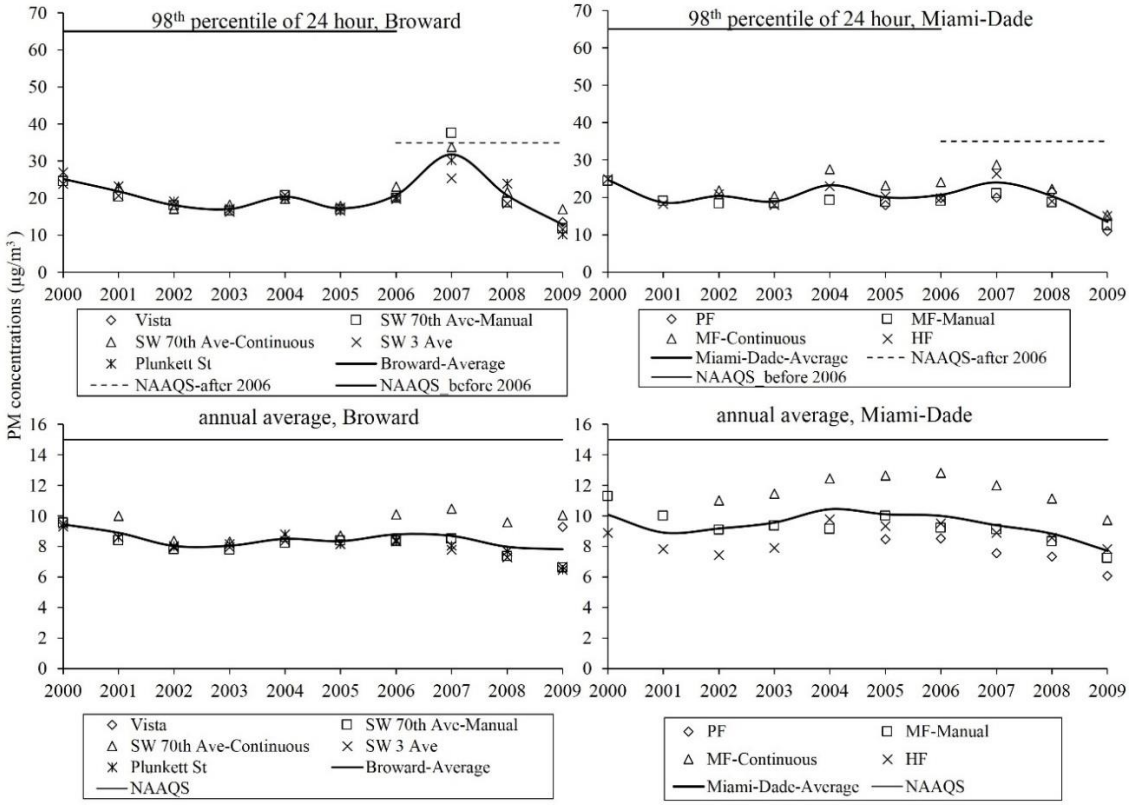

Figure 3.10 Trends of the 98th percentile of 24 hour and annual average $PM_{2.5}$ concentrations in Broward and Miami-Dade County. County averaged data are shown in solid lines.

Figure 3.10 provides trends of the 98th percentile of 24 hour $PM_{2.5}$ concentration and annual average concentrations in Broward and Miami-Dade County. The highest measured annual average $PM_{2.5}$ concentration is 10.5 $\mu g/m^3$ (SW 70th Ave site, 2007) in Broward and 12.8 $\mu g/m^3$ (MF site, 2006) in Miami-Dade, which are below the 2009 regulatory standard of 15 $\mu g/m^3$. The highest values of the 98th percentile of 24 hour average $PM_{2.5}$ concentrations between 2000 to 2009 is 37.6 $\mu g/m^3$ (SW 70th Ave site, 2007) in Broward and 28.7 $\mu g/m^3$ (MF site, 2007) in Miami-Dade. The measured value of 37.6 $\mu g/m^3$ in Broward County slightly exceeds the regulatory standard of 35 $\mu g/m^3$, which does not necessarily imply regulatory non-attainment for the same reasons discussed for ozone. Although the measured $PM_{2.5}$ concentrations are generally lower in 2009 than 2000 in both counties, no apparent temporal trend can be observed.

3.2.2. Selected Mobile Source Air Toxics

Mobile source air toxics (MSATs) are a subset of Hazardous Air Pollutants (HAPs); the latter refers to over 180 air pollutants that are not regulated by National Ambient Air Quality Standards, but have been defined in the Clean Air Act as they may also cause serious health or environmental effects. As implied by their name, mobile source air toxics have substantial vehicular emission contribution, and hence can be affected significantly by transportation infrastructure changes. Here three mobile source air toxics were selected: 1,3-butadiene, acetaldehyde and benzene. All of them are human carcinogens (Agency for Toxic Substances and Disease Registry, 2007, 2009; National Toxicological Program, 2011). No regulatory environmental concentration standards are defined in the national ambient air quality standards for the three selected pollutants.

Table 3.5 List of mobile source air toxic monitoring stations and available data period

County	Station ID	Abbreviation	1,3-Butadiene	Acetaldehyde	Benzene
Broward	12-011-1002	SW 70th Ave	02-09	05-07	00-09
Broward	12-011-2004	SW 3 Ave	02-08	02-03	00-08
Broward	12-011-3002	Plunkett St	02-08		00-08
Broward	12-011-5005	Winston	02-09		00, 02-09
Miami-Dade	12-086-0020	NW 36th St	02-05		02-05
Miami-Dade	12-086-0029	Perdue Med	02-05		02-05
Miami-Dade	12-086-4002	Annex		02-03	

Table 3.5 provides a list of monitoring stations where concentrations of the selected mobile source air toxics were collected. In Miami-Dade County measurement of mobile source air toxics was discontinued in 2006, and as such no data are available after this time. Typically pollutants were first captured in canisters then transferred to laboratories and analyzed using techniques such as Gas Chromatography/Mass Spectrometry (GC/MS) or Gas Chromatography/Flame Ionization detection (GC/FID).

3.2.2.1. 1,3-Butadiene

Under exposure to 1,3-butadiene, irritation to skin, eyes or the respiratory tract is possible. It is also a known human carcinogen (by inhalation). Occupational exposure to 1,3-butadiene has been found to correspond to increased incidences of leukemia and respiratory, bladder, stomach, and lymphato-hematopoietic cancers (Agency for Toxic Substances and Disease Registry, 2009).

Figure 3.11 shows the highest 24 hour and annual 1,3-butadiene concentrations measured in the two counties. The measured highest 24 hour 1,3-butadiene concentrations are 1 ppb (Plunkett site, 2003) in Broward County and 0.9 ppb (Perdue Med site, 2003) in Miami-Dade County. The highest annual average 1,3-butadiene concentrations are 0.13 ppb (Plunkett site, 2003) in Broward County and 0.11 ppb (NW 36 AVE site, 2005) in Miami-Dade County.

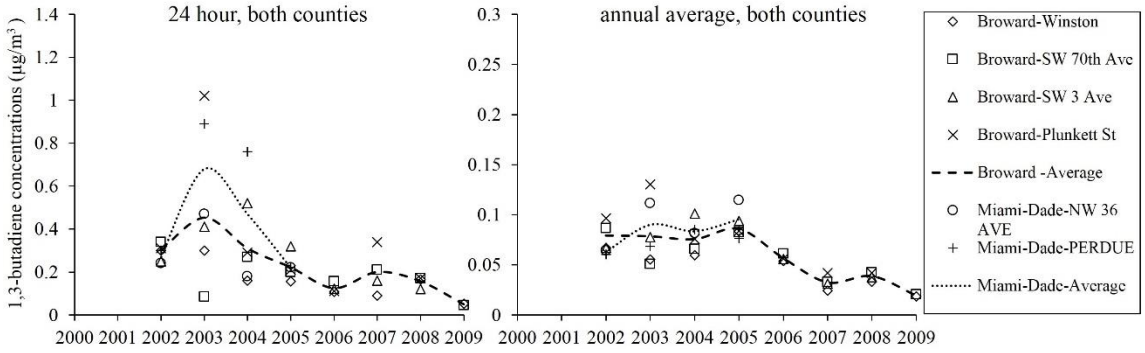

Figure 3.11 Trends of the highest 24 hour and annual average 1,3-butadiene concentration in Broward and Miami-Dade County.

A generally declining trend can be observed for the highest 24 hour and annual 1,3-butadiene concentrations in Broward County. In Miami-Dade County, data are only available from 2002 to 2005, and no apparent trend can be observed.

3.2.2.2. Acetaldehyde

Acetaldehyde is widely used as industrial solvent, it is volatile and highly flammable. Short term exposure to acetaldehyde may cause irritation to skin, eyes and respiratory tracts. The measured highest 24 hour and annual average acetaldehyde concentrations in two counties are shown in Figure 3.12. Only a few data points are available from 2000 to 2009 and no trend can be inferred. It is worth noting that in 2006 an abrupt increase of the highest 24 hour acetaldehyde concentration was observed at the SW 70th Ave site in Broward County, the reason remains unknown.

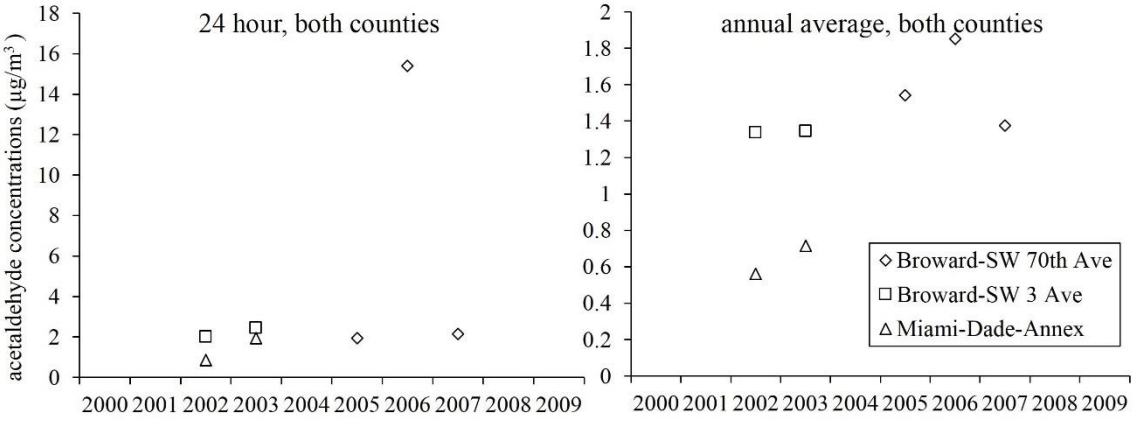

Figure 3.12 Trends of the highest 24 hour and annual average acetaldehyde concentration in Broward and Miami-Dade County.

3.2.2.3. Benzene

Under room temperature benzene is a clear liquid with a sweet odor. It is also volatile and highly flammable. Benzene is primarily used as a solvent and is mainly produced from petroleum products. As a known human carcinogen, chronic exposure to benzene may cause blood disorders and damage immune system (Agency for Toxic Substances and Disease Registry, 2007).

Figure 3.13 provides the highest 24 hour and annual average benzene concentrations in Broward and Miami-Dade County from 2000 to 2009. The measured

highest 24 hour average benzene concentrations are 6.3 ppb (Plunkett site, 2003) in Broward County and 1.3 ppb (NW 36 AVE site, 2002) in Miami-Dade County, while the measured highest annual average benzene concentrations are 1.6 ppb (Plunkett site, 2003) in Broward and 0.53 ppb (NW 36 AVE site, 2005) in Miami-Dade County. Substantial concentration variability are observed in the multi-year results for benzene. Although no apparent trend can be observed, the average benzene concentration from 2005 to 2009 is lower than that from 2000 to 2004.

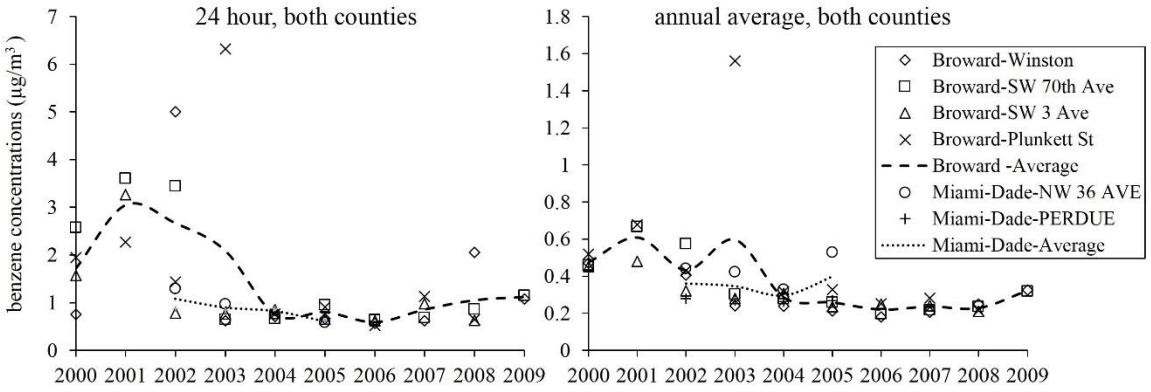

Figure 3.13 Trends of the highest 24 hour and annual average benzene concentration in Broward and Miami-Dade County.

3.2.3. Air Quality Index

Air Quality Index (AQI) is a comprehensive index (ranging from 0 to 500) calculated based on the measured pollutant concentrations of criteria air pollutants including CO, NO_2, O_3, PM and SO_2. It is used to conceptually represent air quality, with a value of 100 generally corresponding to NAAQS standard for criteria air pollutants. Six distinct levels were designated to the air quality index: good, moderate, unhealthy for sensitive groups, unhealthy, very unhealthy and hazardous. These levels and their interpretations are provided in Table 3.6.

Historical air quality index values in Broward and Miami-Dade County were retrieved from the Broward County Environmental Protection and Growth Management Department (EPGMD) and Miami-Dade County Department of Environmental Resources Management (DERM). Trends found in the air quality index are shown in Figure 3.14. In both counties "good" air quality days dominate, with an average of 11% "moderate" days and 0.5% "unhealthy for sensitive groups" days in Broward County, and an average of 9% "moderate" days and 0.4% "unhealthy for sensitive groups" days in Miami-Dade County. There are only 3 "unhealthy" days (2 in 2007 and 1 in 2001) observed in Broward County, accounting for only 0.1% of the total observations. Overall these results suggest slightly better air quality in Miami-Dade than Broward County.

Table 3.6 Air quality index levels and interpretation

air quality index levels of health concern	value	interpretations
good	0-50	air quality is considered satisfactory, and air pollution poses little or no risk.
moderate	51-100	air quality is acceptable; however, for some pollutants there may be a moderate health concern for a very small number of people who are unusually sensitive to air pollution.
unhealthy for sensitive groups	101-150	members of sensitive groups may experience health effects. the general public is not likely to be affected.
unhealthy	151-200	everyone may begin to experience health effects; members of sensitive groups may experience more serious health effects.
very unhealthy	201-300	health alert: everyone may experience more serious health effects.
hazardous	> 300	health warnings of emergency conditions. the entire population is more likely to be affected.

*Source: http://airnow.gov/index.cfm?action=static.aqi

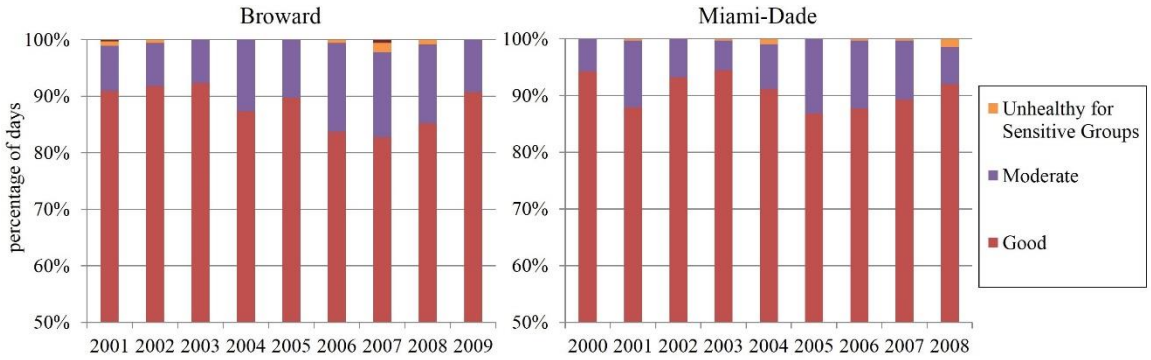

Figure 3.14 Trend of air quality index in Broward and Miami-Dade County.

3.2.4. Summary of Baseline Air Quality Findings

Available data on pollutant concentration levels and values for the four criteria air pollutants (CO, NO_2, PM (PM_{10} and $PM_{2.5}$) and O_3), three mobile source air toxics (1,3-butadiene, acetaldehyde and benzene), and air quality index were collected for the time period 2000 to 2009. The collected data were compiled, multi-year trends were plotted and compared against the national ambient air quality standards (when available).

Overall the measured ambient concentration levels of CO and PM_{10} in the two counties are below the National Ambient Air Quality Standards. Some values of fourth highest 8 hour O_3, as well as 98^{th} percentile of 24 hour $PM_{2.5}$ concentrations exceed the corresponding standard slightly, however the observed exceedance do not necessarily imply regulatory non-attainment due to the different metrics used.

Regarding temporal trends of pollutant concentrations, declining concentrations are observed for CO, NO2 and 1,3-butadiene, as well as benzene, in Broward County. No apparent trend can be observed for the other pollutants. In addition, the air quality index suggests slightly better air quality regarding criteria air pollutants in Miami-Dade than Broward County. In both counties, only a very small number of days from 2000 to 2009

can be categorized as “unhealthy for sensitive groups” and even fewer days are considered “unhealthy”; the latter occurs in Broward County only.

3.3. Emission Estimation

Changes in pollutant emissions from the study corridor due to implementation of the high-occupancy toll lane project are critical for assessing the impact of the project on air quality. Here pollutant emissions from the corridor were estimated by combining traffic data estimated by a traffic micro-simulation model CORSIM (CORridor-microscopic SIMulation) (McTrans, 2008) with emission factors estimated by the MOBILE6.2 model (U.S. Environmental Protection Agency, 2004a). The MOBILE6.2 model is designed specifically for estimating on-road mobile source emissions from vehicles, and has been widely used by federal, state, regional and local level planning agencies and organizations in many applications related to mobile source emissions estimation. Data from the CORSIM model were provided by the Center for Urban Transportation Research (CUTR) at the University of South Florida. Five pollutants: CO, NO_x, PM_{10}, benzene and HC were selected as the study pollutants. Methods and results of emission estimation are provided in following sections.

3.3.1. Emission Factor Estimation

To be consistent with the CORSIM model, vehicle type distributions used in the CORSIM (Table 3.7) model were mapped to the MOBILE6.2 vehicle type distributions (Table 3.8). The method used for mapping the two vehicle type distributions is provided in Table 3.9. Three vehicle type distributions were mapped, corresponding to the before scenario (before implementation of the high-occupancy toll lane project), general purpose

lanes in the after scenario (after implementation of the high-occupancy toll lane project) and high-occupancy toll lanes in the after scenario.

Table 3.7 Vehicle type distributions used in the CORSIM model

vehicle type	CORSIM vehicle type ID	fleet composition
passenger car	1	25%
	2	75%
truck	3	31%
	4	36%
	5	24%
	6	9%
carpool	8	25%
	9	75%

Table 3.8 Vehicle type distributions used in the MOBILE6.2 model

MOBILE6.2 vehicle class ID	MOBILE6.2 vehicle class description
1	LDV Light-Duty Vehicles (Passenger Cars)
2	LDT1 Light-Duty Trucks 1
3	LDT2 Light-Duty Trucks 2
4	LDT3 Light-Duty Trucks 3
5	LDT4 Light-Duty Trucks 4
6	HDV2B Class 2b Heavy-Duty Vehicles
7	HDV3 Class 3 Heavy-Duty Vehicles
8	HDV4 Class 4 Heavy-Duty Vehicles
9	HDV5 Class 5 Heavy-Duty Vehicles
10	HDV6 Class 6 Heavy-Duty Vehicles
11	HDV7 Class 7 Heavy-Duty Vehicles
12	HDV8A Class 8a Heavy-Duty Vehicles
13	HDV8B Class 8b Heavy-Duty Vehicles
14	HDBS School Buses
15	HDBT Transit and Urban Buses
16	MC Motorcycles

Transit buses were not included in the CORSIM simulation for the before scenario. To account for emissions from buses, bus populations on the corridor were obtained and integrated into the CORSIM vehicle type distribution by adjusting the population fractions of the other vehicle types proportionally. In the CORSIM modeling

for the after scenario, General Purpose Lanes (GPL) and high-occupancy toll lanes were modeled separately and transit buses were assumed to be running on high-occupancy toll lanes only. Vehicle type distribution data from 29 counting sites located on the ramps of the I-95 modeling section were also obtained and compared with the vehicle distribution assumption used in the CORSIM model for verification purposes, and they were found to be similar.

Table 3.9 Mapping of CORSIM vehicle type distributions to MOBILE6.2 vehicle type distributions

CORSIM vehicle class ID	corresponding MOBILE6.2 vehicle classes	vehicle fleet composition		
		before scenario all lanes	after scenario	
			general purpose lanes	high-occupancy toll lanes
1, 2, 8,9	LDV, LDT1, LDT2, LDT3 LDT4	95.86%	96.00%	95.60%
3	HDV2B - HDV7	1.24%	1.24%	1.23%
4, 5	HDV8A	2.40%	2.40%	2.39%
6	HDV8B	0.36%	0.36%	0.36%
7	HDBS, HDBT	0.15%	0.00%	0.42%

The mapped vehicle type distributions were then further allocated to each MOBILE6.2 vehicle type using default 2009 VMT distribution data within MOBILE6.2 (U.S. Environmental Protection Agency, 2001, 2004a). Results of the allocated vehicle type distributions are shown in Table 3.10.

Only freeway links were included in the CORSIM simulation. In order to be consistent with the CORSIM model, an external "VMT by facility" file was applied to the MOBILE6.2 model to allocate all vehicle mileage travelled data to freeway links. Further, to reflect average speed distributions on each link and their temporal variations, external "Speed VMT" files were created for each link and were included in MOBILE6.2 modeling for individual links. CORSIM simulated link speed for four rush hours (7-9 am

and 3:30-5:30 pm) and speed data were averaged to obtain hourly speed information for these times. Speed at other hours were assumed to be 55 mph, the speed limit on the corridor.

Table 3.10 Allocated vehicle type distributions

MOBILE6.2 vehicle class ID	MOBILE6.2 default 2009 VMT distribution	before scenario fleet composition	after scenario fleet composition	
			general purpose lanes	high-occupancy toll lanes
1	36.69%	40.27%	40.33%	40.16%
2	8.69%	9.54%	9.55%	9.51%
3	28.94%	31.76%	31.81%	31.68%
4	8.92%	9.79%	9.80%	9.76%
5	4.10%	4.50%	4.51%	4.49%
6	3.89%	0.72%	0.72%	0.71%
7	0.38%	0.07%	0.07%	0.07%
8	0.32%	0.06%	0.06%	0.06%
9	0.24%	0.04%	0.04%	0.04%
10	0.87%	0.16%	0.16%	0.16%
11	1.03%	0.19%	0.19%	0.19%
12	1.12%	2.40%	2.40%	2.39%
13	3.98%	0.36%	0.36%	0.36%
14	0.20%	0.10%	0.00%	0.28%
15	0.10%	0.05%	0.00%	0.14%
16	0.54%	0.00%	0.00%	0.00%

Fuel and meteorological parameters used in the MOBILE6.2 estimation were extracted from the NCD (National Mobile Inventory Model (NMIM) County Database) database (U.S. Environmental Protection Agency, 2005a). Default data were used for other data such as the diesel sale fraction distributions among vehicle types.

MOBILE6.2 modeling were performed for both the before and after scenarios. In the after scenario, general purpose lanes and high-occupancy toll lanes were modeled separately to account for differences in vehicle fleet composition. Emission processes that could occur on freeways were included. Specifically the included emission processes are

running exhaust, running evaporative emissions and seven types of particulate matter emissions: exhausted SO4, exhausted lead, organic carbon and elemental carbon from diesel vehicle exhausts, total carbon, brake-wear PMs and tire-wear.

Emission factors were estimated for all vehicles, as well as for buses alone. The estimated emission factors were resolve by year, month, pollutant and link. Overall, over 100,000 emission factors were estimated, and all emissions factors show a consistent decreasing trend since year 2005.

3.3.2. Annual Traffic Extrapolation

As previously mentioned, CORSIM simulated traffic volume data for 4 rush hours in one typical day. The data were extrapolated to other hours of the day and further extrapolated to a whole year for emission estimation purposes. Diurnal (diurnal profile by hour) and monthly (annual profile by month) traffic variation profiles were applied during this extrapolation. The profiles (Figure 3.15) differ at northbound and southbound I-95, and they were derived from hourly vehicle counting data obtained from one traffic monitoring site located on I-95 (site ID: 860331), approximately 5 miles away from the north end of the modeling section of I-95.

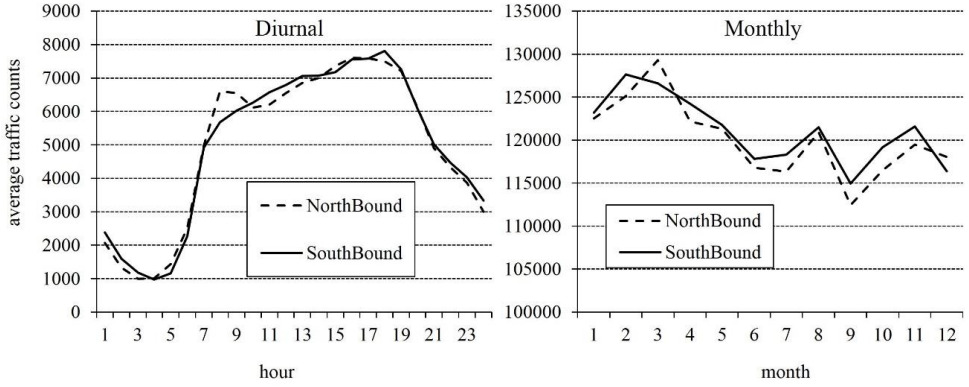

Figure 3.15 Diurnal and monthly traffic variation profiles used in traffic volume extrapolation.

On-road mobile source emissions for each link were estimated by multiplying the emission factor by the length of the corresponding link and extrapolated daily total traffic volume for that link. Monthly and annual emissions were calculated by aggregating these estimated daily emissions.

3.3.3. Emission Estimation Results

Pollutant emissions were calculated for five consecutive years from 2005 to 2009. As an example, results for the year 2009 are provided in Table 3.11. The estimated total emissions for CO, NO_x, benzene and PM_{10} increase slightly with the implementation of the high-occupancy toll lane project. The magnitude of this increase ranges from 0.6% for benzene to 3.4% for CO. Total emissions for HC decreased slightly by 1.5%. Emissions from buses show a consistent decrease with implementation of the high-occupancy toll lane project, with largest decrease for benzene (14.3%) and smallest decrease for NO_x (0.7%).

Table 3.11 Estimated annual emissions for year 2009

pollutants	before scenario total	after scenario total	before scenario buses alone	after scenario buses alone
CO	6657	6892	2.12	1.91
NO_x	623.2	640.4	14.27	14.17
PM_{10}	20.28	20.69	0.25	0.24
benzene	12.58	12.65	0.0024	0.0021
HC	604.1	595.0	0.22	0.2

3.3.4. Discussions of Emission Estimation

The patterns of estimated emission changes are similar to that found in Kall et al. (2009), where slightly increased emissions of CO, NO_x and PM_{10} and slightly decreased emissions of HC were observed due to the implementation of a high occupancy toll lane

project on I-85 near Atlanta, GA. To better understand the observed emission changes in this study, individual factors affecting the results of estimation are discussed.

On-road mobile source emissions from the corridor are mainly determined by two contributing parameters: vehicle mileage travelled on the corridor and emission factors. The former were estimated by the CORSIM model and the latter were estimated by the MOBILE6.2 model. Table 3.12 provides a comparison of the percentage changes in annual emissions, emission factors and annual total average vehicle mileage travelled for 2009 both before and after implementation of the high-occupancy toll lane project. The CORSIM estimated total vehicle mileage travelled increased by approximately 2% in the after scenario. Average emission factors for CO, NO_x and PM_{10} also increased slightly in the after scenario. The increase for both contributing parameters led to an increase in annual emissions for these pollutants. For HC, the average emission factor decreases by a larger magnitude (-3.7%) than the increase in vehicle mileage travelled (2%), which results in overall decrease in annual HC emissions. The average emission factor for benzene is slightly lower in the after scenario, yet the relatively larger increase in vehicle mileage travelled leads to an overall small increase in annual emissions.

Table 3.12 Percentage changes (after scenario versus before scenario) in annual emissions, emission factors and annual total mileage travelled for year 2009.

pollutant	annual emissions	emissions factors	annual vehicle mileage travelled
CO	3.50%	1.20%	
NO_x	2.80%	1.30%	
PM_{10}	2.00%	0.74%	2%
benzene	0.54%	-1.70%	
HCs	-1.50%	-3.70%	

* Change in emissions factors were estimated based on simple average emission factors across all links.

To further understand the observed change in emission factors, a sensitivity analysis was performed for CO, NO_x and HC to evaluate the speed-emission factor relationship in the MOBILE6.2 model. The results are shown in Figure 3.16. The relationships for CO and NO_x are 'V' shaped, with lowest emission factors observed at approximately 30 mph. A constantly declining pattern is observed for HC. Simulation results from the CORSIM model suggest that with implementation of the high-occupancy toll lane project average travelling speeds on the study corridor are expected to increase from approximately 20-30 mph to 45-50 mph. The increased travelling speed will lead to decreased emission factors for HC, but not for CO and NO_x due to their unique speed-emission factor relationships.

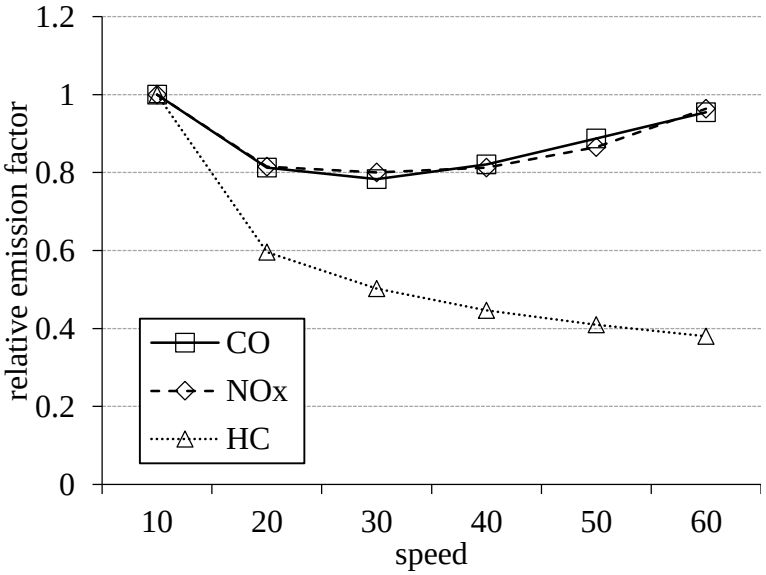

Figure 3.16. Speed-emission factor relationships in the MOBILE6.2 model

Regarding emissions from buses, decreases were observed for all pollutants. Similarly to the previous results, bus emissions are also impacted by changes in vehicle mileage travelled and emission factors. Despite this, the speed-emission factor relationship for buses is different to that shown in Figure 3.16, hence the direction of

change in these bus emissions does not remain the same as previously found when the project is implemented.

The results contribute to the field of study by showing that transportation infrastructure changes (such as the construction of high occupancy toll lanes similar to the one found in this study) could improve the performance of the network, including increasing travelling speed and reducing travelling time. However, the impact of such changes on pollutant emissions from on-road mobile sources are rather more complex, due primarily to the non-linear relationships between emission factors and vehicle speed. When vehicle mileage travelled was held constant, improvement in roadway performance does not necessarily lead to decreased emissions.

3.3.5. Limitations and Uncertainties in Emission Estimation

It has to be noted that there are substantial amount of uncertainties involved in the emissions estimation. One of the largest uncertainty may be came from the CORSIM modeled traffic characteristics (vehicle volumes). The CORSIM results suggest a 3.1% increase in vehicle mileage travelled for northbound I-95 and a 1.9% increase for the southbound direction. These CORSIM estimated changes may not fully account for vehicle volume changes on the corridor due to implementation of the managed lane project. Furthermore, changes of traffic characteristics on surrounding transportation networks were not modeled by the CORSIM, pollutant emissions from these roadways may also impact the air quality in surrounding areas.

There are also limitations in the estimated emission factors. The MOBILE6.2 model which was used to derive the emission factors in this study was not designed to capture microscopic vehicle behaviors such as acceleration and deceleration, and these

vehicle behaviors may be important at the roadway link level. In addition, evaluations of the MOBILE6.2 model have shown that the uncertainties within the estimated emission factors for NO_x and HC range from 20% to 55% (Committee to Review EPA's Mobile Source Emissions Factor (MOBILE) Model, 2000). The estimated range of uncertainties are large than the estimated change in pollutant emissions.

Vehicle fleet composition may also affect the estimated emissions. It is well known that some vehicle categories such as heavy duty vehicles and buses on average emit more pollutants than other vehicles such as passenger cars. Recall that the vehicle fleet compositions used in the CORSIM model were mapped to the MOBILE6.2 vehicle classes; the mapping process may lead to further uncertainties. Additionally, vehicle fleet composition in the MOBILE6.2 modeling was held constant temporally, which may impact the estimated total amount of emissions as temporal variations of fleet composition are not accounted for. Furthermore, the CORSIM model data provided assumed that no bus ridership and carpooling changes would occur due to implementation of the high occupancy toll lane project, yet one of the designed purposes of this project is to encourage the use of buses and carpooling. The total vehicle mileage travelled could be reduced if this purpose is fulfilled.

The extrapolated traffic volume is another uncertainty in emission estimation. By simply applying traffic variation profiles the extrapolated traffic volume may not be fairly representative. Other uncertainties include the 55 mph speed assumption for roadway links and the mapping method use in vehicle type distributions.

3.3.6. Summary of Emission Estimation Findings

Emissions from the study corridor of five selected pollutants: CO, NO_x, PM_{10}, benzene and HC, were estimated for both before and after the implementation of the high-occupancy toll lane project. The MOBILE6.2 model was used to estimate link level emission factors for the corridor, which were then combined with traffic data estimated by the CORSIM model to calculate pollutant emissions.

Results show a slight emission increase for CO, NO_x, PM_{10} and benzene, and a slight decrease for HC following implementation of the project. Pollutant emissions from transit buses consistently decrease for all five pollutants. Increased vehicle mileage travelled, as well as changes in emission factors, contribute to the observed changes in pollutant emissions. The change in emission factors can be explained by the speed-emission factor relationships used for different pollutants in the MOBILE6.2 model.

Emission estimation results of this study are consistent with previous literature (Kall et al., 2009). The results for all vehicles suggest that transportation infrastructure changes may improve performance of the roadway network, but not necessarily lead to reduced on-road mobile source emissions.

3.4. Dispersion modeling

The impact of the high-occupancy toll lane project on pollutant concentration levels was estimated through dispersion modeling. A steady state Gaussian dispersion model, AERMOD, was employed. Phases 1A and 1B of the project, the same sections as for emission estimation, were included in the modeling. Three pollutants: benzene, CO and NO_x were selected as the study pollutants. Inputs to the AERMOD model include

meteorological data, receptor locations, and emission data. Details of these inputs are provided below.

3.4.1. Meteorological Data

Based on recommendations from the Environmental Protection Agency (U.S. Environmental Protection Agency, 2005b), five consecutive years (2005-2009) of meteorological data were collected and used in the AERMOD modeling. Two types of meteorological data were considered: surface observation data and upper air sounding data.

Surface observation data includes temperature, wind and cloud cover information collected at ground level. The surface observation data collected are 2005-2009 Integrated Surface Hourly Database (ISH/ISD/ISHD) measured at the Miami International Airport. Data were retrieved from NCDC (National Climatic Data Center) (ftp://ftp.ncdc.noaa.gov/pub/data/noaa) and are in TD-3505 format.

Upper air sounding data includes pressure, temperature, relative humidity and wind information at different elevations above ground. The 2005-2009 upper air sounding data were also collected at Miami International Airport station, and were retrieved from the NOAA/ESRL Radiosonde Database (http://www.esrl.noaa.gov/raobs/).

3.4.2. Receptor locations

For dispersion models such as AERMOD, a receptor is a user specified location where pollutant concentrations will be estimated. The receptors used in dispersion modeling consisted of two networks (Figure 3.17): a 5 km spaced network that covers all of Broward County and the upper part of Miami-Dade County, and a more densely distributed receptor network located near the modeled corridor. For the latter network

horizontal distances between receptors and the corridor were set to 100 m, 500 m, 1000 m, 2000 m, 3000 m, 4000 m and 5000 m, and vertical distances between the two rows of receptors are 500m.

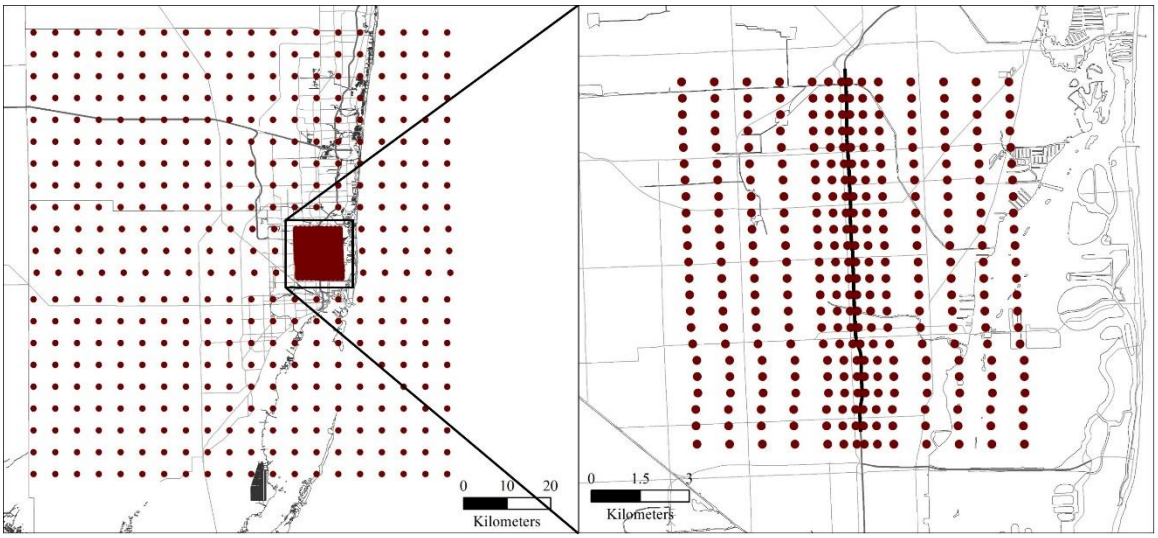

Figure 3.17 Receptors networks used in dispersion modeling.

3.4.3. Source Specification

The corridor was modeled as area sources (roadways are represented by rectangles) in AERMOD, and each link was modeled individually. Coordinates of all links were extracted from the CORSIM model and converted to UTM coordinates. The width of each area source was calculated by multiplying the number of lanes by the width of each lane. A maximum aspect ratio of 10 was applied to each source; a value of 10 is recommended by the USEPA (U.S. Environmental Protection Agency, 2004b) for dispersion modeling practices as sources with an aspect ratio larger than 10 may generate distorted and unrealistic concentration distributions near emission sources. Area sources were further split to ensure appropriate aspect ratios under 10.

Previously estimated pollutant emissions as described earlier were averaged to calculate seasonally and diurnally varied emission rates for each area source. Emission scaling factors were also estimated for each source and applied in the modeling.

3.4.4. Other Parameters

Other parameters including initial vertical dispersion parameter (σz) and surface characteristics were specified for the AERMOD model. The initial vertical dispersion parameter (σz) is used to represent initial mixing of the pollutants such as mechanically induced mixing on roadways (U.S. Environmental Protection Agency, 2004b). A value of 2 was assigned based on past literature (Venkatram et al., 2009). Surface characteristics including noontime albedo, Bowen ratio and surface roughness length are used to estimate boundary layer parameters, which are vital for pollutant dispersion. Noontime albedo refers to the percentage of incoming solar radiation that is being reflected by the ground at noontime. The Bowen ratio is defined as the ratio of upward sensible heat flux and latent heat flux and is an indicator of the moisture content at the surface. The surface roughness length is the height at which the wind speed is assumed to be zero to account for the effect of surface roughness. Ranges of the three parameters, as well as their selected values, are presented in Table 3.13. Values for each parameter were chosen based upon recommendations from previous literature (U.S. Environmental Protection Agency, 1999, 2004b).

Hourly pollutant concentrations were estimated for the three selected pollutants: benzene, CO and NO_x, from 2005 to 2009 for both the before and after scenarios. The highest and second highest 1 hour and 8 hour, as well as the annual average pollutant concentrations were calculated at each receptor.

Table 3.13 Ranges and chosen values of surface characteristics parameters

parameters	range	chosen value
albedo	0.1 (thick forests) - 0.65 (fresh snow)	0.16
Bowen ratio	0.1 (over water) - 10.0 (desert)	1
surface roughness length	0.01 m (calm water) - 1 m (forest or urban area)	1

3.4.5. Results of Dispersion Modeling

To evaluate the performance of the AERMOD model, the modeled highest 1 hour and 8 hour CO concentrations between 2005 and 2008 were compared with measured concentrations at the Annex monitoring station (Table 3.14), which is located in close proximity to the modeled corridor. The modeled highest 1 hour CO concentrations are close to the measured concentrations in all four years, however the modeled highest 8 hour CO concentrations are significantly lower than the measured values. As a primary pollutant with substantial mobile source contributions, CO concentrations at short term temporal metrics such as 1 hour are expected to be impacted significantly by nearby traffic, especially at rush hours. For longer term pollutant concentrations, contributions from other emissions (not modeled by AERMOD) are expected to be important. This may help explain why the modeled highest 1 hour CO concentrations are close to measured values but the modeled highest 8 hour CO concentrations are somewhat lower. Overall, performance of the AERMOD model is considered reasonable.

Table 3.14 Comparisons between the modeled and measured highest 1-hour and highest 8 hour CO concentrations at Annex monitoring station. Measured concentrations are shown within parentheses.

	modeled and measured CO concentrations (μg/m3)			
	2005	2006	2007	2008
highest 1 hour	627 (725)	581 (575)	478 (437)	378 (322)
highest 8 hour	137 (288)	150 (230)	99 (242)	106 (242)

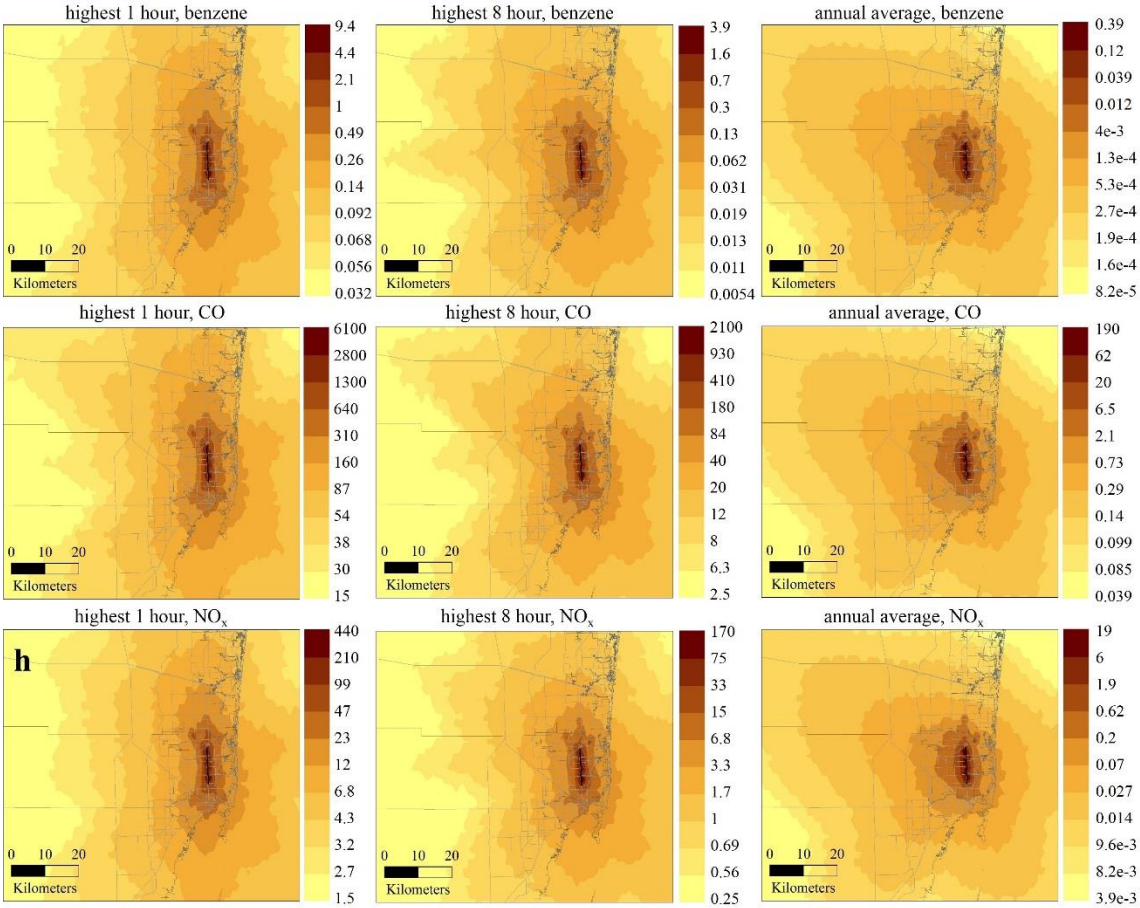

Figure 3.18. Modeled spatial distributions of the highest 1 hour, highest 8 hour and annual average (across all five years) concentration distributions for benzene, CO and NO_x in the before scenario.

Figure 3.18 shows examples of the modeled spatial distribution of pollutant concentrations. Concentration plots shown in the figure include the highest 1 hour, highest 8 hour and annual average (across all five years) concentration distributions for benzene, CO and NOx. Spatial distributions are similar for each of the modeled concentrations, with higher concentrations found near the modeled corridor and decreasing concentrations corresponding to increasing distances from the corridor. Concentration distributions in the after scenarios are similar and hence are not shown here. Additionally, Figure 3.19 provides the trends of domain averaged pollutant concentrations of the three selected pollutants from 2005 to 2009. The domain averaged

pollutant concentrations show a steady decrease from 2005 to 2008, but a slight increase in 2009. Meteorological conditions in 2009, specifically a larger number of hours with calm winds, may be responsible for the observed concentration increase here.

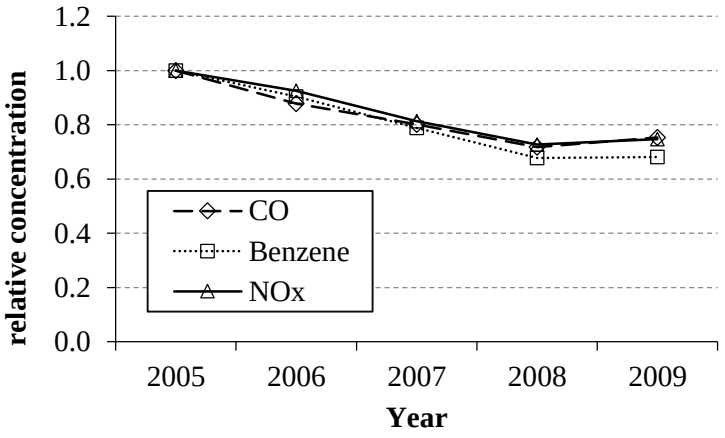

Figure 3.19. Trends of the domain averaged pollutant concentrations from 2005 to 2009. All concentration values shown are normalized to concentration values in 2005.

Changes in pollutant concentrations after implementation of the high-occupancy toll lane project are shown in Figure 3.20. Throughout the majority of the modeling domain pollutant concentrations are seen to increase slightly when the project is in place. Decreased concentrations were observed only at the northern end of the corridor. Spatial re-distribution of pollutant emissions as a result of changing vehicle mileage travelled may be responsible for the observed concentration decrease in this region.

Table 3.15 provides a summary of the estimated pollutant concentrations for both the before and after scenarios. The modeled concentrations of CO (both 1 hour and 8 hour average) are below regulatory standards for corresponding times. Note that regulatory standards are available for NO_2 but not for NO_x. Assuming standard temperature and atmospheric pressure, the national ambient air quality standards for NO_2 are equivalent to 100 and 188 $\mu g/m^3$ at annual and 1 hour averaging time respectively. In

both the before and after scenarios the modeled annual average NO_x concentrations are below the converted annual average NO_2 concentration standards, but the modeled maximum 1 hour NO_x concentrations exceed the corresponding NO_2 standard. The fraction of NO_x that is NO_2 varies substantially, hence the observed exceedance does not necessarily imply regulatory non-attainment.

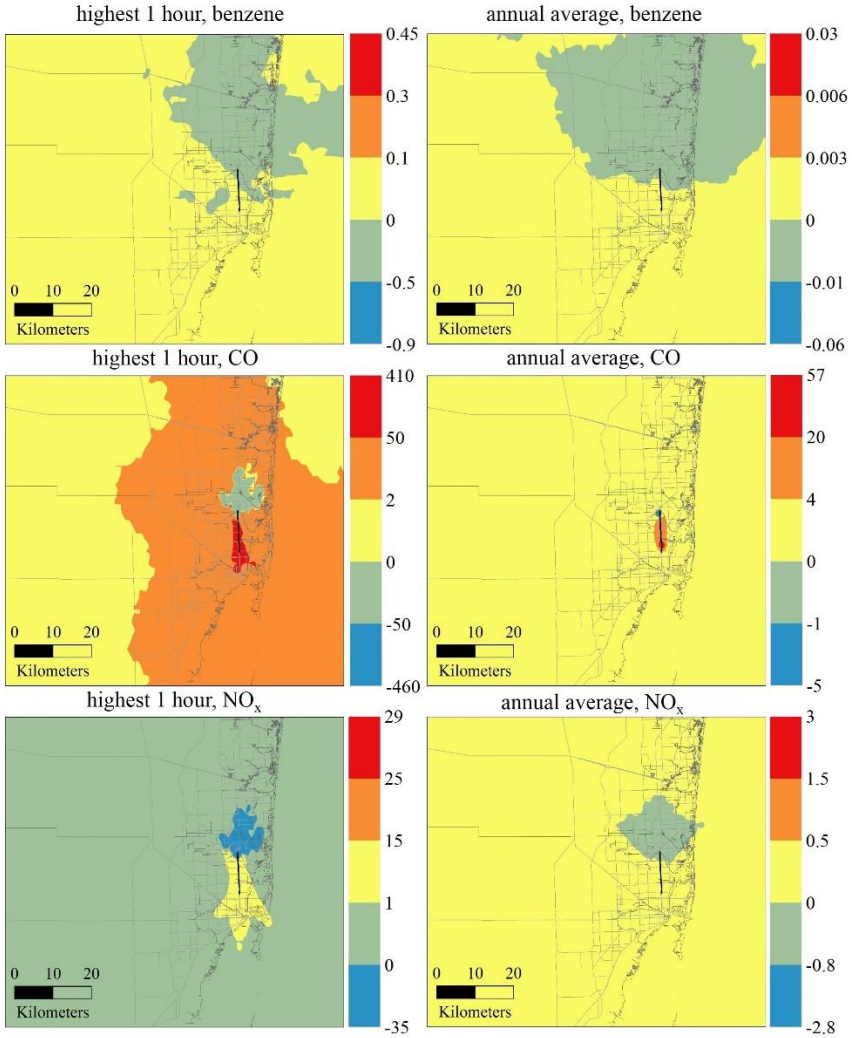

Figure 3.20 Changes in pollutant concentrations (after-before) after implementation of the high-occupancy toll lane project.

Table 3.16 provides the changes in domain average pollutant concentrations after implementation of the high-occupancy toll lane project. The highest 1 hour and annual average pollutant concentrations increase slightly in the after scenario compared to the

before scenario. The highest 8 hour CO and NO_x concentrations also increase, but a decrease is seen for benzene.

Table 3.15 Summaries of the modeled benzene, CO and NO_x concentrations for both before and after scenario. Modeled pollutant concentrations in the after scenario are shown within parentheses.

	concentrations ($\mu g/m^3$)			
pollutant	NAAQS levels	highest 1 hour	highest 8 hour	annual average
benzene	not applicable	0.03 – 9.4 (0.03 – 9.3)	0.005 – 3.9 (0.005 – 3.7)	8.0e-5 – 0.4 (8.0e-5 – 0.4)
CO	40,000 (highest 1 hour)	15 – 6100 (15 - 6200)	3 - 2,100 (3 – 2,100)	0.04 - 200 (0.05 - 230)
	10,000 (highest 8 hour)			
NO_x	not applicable*	1.5 - 440 (1.5 - 450)	0.3 - 170 (0.3 - 168)	0.004 - 19 (0.004 - 19)

* National Ambient Air Quality Standards for NO_2 are equivalent to 100 and 188 $\mu g/m^3$, at annual and 1 hour averaging time

Table 3.16 Changes in domain average pollutant concentrations after implementation of the high-occupancy toll lane project.

	concentrations ($\mu g/m^3$)		
pollutant	highest1-hour	highest 8-hour	annual average
benzene	0.0006	-0.0013	0.0001
CO	18	4.9	3.1
NO_x	1.1	0.27	0.033

3.4.6. Discussion of Dispersion Modeling

The chosen pollutants included in dispersion modeling are largely inert and only on-road mobile source emissions from the corridor were included. Hence pollutant concentrations are expected to be higher near the corridor, as shown in Figure 3.18. In addition, results of emission estimation show slightly increase for benzene, CO and NO_x emissions, and therefore generally increased pollutant concentrations are expected in the after scenario.

Implementation of the high occupancy toll lane project also leads to spatial re-distribution of the vehicle mileage travelled. At the northern end of the corridor, vehicle mileage travelled was reduced and shifted toward the south, resulting in lower pollutant emissions here which in turn leads to lower pollutant concentrations nearby in the after scenario.

3.4.7. Limitations and Uncertainties in Dispersion Modeling

It would seem that pollutant emissions from the corridor impact the results of dispersion modeling and contribute most to the inherent level of uncertainty. In addition, the model selection may lead to further uncertainties. Specifically, the chosen AERMOD model is a steady-state Gaussian plume model and lacks the ability to characterize spatially varying meteorological conditions which may ultimately impact the modeling results.

Buildings also impact pollutant concentrations in surrounding areas by interfering with or inhibiting pollutant transport. Most of the buildings near the study corridor are low in height, but some high-rise buildings, especially those located in extensively urbanized areas such as along Miami Beach, could impact pollutant concentration distributions nearby.

3.4.8. Summary of Dispersion Modeling Findings

The impact of the corridor on air quality before and after the implementation of the managed lane project was estimated using the Gaussian dispersion model AERMOD. Changes in pollutant concentrations of benzene, CO and NO_x were estimated. Comparisons between the modeled and measured CO concentrations at the Annex monitoring stations suggest reasonable model performance. The modeled CO

concentrations are substantially lower than the regulatory concentrations established in the National Ambient Air Quality Standard. Regarding the spatial distribution of pollutants, higher concentrations were found near roadways, with decreasing concentrations corresponding to increasing distance from the corridor. For the majority of the modeling domain a slight increase in pollutant concentrations was found after implementation of the high-occupancy toll lane project. Contrarily, at the northern end of the corridor, concentration decreases were observed. Spatial re-distribution of pollutant emissions is likely to be responsible for such decrease.

Overall the high-occupancy toll lane project appeared to lead to increased pollutant concentrations across the majority of the modeling domain and decreased concentrations at northern end of the corridor, although the magnitude of the concentration changes was relatively small. It needs to be noted that emission estimation contributes most significantly to the uncertainties prevalent in dispersion modeling.

3.5. Conclusion On the Air Quality Impact of the I-95 Managed Lane Project

On-road mobile sources are major contributors to air pollutant emissions. Transportation projects may substantially influence traffic patterns and hence may consequently impact on-road mobile source emissions, as well as air quality nearby. Here air quality impacts of the "95 Express" managed high-occupancy toll lane project (Phases 1A and 1B) were assessed. First, ten years (2000-2009) worth of data on pollutant concentrations for four criteria air pollutants (CO, NO_2, PM (PM_{10} and $PM_{2.5}$) and O_3) and three mobile source air toxics (1,3-butadiene, acetaldehyde and benzene) alongside the air quality index were collected for Broward and Miami-Dade County, where the project was implemented. The collected data were compiled and multi-year trends of the

pollutant concentrations were analyzed. Following this, pollutant emissions from the corridor were estimated for five selected pollutants: CO, NO_x, PM_{10}, benzene and HC by combining outputs from a traffic micro-simulation model CORSIM (CORridor-microscopic SIMulation) with emission factors estimated by the MOBILE6.2 model. Dispersion modeling was then performed using the AERMOD model to estimate pollutant concentrations in the study domain due to emissions from the corridor, for periods both before and after implementation of the project. Changes in pollutant concentrations, as well the spatial distribution of these concentrations, were evaluated.

The collected pollutant concentration data from regulatory monitoring stations show that the measured ambient concentration levels of CO and PM_{10} in the two counties are below the values established by the National Ambient Air Quality Standards. In some years the highest 1 hour NO_2, fourth highest 8 hour O_3, as well as 98^{th} percentile of 24 hour $PM_{2.5}$ concentrations were seen to exceed their corresponding standards slightly. From 2000 to 2009, declining trends were observed for concentrations of CO, NO_2, and 1,3-butadiene in the two counties, and benzene in Broward County only. No clear trend can be observed for the other pollutants. Regarding the air quality index, values of the index suggest slightly better air quality in Miami-Dade than Broward County (regarding criteria air pollutants). In both counties, only a very small number of days from 2000 to 2009 can be categorized into index levels lower than “moderate”.

The estimated on-road mobile source emissions from the corridor show increased emission increases for CO, NO_x, PM_{10} and benzene, but decreased for HCs, after implementation of the high-occupancy toll lane project. Emissions from buses consistently decrease for all pollutants. Change in total vehicle mileage travelled, as well

as changes in emission factors, contribute to the observed emission changes. However, it needs to be mentioned that substantial uncertainties were involved in emission estimation. Mostly from vehicle mileage travelled data estimated by CORSIM model and emission factors estimated by MOBILE6.2 model

Dispersion modeling was then performed for benzene, CO and NO_x to estimate pollutant concentration levels in the study domain, which were attributable to emissions from the corridor, for the periods both before and after implementation of the project. Results show slightly increased pollutant concentrations within the majority of the study domain as the result of the project. Concentration decreases were observed at the northern end of the corridor which was assumed to be due to the re-distribution of pollutant emissions. Overall, the results suggest no substantial impact of the managed lane project on air quality nearby.

Finally, this study also demonstrates that although changes in transportation infrastructures could lead to improved performance in terms of higher vehicle travelling speed and reduced congestion and travelling time, the improved performance does not necessarily result in less on-road mobile source emissions. Rather, these are determined by vehicle mileage travelled as well as the relationships between vehicle speed and emissions.

CHAPTER 4

SPATIOTEMPORAL DISTRIBUTIONS OF AMBIENT OXIDES OF NITROGEN, RESIDENTIAL EXPOSURES, AND EXPOSURE INEQUALITY IN THE TAMPA AREA

Note: This is an Author's Original Manuscript of an article whose final and definitive form, the Version of Record, has been published in the Journal of the Air and Waste Management Association [2013] [copyright Taylor & Francis], available online at: http://www.tandfonline.com/[10.1080/10962247.2013.800168]

4.1. Introduction

Eliminating inequalities in exposures and impacts of air pollutants is a goal in fields from public health and air quality management, to transportation engineering and urban planning (National Research Council, 2004; U.S. Department of Transportation, 1997; US Department of Health and Human Services, 2000). Air pollution in urban areas has important health impacts (Cohen et al., 2004), particularly for children (American Academy of Pediatrics Committee on Environmental Health, 2004). Previous work indicates that exposures and impacts are disproportionate for some disadvantaged population groups, including blacks, Hispanics, and low-income earners (Payne-Sturges & Gee, 2006; Perlin et al., 1999). Recent work has begun to recognize the effects of urban design on emissions (Stone et al., 2007), exposure (Hixson et al., 2010; Schweitzer

& Zhou, 2010), and subgroup inequalities (Frumkin et al., 2004). However, the strength and shape of the relationships between urban form, air quality, and environmental inequality is poorly understood, but both appear to differ by pollutant type (Marshall, 2008) and scale of study (Buzzelli & Jerrett, 2007).

To better understand the complexity involved, there is a need to characterize distributions of urban air pollutants at high spatial resolution and for multiple temporal scales. The relative contributions of different source types to exposures are also needed. Mechanistic air quality modeling is one useful method for estimation at multiple spatial and temporal scales. However, methods for estimating concentrations and evaluating model performance at high resolution, while limiting computational burden, still need further development.

The work described here is part of a study of concentrations of several urban air pollutants in the Tampa area, using both measurement and modeling (Evans & Stuart, 2009; Fridh & Stuart, 2012; Stuart et al., 2009; Stuart & Zeager, 2011). Here, we discuss the development and initial application of a modeling system used to estimate spatially-resolved NO_x distributions and to study impacts of spatial and temporal variability in concentrations on inequalities in exposure. Estimates of concentration and ambient residential exposure are presented. Model performance as a function of temporal scale is explored. Finally, we discuss results and implications for social inequality and urban design in the study area and beyond.

4.2. Study Area and Scope

The study area of Hillsborough County Florida, where Tampa is located, is shown in Figure 4.1. Tampa is part of a fast growing metropolitan region on the west coast of

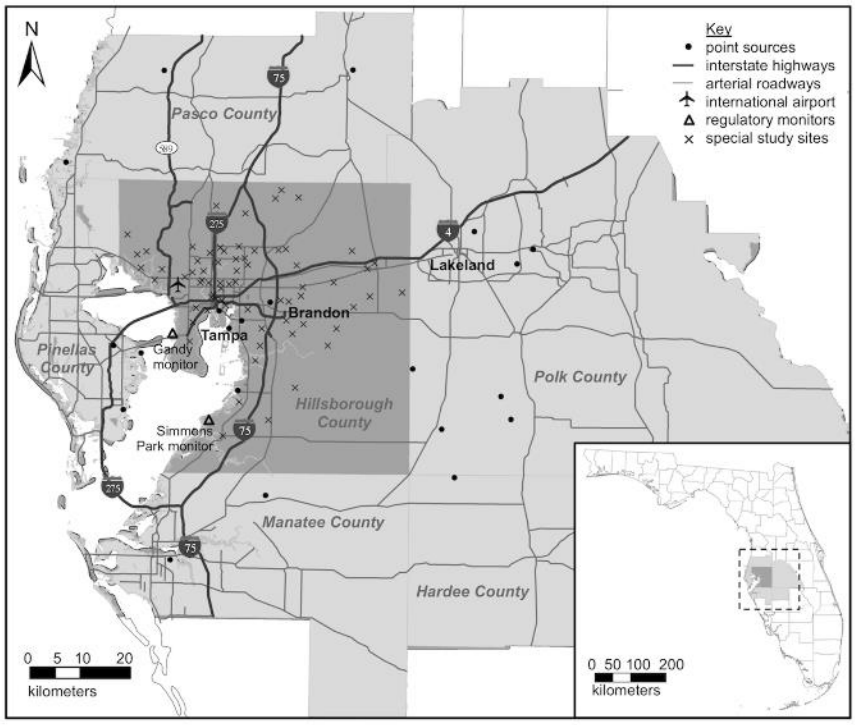

Figure 4.1 The study area (Hillsborough County) and the five surrounding counties in the emissions domain, including source and monitoring locations for NO_x. The inset provides the study area in the context of the state of Florida. The dashed line box outlines the meteorological domain. Sources: county boundary and roadway GIS shapefiles (Florida Department of Transportation); point source coordinates (2002 National Emissions Inventory); monitor coordinates (US Environmental Protection Agency Air Quality System Data Mart).

Florida with a variety of air pollution sources and a diverse residential population (Stuart et al., 2009). A focus on the county, rather than the metropolitan area, allows a large mix of land uses for study of social inequality and urban design. We chose oxides of nitrogen (NO_x) as the focus pollutant here because it is a common urban pollutant and has detailed evaluation data available, including data from our previous measurement study (Stuart & Zeager, 2011). Further, NO_2 , a component of NO_x, is used as a surrogate for the complex mix of traffic pollution in health outcomes analyses (HEI Panel on the Health Effects of Traffic-Related Air Pollution, 2010). It also has established National Ambient Air Quality Standards (NAAQS), and has been associated with respiratory responses for susceptible individuals, particularly children, even at levels below the

NAAQS (U.S. Environmental Protection Agency, 2008a). Due to the availability of emissions data from the US National Emissions Inventory for a time frame comparable to detailed US census data (from 2000), we chose 2002 as a baseline study year to represent near current era effects.

4.3. Methods

4.3.1. Estimation of NO_x Emissions

On-road mobile sources and stationary point sources for Hillsborough County and five surrounding counties (see Figure 4.1) were modeled here. Estimation methods are provided below.

4.3.1.1. On-road Mobile Sources

Two approaches are generally used to estimate on-road mobile source emissions, bottom-up and top-down approaches (Cook et al., 2006). In a bottom-up approach, emissions from roadway links are estimated from traffic activity data. Generation of high-resolution emissions is data intensive and computationally cumbersome for large roadway networks. M. Hatzopoulou and Miller (2010) applied a bottom-up method for the Greater Toronto area, but her temporal modeling domain was limited by the large number of sources. In a top-down approach, the domain is split into spatial zones, with total domain emissions allocated using spatial surrogates (such as population density or roadway density). The top-down approach requires less input data and fewer computational resources, but introduces error associated with the surrogate. Kinnee et al. (2004) developed a hybrid method; a bottom-up approach was applied for major interstates and a top-down method was applied for the remaining roadways. However, Kinnee's method used sources with large aspect ratios (some over 100), which exceeds

that recommended (10) in dispersion model guidance (see e.g. U.S. Environmental Protection Agency (2004b)). Here, we developed and applied a method that builds on the above approaches.

Roadway data, including locations, attributes, and annual average daily traffic counts were extracted from Florida Department of Transportation files (Florida Department Of Transportation, 2002). Available link attributes include traffic count, roadway function class, maximum speed, number of lanes, and median width. Roadways in Hillsborough County were categorized into two classes, those with traffic count data (called major roads here) and those without (minor roads). This results in a similar classification to that of primary roadways, defined by the Census Bureau (census feature class codes between A10 and A28) (U.S. Census Bureau, 2010). A bottom-up approach was used to estimate emissions from major roads; a top-down approach was used for the remaining on-road mobile emissions.

Hourly running emissions for major roadway links (E_M in g per hr), were calculated as:

$$E_{M,hl} = A_{hl} L_l F_{hl}$$

where A_{hl} is the estimated hourly traffic count for hour h and link l (vehicles per hr), L_l is the length of link l (miles), and F_{hl} is the emissions factor (g per vehicle mile). Hourly traffic counts on each link were estimated by summing the average daily traffic counts for each link over the year (i.e. multiplying by 365 days) and then distributing the annual traffic count to each hour of the year using aggregate profiles of the annual (varying by month) and diurnal (varying by hour) cycle of traffic for the county; annual and diurnal profiles were derived from hourly data at all county traffic counting sites. Emission

factors were estimated using the MOBILE6.2 model, using default vehicle distributions. 192 emission factors were calculated to account for differences by month and for all combinations of roadway function class and speed. Monthly fuel parameters, temperature, and humidity were extracted from the National Mobile Inventory Model County Database (U.S. Environmental Protection Agency, 2005a).

When aggregated, major roadway emissions accounted for 79% of the total county emissions from on-road mobile sources in the National Emissions Inventory. For the remaining emissions, a top-down estimation approach was applied. The remaining emissions in the county ($E_{R,T}$) were spatially allocated to a grid with 1 km resolution based on minor roadway density (Saide et al., 2009). Annual remaining emissions (E_R in g per yr) for each grid cell (j) were calculated as:

$$E_{R,j} = \frac{\sum_l L_{lj}}{\sum_j \sum_l L_{lj}} E_{R,t}$$

where L_{lj} is the length of each minor roadway link l in cell j. $E_{R,t}$ is the county total remaining emissions. Hourly emissions for each cell were estimated using the same profiles discussed above.

For the five surrounding counties in the emissions domain, a top-down method was applied for all on-road mobile source emissions. As high resolution is not needed outside the focus area, a 5 km resolution grid was used. Annual emissions (E_X in g per yr) in each external grid cell (k) were spatially allocated as:

$$E_{X,k} = \frac{\sum_l L_{P,lk}}{\sum_k \sum_l L_{P,lk}} E_{P,t} + \frac{\sum_l L_{O,lk}}{\sum_k \sum_l L_{O,lk}} E_{O,t}$$

where $L_{P,lk}$ is the length of each primary roadway link l in grid cell k, $L_{O,lk}$ is the length of each other roadway link, $E_{P,T}$ is total primary roadway emissions, and $E_{O,T}$ is total other

roadway emissions. The calculation was done on a county basis. The contribution of primary versus other roadways to total on-road mobile emissions in the National Emissions Inventory was assumed to be the same as for Hillsborough County (79% and 21%, respectively). We treat the two classes separately because primary roadways are expected to have more emissions. Hourly emission rates for each cell were estimated using the same temporal profiles discussed above.

4.3.1.2. Stationary Point Sources

Forty eight stationary point sources in the six county area were included. Together, they emit over 95% of point source emissions in the National Emissions Inventory for the area. Annual emission rates were taken directly from the inventory. Temporal allocation factors based on source classification code were applied to determine hourly emissions; factor profiles define variations by month, by day of the week, and by hour of the day (U.S. Environmental Protection Agency, 2007a).

4.3.2. Dispersion Modeling for Concentrations

To estimate the spatial distribution of NO_x concentrations in Hillsborough County, the CALPUFF dispersion model was used. CALPUFF is an established Gaussian puff model that represents the release, transport and dispersion of pollutants from multiple sources (Scire et al., 2000). CALPUFF is particularly useful under conditions where the steady-state assumptions of plume dispersion break down (U.S. Environmental Protection Agency, 2005b). Tampa is a coastal city with a complex and temporally varying wind field associated with the sea breeze. Methods used to model NO_x dispersion with CALPUFF are discussed below.

4.3.2.1. Source Parameters

Detailed source information, including geographic location and release parameters (e.g. release height, extent, temperatures, velocity), are required for dispersion modeling. Specific parameters used for each source type are described here; for all other parameters, we used the default values. Overall, hourly emissions and source parameters for 5200 major roadway link sources, 3000 grid-based area sources of other mobile emissions, and 48 stationary point sources were modeled.

For major roadway links, we used an area source representation with roadway links re-discretized to ensure a maximum aspect ratio of 10. The approach was based on recommendations in dispersion model guidance (see e.g. U.S. Environmental Protection Agency (2004b)) and sensitivity testing we performed to ensure applicability to CALPUFF. We calculated the area source width as the number of lanes multiplied by the lane width (assumed to be 3.65 m (Kinnee et al., 2004)) plus the median width (provided with the road data). For the other source parameters, we used an effective release height of 1.5 m, an effective rise velocity of 0.5 m/sec (Kalthoff et al., 2005), and an effective radius calculated by assuming area equivalence. For the effective release temperature, we used the diurnal cycle of monthly-average hourly ambient temperature in Hillsborough County from the National Mobile Inventory Model (U.S. Environmental Protection Agency, 2005a). The initial vertical dispersion length was treated as a calibration parameter. It was adjusted to obtain results (at a collocated receptor) comparable to the measured monthly means from a regulatory monitoring site (Gandy: 27°53'32" N, 82°32'19" W, one of the two NO_x monitoring sites in the county).

Ultimately, a value of 100 m was used for links located near downtown Tampa (approximately 12 km^2), and 30 m was used elsewhere.

Other roadway emissions (minor roadways in county and all on-road mobile sources in surrounding counties) were treated as gridded area sources, with dimension equal to those used to estimate emissions. Other parameters were set to the same values used for major roadways. For stationary sources, the required point-source data are tabulated in the National Emissions Inventory. A vertical momentum flux factor of one (Scire et al., 2000) was used.

4.3.2.2. Meteorological and Geophysical Data.

A full year (2002) of meteorological data with one hour temporal resolution and 4 km spatial resolution were used to drive CALPUFF. CALPUFF-ready meteorological (and geophysical) data for the domain were obtained in pre-processed form from VISTAS (Visibility Improvement State and Tribal Association of the Southeast). Details of the meteorological pre-processing from MM5 data are provided in (TRC Environmental, 2007). We performed no re-interpolation of the data. To capture re-circulation of pollutants due to the land-sea breeze in the area, we ran CALPUFF simulations with a meteorological domain that extended 60 km to each side of Hillsborough County (shown in Figure 4.1).

4.3.2.3. Model Execution and Post-Processing

Hourly ground-level concentrations were calculated for a 68 by 68 km^2 receptor grid with 1 km spatial resolution covering Hillsborough County plus two discrete receptors at the county measurement sites. NO_x was treated as a non-reactive tracer, with no deposition processes enabled. Temporal summary values at receptor sites were

calculated via post-processing. These included weekly and monthly averages, and annual cumulative distribution statistics. We used values on the receptor grid to generate spatial fields, and for spatial interpolation (using kriging in ArcGIS) to categorical fields (contours).

4.3.2.4. Model Evaluation.

Evaluation against two types of measurement data was performed. For evaluation of temporal performance, we compared model results with measurements at the two regulatory monitors in the county (Gandy and Simmons Park), which provide hourly-resolved data for the model year. For spatial evaluation, we compared modeled fields with data from a passive sampling field campaign that measured NO_2 at 75 locations in the county over one week in March 2008 (Stuart & Zeager, 2011). The location of all monitors using in the evaluation are provided in Figure 4.1.

4.3.3. Analysis of Exposures and Inequality

Modeled spatial distributions of NO_x were compared with that of residential block group data from the 2000 US census (Florida Geographic Data Library, 2012). We focused on population subgroups representing a few categories of race-ethnicity (black, Hispanic, white), economic status (annual income categories ranging from less than $20,000 to greater than $100,000), and age (less than 5, between 5 and 65, and greater than 65 years). Race-ethnicity and economic status have been associated with air pollution exposure inequalities (Mennis & Jordan, 2005), while young children and older adults are susceptible to effects of air pollution (Sacks et al., 2011). Exposure analyses were performed using three summary statistics of the cumulative temporal distribution of

hourly concentration (annual average, 98th percentile, and maximum), to represent chronic to acute exposures.

For each statistic, we assessed exposure inequalities between subgroups in three ways. First, we calculated a population-weighted average exposure (X) for each subgroup (i) as:

$$X_i = \sum_j \frac{C_j p_{ij}}{P_i}$$

where the concentration field was divided into discrete intervals with index j; for example, we used seven intervals with a 5 μg/m^3 increment for the annual average field. C_j is the midpoint value in interval j, p_{ij} is the population (number) of subgroup i residing in the spatial area of interval j, and P_i is the total population of subgroup i in the county. We calculated the p_{ij} from census data using ArcGIS tools to determine the overlapping areas for block groups with concentration intervals. Population-weighted subgroup exposures were then compared.

Second, we used the subgroup inequality index (Stuart et al., 2009) to explore trends in inequality as a function of concentration. The index (I) is defined as:

$$I_{i,j,c} = \log\left(\frac{p_{i,jc,} / P_{j,c}}{F_i}\right)$$

The term p_{ij} / P_j represents the fraction of the population living within an area j that is categorized as subgroup i. F_i is the fraction the subgroup comprises of the total county population. The index measures the degree to which a subgroup is disproportionately residing in a particular area compared to a larger whole (the county). Positive values indicate disproportionately high representation in the area. Stuart et al. (2009) provide discussion of the index applied to source proximity areas. Here, we measure inequalities

for concentration areas, by defining the area *j* as that with concentrations greater than cutoff value *j* (defined by a contour line).

Finally, to assess the statistical significance of disproportionate exposures and linear trends, we performed Cochran-Armitage trend testing. A test was performed on the population of each subgroup (and the remaining population in a concentration interval area) versus the concentration interval category level (with the midpoint as the score value). The null hypothesis is that there is no trend in subgroup population fraction with increasing concentration. SAS (version 9.3, SAS Institute Inc. (2011)) was used for statistical testing.

4.4. Results

4.4.1. Model Performance

Figure 4.2 shows box plots of the annual distribution of hourly concentration at each regulatory monitoring site, along with the summary statistics used for exposure analyses. The measured temporal distributions are represented well by the modeled values at both sites. A good match is seen for the central tendency statistics (annual median and mean), quartiles of the cumulative distribution, and for the 5^{th} and 95^{th} percentiles. The simulated annual average concentration at both monitoring sites is within 8% of the measured values. Model performance declines somewhat for the highest values. The simulated 98^{th} percentile values are within 1% and 30% of those measured, at the Gandy and Simmons sites, respectively. The percent differences for the maximum one-hour concentrations are 35% and 42%, respectively.

Although model results represent annual cumulative distribution statistics well, we do not expect to match the hour by hour concentrations, due to the stochastic nature of

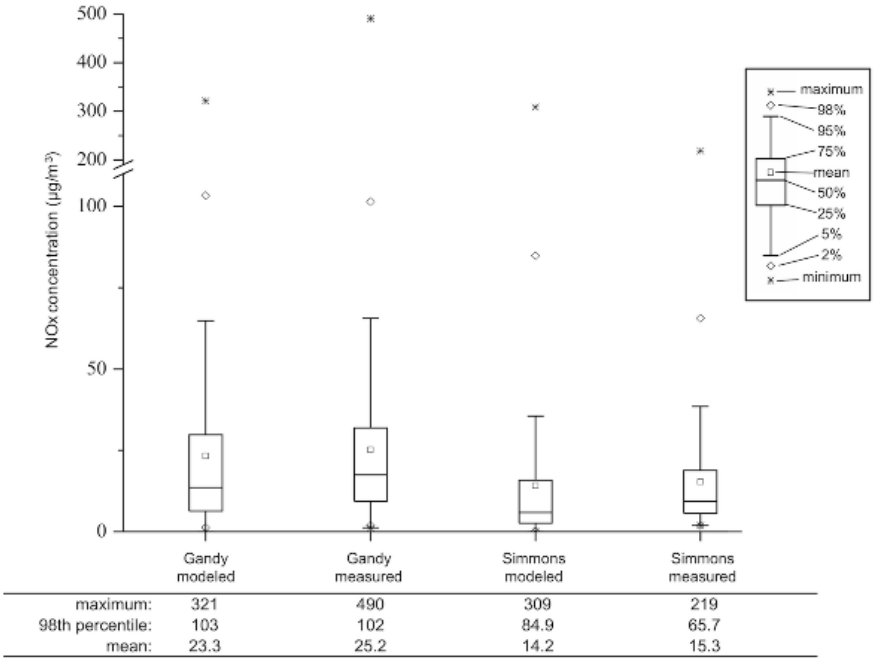

Figure 4.2 Cumulative distribution box plots of the measured and modeled hourly NO_x concentrations for year 2002 at the two regular monitoring sites in the county, Gandy (monitor ID: 12-057-1065-42602-1) and Simmons Park (12-057-0081-42602-1). Simmons was purely an evaluation site, while monthly average data at Gandy were used to calibrate the initial vertical dispersion parameter. Values for hours with no measurement data have been excluded.

the problem and uncertainties in the hourly allocation of emissions. However, we are interested in the limits of model performance at increased temporal resolution, as they inform use of temporal averages to estimate exposure. Figure 4.3 shows scatter plots of paired monthly and weekly averages of the modeled versus measured data. All modeled monthly averages are within a factor of two of the measured values, while 90% of the modeled weekly averages are within that factor, indicating reasonable model performance. U.S. Environmental Protection Agency (2009) discusses this and other model performance metrics). Table 4.1 provides additional metrics of performance for each averaging period. Results are consistent with degraded performance as the temporal resolution of the matching increases. Figure 4.4 shows a time series comparison for the weekly averages. The model follows many fluctuations of the measured values, but does

not capture the highest winter values. A histogram of residuals (not shown) indicates a relatively normal distribution, but with an extreme value for the highest measurement in January.

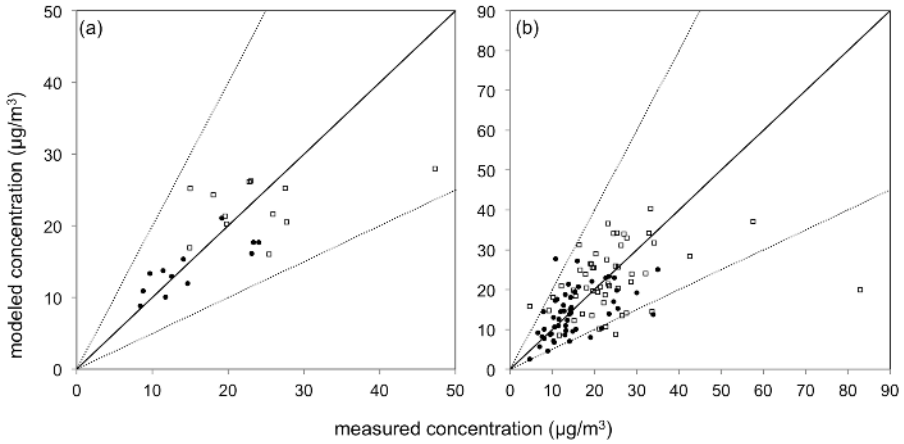

Figure 4.3 Modeled versus measured NO_x concentrations for average (a) monthly and (b) weekly values in 2002. The solid (1:1) line indicates a perfect match between measured and modeled values. The dotted (1:2 and 2:1) lines indicates a factor of 2 between the measured and modeled concentrations. Filled circles indicate Simmons Park data; open squares indicate Gandy data.

Table 4.1 Model performance as a function of temporal averaging period

evaluation statistic	averaging period	
	month	week
normalized bias (%)	1.0%	4.0%
bias ($\mu g/m^3$)	-1.1	-1.2
root mean squared error ($\mu g/m^3$)	6.0	9.7
absolute average gross error ($\mu g/m^3$)	4.4	6.3
residual standard deviation ($\mu g/m^3$)	5.9	9.6
Pearson correlation	0.70	0.51

Spatial performance is usually difficult to assess, due to lack of data at high spatial resolution. We compared the spatial footprint of modeled concentrations to measurement data from a previous NO_2 field campaign with measurement at 75 locations (shown in Figure 4.1). The comparison is not direct due to the mismatch in the temporal period (the data is for a one week average during spring 2008) and pollutant focus (NO_x

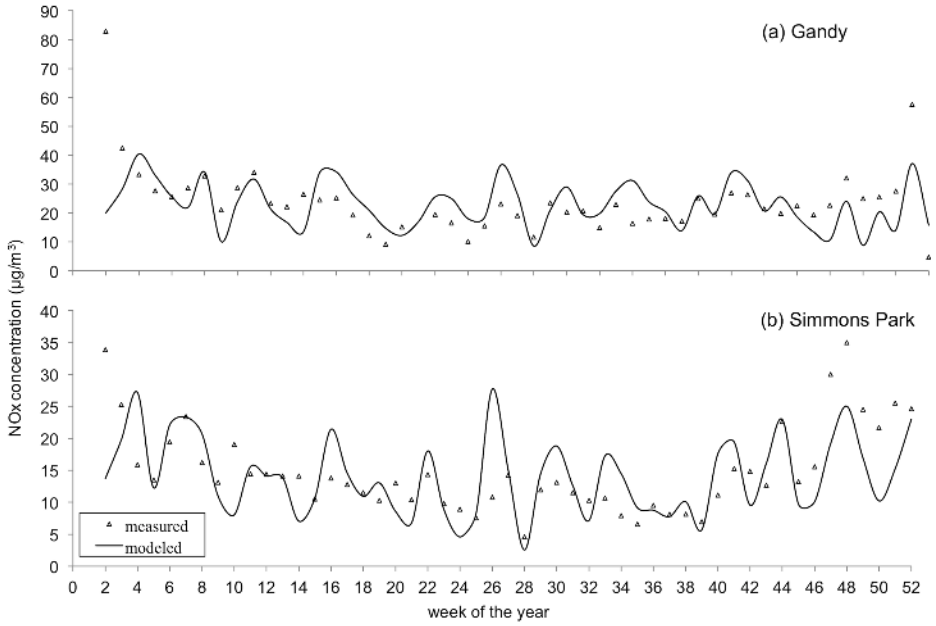

Figure 4.4. Trends of weekly average NO_x concentrations for the modeled and measured data in 2002. a) provides the comparison at the Gandy site, and b) provides the comparison at Simmons Park. Simmons was purely an evaluation site, while monthly average data at Gandy were used to calibrate the initial vertical dispersion parameter.

versus NO_2). Nonetheless, the same spatial pattern is qualitatively observable (see Stuart & Zeager (2011) for a measurement plot). Quantitatively, the Pearson correlation between measured and modeled values at the measurement locations was 0.72, 0.68, and 0.58, respectively, for each of the three temporal distribution statistics used for exposure analyses (annual, 98th percentile, and maximum). The model results capture a large proportion of the spatial variability measured during the field campaign, with better closure between modeled and measured data for the annual average.

4.4.2. Spatial Distributions of Concentration and Source Contributions

Table 4.2 provides spatial statistics for modeled NO_x in the study area. Annual average values varied by up to an order of magnitude between grid locations. Levels at all locations were below the annual average National Ambient Air Quality Standard (NAAQS) level for NO_2 (equivalent to 100 µg/m^3 at standard ambient temperature and

pressure), but the 98th percentile value exceeds the new hourly NAAQS for NO_2 (equal to188 $\mu g/m^3$) in a small area where ground-level point-source emissions are high. The fraction of NO_x that is NO_2 varies, but has been found to be about 0.8 on average in the Tampa area (Poor, 2008). Applying this fraction, we estimate that a few hourly NO_2 concentrations in 2002 in some areas may have been above the hourly NAAQS level. (Note that the hourly NO_2 NAAQS standard did not exist in 2002).

Table 4.2 Spatial statistics of NO_x concentration ($\mu g/m^3$) in 2002

spatial statistic	temporal statistic[a]		
	average	98th percentile	maximum
domain average	12	69	254
standard deviation	5	24	122
range	5 - 44	36 - 231	100 - 1591

[a]These refer to summary statistics of the annual distribution of hourly values in 2002.

Figure 4.5 provides the spatial distributions of annual average, 98th percentile, and maximum NO_x concentrations. All distributions have the general pattern of a highs focused primarily over central Tampa, where three major interstate highways converge, the roadway network is dense, and a few point sources are located. Overall, the spatial distributions are highly correlated. Pairwise Pearson correlations are 0.95 (annual average versus 98th percentile), 0.80 (98th percentile versus maximum), and 0.75 (annual average versus maximum). However, differences are also observed. The highest annual average concentrations are along the interstate highways, particularly near the Tampa International Airport, with local highs along other roadways visible. The spatial distributions of 98th percentile and maximum concentration also show local highs along

large roads and roadway intersections. However, the highest values are seen near to a few point sources near a major port facility (Port Sutton).

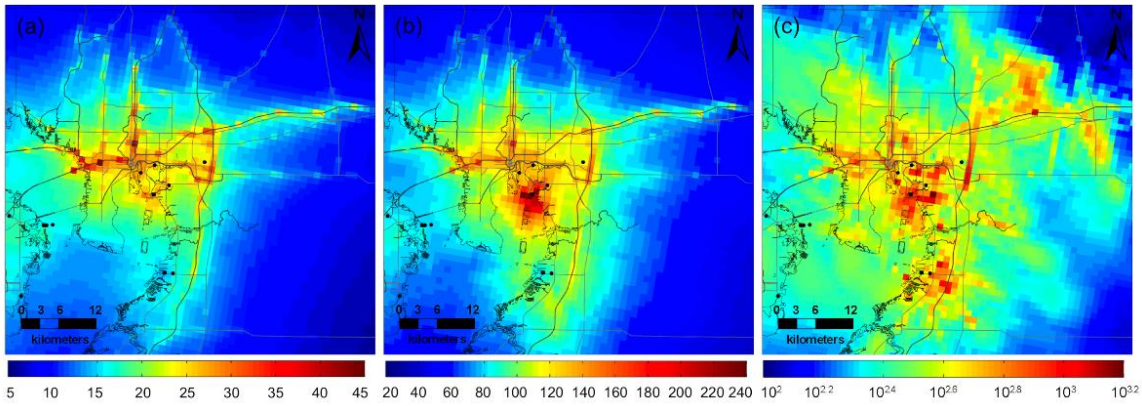

Figure 4.5 Modeled spatial distributions of NO_x concentration ($\mu g/m^3$) in Hillsborough County in 2002 for three statistics of the temporal distribution of hourly values, specifically (a) annual average, (b) 98th percentile and (c) maximum values. The resolution shown is that of the model output (1 km^2). Filled circles indicate point emission sources of NO_x, and major roadways are shown as black lines. Sources of mapping data are provided in the Figure 4.1 caption.

Table 4.3 Contributions of each source category to emissions and concentrations of NO_x in 2002

source category	emissions contribution	concentration contribution[b]		
		average	98th percentile	maximum
major roadways in the study area	12%	35%	31%	40%
minor roadways in the study area	3%	6%	5%	6%
external[a] on-road mobile sources	30%	22%	15%	13%
stationary point sources	55%	37%	49%	41%

[a]The term *external* refers to sources in the five counties surrounding Hillsborough County. [b]The average, 98th percentile, and maximum refer to summary statistics of the 2002 annual distribution of hourly concentrations for Hillsborough County.

Table 4.3 provides a summary of source contributions to emissions and concentrations. On-road mobile source emissions within Hillsborough County contributed 15% of the NO_x emissions in the six county area, however they contribute

41%, 36%, and 46% of the annual average, 98th percentile, and maximum concentrations, respectively. The contribution of in-county major roadways to annual average concentrations was approximately three times their contribution to emissions. The contribution of in-county minor roadways to concentrations was also greater (by two times) than that to emissions, but they only contribute a small fraction overall. Conversely, point sources throughout the domain contributed over half of the total emissions, but were only responsible for around 40% of the concentrations.

4.4.3. Average Exposures and Inequalities

Table 4.4 provides estimated population-weighted group average exposures to NO_x for racioethnic, income, and age subgroups. Among racioethnic groups, estimated average exposures for black residents were highest, followed by Hispanic residents. Whites had the lowest average exposures. Both the black and Hispanics subgroups had average exposures higher than the overall county average (12 - 15% and 3 - 6% higher, respectively), while the average exposure of white residents was slightly lower than the county average (2 - 3%). Qualitative differences were consistent for all temporal statistics of concentration studied (annual average, 98th percentile, and maximum). A similar inequality was found for income groups. Residents with annual incomes less than $20,000 had the highest average exposures. However, the average exposure for the lowest income subgroup was not as high as that for the black subgroup. (Note that any individual could be categorized in both these groups.) Average exposures decreased with increasing income, achieving the county average for income between $40,000 and $60,000. Average exposures for the highest income group (greater than $100,000) was 6% less than the county average. Differences by age were much smaller and largely

indistinguishable. However, residents older than 65 years had slightly higher than average exposures (0 - 2%).

Table 4.4 Estimated group-average exposure to NO_x for racioethnic, income, and age categories

population subgroup		group average exposure ($\mu g/m^3$)[a]		
		average	98th percentile	maximum
race or ethnicity	black	19.9	102	395
	Hispanic	18.2	94.5	356
	white	16.6	88.6	335
annual income (thousands of dollars)	less than $20	18.6	96.3	361
	$20 to $40	17.8	93.0	349
	$40 to $60	17.2	90.5	343
	$60 to $100	16.3	87.3	332
	more than $100	16.2	86.3	326
age (years)	more than 65	17.3	92.5	347
	less than 5	17.2	90.7	345
	5 to 65	17.2	90.6	344
county average		17.2	90.8	344

[a]Average, 98th percentile, and maximum refer to summary statistics of the 2002 annual distribution of hourly concentrations for Hillsborough County, from which exposures were estimated.

Figure 4.6 provides plots of the subgroup inequality index as a function of concentration. The index measures the degree of disproportionate representation of a subgroup in a defined area (defined here as the area with concentration exceeding a cutoff value). For annual average concentrations, index values are positive and increase as concentration increases for the black, Hispanic, and lowest income (less than $20,000) resident groups, as well as young children (less than 5 years). In areas with the highest concentrations (greater than 35 $\mu g/m^3$), the highest index value was observed for blacks; the value (0.5) indicates that the fraction of blacks living in these areas is approximately

three times ($10^{0.5}$) their fraction in the county overall. The fraction of the lowest income group in high concentration areas is approximately 2 times that in the county. For the age category, index values are very close to zero until the highest concentrations are reached (greater than 30 μg/m^3). For these high areas, children less than 5 years are overrepresented.

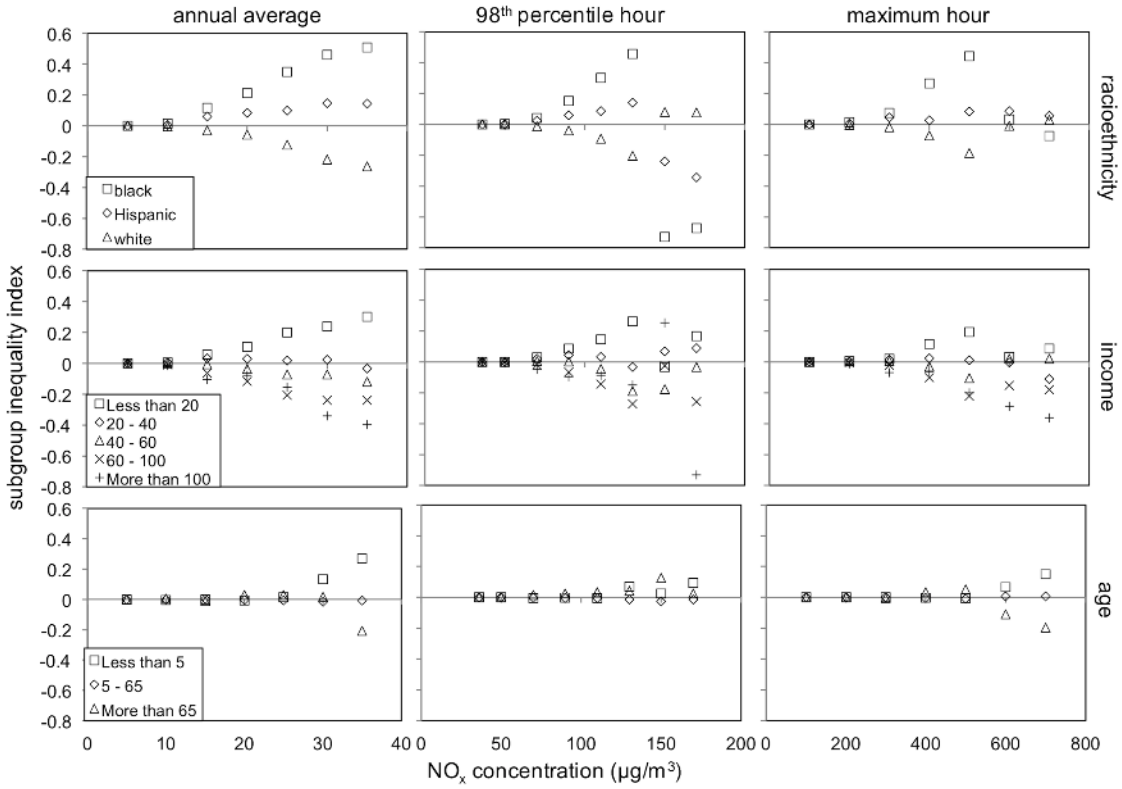

Figure 4.6 Estimated subgroup inequality index for selected populations as a function of NO_x concentration in 2002. The index is calculated as $I_{ij} = \log [(p_{ij} / P_j) / F_i]$. The term p_{ij} / P_j is the fraction of the population, P_j, living within the concentration area, j, that is categorized as subgroup i. F_i is the fraction of the total county population that is that subgroup. Marker location on the concentration axis indicates the lower limit concentration value (i.e. the contour line value) used to define area j for each index calculation. An index value of 0.3 means that the fraction of people who are that subgroup living where levels are greater than the concentration cutoff value is $10^{0.3}$ (or 2) times their fractional representation in the county. An index value of -0.3 indicates that the fraction is $10^{-0.3}$ (or 1/2) that in the county. Row headings provide the category of population subgroup studied. The column headings indicate the temporal distribution statistic used to quantify concentration. Income amounts are in units of thousands of dollars per year; age is in units of years.

Conversely, the index is negative and generally becomes more negative as the annual average concentration increases for the white and highest income groups. In areas with highest concentrations, the fraction of white and highest income (greater than $100,000) residents is only half and less than half, respectively, of their fraction in the county. The index value for residents aged older than 65 years is also negative for concentrations greater than 35 $\mu g/m^3$, but is slightly positive between 20 and 35 $\mu g/m^3$. The group average (over all concentrations, Table 4.3) remains higher than the county average due to larger total population numbers in this mid-range.

For the short-term concentration statistics (98^{th} percentile and maximum), the results are more variable than for annual averages. Trends in index value with increasing concentration are similar to those seen for the annual average, up until the highest two or three concentration levels. For these, the trend was often not monotonic and sometimes fluctuated between positive and negative values. Notably, the index value for blacks for the highest concentration hours (98^{th} percentile and maximum) was negative; i.e., this group was underrepresented in areas with the highest hourly values.

Results of Cochran-Armitage trend testing are shown in Table 4.5. Large negative test z-values support the alternative hypothesis of a statistically significant increasing linear trend in subgroup population fraction with increasing concentration for blacks and Hispanics, and a decreasing trend for whites. For income, results indicate an increase in population fraction with concentration for income categories less than $40,000, and a decrease for incomes over $40,000. Z-values for the age groups were small in magnitude, but indicate a slightly increasing trend for residents aged older than 65 years, and a decreasing trend for those ages 5 to 65 years. (Note that the test weighs

data from the lower concentration intervals more than from the high concentration intervals because there are may more people overall in the low intervals.) The trend test results were consistent irrespective of the concentration measure used (annual, 98th maximum) to define the concentration intervals.

Table 4.5 Cochran-Armitage trend test z statistic values

population subgroup		z-statistic value[a]		
		average	98th percentile	maximum
race or ethnicity	black	-206	-217	-210
	Hispanic	-85	-79	-56
	white	178	183	171
annual income (thousands of dollars)	less than $20	-76	-77	-55
	$20 to $40	-30	-30	-19
	$40 to $60	13	13	6.2
	$60 to $100	59	58	38
	more than $100	51	53	42
age (years)	more than 65	-8.9	-29	-7.7
	less than 5	*(0.3)*	*(1.3)*	*(-0.5)*
	5 to 65	7.2	23	6.7

[a]Values in parentheses were not statistically significant (p-value greater than 0.05). All others values had p-values less than 0.0001. Average, 98th percentile, and maximum refer to summary statistics of the 2002 annual distribution of hourly concentrations for Hillsborough County.

4.5. Discussion

4.5.1. Inequalities in Exposure to Air Pollution

This study extends our previous work using complementary methods (Evans & Stuart, 2009; Fridh & Stuart, 2012; Stuart et al., 2009; Stuart & Zeager, 2011) on air pollution concentrations, exposures, and exposure inequality in the Tampa area. Here, we contribute results based on highly-resolved estimates of NO_x concentrations through use of dispersion modeling. The results provide evidence for disproportionately high

residential exposures to NO_x (and potentially other traffic-related pollutants) for the black, Hispanic and low income population subgroups, particularly for chronic exposures. For the long-term (annual) average concentration, we found inequalities that persist across concentration levels (and hence sub-county spatial scales). Inequalities were also apparent across the temporal statistics considered (representing chronic to acute exposures). However, for the short-term measures (98th percentile and maximum concentration), inequalities varied substantially and even reversed at the highest concentration levels. Inequalities between age groups were small and nonlinear with concentration. However, we did see suggestive evidence of disproportion exposure of young children to the highest concentrations. These results provide a unique examination of differences and consistency in disparties across multiple time scales and concentration levels.

4.5.2. Attribution of Concentrations and Effects to Emission Sources

One explanation for disproportionately high exposures of disadvantaged groups to urban pollution is the tendency of these groups to live (and attend schools) in close proximity to roads with high traffic volumes (Green et al., 2003). Studies have also found disproportionate contributions to ambient concentrations from on-road mobile sources (Leksmono et al., 2006), and from area sources generally (Irwin & Brown, 1985). Our results support disproportionate contributions from on-road mobile source emissions to NO_x across temporal scales. We found contributions of roads in the study area to concentrations to be two to three times greater than their contributions to emissions. The influence was greatest for the long-term (annual) average, but persisted across the temporal statistics studied. However, stationary sources also contribute to

concentrations, particularly for the short-term measures (98th percentile and maximum). Hence, both types of sources need to be well-characterized for intra-urban exposure estimation; a focus on roadway sources may be warranted for chronic exposures, while point sources cannot be neglected for acute exposures.

4.5.3. Differences in Spatial Concentration Distributions by Time Scale

Many studies have modeled spatial distributions of air pollution and applied the results for exposure estimation (Jerrett et al., 2005). Differences in spatial distributions for distinct time scales are seldom discussed. Here, the spatial fields of NO_x were correlated for the three temporal statistics studied (annual average, 98^{th} percentile, and maximum), but differences were apparent. A roadway dominated pattern (highs surrounding roads) was clear, particularly for the annual average, but highs near point sources emerge for the high hour fields. Hence, the temporal statistic selected for exposure and effects analyses may be important. As effects may be due to acute or chronic exposures (or both) (HEI Panel on the Health Effects of Traffic-Related Air Pollution, 2010), multiple temporal measures may be needed. Further, exposure estimation methods that explicitly resolve temporal variations are needed. Many approaches, such as proximity-based methods and land use regression, do not account well for temporal variations. Modeling used to represent short-term exposures should evaluate results for short-term measures. We were not able to fully capture the highest statistics of the measured cumulative frequency distribution (98^{th} percentile and maximum). However, the 95^{th} percentile values, and weekly and monthly averages, were represented quite well. Further, this work demonstrates the importance of considering the stochastic nature of concentrations, by assessing concentrations and exposures in a

probabilistic manner (e.g. using cumulative distribution statistics). However, more work is needed to develop and evaluate methods that represent exposures for multiple time scales.

4.5.4. Implications for Urban Design

Past studies suggest that compact urban form with mixed land-use may reduce on-road mobile emissions when compared with sprawl growth (Kahyaoğlu-Koračin et al., 2009; Stone et al., 2007). Reductions in emissions may not necessarily reduce human exposure (Schweitzer & Zhou, 2010) or exposure inequality. Results here suggest that co-location of populations and concentrations is complex and changes with temporal scale. However, results are consistent with the current focus on mobile sources emissions, particularly for long-term exposures. Policies that remove motor-vehicle emissions from areas where people, particularly blacks and low income earners, live and spend time are suggested. These could include avoiding high density populations for new road construction (Chakraborty, 2009), promotion of electric vehicles for urban core use (including for public transit), and promotion of the human-powered travel modes (biking and walking). However, motor vehicle emissions nearby must also decrease as these modes increase; otherwise, activity exposures and exposure inequality may increase.

4.5.5. Limitations

One of the largest sources of uncertainty in air pollution modeling is emissions information. To model spatiotemporal distributions of concentration, detailed assignment of traffic activity is needed. We applied scaling profiles for the annual and diurnal cycles, derived from aggregated local traffic count data, to estimate hourly emissions. This approach does not represent all variability, particularly differences between

weekdays and weekends (e.g. Fujita et al. (2003)), and between roadways. Travel demand modeling may be an improved approach for spatiotemporal allocation of traffic activity (Hatzopoulou & Miller, 2010). Nonetheless, our evaluation suggests that we have represented temporal variations reasonably down to weekly resolution. We also capture up to the 95th percentile summary statistic of the cumulative distribution of hourly values well, with somewhat degraded performance for the highest hour values (98th percentile and maximum). Hence, exposure results based on the high hour values are less certain than those based on the annual average, and should be viewed primarily as illustrative of potential differences in patterns.

Emission factors also provide a source of error. We disaggregated emission factors by month (representing changes in meteorology and fuel parameters), roadway function class, and speed category. Dependence on speed is a known source of error as the relationship between emissions and speed is largely empirically derived (Brzezinski et al., 2001). Further, we used maximum speeds due to data availability. Bai et al. (2007) suggested a speed adjustment based on traffic volume, which was not applied here. Additionally, local deviations from default county distributions of vehicle type and age can impact emissions factors (Lindhjem et al., 2012). Finally, we used MOBILE6.2 rather than the MOVES estimator, which has replaced MOBILE6.2 since this work began. In a recent study of two metropolitan areas, Lindhjem et al. (2012) found differences in NO_x emissions estimated using MOVES versus MOBILE6. More inter-comparison work is needed to fully evaluate the differences and their general implications.

Other sources of error are the spatial allocation of other roadway emissions, source parameters, and missing emission sources. Spatial allocation of minor road emissions (and other vehicle emission such as hot soak and cold start emissions) was based on minor roadway density, one of a few possible surrogates (e.g. Saide et al. (2009)). The surrogate choice is not expected to impact concentrations much, as these emissions are small. However, allocation of emissions to 1x1 km^2 grid cells could dilute their modeled contribution. Results may also be limited by missing sources. Exclusion is due to lack of data (for sources missed by the national inventory) or modeling tractability (for diffuse and minor sources). Together, the emissions included here account for 76% of the total NO_x emissions in the 2002 National Emission Inventory for the domain. Due to the likely small magnitude of missing sources, we do not expect substantial impacts on concentrations or exposures; however, impacts cannot by ruled out.

Dispersion modeling assumptions and other types of data can also lead to uncertainties in concentration results. Meteorological data can be a source of error. We used a full year of data, and therefore expect high fidelity in the temporal representation. However, the data used have a spatial resolution of 4 km, which is limited for representing differences at 1 km resolution. Further, chemical reaction and deposition processes were not included. These processes are not expected to influence the high concentration areas near sources (due to time scales longer than that for dilution (Seinfeld & Pandis, 1997)), but exclusion could lead to overestimation of concentrations overall. Finally, the initial vertical dispersion length parameter for road link area sources is uncertain; it depends on many factors including traffic-induced turbulence and nearby structure heights (Rao et al., 1979; U.S. Environmental Protection Agency, 2004b).

Here, we use it as a calibration parameter; this improves model results, but limits their generalizability.

Uncertainties are also present in the exposure estimation. Accurate and precise estimation of personal exposures requires spatiotemporal matching of a person's location and the pollutant concentrations in their breathing zone. Ideally, this would include characterizing spatiotemporal population activity patterns and pollutant levels in non-ambient microenvironments (inside homes, schools, workplaces, vehicles, etc.). Although we are currently working on path-following exposure estimation (Gurram et al., 2012), we do not disaggregate these elements here. Instead, we use residential locations and ambient concentration to represent population location and exposure concentration, respectively. Furthermore, for subgroup exposures, we assume that demographic characteristics are homogeneously distributed within a census block group, due to the resolution of the census data. Temporally, we specifically consider multiple statistics of the concentration distribution, improving upon most current studies. Nonetheless, we are only simulating one year of data for both population residence location and concentrations. Both of these distributions change in time. Notably, emissions of NO_x from the 2008 National Emissions Inventory for Hillsborough County are 46% lower that in 2002. This same percentage decrease is seen in emissions estimates for the US as a whole between 2012 and 2002 (U.S. Environmental Protection Agency, 2012a). Hence, the exposures and their social distribution found here may not represent current or future exposures.

To study the social distribution of exposure, we used a few approaches. There are many methods and indices used to investigate inequality; several reviews on the subject

have been written (e.g. Levy et al. (2006)). The metrics used here allow us to compare exposures between groups and explore changes with concentration. However, we do not quantify the processes that lead to unequal outcomes or address the fairness of inequalities.

We note that this work characterizes NO_x concentrations and exposures in the Tampa area. Although NO_x has been used as a surrogate to represent the complex mix of primary pollution from traffic, results are not applicable to pollutants formed in the atmosphere (secondary pollutants), such as ozone. Further, results are specific to the Tampa area and the time period of the data used for estimation (early 2000s); they contribute a case study to the body of knowledge across localities and times.

4.6. Conclusions

We modeled NO_x concentrations in 2002 and estimated residential exposures for the Tampa area at high spatiotemporal resolution. Implications for social inequality and urban design were discussed. Contributions include the description of a hybrid approach for estimating link-level roadway emissions that allows characterization of concentrations at high spatiotemporal resolution while limiting computational resource needs. Differences in concentration fields, source contributions, exposures, and inequality across multiple temporal scales are presented. This focus is fairly novel, as many exposure methods do not explicitly consider time scale. Further, we present a detailed evaluation of model performance across temporal scales, adding knowledge on limitations and robustness of exposure estimation using dispersion modeling. Findings and conclusions suggested by this work are the following:

1. Spatial distributions of NO_x were highly correlated, but have differences, for the three statistics of the cumulative temporal distribution studied (maximum hour, 98^{th} percentile hour, and annual average).
2. Contributions of on-road mobile sources to ambient NO_x concentrations in 2002 were disproportionate to their emissions. Point sources contributions are also substantial; their influence is more evident for the high hour (maximum and 98th percentile) fields.
3. The black, lowest income (less than $20 K), and Hispanic subgroups were likely exposed to disproportionately high average NO_x at their residences. The white and the highest income (greater than $100K) subgroups were found to be disproportionately un-exposed.
4. Persistent exposure inequalities were found across temporal scales, with generally increasing inequalities as NO_x level increased. However, the relationship is complex; it reversed for the highest concentration hours for some groups (notably blacks).
5. Decreased overall emissions may not decrease population exposures or improve exposure equality. Urban planning should focus on designs, infrastructure, and policies that reduce on-road mobile source emissions in areas with high density of disadvantaged subgroups.

The methods and results presented here can be used for study of impacts of urban growth on health and to improve urban planning toward more equitable and sustainable design. Our current work is focused on applying and improving these methods to other

urban pollutants, particularly air toxics, for both near current era and potential future urban forms.

CHAPTER 5

EMISSIONS, CONCENTRATIONS, EXPOSURES, AND EXPOSURE INEQUALITY FOR MULTIPLE TRAFFIC-RELATED AIR POLLUTANTS IN THE TAMPA AREA

5.1. Introduction

Although NO_x is an established surrogate for multiple traffic-related air pollutants, we are also interested in investigating and comparing patterns of emissions, concentrations, and exposures for other select air toxic pollutants. Here we investigate four additional pollutants for the same study period: 1,3-butadiene, benzene, acetaldehyde and formaldehyde. These pollutants are among the 33 urban air toxics (UAT), which have been shown to significantly impact human health and public welfare in urban areas of the US (U.S. Environmental Protection Agency, 2008b). They are also mobile source air toxics (MSAT) (ENVIRON International Corporation, 2006) and have substantial mobile source contributions. Further, these four pollutants are all known human carcinogens (Agency for Toxic Substances and Disease Registry, 2007; National Toxicological Program, 2010, 2011), and long-term exposure to these pollutants may increase the risk of cancer. In addition, formaldehyde and acetaldehyde have substantial contributions from secondary formation in the atmosphere, while 1,3-butadiene and benzene are primary pollutants.

Furthermore, during the course of this study the MOBILE6.2 model for on-road mobile source emissions used in Chapter 4 was replaced by the Motor Vehicle Emission

Simulator (MOVES) model (U.S. environmental Protection Agency, 2010b). Hence, I re-estimated NOx emissions, concentrations, and exposures using the new model.

5.2. Overview of Method

Figure 5.1 illustrates an overview of the methods used to estimate air pollution exposure and exposure inequalities. First, emissions of the five selected pollutants were estimated for the study area. The estimated emissions were consequently applied to calculate spatiotemporal resolved pollutant concentrations, which were then combined with demographic data to estimate human exposure to air pollution and exposure distributions among chosen population subgroups. Details of each steps are presented separately in following sections.

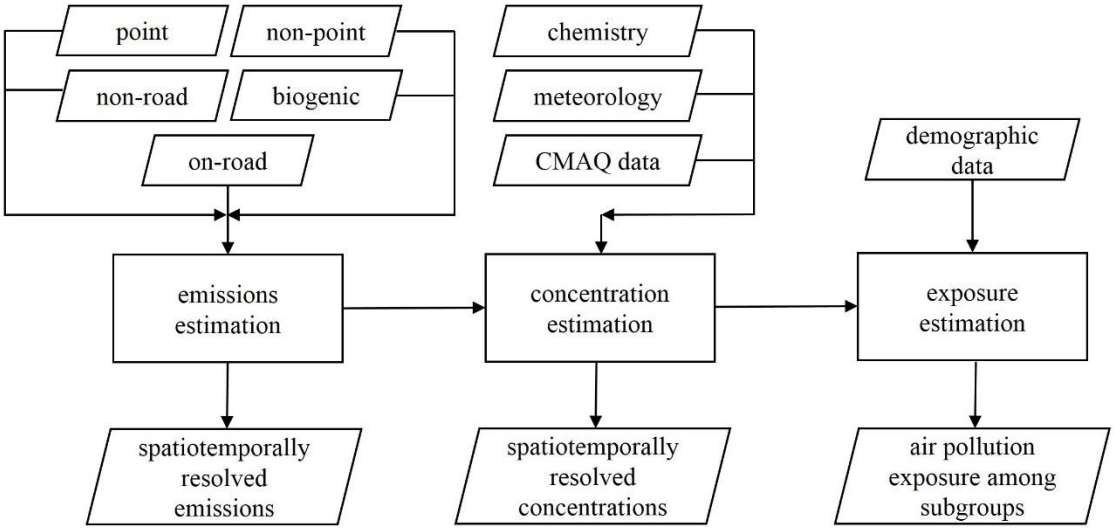

Figure 5.1 Overview of the methods

5.3. Emission Estimation

Emissions of the five selected pollutants were estimated for the Tampa area. Five emission categories were included in emission estimation: stationary point, on-road mobile, non-road mobile, non-point and biogenic emissions. Methods and results for each of the emission categories were provided below.

5.3.1. Methods of Emission Estimation

The study area here is similar as in Chapter 4. Pollutant emissions within Hillsborough County, where Tampa is located, as well as 50 km outside the county, were included. 50 km is a commonly recognized distance beyond which the impacts of directly emitted pollutants are expected to be small. Location of the domain for emissions estimation is shown in Figure 5.2. Size of the domain is 160 km by 160 km. Emissions from 12 counties within the emission domain were included in emission estimation. Estimation methods for each of the emission category are described below.

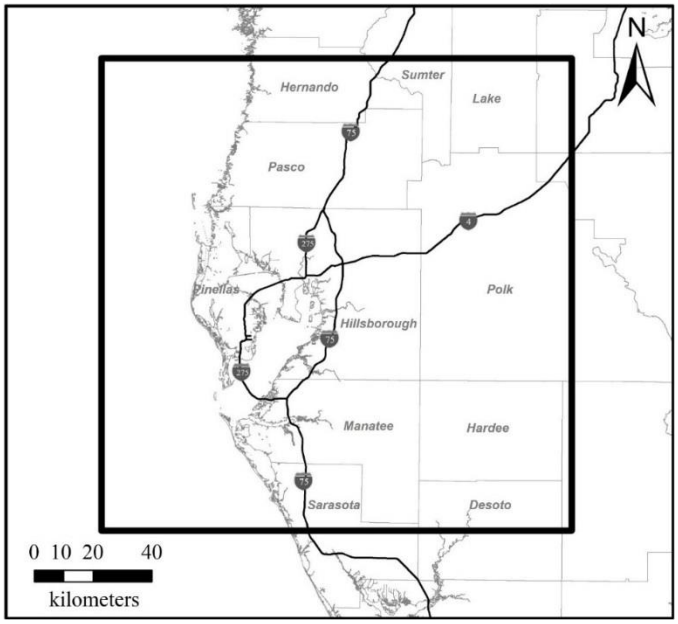

Figure 5.2 Domain of emissions estimation.

5.3.1.1. On-Road Mobile Sources

A similar hybrid method as used in Chapter 4 was applied for on-road mobile source emissions. Within Hillsborough County, all roadways are divided into two categories: major roadways and minor roadways (Figure 5.3). Major roadways are roads with traffic count (annual average daily traffic (AADT)) data available in 2002, and all

other roads are classified as minor roadways. Different approaches were applied for major and minor roadways.

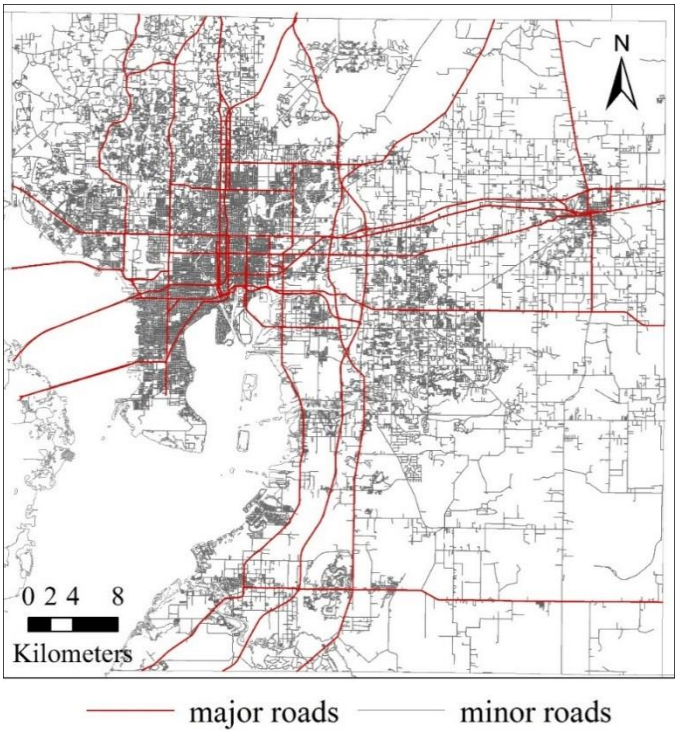

Figure 5.3 Major and minor roadways in Hillsborough County, FL, and annual average daily traffic on major roadway links

5.3.1.1.1. Major roadways within Hillsborough County

A detailed bottom-up approach was applied on major roadways in Hillsborough County, as emissions from these roadways are expected to be substantial and have significant impacts on nearby pollutant concentrations. Generally, emissions from individual major roadway links are estimated by:

$$E_{l,h} = T_{l,h} F_{l,s,h} L_l$$

where: $E_{l,h}$ is the estimated on-road mobile source emissions (grams per hour) for link l at hour h; $T_{l,h}$ is traffic volume (vehicles per hour) on link l at hour h; $F_{l,s,h}$ is the emission factor (grams per mile per vehicle) for link l at hour h at average speed s. It is an

estimation of the average amount of pollutant emissions from vehicles travelling certain distances on roadways; and L_l is the length (mile) of link *l*.

Length of individual roadway link was calculated from Geographic Information Systems (GIS) data obtained from the Florida Department of Transportation (Florida Department Of Transportation, 2002). Traffic volume (vehicles per hour) on major roadway links were estimated for each link and each hour by applying temporal traffic variation profiles on annual average daily traffic for the corresponding link. There are four profiles used: annual profile by month, weekly profile by day, weekday diurnal profile by hour, and weekend diurnal profile by hour (Figure 5.4). These profiles were derived from hourly traffic counting data within Hillsborough County, which were also obtained from the Florida Department of Transportation (Florida Department Of Transportation, 2002).

Here, MOVES (instead of the MOBILE6.2 model) was used to estimate emission factors, using a more sophisticated method (Figure 5.5). In this method, hourly average travelling speeds on each major roadway link were first calculated, and emissions factors were then estimated using MOVES model. By applying the estimated speed information, appropriate emission factors were assigned to corresponding roadway links. Hourly resolved link emissions were then calculated using the estimated link volume and emission factors.

First, two roadway link characteristics were identified for each major roadway link: area type and roadway type. Area type refers to the type of surrounding areas (urban, rural etc.) where the link is located, and roadway type refers to the function class (freeway, collectors etc.) of the corresponding roadway link. These attributes were

obtained from Tampa Bay Area Regional Transportation Authority (TBARTA) and were used by the Tampa Bay Regional Planning Model (TBRPM), which is the designated travel demand model for transportation planning in the Tampa Bay area (Gannett Fleming Inc, 2010). For convenience, area and roadway types as defined in the TBRPM model are herein referred as TBRPM area and roadway types. Appendix A-1 and A-2 provides complete lists of the TBRPM area and roadway types used in this study.

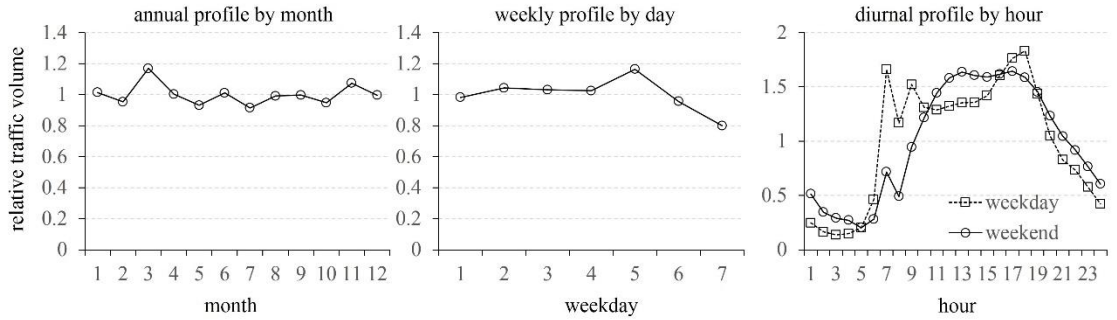

Figure 5.4 Temporal traffic variation profiles used to estimate hourly traffic volumes on each roadway link. Traffic volume shown are relative to mean traffic volumes at corresponding temporal scales.

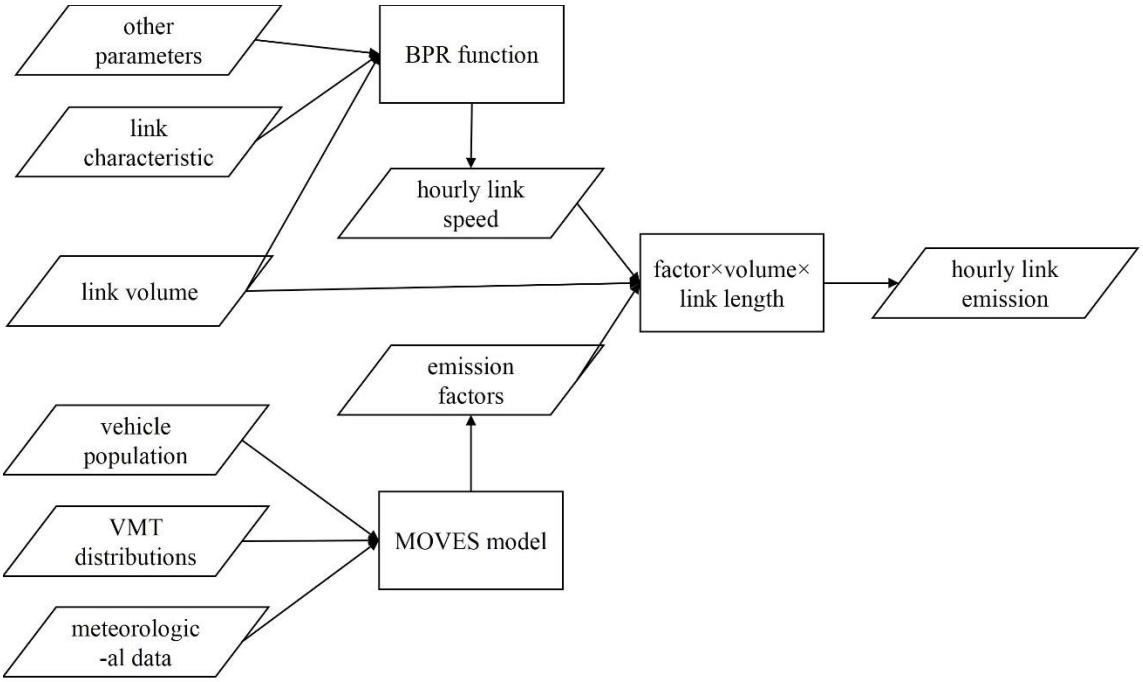

Figure 5.5 Overview of the methods for estimating on-road mobile source emissions for major roadway links.

Additional link characteristics, including number of lanes and median width, were also identified for all major roadway links. This information was also obtained from the Florida Department Of Transportation (2002). Roadway mileage markers were used as criteria for determining the attributes, and links were further divided when necessary. For example, if one roadway link starts from mileage 1 and ends at mileage 2, however there are two lanes at each direction from mileage 1 to 1.5 but there are three lanes at each direction from mileage 1.5 to 2. In this case, the roadway link is broke into two links at mileage 1.5 to ensure consistent attributes along the link.

Roadways with steep curves and complex geometries are consist of many short links. Modeling of these short links individually can be very computational expensive. Considering computational tractability, a regression algorithm was applied to reduce the total number of links. Specifically, the developed algorithm will attempt to linearly fit a regression line along the same roadway with as many links as possible, as long as the maximum error (perpendicular distances of each link nodes to the regressed line) are within the threshold of 20 m. "Nodes" refer to the two end points of each link. When the threshold was not exceeded, original roadway links were replaced with the regressed line. The total number of links was reduced by approximately 1/3 by applying this algorithm, which saved approximately 2000 CPU hours for dispersion modeling.

As shown in Chapter 3, speed of vehicles travelling on each link is important as vehicular emissions varies at different speeds. Unfortunately detailed speed information at link level are normally not readily available. Past studies have relied on travel demand models for such information; however, the temporal coverage of travel demand models are generally limited.

In this study, I developed a method that can be readily applied to estimate hourly resolved speed information for individual roadway links. Specifically, average travelling speeds were estimated by applying the Bureau of Public Roads (BPR) function, which is a widely used empirical function to estimate vehicle speed on roadways:

$$S_{l,h} = \frac{S_{l,f}}{1 + \alpha_l \left(\frac{V_{l,h}}{C_l} \right)^{\beta_l}}$$

where $S_{l,h}$ is the estimated average speed for link l in hour h; $S_{l,f}$ is the free flow speed for link l; $V_{l,h}$ is the traffic volume on link l in hour h; C_l is the roadway capacity for link l; α_l and β_l are corresponding parameters for link l;

Free flow speed ($S_{l,h}$), α_l and β_l for each link are determined by the combination of TBRPM area and roadway types of the corresponding link. This information was also extracted from the Tampa Bay Regional Planning Model. Look-up tables for freeway flow speed and the two parameters are provided in Appendix A-3 and A-4.

Information on roadway capacity (C_l) of each link was obtained from the 2009 FDOT Quality/Level of Service Handbook (Florida Department of Transportation, 2009). In this handbook, a different area and roadway classification method was used. For convenience, these area and roadway types are herein referred as LOS handbook area and roadway types. Appendix A-5 and A-6 provides lists of the LOS handbook area and roadway types.

TBRPM area and roadway types of each link were first mapped to the LOS handbook area and roadway types, using methods provided in Appendix A-7 and A-8. Link capacity was then obtained from a capacity look-up table (Appendix A-9), which was extracted from the 2009 FDOT Quality/Level of Service Handbook. In accordance

with the handbook, capacity adjustments were also performed for certain links, as listed in Appendix A-8. Linear interpolation or extrapolations were performed when the number of lanes did not match the look-up table.

Table 5.1 Mapping method from Florida Department of Highway Safety and Motor Vehicles (FHSMV) vehicle types to MOVES vehicle types

FHSMV vehicle type	description	Mapped to MOVES vehicle type
Passenger cars	Passenger cars < 2499 lbs	21
	Passenger cars between 2500 and 3499 lbs	
	Passenger cars > 3500 lbs	
	Antique passenger cars	
Lease vehicles	semi annual lease	
	passenger car	
	short term lease[a]	31+32
Buses, ambulances and hearses	Buses > 9 passenger	41+42+43
	Buses, half year, > 9 passenger	
	Buses, unknown	
	Ambulances and hearses[b]	
Trucks (exclude tractors)[c]	Trucks (exclude tractor) - < 1999 lbs	31+32
	Trucks (exclude tractor) - 2000-3000 lbs	
	Trucks (exclude tractor) - > 3001 lbs	
	Trucks (exclude tractor) - antique	
Mobile home and park trailers	Mobile home - military	Excluded[d]
	Mobile home	
	Park trailer	
	5th wheel trav trailer < 35 ft	
	5th wheel trav trailer > 35 ft	
Trailers	Private trailer < 500 lbs	
	Private trailer > 500 lbs	
	Trailer for hire < 1999 lbs	
	Trailer for hire >= 2000 lbs	
	Semi trailer - flat	
	Semi trailer - permenant	

[a]Assumed to be truck rentals; [b]assumed to be light trucks (including vans); [c]These are private owned light duty trucks; [d]these are excluded because they either have no engine or not running on road; [e]This item was excluded due to insufficient information and small number of vehicles;

Table 5.1 (continued) Mapping method from Florida Department of Highway Safety and Motor Vehicles (FHSMV) vehicle types to MOVES vehicle types

FHSMV vehicle type	description	Mapped to MOVES vehicle type
Motorcycles	Motorcycles	11
	Moped/motorized bike	
	Antique motorcycle	
Demonstrators	Demonstrators - Dealer plates	Excluded[d]
	Boat trailer	
Truck tractors	truck tractor forestry, full year	51+52+53+61+62
	truck tractor forestry, half year	
	GVW truck/tractor, full year	
	GVW truck/tractor, half year	
	GVW truck/tractor, wrecker	
	tractor crane	Excluded[d]
other vehicles	miscellaneous base tax fees	
	horseless carriage	
	goat	Excluded[e]
	x-series exempt	See section 3.2.1.2.1
	government vehicles	
	non-resident military	
miscellaneous	transporter	61+62
	trucks, agriculture use	51+52+53
	All other vehicles	Excluded[e]
recreational	auto - motorcoach < 4499 lbs	54
	auto - motorcoach >= 4499 lbs	
	camp trailer	Excluded[d]

[a]Assumed to be truck rentals; [b]assumed to be light trucks (including vans); [c]These are private owned light duty trucks; [d]these are excluded because they either have no engine or not running on road; [e]This item was excluded due to insufficient information and small number of vehicles;

In addition to hourly link speed and volume data, emission factors (grams per vehicle per mile) were estimated using the MOVES model and organized as a look-up table. Appropriate emission factors for individual links were retrieved from the look-up table based on combinations of link characteristics such as roadway type, area type and speed.

MOVES model was executed under the county scale. Three sets of data were prepared using local specific information for the MOVES model: vehicle population (also referred to as source type population in MOVES), vehicle mileage travelled (VMT) distribution by MOVES vehicle and roadway types, and meteorological data. Defaults were applied for other required input datasets such as ramp fraction, vehicle age distribution and fuel properties.

Vehicle population data were obtained from the Florida Department of Highway Safety and Motor Vehicles (FHSMV) (Florida Department of Highway Safety and Motor Vehicles, 2002, 2003). The raw data, which was provided by fiscal year, were averaged to obtain population data for calendar year 2002. In addition, FHSMV uses a different vehicle classification system (herein referred as FHSMV vehicle types), which were mapped to aggregated MOVES vehicle types (herein referred as MOVES vehicle types). Appendix A-10 listed the vehicle types as used by the MOVES model, and Table 5.1 provides list of FHSMV vehicle types and the mapping method applied here.

During the mapping process, three FHSMV vehicle types were treated specially: X-series exempt vehicles, government vehicles and non-resident military vehicles. X-series exempt vehicles are vehicles owned by churches and non-profit organizations, and government vehicles are "yellow tag" vehicles owned by the government. The fleet compositions of these two categories were assumed to be 50% passenger cars (MOVES ID 21, see Appendix 10) and 50% light trucks (MOVES ID 31+32), given no further information available. Non-resident military vehicles are vehicles owned by military personnel stationed in the study area and are resident of another state. This category was assumed to be 84% passenger cars and 16% light trucks. Total vehicle population of

these three categories account for less than 0.5% of the total vehicle population for the whole county. Hence these simplified assumptions are not expected to significantly impact vehicle fleet compositions.

The mapped vehicle populations for each aggregated MOVES vehicle type category were then distributed to each specific MOVES vehicle type using MOVES default population data for Hillsborough County, assuming same fractions within each aggregated vehicle type.

The second input dataset to the MOVES model is vehicle mileage travelled data and its distribution by MOVES vehicle and roadway types (See Appendix A-11 for a list of roadway types). There are five components of the vehicle mileage travelled and distribution data: annual total vehicle mileage travelled by vehicle class, vehicle mileage travelled fraction distribution by month, weekday, hour, and also by MOVES roadway type. County total vehicle mileage travelled data for 2002 were available from Florida Department of Transportation (Florida Department of Transportation, 2003), and data are provided for different area and roadway types. However, the area and roadway classification method used in the report (herein referred as VMT area and roadway types) are different from those as in the MOVES model. The method used to map VMT area and roadway types to MOVES roadway types are provided in Table 5.2. The same vehicle mileage travelled distribution by MOVES roadway type were applied for all MOVES vehicle types, given no further information available. Regarding the temporal variation of vehicle mileage travelled data, the four temporal traffic variation profiles derived previously were applied.

The third input dataset to the MOVES model is meteorological data including diurnal temperature and humidity data for 12 months. These data were extracted from the NMIM (National Mobile Inventory Model) model (U.S. Environmental Protection Agency, 2005a) NCD (NMIM County Database) database.

Table 5.2Mapping method from VMT area and roadway type to MOVES roadway types.

	VMT area types		
	rural	small urban	large urbanized
interstate	RR	UR	UR
turnpike & freeway	NONE	NONE	UR
other principal arterials	RU	UU	UU
minor arterials	RU	UU	UU
urban major collector	RU	UU	UU
rural minor collector	RU	NONE	NONE
locals	RU	UU	UU

*Urban restricted (UR), rural restricted (RR), urban unrestricted (UU) and rural unrestricted (RU) roads. NONE indicates that there are no roads with such combination

Overall, approximately 6 million emission factors were estimated. Appropriate emission factors for each link were then retrieved from these emission factors based on a combination of link characteristics including roadway type, area type and speed. The MOVES model uses a different definition of area and roadway types. Hence the Tampa Bay Regional Planning Model (TBRPM) area and roadway types were mapped to MOVES roadway types during the assignment of emission factors. The mapping method is provided in Appendix A-12. In addition, MOVES emission factors were resolved by speed bins with 5 mph interval. When the estimated link speed fell between two speed intervals, linear interpolations were performed. Finally, hourly link emissions were calculated by combining emission factors, link length and hourly link volume for the corresponding link.

5.3.1.1.2. Minor roadway emissions in Hillsborough County

For minor roadways within Hillsborough County that have no traffic counting data available, a top-down approach was applied. First, the MOVES model was used to estimate total on-road mobile source emissions for Hillsborough County. Emissions from major roadways were subtracted from the estimated total. The remaining emissions were spatially allocated to a 1 km by 1 km grid network overlaid on Hillsborough County using proportionally to total minor roadway length in each grid cell.

5.3.1.1.3. On-road mobile source emissions in surrounding counties

For on-road mobile source emissions in surrounding counties, a similar top-down approach was used. There are two considerations for choosing this approach. First, emissions from surrounding counties are not expected to substantially impact spatial concentration distributions as those major roadways within Hillsborough County, hence there is no need to accurately characterize the geometry of roadways. Second, the detailed bottom-up approach is very data and computation intensive and it may be impractical to apply bottom-up approach to all counties.

The MOVES models were first used to estimate total on-road mobile source emissions for 11 counties included in emission estimation (Figure 5.3). Input datasets to the MOVES model were prepared in the same way as described above. Then, the estimated county total emissions were divided into two parts: emissions from primary roadways and emissions from secondary roadways. Here, primary roadways refer to roadways with census feature class codes between A10 and A28 (U.S. Census Bureau, 2010) and all other roads are classified as secondary roadways. Emission fractions of the

two categories are assumed to be the same as the fraction of emissions between major and minor roadways within Hillsborough County. Finally, grid networks were overlaid on these counties and on-road mobile source emissions were allocated to the grid network. Emissions from primary roadways were allocated proportionally to total primary roadway length in each grid cell, and emissions from secondary roadways were allocated proportionally to total secondary roadway length in each grid cell.

Two grid networks were used in the spatial allocation of on-road mobile source emissions (Figure 5.6). A 5 km by 5 km grid network was used for benzene, 1,3-butadiene and NO_x. For acetaldehyde and formaldehyde, a 1 km by 1 km grid network was used for the purpose of combining CMAQ data (see section 5.4.1.7). The four temporal traffic variation profiles used for major roadway were also applied to estimate hourly resolve emissions.

5.3.1.2. Stationary point sources

Stationary point sources are generally industrial stacks. Here, stationary point emissions were modeled for acetaldehyde, formaldehyde and NO_x. Point emissions of 1,3-butadiene and benzene were excluded due to their small contribution to the total amount (less than 1%). Considering computational tractability, a total of 35 point sources were included for acetaldehyde, 60 for formaldehyde and 159 for NO_x. Emissions from these sources contribute to more than 98% of total emissions from point sources. Locations of these sources are shown in Figure 5.7. Most of the stationary point sources are located in Hillsborough, Pinellas and Polk counties, and many are clustered around the Tampa Bay area.

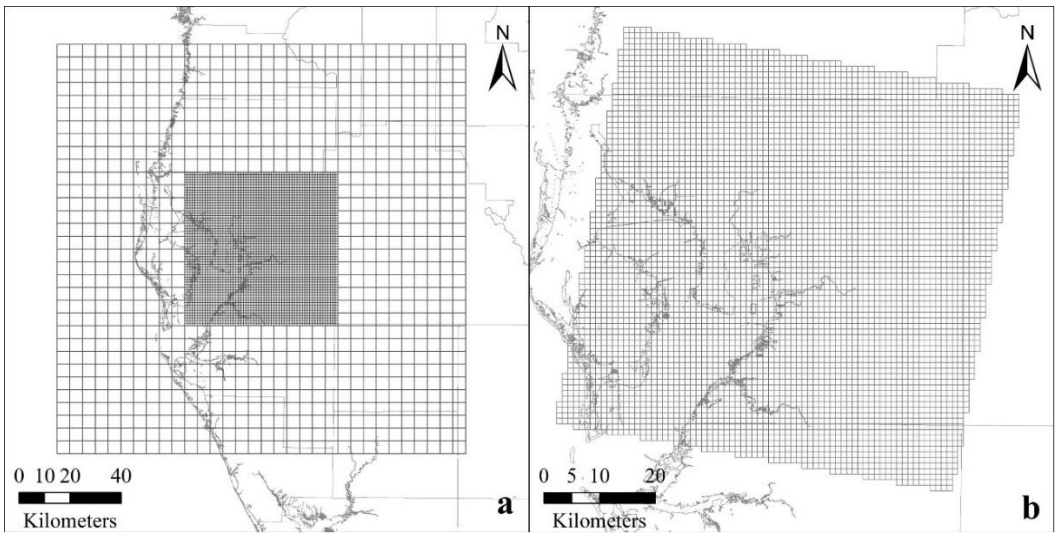

Figure 5.6 Two different grid networks used to allocate on-road mobile source emissions. a) shows grid network for 1,3-butadiene, benzene and NO_x; and b) shows grid network for acetaldehyde and formaldehyde.

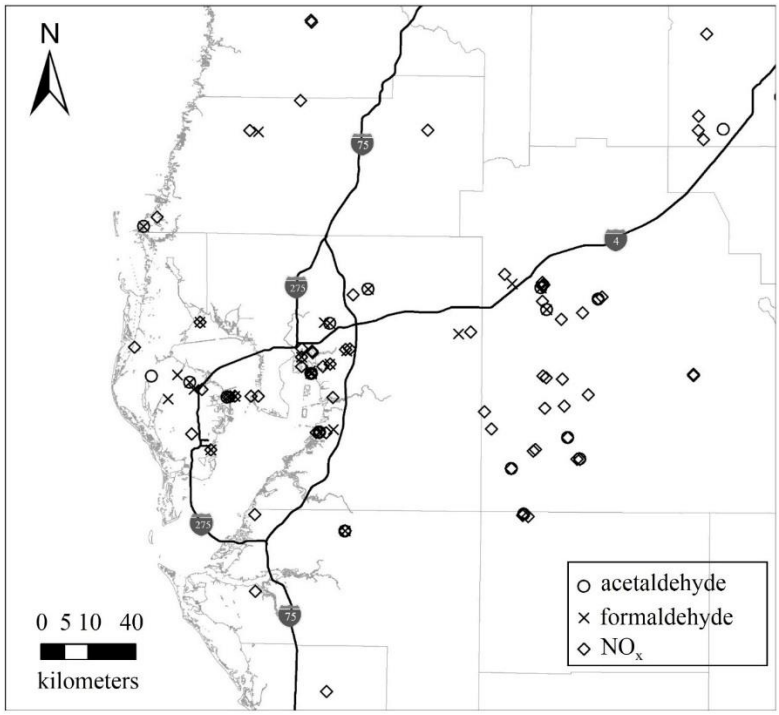

Figure 5.7 Stationary point sources of acetaldehyde, formaldehyde and NO_x included in the modeling

Characteristics of these stationary point sources, including location, annual emission, stack height and diameter, exit gas temperature and velocity, and rain hat information, were obtained from the 2002 National Emission Inventory (NEI) (U.S.

Environmental Protection Agency, 2006). Temporal variations of emissions were characterized by four profiles: annual profile by month, weekly profile by day and diurnal profile by hour (different for weekday and weekend days). These profiles were obtained from U.S. Environmental Protection Agency (2007a). Different factors were assigned to individual point source based on its corresponding source classification code. Hourly emission rates were estimated for each point source.

5.3.1.3. Biogenic emissions

Biogenic emissions are emissions emitted from natural sources such as forests. These emissions are significant for acetaldehyde and formaldehyde, and are neglected for the other three pollutants due to the small amount of emissions. Annual total biogenic emissions of formaldehyde were obtained from the 2002 National Emission Inventory. Emissions for acetaldehyde are not directly available, but they are assumed to be the same as formaldehyde since their emission factors are identical in the BEIS (Biogenic Emission Inventory System) model (U.S. Environmental Protection Agency, 2010a), which is the model used to generate biogenic emissions for the 2002 National Emission Inventory.

To account for temporal variations of biogenic emissions, two variation profiles were applied: annual profile by month and diurnal profile by hour. The annual profile was derived directly from national emission inventory data. The diurnal profile was derived from outputs of a standalone version of the BEIS model (version 2.3).

Three datasets were prepared for the BEIS model: temperature, cloud cover and PAR (Photosynthetically Active Radiation) data. Temperature data were extracted directly from the database of NMIM model. Cloud cover data were extracted from

surface meteorological observation data from VISTAS (Visibility Improvement State and Tribal Association of the Southeast) for 2002 (Morris et al., 2007). Hourly cloud cover data were extracted from two stations located within Hillsborough County (World Meteorological Organization (WMO) ID 722110 and 747880), and averaged at each hour. Photosynthetically active radiation refers to solar radiation absorbed by plants that are used in photosynthesis. Diurnal photosynthetically active radiation for 12 months in 2002 were estimated by:

$$P_{h,m} = S_{h,m} f_{P,m} F_P$$

where $P_{h,m}$ is the estimated photosynthetically active radiation for hour h in month m (μ mol $m^{-2}s^{-1}$); $S_{h,m}$ is the solar radiation intensity at hour h in month m (W/m^2); $f_{P,m}$ is the fraction of incoming solar radiations that is photosynthetically active radiation in month m; and F_P is a conversion factor (4.57 μ mol s^{-1} W^{-1}) (Escobedo et al., 2009).

Solar radiation intensity ($S_{h,m}$) were obtained from National Solar Radiation Database (NSRD) (National Renewable Energy Laboratory, 2007). Hourly radiation data from two stations located within Hillsborough County (world meteorological organization ID 722021 and 722110) for 2002 were extracted and averaged at each hour. $f_{P,m}$ were retrieved from Global Terrestrial Observing Network (GT-NET) Fraction of Absorbed Photosynthetically Active Radiation (FAPAR) satellite observation data. Monthly data in 25 grid cells covering Hillsborough County were extracted and averaged at each month.

The estimated diurnal profile by hour for 12 months were averaged to obtain a single diurnal emission variation profile. Figure 5.8 provides the final diurnal profiles applied in emissions estimation, together with the annual profile by month derived from

monthly biogenic emission data within the 2002 National Emission Inventory. Biogenic emissions are the highest in summer time at annual scale, and are the highest around 3 pm at daily scale.

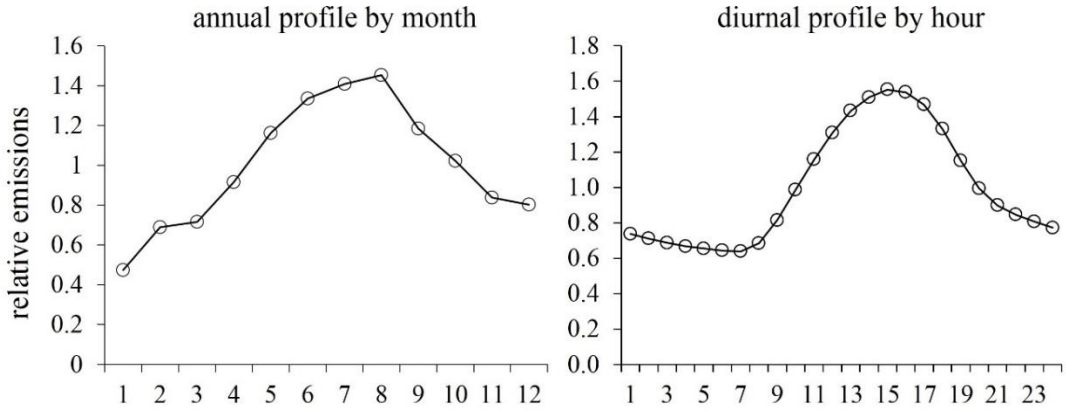

Figure 5.8 Derived annual profile by month and diurnal profile by hour for estimating hourly biogenic emissions. Emission shown in the figure are relative to average emissions at corresponding temporal scales

Biogenic emissions of acetaldehyde and formaldehyde were spatially allocated to 1 km grid network as shown in Figure 5.6, proportionally to forest land area (km^2) within each grid cell. Land use data containing the spatial distribution of forest were retrieved from Southwest Water Management District. The developed annual profile by month and diurnal profile by hour were applied to estimate hour resolved emissions.

5.3.1.4. Non-road mobile and non-point emissions

Non-road mobile emissions refer to emissions from motor engines running off-road, such as lawn mowers, recreational watercrafts etc. Non-point emissions refers to emissions from sources that are characterized as an "area" such as landfills. The annual total amount of non-road and non-point emissions are available from the 2002 National Emissions Inventory, and were spatially allocated to the two grid networks as shown in Figure 5.6. Each source category contains thousands of emissions records, organized by Source Classification Codes (SCC), corresponding to emissions from different processes,

such as emissions from farming equipment, dry cleaning equipment, or recreational watercrafts. A total of 76 spatial surrogates were used during the spatial allocation. Each surrogate is a spatial metric based upon which fractions of emissions within each grid cell can be calculated and allocated. Examples of surrogates including forest land area, industrial land area, and population within each grid cell. The surrogates were manually derived using data obtained from EPA (U.S. Environmental Protection Agency, 2007b). For the forest area surrogate, data retrieved from Southwest Water Management District were used as they contained more detailed information. Appropriate surrogates were assigned corresponding to the source classification codes of each emission records, using recommendations from the EPA (U.S. Environmental Protection Agency, 2007b).

Regarding the temporal variation of non-point and non-road emissions, four profiles were applied: annual profile by month, weekly profile by day and diurnal profiles by hour (weekday and weekend days). These profiles were also obtained from the EPA, and different profiles were assigned corresponding to the source classification codes of each record (U.S. Environmental Protection Agency, 2007a) .

NO_x emissions from commercial marine vessels and marine ports were treated specially (no special treatment for other pollutants). NO_x emission data from Jungers et al. (2006) were used instead of data from the 2002 National Emissions Inventory. The data from Jungers et al. (2006) were calculated using a detailed bottom-up approach based on detailed marine vessel activities, whereas emissions for the 2002 National Emissions Inventory for Hillsborough County were calculated by allocating estimated national level (whole US) emissions using a simplified top-down allocation approach. Therefore data from Jungers et al. (2006) are considered more representative.

Annual NO_x emissions from commercial marine vessels and marine ports were spatially allocated to emission grid cells as shown in Figure 5.9. Grid networks shown in the left are for benzene, NO_x, and 1,3-butadiene, while grid network to the right are for acetaldehyde and formaldehyde (see Figure 5.6). Constant temporal emission profiles were applied for emission from commercial marine vessels and marine ports.

5.3.2. Results of Emission Estimation

Figure 5.10 shows the estimated on-road mobile source emissions from major roadway links for the five selected pollutants. For comparison purposes, annual average daily traffic for 2002 are also shown in the figure. Major Interstates including I-75, I-4 and I-275 have the highest traffic volume. Traffic volumes are concentrated in downtown Tampa area, where the three interstates merges. The spatial distribution of pollutant emissions varies slightly for different pollutants, but generally follow the same pattern as annual average daily traffic. The highest emissions are found along the major interstates. NO_x emission estimation results using MOBILE6.2 model are similar and hence are not shown.

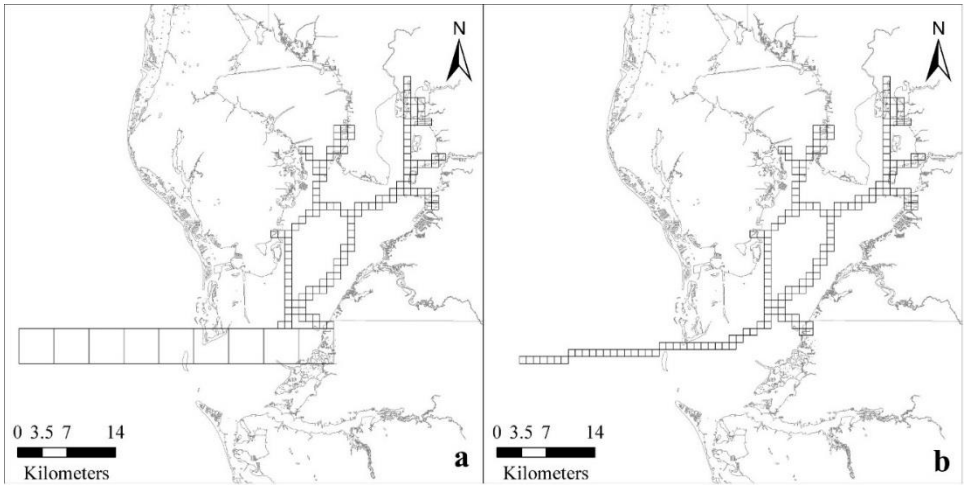

Figure 5.9 Emission grids where commercial marine vessels and marine ports emissions were allocated. a) shows the emission grids for 1,3-butadiene, benzene and NO_x; b) shows emission grids for acetaldehyde and formaldehyde.

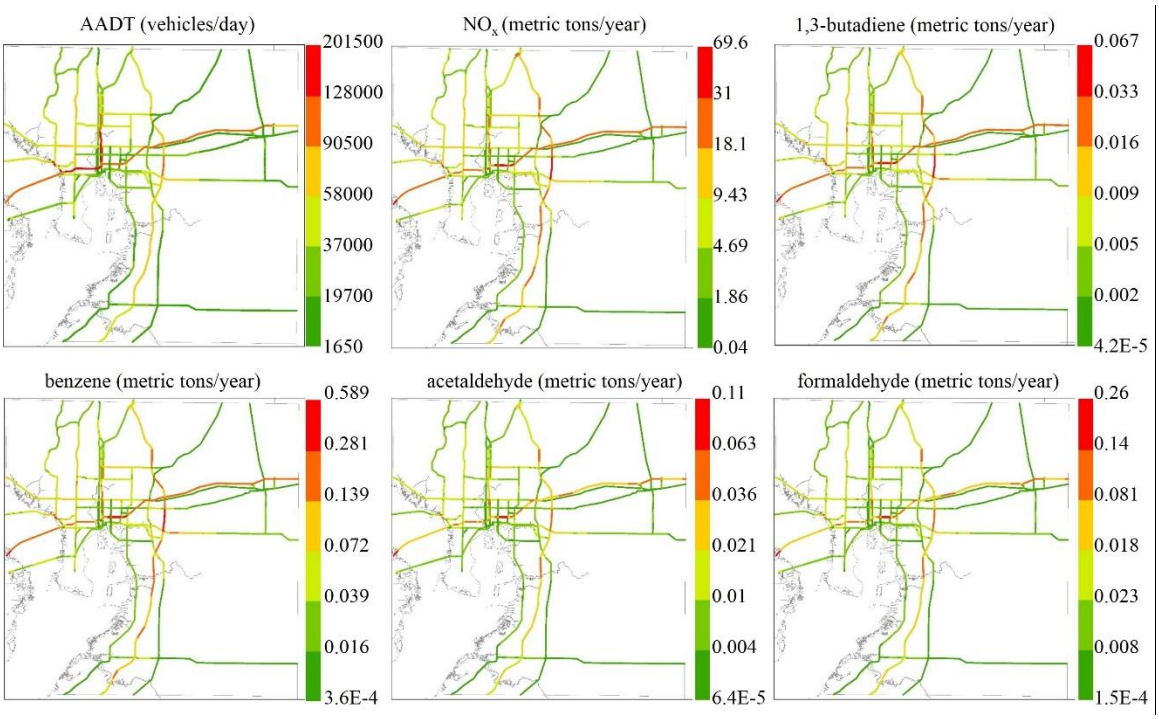

Figure 5.10 Estimated major roadway link emissions for NO_x, 1,3-butadiene, benzene acetaldehyde, and formaldehyde. Annual average daily traffic are also shown.

Table 5.3 shows the estimated total on-road mobile source emissions for 12 counties (Hillsborough and 11 surrounding counties). Emission estimates from the 2002 National Emission Inventory (NEI) were also listed for comparison purposes. NOx emission estimated by MOVES model is 79% higher than data from the inventory, which used MOBILE6.2 model. The estimated emission is also higher (21%) for acetaldehyde, but are lower for the rest air toxics. County specific emissions are shown in Table 5.4.

Table 5.3 Estimated annual total on-road mobile source emissions for 12 counties

pollutant	annual emissions (metric tons)	
	MOVES	2002 NEI
1,3-butadiene	291	355
acetaldehyde	423	349
benzene	2500	3060
formaldehyde	961	1020
NO_x	197000	110000

Table 5.4 County total on-road mobile source emissions for 2002 as estimated by MOVES model and in the 2002 National Emission Inventory

pollutant	county	annual emissions (metric tons)		pollutant	county	annual emissions (metric tons)	
		MOVES	2002 NEI			MOVES	2002 NEI
NO_x	Desoto	1556	1045	1,3-butadiene	Desoto	1.5	3
	Hardee	1727	613		Hardee	1.5	1.7
	Hernando	5831	3338		Hernando	7.8	9.2
	Hillsborough	44366	23175		Hillsborough	62.3	78.2
	Lake	9339	3828		Lake	13.1	10.6
	Manatee	14615	6278		Manatee	28.2	18.6
	Orange	39484	22182		Orange	56.7	76.8
	Pasco	12921	8476		Pasco	19.7	24.8
	Pinellas	26947	18257		Pinellas	49.6	67.2
	Polk	21511	12138		Polk	26.7	36.1
	Sarasota	13444	7386		Sarasota	20.3	22.6
	Sumter	5290	3285		Sumter	3.7	5.9
benzene	Desoto	12.5	25.7	acetaldehyde	Desoto	3.1	3.1
	Hardee	12.2	14.4		Hardee	3.1	1.7
	Hernando	67.1	78.4		Hernando	11.7	9.4
	Hillsborough	534	674		Hillsborough	93.1	76.1
	Lake	112.2	90.3		Lake	19.5	10.9
	Manatee	240.5	160.4		Manatee	36.2	18.8
	Orange	486.7	667.7		Orange	83.2	74.1
	Pasco	169.2	212.5		Pasco	27.9	25
	Pinellas	433.3	581.9		Pinellas	60.5	64.4
	Polk	225.4	310.5		Polk	44.7	36.3
	Sarasota	175.7	195.7		Sarasota	28.3	22.6
	Sumter	30.4	48.3		Sumter	8.2	6.7
formaldehyde	Desoto	6.9	8.9				
	Hardee	7	5.1				
	Hernando	26.4	27.4				
	Hillsborough	212.9	222.4				
	Lake	44	31.7				
	Manatee	82	54.7				
	Orange	187.9	216.3				
	Pasco	63	72.7				
	Pinellas	139.8	188.4				
	Polk	100.7	105.7				
	Sarasota	63.9	66				
	Sumter	18.3	19.3				

Figure 5.11 shows the allocated emissions at two grid networks. The emissions include minor roadway emissions within Hillsborough County, on-road mobile source emissions in other counties, non-road, non-point and biogenic emissions. For NOx, 1,3-butadiene and benzene, urbanized areas generally have higher pollutant emissions, especially in downtown Tampa, Pinellas County, and the Brandon area. Rural areas generally have lower pollutant emissions. Emissions from shipping lanes are visible for NO_x, acetaldehyde and formaldehyde, and marine port emissions can clearly be seen for acetaldehyde and formaldehyde.

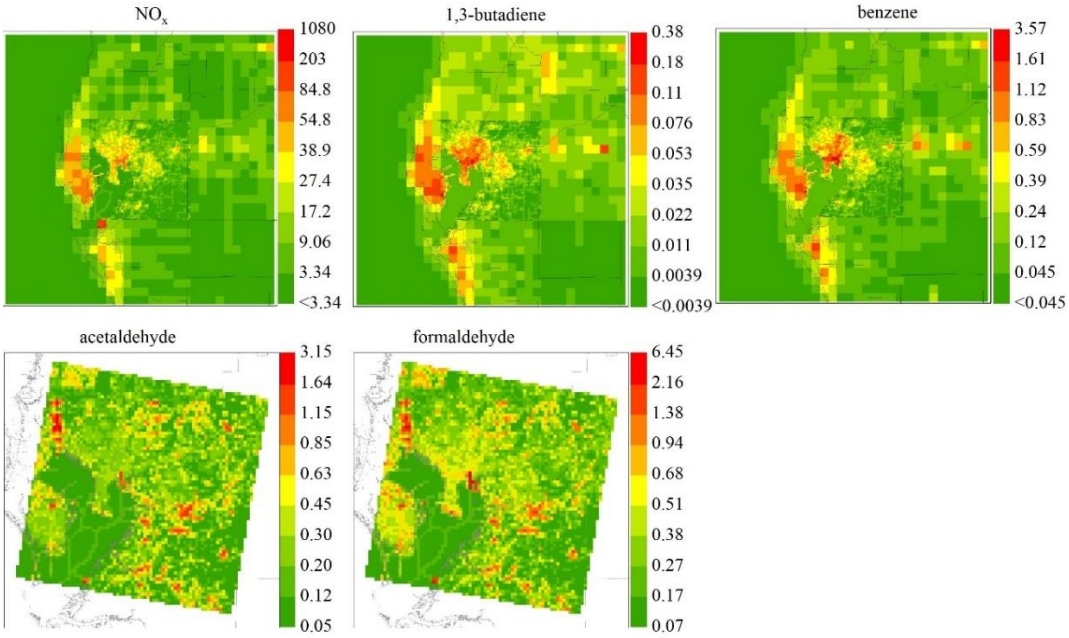

Figure 5.11 Allocated emissions for NO_x, 1,3-butadiene, benzene, acetaldehyde and formaldehyde. Emissions shows are metric tons (annual total) per square kilometers.

Table 5.5 and Figure 5.12 provides a summary of emissions for each category that was included in the modeling. It can be seen that emission distributions among different categories vary for different pollutants. Generally, point sources contribute to a small percentage of emissions, except for NO_x, for which 32% emissions are from point sources. On-road mobile sources (major roadways and other on-road mobile sources)

contribute substantially (over 50%) to their corresponding anthropogenic emissions (excluding biogenic emissions). For acetaldehyde and formaldehyde, biogenic emission contribute to 72% and 51% to their total emissions included in the study area. Non-road mobile sources also have important emission contributions, with highest percentage of 27% for 1,3-butadiene and smallest percentage of 10% for acetaldehyde.

Table 5.5 Emission summary for stationary point, on-road mobile, non-point, non-road and biogenic emissions included in the model

	annual emissions (metric tons)				
	1,3-butadiene	acetaldehyde	benzene	formaldehyde	NOx
point	N/A	8.8	N/A	22.2	87100
major roadways	18.9	28.7	162	65.8	19200
other on-road*	193	115	1660	262	121000
non-road	106	94.7	883	226	32810
non-point	76.7	12.5	636	56.8	9310
biogenic	N/A	659	N/A	659	N/A
Total	395	919	3340	1290	269000

* Other on-road emissions refers to the combination of minor roadway emissions within Hillsborough County and all on-road mobile source emissions in surrounding counties that are included in the modeling.

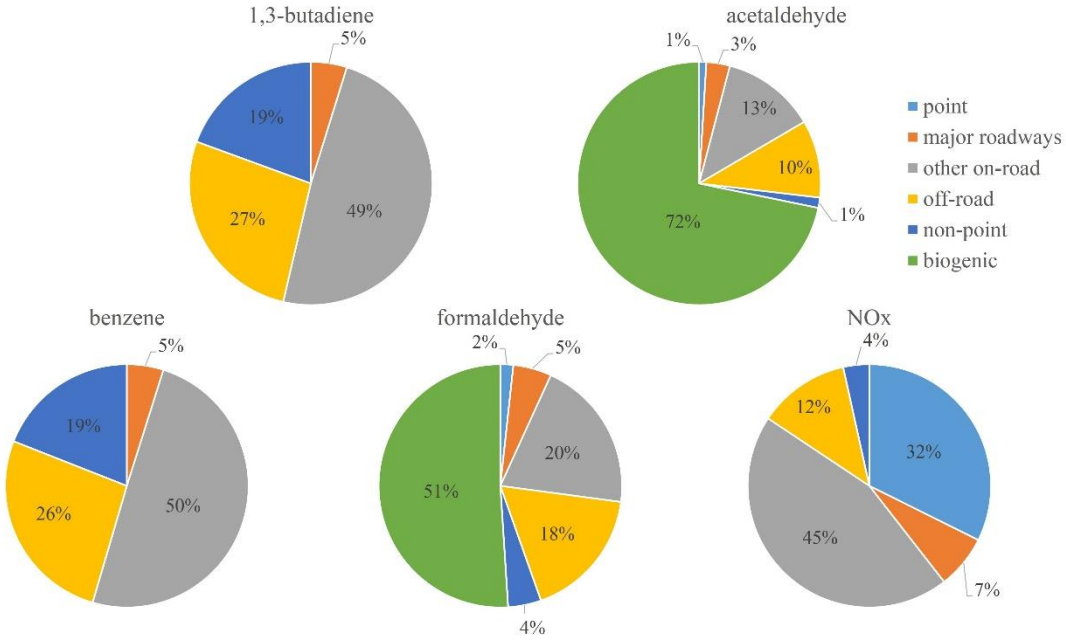

Figure 5.12 Percentage of emissions from each category for the five selected pollutants.

5.3.3. Discussion of Emission Estimation

On-road mobile, stationary point, non-road mobile, non-point and biogenic emissions of the five chosen pollutants were estimated for the study domain. As shown in Figure 5.12, the estimated amount of emissions from different emission categories show significant contributions from mobile source emissions (including both on-road and non-road mobile sources). More than 50% of anthropogenic emissions in the modeling domain were from mobile sources. These results further confirmed the importance of urban growth forms regarding air pollution concentration and exposures, as urban growth forms may have significant impacts on the amount and spatial distributions of mobile source emissions (see Chapter 2).

In this study on-road mobile source emissions were estimated using MOVES model for 12 counties included in the modeling domain. The 2002 National Emissions Inventory (NEI) contains estimated on-road mobile source emissions for these counties, but data from the inventory were not used as they were estimated using the MOBILE series model, which is the precedent model of MOVES. Comparison between the estimated emissions using MOVES model and data from the inventory shows that the estimated emissions using MOVES model for 12 counties are substantially higher for NO_x (+79%) and acetaldehyde (+21%), and are lower for 1,3-butadiene (-18%), benzene (-18%) and formaldehyde (-6%). Similar differences were also found in other studies (Fujita et al., 2012; Indiana Department of Environmental Management, 2012; Pennsylvania Department of Environmental Protection, 2013). This finding suggests that data for on-road mobile source emissions in the 2002 national emissions inventory may

be outdated, and also justified the use of MOVES model for on-road mobile source emission estimations.

The estimated emissions include all five emission categories in the 2002 National Emission Inventory, such comprehensive coverage on emissions are seldom found in past studies that uses non-steady state Lagrangian chemical transport models. In this study, a full sets of tools were developed for automated emission estimation purposes, and to my knowledge, no similar tools are currently available for non-steady state Lagrangian chemical transport models.

It is commonly recognized that average vehicle travelling speed substantially impact emissions from motor-vehicles (Bai et al., 2007). However detailed speed information are normally not readily available. When estimating on-road mobile source emissions, the US Environmental Protection Agency recommends using output from travel demand models to characterize speed for roadways (Hatzopoulou & Miller, 2010; U.S. environmental Protection Agency, 2012c; Wang et al., 2009). However producing such output data could be costly. Further, travel demand models generally do not attempt to model large time spans, hence their outputs are temporally restricted. In this study, an innovative speed estimation approach was developed by adopting the Bureau of Public Roads (BPR) function, which are commonly used in the field of transportation modeling. Spatiotemporal resolved speed information were estimated at roadway link level. This approach can be readily applied in other areas to better characterize the impact of speed on on-road mobile source emissions.

5.3.4. Limitations and Uncertainties of Emission Estimation

In emission estimations for on-road mobile source emissions from major roadways, hourly traffic volume on individual roadway links were estimated by temporally interpolating annual average daily traffic data on each link. The interpolated traffic volume data may not accurately represent actual traffic volume on roadway links.

Emission factors and county total on-road mobile source emissions estimated by MOVES model may also contain uncertainties. Specifically, three datasets were prepared for MOVES using local representative data, and defaults were applied for other required datasets such as vehicle age distribution, which may impact the estimated emissions and emission factors. In addition, hourly link speeds were calculated in this study to characterize the impact of vehicle travelling speed on emissions. A single average speed was estimated at each hour for each link, which was then used to retrive appropriate emission factors. It was recommended that to apply a "speed profile", rather than a single speed value, to better characterize the impact of speed on emission (U.S. environmental Protection Agency, 2012c). However this approach was not applied due to lack of information.

When estimating biogenic emissions, an old but standalone version of BEIS model (version 2.3) was used. The latest version of BEIS model (version 3.12) was built into SMOKE (Sparse Matrix Operator Kernel Emissions) model, which is an emission processing software designed for CMAQ model (University of North Carolina at Chapel Hill, 2010). However it is infeasible to run SMOKE model due to lack of data. In addition, it was assumed all biogenic emissions were from forests while spatially allocating biogenic emissions. Other plant areas such as lawns may also contribute to

biogenic emissions, and they were neglected. However, emissions from these plant areas are not expected to be substantial.

5.4. Concentration Estimation

The estimated pollutant emissions, together with chemistry data, meteorological data and output data from the CMAQ model, were used to calculate ambient concentration levels of the five selected pollutants in Hillsborough County, FL. The CALPUFF model was used to estimate ambient pollutant concentrations due to local emissions. For acetaldehyde and formaldehyde, the CALPUFF estimated pollutant concentrations were further combined with concentration estimated from the CMAQ model to account for atmospheric formations of acetaldehyde and formaldehyde. Methods used in concentration estimation are presented below, followed by results and discussion.

5.4.1. Methods of Concentration Estimation

5.4.1.1. Source Specifications

First, CALPUFF model was used to estimate the spatial and temporal distribution of concentrations for the five selected pollutants. For major roadway sources within Hillsborough County, each link was modeled individually as an area source (a rectangle). The use of area source representation for roadways is commonly found in previous studies (Cook et al., 2008; Isakov & Venkatram, 2006; Stein et al., 2007). The widths of the area sources for major roadway links are calculated as:

$$w_l = m_l + n_l w$$

where w_l is the width of the area source for link l; m_l is the median width of link l; n_l is the number of lanes for both directions on link l; and w, the width of each lane, is

assumed to be 3.65 m (Kinnee et al., 2004). A maximum aspect ratio of 10 was applied for each area source. This value is recommended for dispersion modeling (U.S. Environmental Protection Agency, 2004b). The total number of sources generated for major roadways are approximately 4800.

For other emission sources, including minor roadways within Hillsborough County, on-road mobile sources in surrounding counties, non-point, non-road mobile sources and biogenic sources, the emission grids (Figure 5.6) were modeled as area sources. Overall, there are approximately 4800 area sources for 1,3-butadiene, benzene and NO_x, and 5300 area sources for acetaldehyde and formaldehyde.

The same effective release height (1.5 m) and effective rise velocity (1.5 m/s) as used in Chapter 4 were used in dispersion modeling. The initial vertical dispersion parameter (σ_z) was used in model calibration. A value of 100 m was assigned to area sources located in the downtown Tampa area and 30 m was assigned to other area sources. Some of the recommendations for initial vertical dispersion parameters are provided by U.S. Environmental Protection Agency (2004b). The use of 100 m and 30 m for initial vertical dispersion parameters are justifiable for two reasons: a) Many high-rise buildings are located in downtown Tampa, these buildings will lead to substantial vertical mixing, hence a higher value of initial vertical dispersion parameter is needed; b) The chosen values of 30 m and 100 m are still within a reasonable range.

5.4.1.2. Terrain and Meteorological Data Preparation

Meteorological data are critical in dispersion modeling as it directly impacts how pollutants are transported in the atmosphere. In this study, the CALMET model was used to generate a new meteorological dataset for CALPUFF. CALMET is the meteorological

processor for CALPUFF. It has the capability to produce three-dimensional meteorological field data (such as wind and temperature) by incorporating multiple datasets such as geophysical, surface and upper air observations, precipitation, and outputs from other numerical meteorological models.

The size of the selected meteorological domain is 400 km by 400 km, centered in Hillsborough County. This was to capture the re-circulation of pollutants due to land sea breeze, which is common in coastal area such as the Tampa area. In this study, seven datasets were input into the CALMET model: terrain elevation, land use and land cover, surface meteorological observation, upper air sounding, precipitation, buoy data and output data from MM5 (Fifth-Generation Penn State/NCAR Mesoscale Model) (Dudhia et al., 2005). Among these datasets, surface meteorological observation, upper air sounding, and precipitation data were obtained from VISTAS (Visibility Improvement State and Tribal Association of the Southeast) (Morris et al., 2007). Below a brief description of the other datasets are provided.

Two datasets were used to generate terrain elevation data for CALMET: SRTM1 (Shuttle Radar Topography Mission, version 2.1) (http://dds.cr.usgs.gov/srtm/) and USGS90 (U.S. Geological Survey) DEM (Digital Elevation Models) data (http://edc2.usgs.gov/geodata/index.php). Resolution of the data is 1 arc second (approximately 30 m) for SRTM1 and 3 arc seconds (approximately 90 m) for USGS90. Missing values were found for SRTM1 data at some areas in the northern part of the domain, and the missing data were replaced with USGS90 data. The study area is a coastal area. To correct any potential errors in the collected terrain data regarding the shape of coastlines, another dataset that contains accurate representations of coastline

shapes, the GSHHS (Global Self-consistent, Hierarchical, High-resolution Shoreline Database) (http://www.ngdc.noaa.gov/mgg/shorelines/gshhs.html) was applied. The 1992 National Land Cover Database (NLCD) (http://www.mrlc.gov/), with 30 m resolution, was used to generate land use and land cover data for CALMET.

Buoy data refer to data obtained from buoys deployed in the sea, which collect air and water temperatures, as well as wind and wave parameters. Eight buoy stations were identified for 2002 and data from these buoys were collected from the National Oceanographic Data Center (NODC) (http://www.nodc.noaa.gov/) and the National Data Buoy Center (NDBC) (http://www.ndbc.noaa.gov/). The collected data were further processed for CALMET using the BUOY processor, which is part of the CALMET model.

The collected meteorological observation data (surface and upper air) are at discrete locations. Outputs from numerical meteorological models provide continuous meteorological field information that is important for dispersion modeling. Here, output from MM5 model was obtained from VISTAS (Visibility Improvement State and Tribal Association of the Southeast) and were further processed using CALMM5, which is a processor designed to extract MM5 data to be used by CALMET model. Spatial and temporal resolution of the raw MM5 data is 12 km and 1 hour.

The CALMET model was then used to generate a meteorological dataset for CALPUFF. Spatial and temporal resolution of the generated dataset is 1 km and 1 hour. The generated data were also compared with an evaluation dataset provided by VISTAS (Visibility Improvement State and Tribal Association of the Southeast), which has 4 km spatial resolution and 1 hour temporal resolution. The evaluation dataset were produced

externally by CALMET. Comparisons indicate limited improvements for the new datasets over the evaluation dataset, which was mainly due to the spatial resolution of MM5 data used. In addition, the new meteorological dataset requires massive computational resources, which limited its usage. Therefore, the evaluation dataset were used in dispersion modeling, and the newly generated new dataset was not used.

5.4.1.3. Chemical Deposition Parameters

After being released into the atmosphere, pollutants also undergo removal processes including dry and wet deposition. Dry deposition is the removal of pollutants when they come into contact with the surface (earth surface or plant cover), and wet deposition refers to the removal of pollutants through precipitation.

In CALPUFF model, five parameter determines pollutant removal through dry deposition: diffusivity, alpha star, reactivity, Henry's law constant and mesophyll resistance. CALPUFF default dry deposition parameters for NO_x was used. Parameters for 1,3-butadiene, benzene and formaldehyde were obtained from Traisantikul (2008). Regarding acetaldehyde, its diffusivity was estimated as (Lyman et al, 1990):

$$D = \frac{10^{-3} T^{1.75} \sqrt{\frac{1}{M_A} + \frac{1}{M_B}}}{P\left(V_A^{\frac{1}{3}} + V_B^{\frac{1}{3}}\right)^2}$$

where D is the estimated diffusivity for acetaldehyde (cm^2/s); T is temperature, which was assumed to be 298.15 K; P is atmospheric pressure, which was assumed to be 1 atm; M_A and M_B is the molecular weight of the air (28.97 g/mol) and acetaldehyde (44.05 g/mol); V_A and V_B is the molar volume of the air (20.1 cm^3/mol) and acetaldehyde (46.4 cm^3/mol).

Alpha star (α*) is the solubility enhancement factor as a result of aqueous phase dissociation of the pollutant. It was assumed to be 1. Reactivity parameters of acetaldehyde was assumed to be 10. Henry's law constant was obtained from R. Sander (1999) and converted to dimensionless (gas/liquid). Mesophyll resistance was calculated as (Wesely, 1989; Traisantikul, 2008):

$$R_m = \frac{1}{\left(\frac{0.034}{H} + 100 f_0\right)}$$

where R_m is the estimated mesophyll resistance for acetaldehyde (s/m); H is Henry's law constant; f_0 is a constant. It is 1.0 for ozone, titanium tetrachloride and divalent mercury; 0.1 for nitrogen oxide and 0 for other substances. Here the value 0 is used.

Table 5.6 Dry and wet deposition parameters for the five selected pollutants

	NO_x	1,3-butadiene	acetaldehyde	benzene	formaldehyde
diffusivity (cm^2/s)	1.7E-1	1.01E-01	1.28E-01	8.96E-02	1.72E-01
alpha star	1	1	1	1	1
reactivity	8	10	10	10	10
mesophyll resistance (s/cm)	5	6.09E+03	8.59E-04	1.64E+02	9.41E-03
henry's law coefficient (dimensionless)	3.5	8.50E+00	2.92E-03	2.29E-01	1.31E-05
liquid precipitation scavenging coefficient (1/s)	0	6.37E-03	2.19E-06	1.72E-04	9.86E-09
frozen precipitation scavenging coefficient (1/s)	0	0	0	0	0

Two parameters determine the wet deposition of pollutants in CALPUFF model: scavenging coefficients for liquid precipitation, as well as frozen precipitations. Unit of the coefficients is 1/s. Default parameters for NO_x were used. Scavenging coefficients of liquid precipitation for other pollutants were estimated by simple scaling from the coefficient of SO_2 using their corresponding Henry's law constant. Frozen precipitation

coefficients were set to 0 since no frozen precipitation occurred in the study area in 2002. The estimated dry and wet deposition parameters are provided in Table 5.6.

5.4.1.4. Chemical Reaction Mechanisms

To account for atmospheric reactions of the chosen pollutants, the default reaction algorithm MESOPUFF II was applied for NO_x. In the MESOPUFF II algorithm, the loss rates of NO_x is statistically determined by a combination of conditions such as solar radiation intensity, temperature, atmosphere stability class, background ozone concentration and NO_x concentration (Scire et al., 2000). Monthly averaged ammonia concentrations needed for the chosen algorithm were extracted from CMAQ data obtained from Community Modeling and Analysis (CMAS) (http://www.cmascenter.org/), and hourly background ozone concentrations were provided by the Visibility Improvement State and Tribal Association of the Southeast (VISTAS).

For other pollutants, diurnal loss rates were applied. The loss rates were manually calculated considering reactions listed in Table 5.7. The selection of reaction pathways were based on the fate of each pollutant in the atmosphere (Finlayson-Pitts & Pitts, 1999; Jacobson, 2005; Seinfeld & Pandis, 1997).

Table 5.7 Reactions included for the 1,3-butadiene, benzene, acetaldehyde and formaldehyde

	OH radical	NO_3 radical	ozone	photolysis
1,3-butadiene	✓	✓	✓	
acetaldehyde	✓	✓		✓
benzene	✓			
formaldehyde	✓	✓		✓

For radical and ozone reactions, fractional loss rates (percentage per hour) at every hour of the year were calculated by assuming pseudo-first order reaction within each hour:

$$l_{p,h} = 1 - e^{-1/t_{p,h}}$$

$$t_{p,h} = \left(\sum_{r=1}^{n} \frac{1}{k_{p,r} C_{r,h}} \right) / 3600$$

where $l_{p,h}$ is the loss rate of pollutant p at hour h; and $t_{p,h}$ is the e-folding time (hour) of pollutant p at hour h due to atmospheric reactions; r is the current reactant with which pollutant p reacts; n is the total number of reactants; $k_{p,r}$ is the reaction rate constant ($cm^3 molecules^{-1} s^{-1}$) for the reaction between pollutant p and reactant r; and $C_{r,h}$ is the concentration of reactant r (molecules/cm^3) at hour h.

Table 5.8 Reaction rate constants for radical and ozone reactions

	reaction rate constants ($cm^3 molecules^{-1} s^{-1}$)		
	OH radical	NO_3 radical	ozone
1,3-butadiene	6.66E-11	1.00E-13	6.30E-18
acetaldehyde	1.50E-11	2.40E-15	
benzene	1.30E-12		
formaldehyde	8.50E-12	5.80E-16	

Hourly concentrations of hydroxyl radical (OH) and ozone were extracted from CMAQ data obtained from Community Modeling and Analysis (CMAS) (http://www.cmascenter.org/). Concentrations of nitrate radical (NO^3) were interpolated using sine curve and assuming 20 pptv concentration at midnight (12 am) (Yvon et al., 1996) and 0 pptv at mid-day (12 pm). Reaction rate constants for radical and ozone reactions were obtained from a number of sources (Agency for Toxic Substances and Disease Registry, 2007, 2009; Finlayson-Pitts & Pitts, 1999; Jacobson, 2005; Liu et al., 1999; Sander et al., 2011; Seinfeld & Pandis, 1997) and are shown in Table 5.8.

Photolysis reactions were also considered for acetaldehyde and formaldehyde, and hourly rate constants were calculated using methods from Finlayson-Pitts and Pitts (1999):

$$k_{p,h} = \sum \phi(\Delta\lambda)\sigma(\Delta\lambda)F_h(\Delta\lambda)$$

where $k_{p,h}$ is the estimated photolysis rate constant (s^{-1}) for hour i; λ is the wavelength of incoming solar radiation (nm); $\phi(\Delta\lambda)$ is the primary quantum yield of pollutant molecules averaged over $\Delta\lambda$; $\sigma(\Delta\lambda)$ is the absorption cross section (cm^2) of the pollutant, averaged over $\Delta\lambda$; $F_h(\Delta\lambda)$ is the actinic flux ($cm^{-2}s^{-1}$) at hour h, summed over $\Delta\lambda$; The wavelength interval ($\Delta\lambda$) used in the calculation is 2 nm and the range of wavelengths used in the calculation are 296-332 nm and 296-360 nm for acetaldehyde and formaldehyde, respectively. The same method was also used in CMAQ model for the calculation of photolysis rate constants (Byun & Schere, 2006).

The actinic flux reflects how much energy is available in the incoming solar radiation to pollutant molecules. Data on actinic flux were obtained from (Finlayson-Pitts & Pitts, 1999), and were adjusted using hourly solar zenith angle data obtained from National Solar Radiation Database by linear interpolation. Quantum yield and absorption cross section data were obtained from (Sander et al., 2011).

The calculated hourly loss rates were then averaged for three time periods: January to February, March to October and November to December, for computational tractability. The calculated diurnal loss rates are shown in Figure 5.13.

For all pollutants, the highest loss rates are observed around 1-2 pm within each time period. Among the three time periods, March to October has the highest rates. Reactions with the OH radical are responsible for such observations, as the concentrations of OH radical is highly related with the intensity of solar radiations. For

1,3-butadiene, slightly higher loss rates were observed at midnight, due to its reaction with NO_3 radicals at night. Among the three pollutants, benzene is the least reactive; hence, the lowest loss rates are observed. The estimated loss rates for the four pollutants are equivalent or on the same order of magnitude as those documented in previous literatures (Millet et al, 2010; Lowe & Ulrich, 1983; Dollard et al, 2001; Rasmussen & Khalil, 1983)

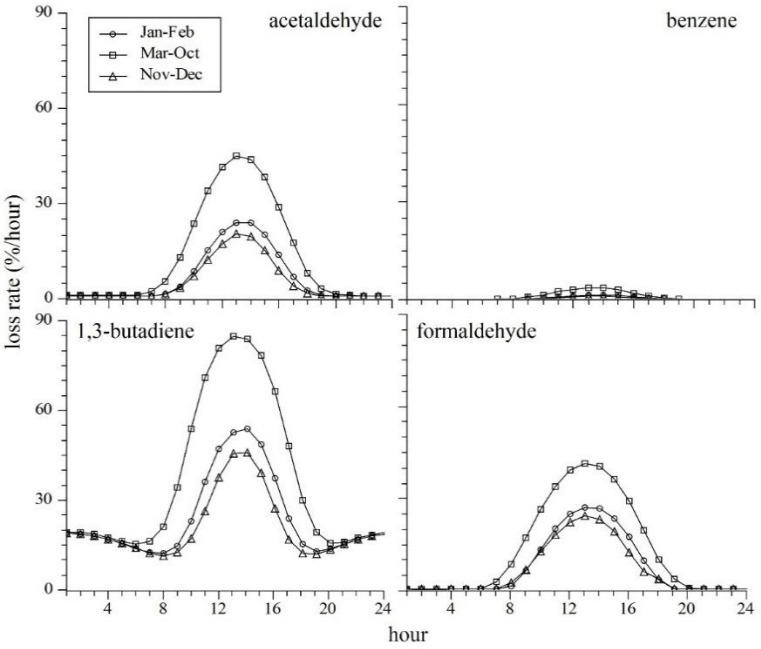

Figure 5.13 Estimated diurnal loss rates of four pollutants.

5.4.1.5. Receptor Specifications

A receptor is a user specified location where pollutant concentrations will be estimated. For 1,3-butadiene, benzene and NO_x, hourly pollutant concentrations were modeled at 1 km receptor grids covering Hillsborough County, as well as at the centroid of 795 census block groups in Hillsborough County, for the entire year of 2002. Concentrations at the locations of monitoring stations of corresponding pollutants were also modeled for the purpose of model evaluation. For acetaldehyde and formaldehyde, the 1 km receptor grids were extended to cover all CMAQ grids that entirely or partially

overlaid on Hillsborough County. The two receptors networks used in CALPUFF modeling were shown in Figure 5.14. Different receptor networks for acetaldehyde and formaldehyde were used for the purpose of combining CALPUFF results with pollutant concentrations estimated by CMAQ model (see section 5.4.1.7).

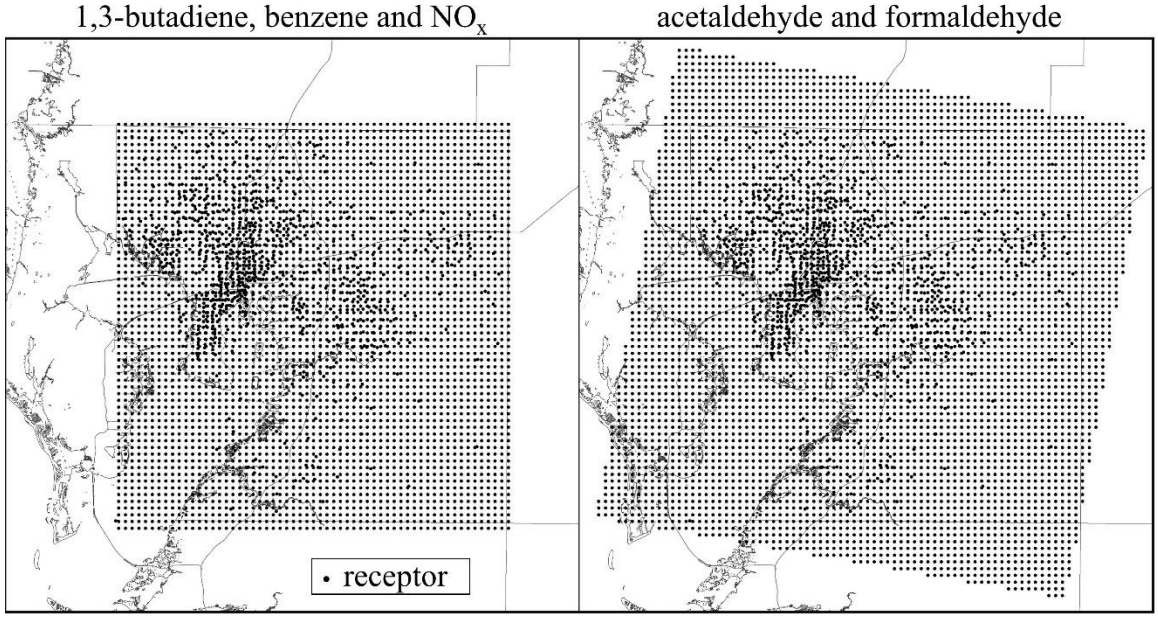

Figure 5.14 Receptor grids used in CALPUFF modeling.

5.4.1.6. Model Execution

Due to the large amount of emissions sources, the whole modeling process was split into 447 cases, which were executed in parallel on the high performance computing cluster at University of South Florida: the CIRCE. The results were combined afterward. For pollutants other than NO_x, the whole year were also split into 3 time periods (January-February, March-October, and November-December) and the previously developed reaction loss rates were applied. A two days overlapping time were applied between time periods for model spin up purposes.

Hourly NO_x concentrations were measured by two regulatory monitoring stations in Hillsborough County in 2002: Gandy (monitor ID: 12-057-1065-42602-1) and

Simmons Park site (monitor ID: 12-057-0081-42602-1) (Figure 5.15). Monthly averaged NO_x concentration measured at Gandy site were used to calibrate the CALPUFF model, by adjusting the initial vertical dispersion parameter. The model is considered calibrated until CALPUFF estimate NO_x concentrations (monthly average) at the Gandy site are comparable with measured concentrations.

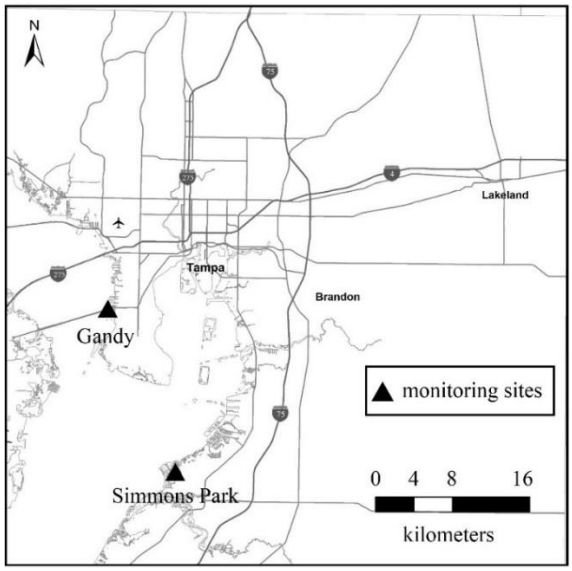

Figure 5.15 Location of regulatory pollutant monitoring sites located within Hillsborough County as of 2002.

5.4.1.7. Combining Background Concentrations

For acetaldehyde and formaldehyde, CALPUFF modeled pollutant concentrations were combined with hourly concentrations from the CMAQ model to account for contributions to pollutant concentrations from other processes not modeled by the CALPUFF model, such as atmospheric formation of pollutants.

As discussed in Chapter 2, two approaches have previously been used to blend concentration estimates from Eulerian grid chemical transport models with dispersion models: simple addition (Cook et al., 2008; Lobdell et al., 2011), and combination of background concentrations from Eulerian grid models with local concentration variability

derived from dispersion models (Isakov et al., 2007). The approach of simple addition has double-counting issues, but there are also substantial uncertainties in the second approach, due partially to fundamentally different designs of the two types of models. In this study, a new empirical based method was developed and applied.

First, in hour *h*, average concentrations as modeled by CALPUFF across all CALPUFF receptors ($C_{h,p}$), as well as average concentrations as modeled by CMAQ across all CMAQ grid cells covering Hillsborough County ($C_{h,q}$), are calculated:

$$C_{h,p} = \frac{\sum_{r=1}^{n} C_{h,p,r}}{n}$$

$$C_{h,q} = \frac{\sum_{g=1}^{m} C_{h,q,g}}{m}$$

where $C_{h,p,r}$ is the pollutant concentration as modeled by CALPUFF at CALPUFF receptor *r* in hour *h*, n is the total number of CALPUFF receptors; $C_{h,q,g}$ is the pollutant concentration as modeled by CMAQ in CMAQ grid cell *g* in hour *h*; and *m* is the total number of CMAQ grid cells;

Generally, spatial averages from the CALPUFF model are expected to be lower than those from the CMAQ model because CMAQ modeling included emissions from outside of the CALPUFF modeling domain, as well as atmospheric formations of pollutants. However, these conditions may not always be met here because of the following reasons: a) CALPUFF and CMAQ models have fundamentally different model design. Although results from the two models are expected to be consistent at larger temporal scale (such as annual average), inconsistent results may occur at very short temporal scale (such as hourly); b) On-road mobile source emissions were estimated by MOVES model in this study (see section 5.4.1.1), whereas in CMAQ modeling, on-road

mobile source emissions were estimated by MOBILE series model. Comparison show significant differences between the modeling results (Table 5.3). The differences in emissions may also lead to higher concentration estimates from CALPUFF model.

For hours when spatially averaged concentrations from CALPUFF are larger than that for CMAQ, no blending is performed and CALPUFF estimated pollutant concentrations are used as final concentrations. For other hours, spatially averaged CALPUFF concentrations were first subtracted from CMAQ spatial averages, and the differences were then spatially distributed to each CMAQ grid cell proportional to CMAQ estimated concentrations in corresponding grid cells. Third-order local polynomial interpolation was then used to estimate adjusted CMAQ concentrations at each CALPUFF receptor location, assuming the distributed CMAQ concentrations are originally at the centroids of the CMAQ grid cells. The interpolated concentrations represent the concentrations of the pollutants that were not captured by the CALPUFF model, i.e., due to impact of emissions from outside of CALPUFF modeling domain and atmospheric formations. Finally, the interpolated CMAQ concentrations were combined with CALPUFF modeled pollutant concentrations at each receptor. This approach was applied for acetaldehyde and formaldehyde, and for all hours included in CALPUFF modeling (whole year of 2002).

5.4.1.8. Model Evaluation

The modeled pollutant concentrations were compared with measured pollutant concentrations at Simmons Park regulatory monitoring sites to evaluate the performance of the model. NO_x was chosen as the evaluation species due to the availability of hourly measurement data.

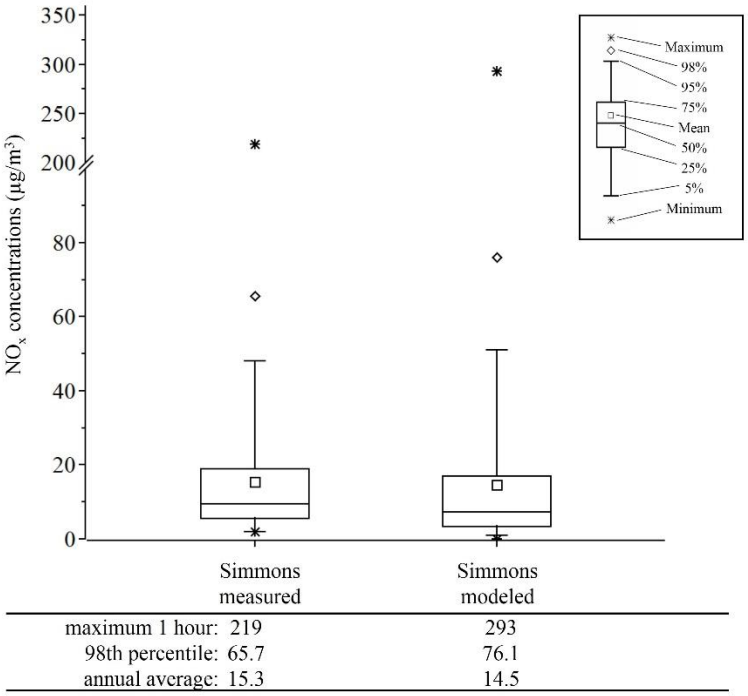

Figure 5.16 Box plot of measured and modeled hourly NO_x concentration distributions at Simmons Park regulatory monitoring site

Figure 5.16 provides a box plot of the modeled and measured hourly NO_x concentration distributions at the Simmons Park monitoring site. The CALPUFF model reasonably captured the statistical distributions of hourly NO_x concentrations, specially the four quartiles, as well as the 98th percentile of concentration distributions.

Pollutant concentrations at different temporal scales are needed to appropriately characterize both short-term and long-term air pollution exposures. Additional statistics are provided in Table 5.9 to further evaluate the performace of CALPUFF model at three different temporal scales: monthly average, weekly average and hourly concentrations.

The calculated values of biases are all negative, indicating that the CALPUFF model slightly underpredicts NO_x concentrations. Magnitude of normalized bias, root mean squared error, standard deviation of residuals and absolute average gross error increases steadily from monthly to hourly metric, indicating more "spread out"

distributions of prediction error, and suggesting degrading model performance with increasing temporal resolution. In addition, the decreasing correlation coefficient indicates that less variations in NO_x concentrations were captured by CALPUFF model with increasing temporal resolution.

Table 5.9 Performance of the CALPUFF model at three temporal scales

statistics	monthly	weekly	hourly
bias ($\mu g/m^3$)	-0.71	-0.77	-0.78
normalized bias (%)	-0.3%	2.1%	35%
root-mean-squared error ($\mu g/m^3$)	3.1	6.1	22
standard deviation of residuals ($\mu g/m^3$)	3.0	6.0	22
absolute average gross error ($\mu g/m^3$)	2.7	4.1	12
correlation coefficient (R)	0.84	0.54	0.31

Overall, best model performance is observed for monthly scale. Model performance generally degrades with the increase of temporal resolution. This result is expected as numerous factors impact short term air pollution concentrations, hence it is infeasible for air quality models to accurately capture pollution concentration variations at very high temporal resolutions given its near stochastic nature.

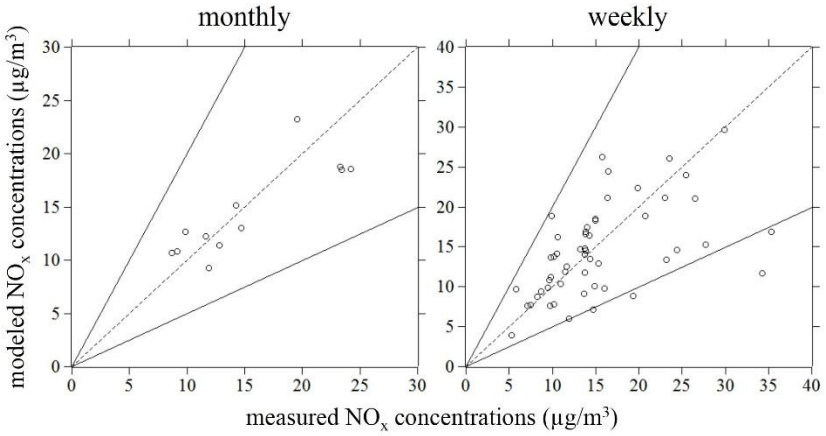

Figure 5.17 Scatter plots of the measured versus modeled NO_x concentrations at three temporal scale.

In air quality modeling, it is generally recognized that model performace is considered reasonable when the modeled concentrations are within a factor of two of the

measured concentrations. Figure 5.17 provides scatter plots of the measured and modeled NO_x concentrations at monthly and weekly temporal scale at the Simmons Park site. The dashed line indicates a 1:1 match and the solid lines indicate a 1:2 or 2:1 ratio between the modeled and measured NO_x concentrations. The percentages of measured NO_x concentrations that are within a factor of two of the modeled concentrations are 100% for monthly and 92% for weekly scales, and suggest good model performance.

5.4.2. Results of Concentration Estimation

5.4.2.1. Estimated NOx Concentrations

Spatial distributions of the estimated annual average, 98th percentile of hourly and highest 1 hour NO_x concentrations are shown in Figure 5.18. Also shown in Figure 5.18 are the previously modeled NO_x concentration distributions, for which only stationary point and on-road mobile source emissions were included, in which the MOBILE6.2 model was used to estimate on-road emissions from major roadways. Further, Figure 5.19 provides population density distributions of black, white population subgroups, as well as annual household income less than $20,000 and more than $100,000 population subgroups.

The modeled pollutant concentrations are generally higher in the updated modeling results, due primarily to the inclusion of more emission sources (non-road, non-point and biogenic sources). At annual average and 98th percentile temporal scales, both previously modeled and the updated NO_x concentration distributions show roadway dominated patterns. In previous modeling results, the modeled highest NO_x concentrations at all three temporal scales are found near the downtown Tampa area, whereas in the updated modeling results, the highest NO_x concentrations are also found

near the Tampa International Airport area. The including of non-road mobile source emissions from airports likely contribute to this observations. At the highest 1 hour temporal scale, no apparent spatial patterns can be observed due primarily to large amount of uncertainties involved in short-term pollutant concentrations. In addition, the modeled highest NO_x concentrations are co-located with highest population density of some population subgroups such as black and the lowest income subgroup (annual household income less than $20,000) (Figure 5.19), and hence these population subgroups are potentially exposed to higher NO_x concentrations.

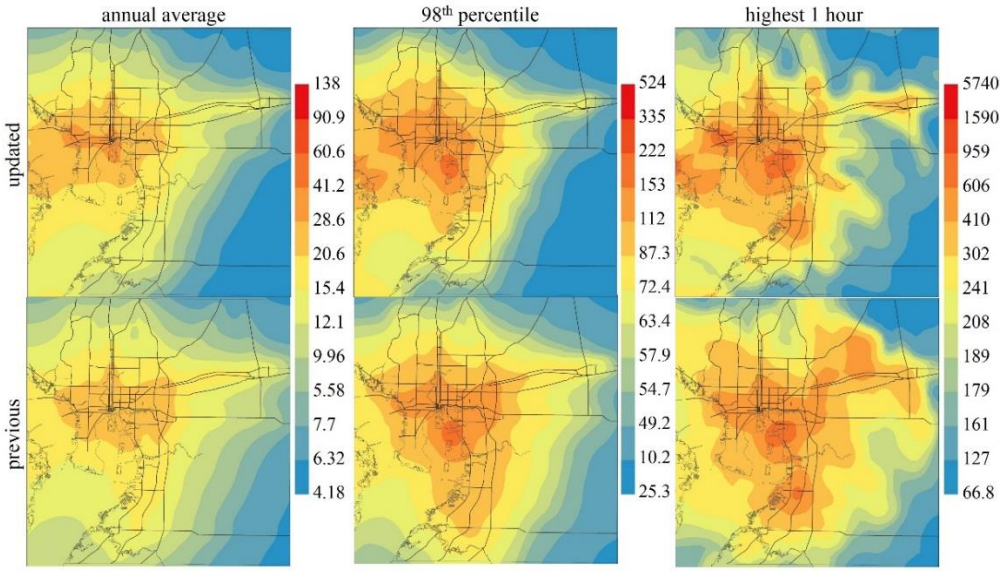

Figure 5.18 CALPUFF modeled annual average, 98th percentile and highest 1 hour NO_x concentrations in the Tampa area (Hillsborough County, FL). Previous modeling results including only stationary point and on-road mobile source emissions are also shown. Maps were generated using kriging from concentration data at CALPUFF receptors.

Table 5.10 shows a summary of NO_x concentrations in previous modeling results and updated modeling results. NO_x concentrations in the updated modeling results are generally higher and show more variations. The National Ambient Air Quality Standard (NAAQS) sets regulatory standards for NO_2. Assuming standard ambient temperature and pressure, the standards for NO_2 are equivalent to 100 $\mu g/m^3$ and 188 $\mu g/m^3$, at annual

and 98th percentile temporal scales. At both temporal scales, the domain averaged NO_x concentrations in the updated modeling are below NAAQS standard, but concentrations at some of the receptor locations exceeded the standard (Figure 5.20). These receptors are located near Tampa International Airport and Port Sutton area, where non-road emissions are high. However it needs to be noted that here the modeled NO_x concentrations are compared with national ambient air quality standards for NO_2, and NO_x is comprised of NO and NO_2. A previous study (Poor, 2008) has estimated a fraction of NO_x that is NO_2 at 0.8 in the Tampa area.

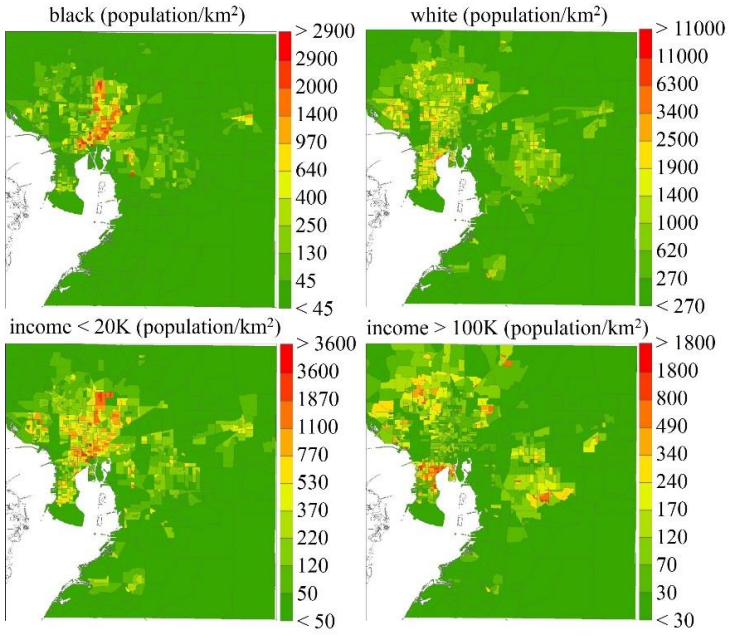

Figure 5.19 Population density distributions (year 2000) in census block groups for black, white, annual household income less than $20,000 (income < 20K) and more than $100,000 (income > 100K) population subgroups.

Table 5.10 Summaries for NO_x concentrations in previous modeling results and updated modeling results.

spatial statistic	temporal statistic		
	annual average	98th percentile	highest 1 hour
domain average	14(12)	72(69)	262(254)
standard deviation	7(5)	32(24)	150(122)
range	4-138(5-44)	25-524(36-231)	67-2738(100-1591)

* Concentration values shown in parentheses are results from previous modeling

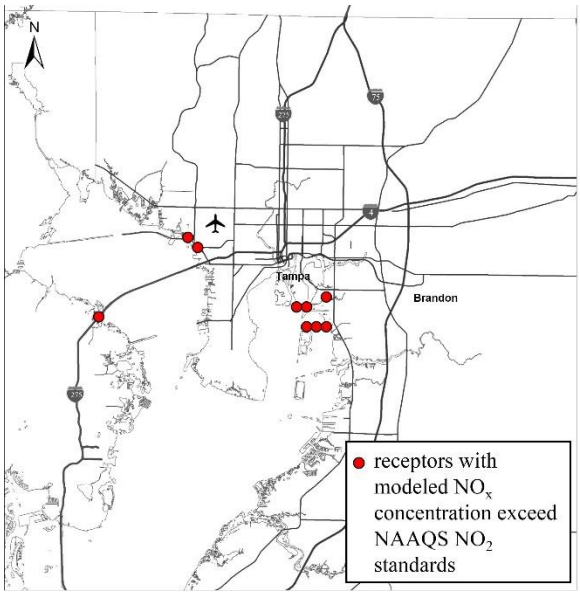

Figure 5.20 Locations of receptors with modeled NO_x concentrations exceed NAAQS NO_2 standards.

5.4.2.2. Estimated 1,3-butadiene and Benzene Concentrations

The spatial distributions of estimated 1,3-butadiene and benzene concentrations at annual and highest 1 hour temporal scales are shown in Figure 5.21. Additionally, summaries for modeled 1,3-butadiene and benzene concentrations are provides in Table 5.11. Unlike NO_x, 1,3-butadiene and benzene were not included in previous modeling.

Table 5.11 Summaries for modeled 1,3-butadiene and benzene concentrations

spatial statistic	1,3-butadiene		benzene	
	temporal metrics ($\mu g/m^3$)		temporal metrics ($\mu g/m^3$)	
	annual average	highest 1 hour	annual average	highest 1 hour
domain average	0.012	0.24	0.19	3.4
standard deviation	0.007	0.18	0.085	1.8
range	0.003-0.21	0.04-4.8	0.07-2.0	1.1-45

Regarding the spatial distributions of 1,3-butadiene and benzene concentrations, the roadway dominated pattern can still be observed, although not as apparent as that for NO_x. Highest pollutant concentrations are also found near the airport area at the annual

temporal scale, and no apparent spatial patterns can be observed at the highest 1 hour temporal scale.

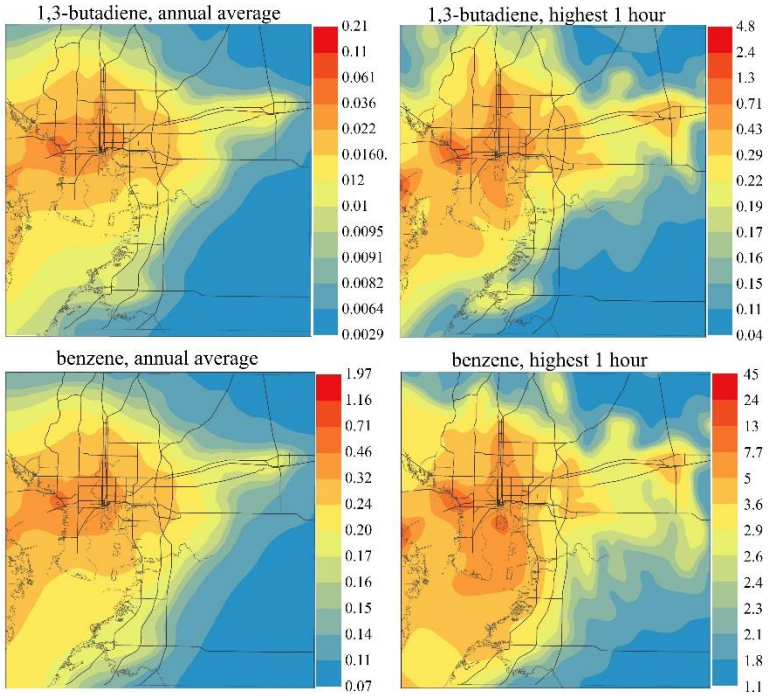

Figure 5.21 CALPUFF modeled annual average and highest 1 hour 1,3-butadiene and benzene concentrations in the Tampa area (Hillsborough County, FL). Maps were generated using kriging from concentration data at CALPUFF receptors.

5.4.2.3. Estimated Acetaldehyde and Formaldehyde Concentrations

For acetaldehyde and formaldehyde, a special approach was used to estimate their concentrations (see section 5.4.1.7), where CALPUFF modeled pollutant concentrations were combined with CMAQ data to account for contributions from processes not modeled by CALPUFF, such as atmospheric formations. Figure 5.22 provides spatial concentration distributions of the two pollutants. Both concentrations as modeled by CALPUFF model, and estimated final pollutant concentrations are shown in the Figure. Summaries of the modeled pollutant concentrations are provided in Table 5.12 and Table 5.13.

Spatial distributions of CALPUFF modeled acetaldehyde and formaldehyde concentrations show similar patterns: at annual temporal scale, generally higher pollutant concentration are found in urbanized areas, and contributions from major roadways are visible. No spatial patterns can be observed for highest 1 hour temporal scale.

Table 5.12 Concentration summaries for the modeled acetaldehyde concentrations

spatial statistic	CALPUFF[1] (μg/m^3)		Combined[2] (μg/m^3)	
	average	maximum	average	maximum
domain average	0.068	1.6	2.0	8.4
standard deviation	0.022	0.48	0.16	1.3
range	0.02-0.4	0.68-8.4	1.64-2.4	6.3-12.4

[1]Pollutant concentrations as modeled by CALPUFF; [2]Combined pollutant concentrations from both CALPUFF and CMAQ model

Table 5.13 Concentration summaries for the modeled formaldehyde concentrations

spatial statistic	CALPUFF[1] (μg/m^3)		Combined[2] (μg/m^3)	
	average	maximum	average	maximum
domain average	0.098	2.1	1.8	8.4
standard deviation	1.047	1.05	0.11	1.8
range	0.03-0.9	0.74-57	1.5-2.5	5.2-57

[1]Pollutant concentrations as modeled by CALPUFF; [2]Combined pollutant concentrations from both CALPUFF and CMAQ model

After combining with CMAQ data, spatial concentration distributions of the two pollutants were changed substantially, especially for acetaldehyde. Concentration levels of the two pollutants were also significantly elevated (Table 5.12 and Table 5.13). These observations indicate that processes not modeled by the CALPUFF model (mainly atmospheric formations) contribute substantially to acetaldehyde and formaldehyde concentrations. This finding confirms the necessarily of combining CMAQ data with CALPUFF modeling results in this study.

5.4.3. Discussion of Concentration Estimation

The estimated pollutant concentration distributions for 1,3-butadiene, benzene and NO_x (updated modeling results) (Figure 5.18, Figure 5.21 and Figure 5.22) at different temporal scales show generally higher pollutant concentrations at urbanized areas such as downtown Tampa, Pinellas County, and Sarasota County. These areas are co-located with highest population density of some subgroups such as black and the lowest income subgroup, hence these subgroups are potentially exposed to higher pollutant concentrations. Regarding the spatial distribution of pollutant concentrations, the distributions change at different temporal scales. This finding suggest different patterns for acute and chronic exposures to air pollution, and pollutant concentration variations at multiple temporal scales should be appropriately characterized for the purpose of exposure estimation. Some air quality modeling methods, such as proximate based methods and land use regression, may not be able to appropriately capture pollutant concentration variation at multiple temporal scales; hence, caution should be taken when applying these methods for exposure estimation.

For acetaldehyde and formaldehyde, pollutant concentrations at their spatial distributions differs before and after combining with CMAQ data (Figure 5.22). The observed changes suggest atmospheric formations contribute substantially to acetaldehyde and formaldehyde concentrations. This finding is expected as the two chosen aldehydes are highly reactive in the atmosphere, and significant fractions of the two pollutants were formed in the air rather than directly emitted (Finlayson-Pitts & Pitts, 1999). The finding further stressed the importance of atmosphere chemistry when modeling for reactive pollutants such as acetaldehyde and formaldehyde.

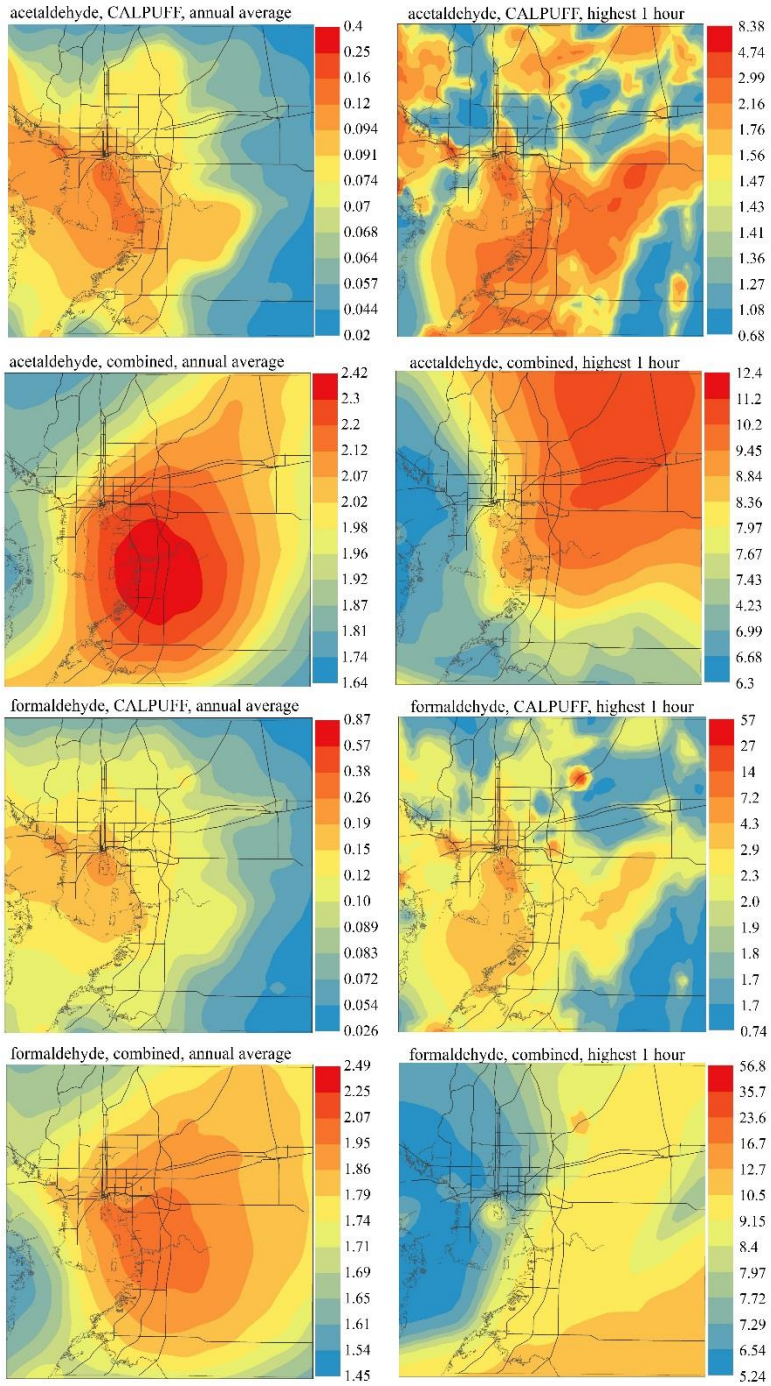

Figure 5.22 Annual average and highest 1 hour acetaldehyde and formaldehyde concentrations in the Tampa area (Hillsborough County, FL), as modeled by CALPUFF and combined with CMAQ data.

5.4.4. Limitation and Uncertainties of Concentration Estimation

Meteorological data used in dispersion modeling could contribute to uncertainties in the estimated pollutant concentrations. The meteorological data were obtained from

Visibility Improvement State and Tribal Association of the Southeast (VISTAS). MM5 model outputs with 12 km spatial resolution were used to develop this dataset, which may not be sufficient to capture variation of meteorological field at 1 km resolutions. Further, meteorological observations, including surface measurements and upper air soundings, were blended into the dataset using the CALMET model, but this approach is not recommended (U.S. Environmental Protection Agency, 2009). Sensitivity analyses were performed, and the "blending" done by CALMET were found to impact modeling results (although the impact is generally small).

The approach used to combine CALPUFF modeling results with CMAQ data also contributes to uncertainties. As described in section 5.4.1.7, the approach used has not been rigorously evaluated. Other approaches have been tested, including inverse distance weighting and those based on geostatistics such as kriging. However they are either impractical or unable to produce convincing results. Discussion of the issues in combining spatially incompatible data are provided in Cressie et al. (2009). In addition, Li et al. (2013) presented a promising hierarchical model, which could contribute to part of the solution.

Other limitations include the use of simplified chemistry algorithm and the blending of CALPUFF and CMAQ data. The chemical loss rates used were calculated by considering several reaction pathways, which are not as conclusive as the chemistry algorithm implemented in Eulerian grid models such as carbon-bound IV. In calculations for photolysis, no cloud attenuations were considered and hence the calculated loss rates for photolysis may be overestimated.

5.5. Exposure and Inequalities Estimation

The estimated pollutant concentrations at multiple temporal scales were combined with 2000 census demographic data to estimate air pollution exposure, and exposure inequalities among different population subgroups. The chosen subgroups include race/ethnicity (black, Hispanic and white), age (age less than 5, between 5 and 65 and age more than 65 years old) and annual household income groups (less than $20,000, between $20,000 and $40,000, between $40,000 and $60,000, between $60,000 and $100,000 and more than $100,000). Methods and results of exposure and inequality estimation are presented in following sections.

5.5.1. Method of Exposure and Inequalities Estimation

Human exposure to air pollution, and exposure inequalities were estimated at census block group level. First, concentrations of the five selected pollutants were calculated at each census block group, using the previously estimated concentration data at CALPUFF receptor locations. For block groups with area less than 1 square kilometers, concentration estimates from receptor located at their centroids were assigned the corresponding block group. For block groups with area larger than 1 square kilometers, average concentrations were calculated from 1 km spaced receptor grids that are located within the corresponding block group.

The calculated block group concentrations were then combined with 2000 census data obtained from Florida Geographic Data Library (FGDL) (http://www.fgdl.org), using two metrics to quantitatively assess air pollution exposure and exposure inequalities: population weighted exposure and subgroup inequality index. The subgroup inequality index is estimated as:

$$I_{i,j,c} = \log\left(\frac{p_{i,jc,} / P_{j,c}}{F_i}\right)$$

Where $I_{i,j,c}$ is the estimated subgroup inequality index for subgroup *i* that live in area *j* within concentration interval *c*; $p_{i,j}$ is the population of subgroup *i* that live in area *j* within concentration interval *c*; $P_{j,c}$ is the total population in area *j* within concentration interval *c*; and F_i is the fraction the subgroup *i* of total county population. A positive index value suggests potential inequalities for the chosen subgroup *i* at corresponding concentration intervals. Air pollution exposure and exposure inequalities were estimated for each pollutant individually and the results are provided below.

5.5.2. Results of Exposure and Inequalities Estimation

5.5.2.1. Exposure and Inequalities for NOx

Table 5.14 provides the estimated population weighted exposure to NO_x air pollution for the chosen subgroups at three temporal scales. Among all subgroups, the black subgroup is exposed to the highest NO_x concentrations: 15% higher exposure than county average in annual and 98th percentile temporal scales and 22% higher in the highest 1 hour scale. The subgroup with the lowest income (less than $20,000) is exposed to the second highest NO_x concentrations at three temporal scales. Among race/ethnicity category, the white subgroup has the lowest NO_x exposure. Among income category, exposures show general decreasing trend with the increase of annual household income; although, exposures for the subgroup with the second highest income ($60,000-$100,000) are lower than that for the highest income subgroup. NO_x exposures for all age subgroups are generally close to the county average, with slightly higher exposures observed for people with older age (> 65).

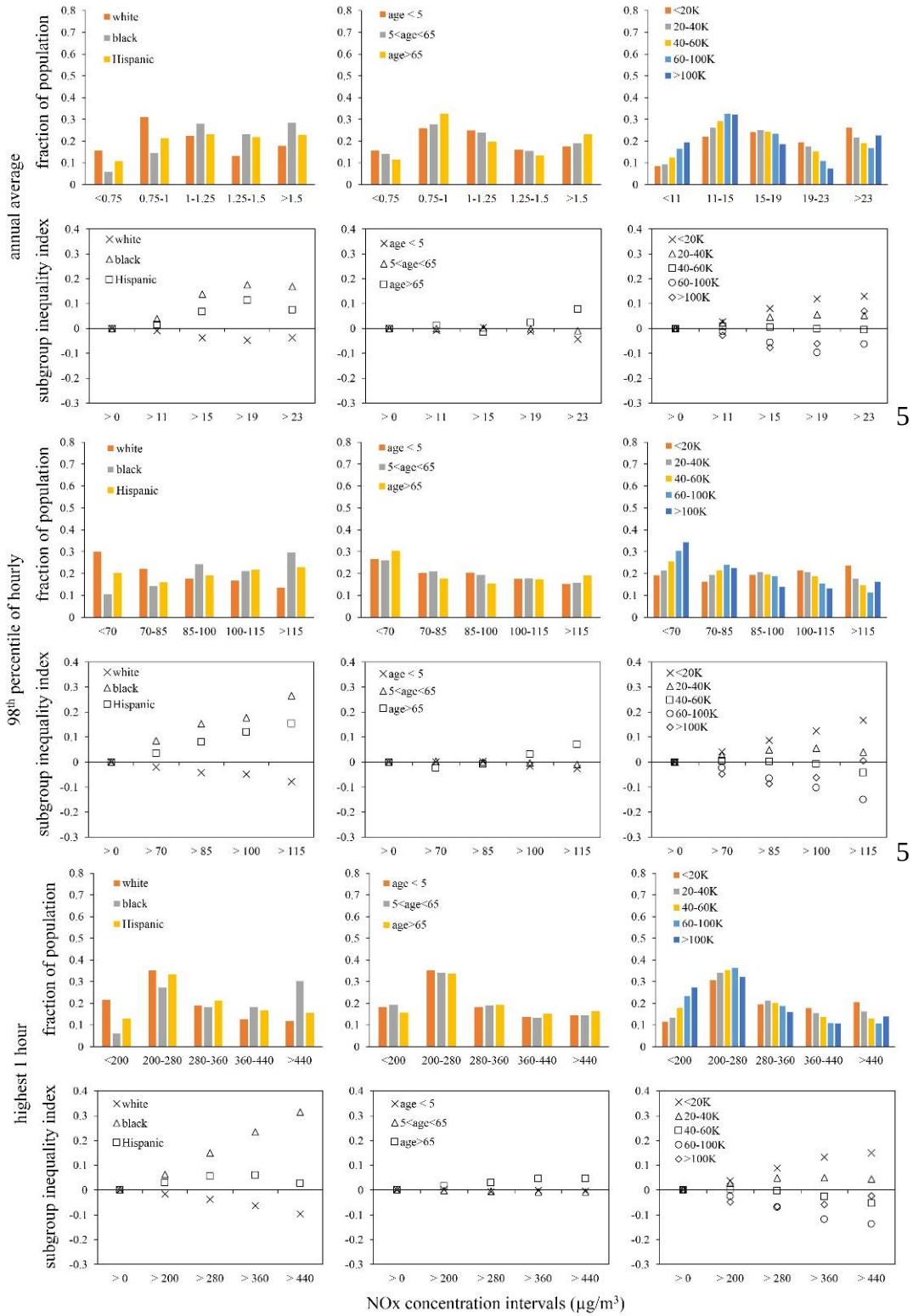

Figure 5.23 Population distributions of the chosen race/ethnic, age and income subgroups for annual average, 98th percentile of hourly and maximum 1 hour NO_x concentrations.

Figure 5.23 shows the population distribution of chosen subgroups at different NO_x concentration intervals. Black and Hispanic subgroups tend to live in areas with higher NO_x concentration and consistently have positive and generally increasing subgroup inequality indices with the increase of NO_x concentrations, while the estimated index value for white subgroup is consistently negative. Estimated subgroup inequality index for age subgroups are generally close to zero, although slightly positive index values are observed for subgroup with age more than 65 at the highest NO_x concentration interval. Among the income category, the fraction of population that are in higher concentration areas tend to decrease with increasing income; hence, the estimated inequality indices shows an overall decreasing trend with the increase of income.

Table 5.14 Population weighted exposure to NO_x for chosen subgroups

subgroups		temporal metrics ($\mu g/m^3$)		
		annual	98th percentile	highest 1 hour
race/ethnicity	black	19.9	102	375
	Hispanic	18.4	95	323
	white	16.6	86	294
age	age > 65	17.5	90	318
	age < 5	17.0	89	307
	age between	17.2	89	306
annual household income	< 20K	18.8	96	339
	20K - 40K	17.9	92	320
	40K - 60K	17.2	89	304
	> 100K	16.7	85	292
	60K - 100K	16.3	85	288
county average		17.2	89	308

Overall, the estimated population weighted exposure (as well as subgroup inequalities index) shows that black, Hispanic subgroups and the subgroup with the lowest income (less than $20,000) are disproportionately exposed to NO_x air pollution, while white and higher income subgroups (between $60,000-$100,000 and more than

$100,000) are disproportionately not exposed. Exposure inequalities for age categories are small, with slightly higher exposure observed for elder subgroup (age > 65).

5.5.2.2. Exposure and Inequalities for 1,3-butadiene and benzene

Table 5.15 shows estimated population weighted exposures to 1,3-butadiene and benzene for chosen population subgroups. Population distribution and corresponding subgroup inequality indices are provided in Figure 5.24 and Figure 5.25. Overall, distributions of population-weighted exposures among subgroups, as well as estimated inequality index for different subgroups are similar with those for NO_x. The same population subgroups (black, Hispanic and lowest income subgroups) were also found to be disproportionately exposed to 1,3-butadiene and benzene air pollution, and white and higher income subgroups are found to be disproportionately not exposed.

Table 5.15 Population weighted exposure to 1,3-butadiene and benzene for chosen subgroups

subgroups		1,3-butadiene		benzene	
		temporal metrics(μg/m^3)		temporal metrics(μg/m^3)	
		annual	highest 1 hour	annual	highest 1 hour
race/ethnicity	black	0.020	0.42	0.28	4.85
	Hispanic	0.018	0.35	0.26	4.27
	white	0.016	0.31	0.23	3.88
Age	age < 5	0.017	0.33	0.24	4.05
	age between	0.017	0.33	0.24	4.03
	age > 65	0.017	0.33	0.24	4.13
annual household income	< 20K	0.018	0.38	0.26	4.51
	20K - 40K	0.017	0.34	0.25	4.21
	40K - 60K	0.017	0.32	0.24	3.99
	60K - 100K	0.016	0.30	0.23	3.79
	> 100K	0.016	0.30	0.24	3.94
county average		0.017	0.33	0.24	4.05

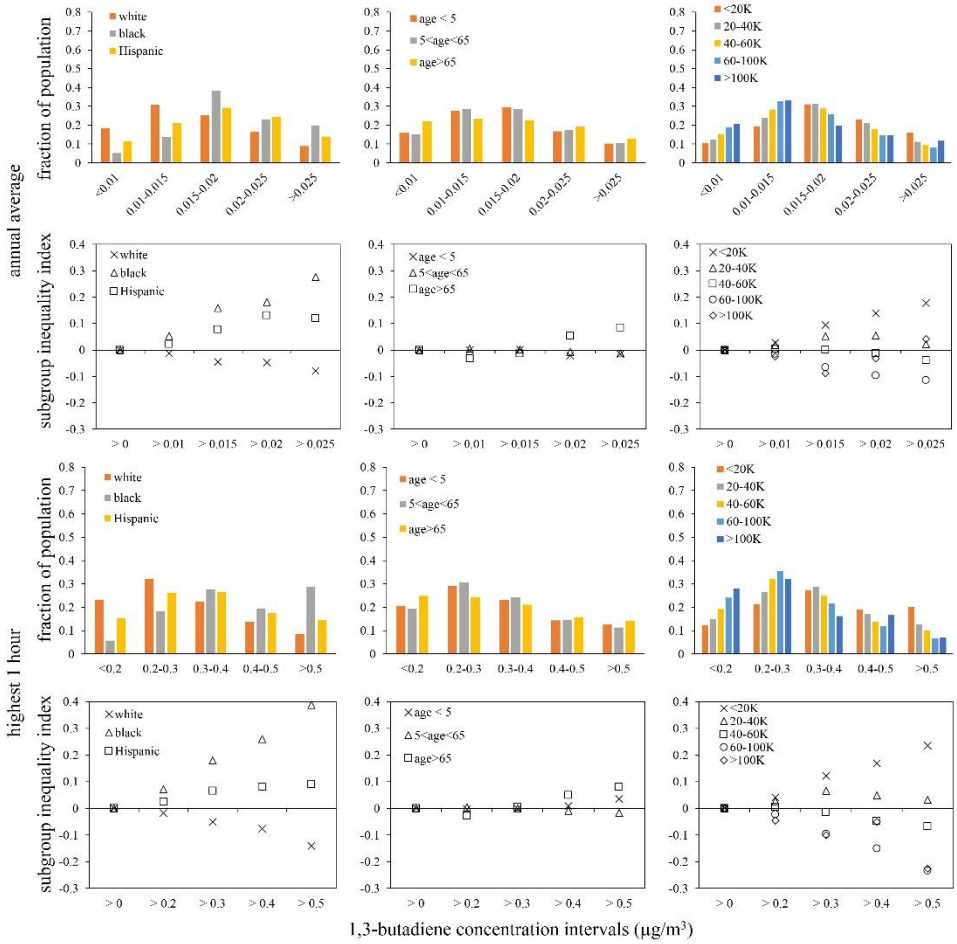

Figure 5.24 Population distributions of the chosen race/ethnicity, age and income subgroups for annual average and maximum 1 hour 1,3-butadiene concentrations.

5.5.2.3. Exposure and Inequalities for acetaldehyde and formaldehyde

For acetaldehyde and formaldehyde, different patterns in population weighted exposures (Table 5.16) and inequality indices (Figure 5.26 and Figure 5.27) were observed. Specifically, population weighted exposure for the two pollutants at both temporal scales show relatively smaller variations among the chosen subgroups. For acetaldehyde, no apparent and consistent trend in inequality index can be observed for any subgroup. For formaldehyde, reverse inequalities are sometimes observed. For example, at highest 1 hour temporal scale, black, Hispanic and the lowest income subgroups are disproportionately not exposed to formaldehyde air pollution while white

and the two of the highest income subgroups are disproportionately exposed. The distinct spatial distribution of acetaldehyde and formaldehyde concentrations (see section 5.4.2.3) contribute to such observations.

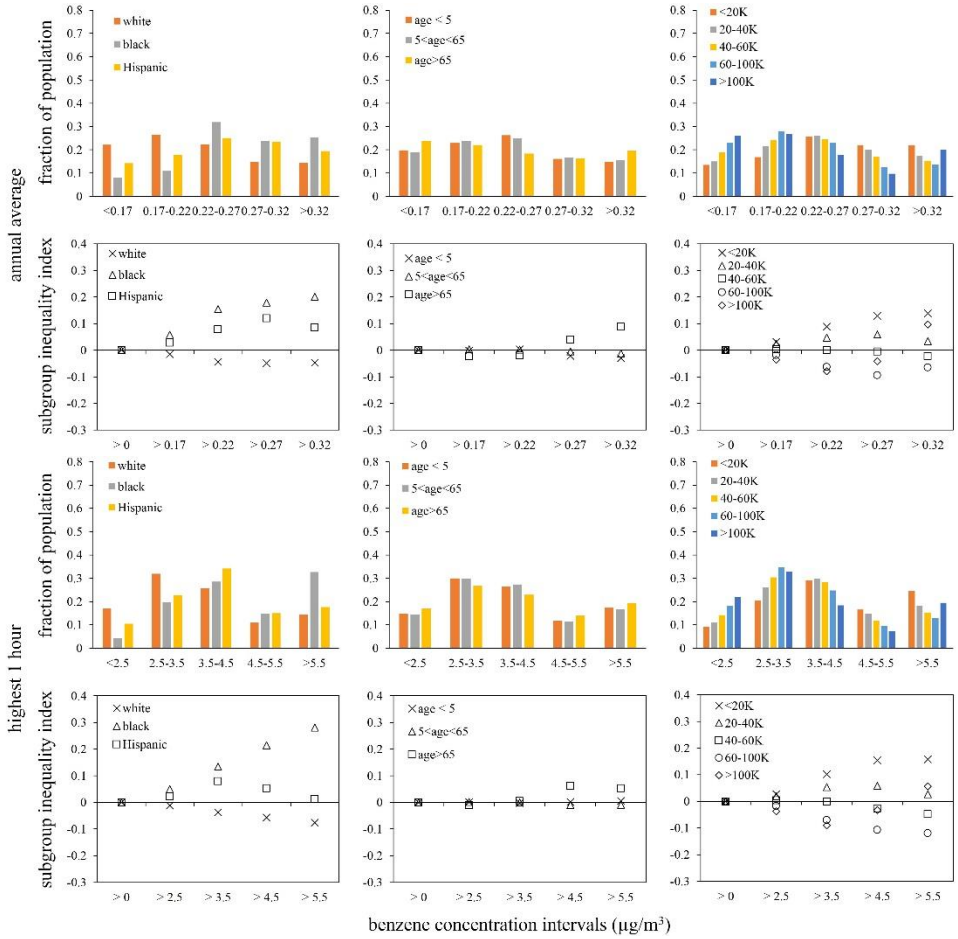

Figure 5.25 Population distributions of the chosen race/ethnic, age and income subgroups for annual average and maximum 1 hour benzene concentrations.

5.5.3. Discussion of Exposure and Inequality Estimation

Inequalities were found for black, Hispanic and lowest income subgroups (annual household income less than $20,000) regarding NO_x, 1,3-butadiene and benzene air pollution; meanwhile white and the two highest income subgroups (between $60,000 to $100,000 and greater than $100,000) were found to be disproportionately not exposed to

these three pollutants. However, rather complex, and sometimes even reversed exposure patterns were found for acetaldehyde and formaldehyde.

Table 5.16 Population weighted exposure to acetaldehyde and formaldehyde for chosen subgroups

subgroups		acetaldehyde		formaldehyde	
		temporal metrics($\mu g/m^3$)		temporal metrics($\mu g/m^3$)	
		annual	highest 1 hour	annual	highest 1 hour
race/ethnicity	black	2.06	8.48	1.85	7.46
	white	2.04	8.48	1.82	7.96
	Hispanic	2.02	8.13	1.81	7.55
age	age > 65	2.06	8.27	1.83	8.03
	age < 5	2.04	8.52	1.83	7.87
	age between	2.04	8.49	1.82	7.84
annual household income	< 20K	2.04	8.34	1.83	7.63
	20K - 40K	2.04	8.37	1.82	7.75
	40K - 60K	2.04	8.43	1.82	7.86
	60K - 100K	2.04	8.50	1.82	7.98
	> 100K	2.02	8.39	1.81	7.82
county average		2.04	8.47	1.83	7.86

These observations are mainly due to spatial distributions of the estimated pollutant concentrations (see section 5.4.2). The spatial distributions of NO_x, 1,3-butadiene and benzene concentrations show generally higher concentrations in urbanized areas such as near downtown Tampa and the Tampa International Airport, where pollutant emissions are high. Hence similar inequalities were found. The CALPUFF modeled acetaldehyde and formaldehyde concentrations also show similar patterns as the other pollutants; the spatial distributions were substantially altered after combining with CMAQ data. Therefore lead to more complex findings regarding exposure and exposure inequalities.

The inequalities found for NO_x, 1,3-butadiene and benzene air pollution are consistent with other studies focused on the same area (Chakraborty, 2009; Chakraborty

& Bosman, 2010; Stuart et al., 2009), although different methods were employed in these studies. Findings for acetaldehyde and formaldehyde contribute to our understandings regarding the exposure inequalities in the Tampa, FL by showing different and sometimes even reversed inequality patterns, suggesting the importance of including multiple pollutants during exposure and inequality assessments.

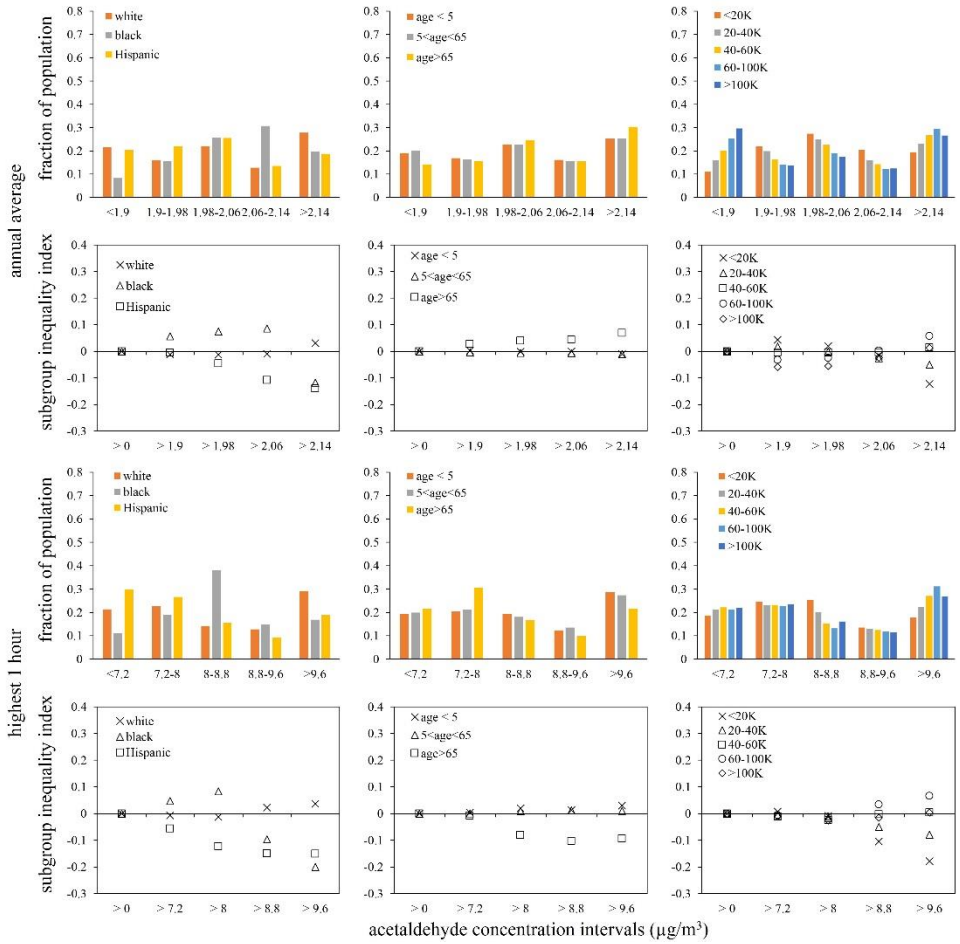

Figure 5.26 Population distributions of the chosen race/ethnicity, age and income subgroups for annual average and maximum 1 hour acetaldehyde concentrations.

5.5.4. Limitation and Uncertainties in Exposure and Inequality Estimation

Air pollution exposures estimated in this study are residential exposures based on modeled ambient pollutant concentrations. Accurate representation of personal exposure to air pollution requires consideration of human activity patterns and pollutant

concentration variations in different micro-environments. However, these factors were not included in this study. In addition, pollutant concentration variations within each census block group were not modeled here.

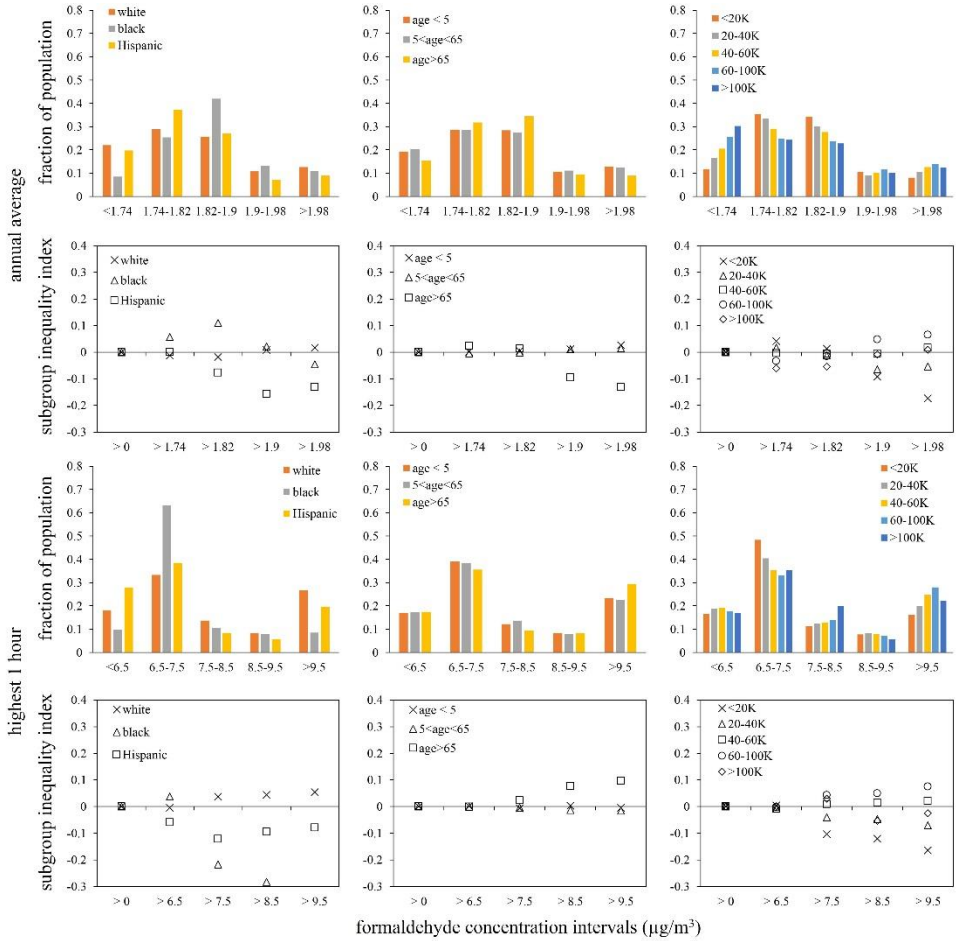

Figure 5.27 Population distributions of the chosen race/ethnicity, age and income subgroups for annual average and maximum 1 hour formaldehyde concentrations.

There are uncertainties in the categorization of population subgroups. Specifically, there are overlapping in the category definition for race/ethnicity groups. A subset of the population may be both white and Hispanic, and they were included in both subgroups. Additional analysis are suggested for future work.

Similar with Chapter 4, human activity patterns and pollutant concentration variability at micro-environments were not incorporated into the exposure estimation in

this study. Residential exposures were estimated instead. Further, while estimating air pollution exposures for one chosen population category (race/ethnicity, age or income category), the other categories were not controlled. More rigorous statistical analysis and tests are suggested for future work.

5.6. Overall Summary and Conclusions

In this study, human exposure to air pollution, and exposure inequalities among chosen race/ethnicity, age and income subgroups were estimated for five selected pollutants : 1,3-butadiene, acetaldehyde, benzene, formaldehyde and NO_x. First, pollutant emissions from five emission categories were estimated for the study area. Spatiotemporal distributions of pollutant concentrations were then estimated using the CALPUFF, a non-steady state Lagrangian chemical transport model, and output data from CMAQ, a Eulerian grid chemical transport model. The estimated pollutant concentrations were combined with demographic data to estimate air pollution exposure and exposure inequalities among chosen population subgroups. Findings from this work are as follows:

1. Compared with on-road mobile source emissions estimated using MOBILE6.2 model, the MOVES estimated emissions are substantially higher for NO_x, higher for acetaldehyde and lower for 1,3-butadiene and formaldehyde.
2. The spatial distributions of CALPUFF modeled pollutant concentrations show similar patterns, with higher concentrations generally found in urban areas and lower concentrations generally found in rural areas.

3. At different temporal scales, the CALPUFF modeled pollutant concentrations show different spatial patterns. The impact of roadways are observable at annual average temporal scale, this pattern diminishes with increasing temporal scales.
4. For acetaldehyde and formaldehyde, processes not included in CALPUFF modeling, including atmospheric formation and long range transportation of pollutants, contribute substantially to pollutant concentrations.
5. Inequalities were found for black, Hispanic and low income (annual household income less than $20,000) population subgroups regarding NO_x, 1,3-butadiene and benzene. Complex, and sometimes even reversed exposure patterns were found for acetaldehyde and formaldehyde, due primarily to their distinct spatial distribution of estimated concentrations.

CHAPTER 6

POTENTIAL IMPACTS OF FUTURE URBAN FORM AND VEHICLE FLEET ELECTRIFICATION ON AIR POLLUTANT EMISSIONS, CONCENTRATIONS, AND EXPOSURES IN THE TAMPA AREA

6.1. Introduction

The question of which urban form best accommodates the rapid expansion of cities whilst maintaining environmental sustainability has been extensively discussed in the field of urban planning. Despite this, it was not until recently that researchers started to notice the impact of urban forms on urban air quality (Breheny, 1996). Appropriate and accurate characterization of urban forms involves the consideration of many factors such as morphology of the city, design of transportation infrastructure and land use policy (Miranda et al., 2008), amongst others. While recognizing the complexity of urban forms, past studies make use of simplified approaches to assess their impact on air quality (Borrego et al., 2006; Ridder et al., 2008; Frank et al., 2000; Kahyaoğlu-Koračin et al., 2009; Liu, 2003; McDonald-Buller et al., 2010; Niemeier et al., 2011; Song et al., 2008; Stone et al., 2007, 2009). Generally, two urban forms have received the most attention: sprawl and compact urban form.

As discussed in Chapter 2, many previous studies have suggested that sprawl and compact urban forms may have a significant impact on urban air quality. This is due primarily to changes in the total amount of emission, as well as the spatial distributions of

these emissions. Many studies have found that overall pollutant emissions are lower in compact than sprawl urban form, however the colocation of pollutant emissions and human population in compact urban form may lead to potentially higher pollution exposures for pollutants with substantial primary contributions. On the other hand, sprawl urban forms may lead to less human exposure to air pollution, despite higher overall pollutant emissions (Hixson. et al., 2010, 2012; Song et al., 2008). The mechanisms by which urban forms impact urban air pollution are still poorly understood.

Past studies are also insufficient regarding how urban forms impact air pollution exposure, particularly disproportionate distribution of exposures among different population subgroups. In addition, although many have pointed out that human exposure to air pollution may be higher in compact urban form, few studies have taken a step further to investigate potential strategies to alleviate this exposure.

To address these issues, I investigated the emissions of five selected pollutants: 1,3-butadiene, benzene, NO_x, acetaldehyde and formaldehyde, in potential future sprawl and compact urban forms. Spatial concentration distributions of these pollutants were estimated through dispersion modeling. Human exposures to air pollution, as well as exposure distributions among race/ethnicity, age and income population subgroups, were then estimated and compared. Furthermore, the effects of vehicle fleet electrification on pollutant emissions, concentration distributions and air pollution exposures were also estimated to evaluate the use of vehicle fleet electrification as a potential strategy to alleviate air pollution exposure in compact urban form.

6.2. Scope of Study

Similar with the modeling study for the year 2002 (see Chapter 4), the focus area of this study is the Tampa, FL area, a populated metropolitan region with a diverse population and well known sprawl development patterns (Glaeser et al., 2001; Stuart et al., 2009). The same five pollutants: 1,3-butadiene, benzene, NOx, acetaldehyde and formaldehyde, were selected as the focus pollutants, as they have significantly impact on human health and public welfare in urban areas in the US (Agency for Toxic Substances and Disease Registry, 2007; National Toxicological Program, 2010, 2011; U.S. Environmental Protection Agency, 2008a, 2008b), and also have substantial mobile source contributions (ENVIRON International Corporation, 2006). The same population subgroups were also used in this study: including race/ethnicity (black, Hispanic and white), age (age less than 5, between 5 and 65 and age more than 65 years old) and annual household income groups (less than $20,000, between $20,000 and $40,000, between $40,000 and $60,000, between $60,000 and $100,000 and more than $100,000).

Future scenarios were developed based upon the One Bay visioning plan (One Bay, 2010), the data for which were provided by the Tampa Bay Regional Planning Council (TBRPC). The One Bay visioning plan contains four alternative planning scenarios for seven counties around the Tampa Bay area in 2050: a "business as usual" sprawl growth scenario; a compact growth scenario designed based on "transient oriented development"; a scenario designed to conserve water resources and wildlife habitats in the area; and a fourth scenario designed based on previously collected public inputs. One Bay is a collaborative organization formed by several metropolitan planning

organizations around the Tampa Bay area and the One Bay visioning plans are considered influential.

The sprawl and compact scenarios in the One Bay visioning plan were chosen for this study. In addition, a vehicle fleet electrification scenario (hereinafter referred to as the electric vehicle scenario) was also created, which is based on compact urban form, but with all on-road vehicles replaced by electric vehicles. The selection of vehicle fleet electrification as the potential strategy to alleviate air pollution exposure in compact urban form is based on the fact that on-road mobile sources were found to contribute to inequalities regarding air pollution exposure in the Tampa area (Chakraborty, 2009). Modeling results for the year 2002 (see Chapter 4) were used as the baseline scenario.

The visioning plan contains predicted land use in the year 2050 for both sprawl and compact scenarios. Seven counties around the Tampa Bay area were included: Hernando, Hillsborough, Manatee, Pasco, Pinellas, Polk and Sarasota County. The same roadway network was used as in the baseline scenario (see Chapter 4).

Figure 6.1 provides comparisons of re-developed land area and land use types in the sprawl and compact scenarios. Overall there are 15 land use types in the visioning plan (Appendix B-1). In the sprawl scenario, a substantial amount of new developments are low-density residential areas, and these new developments spread throughout the whole region included in the visioning plan. For the compact scenario, medium density residential areas dominate the new developments, with significantly fewer low-density residential areas. The developments in the compact scenario are also concentrated in current urban centers and along major interstates, especially in Hillsborough, Pinellas and Sarasota County.

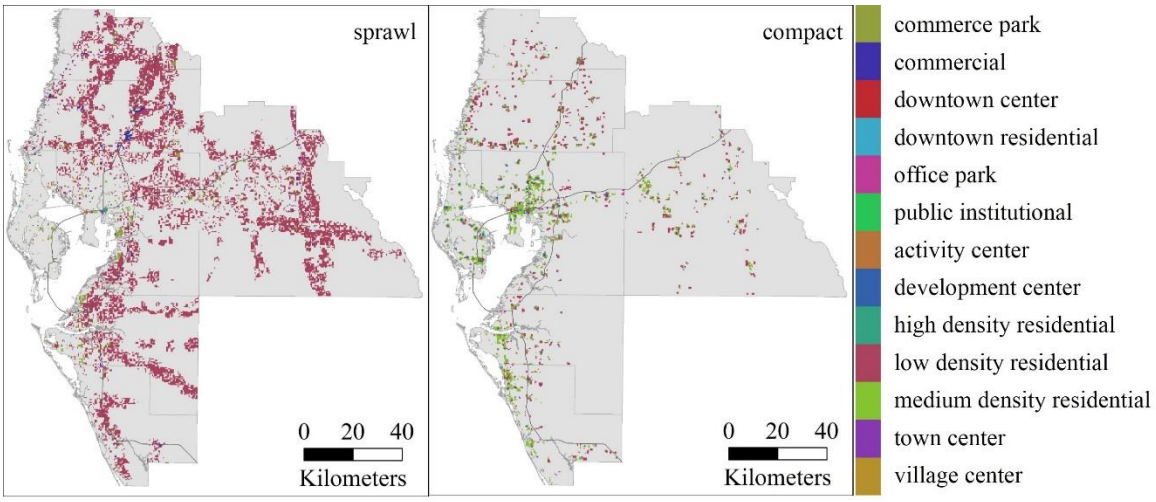

Figure 6.1 Re-developed land area and land use types in sprawl and compact scenarios.

To estimate pollutant concentrations in the future scenarios, emissions of the five selected pollutants were first projected to 2050 for each scenario; The CALPUFF model was used to estimate pollutant concentrations in Hillsborough County (where Tampa is located), following which the estimated pollutant concentrations were combined with projected demographic data to estimate air pollution exposure, as well as exposure among chosen population subgroups. Details of each step are provided in the following sections.

6.3. Emission Estimation for Future Scenarios

Table 6.1 Types of emissions estimated for each scenario

	sprawl scenario	compact scenario	electric vehicle scenario
on-road mobile	projected	projected	excluded
stationary point	projected	projected	projected
off-road mobile	projected	same as sprawl	same as sprawl
non-point	projected	projected	same as compact
biogenic	projected	projected	same as compact

Pollutant emissions from five source categories were projected to the year 2050: on-road mobile sources, stationary point sources, non-point, off-road mobile and biogenic sources (Table 6.1). On-road mobile source emissions were excluded for the electric vehicle scenario as the vehicle fleet is assumed to contain 100% electric vehicles.

Stationary point source emissions were projected for the three different scenarios individually. Off-road mobile source emissions were kept the same for all three scenarios, and non-point and biogenic emissions were projected for the sprawl and compact scenarios.

6.3.1. Methods of Emission Estimation for Future Scenarios

6.3.1.1. On-road Mobile Source Emissions

Travel demand models, combined with emission factor estimation model, have been used in many previous studies to estimate future on-road mobile source emissions (Ridder et al., 2008; Hixson et al., 2010; Song et al., 2008). However, no travel demand model outputs are available for the One Bay visioning plans. Hence, a top-down approach was developed and applied. First, county total on-road mobile source emissions in the future scenarios were estimated using the MOVES model. The estimated total emissions were then spatially allocated based on spatial surrogates developed based on multiple linear regressions. Regarding temporal variation of on-road mobile source emissions, the same traffic variation profiles as used in the baseline scenario were applied.

6.3.1.1.1. County Total On-road Mobile Source Emissions

County total on-road mobile source emissions were estimated for all seven counties included in the One Bay visioning plan. Two input datasets were prepared for the MOVES model: vehicle population in each county and county total vehicle mileage travelled for different vehicle types.

Vehicle populations for each MOVES vehicle class were extrapolated from the baseline scenario (2002) to 2050 using populations in each county. County population in

the year 2002 was calculated based on interpolation of 2000 and 2010 census data, and 2050 populations in each county were calculated based on One Bay visioning data:

$$P_{c,s} = p_H \sum_{k=1}^{15} \left(L_{c,k,s,u} H_{k,u} + L_{c,k,s,d} H_{k,d} \right)$$

where $P_{c,s}$ is the predicted population in 2050 in county c for scenario s; p_H is average person per household, assumed to be 2.46, as defined in the One Bay visioning data; k is land use types as defined in the One Bay visioning plan, and there are 15 different land use types; $L_{c,k,s,u}$ is the total land areas (acres) of land use type k in county c of scenario s that is already developed to some extent in the baseline scenario, but with no further developments in the future scenarios; $H_{k,u}$ is the household density (households per acre) for land use type k that is already developed to some extent but with no further developments in the future scenarios; Similarly, $L_{c,k,s,d}$ is the total land area (acres) of land use type k in county c of scenario s that is newly or re-developed in the future scenario; and $H_{k,d}$ is the household density (households per acre) for land use type k that is re-developed in the future scenario. All of the data mentioned above were obtained from the One Bay visioning plan.

Total vehicle mileage travelled for all seven counties combined are available from the visioning data, but not for each county individually. The total vehicle mileage travelled was allocated to each county based on total vehicle trips generated in corresponding counties, which were calculated by

$$T_{c,s} = \sum_{k=1}^{15} \sum_{m=1}^{32} \left(L_{c,k,s,u} + L_{c,k,s,d} \right) f_{k,m} T_{k,m}$$

where $T_{c,s}$ is the predicted vehicle trips generated in 2050 in county c for scenario s; m is the building types associated with land use type k as defined in the One Bay visioning

plan. Each land use type contains a subset of the 32 building types. A complete list of the building types is provided in Appendix B-2, and assumptions of building type distributions for different land use types are provided in Appendix B-3; $f_{k,m}$ is the fraction of building type *m* that is associated with land use type *k*; and $T_{k,m}$ is the vehicle trip generation rate (trips per acre) for building type *m* that is associated with land use type *k*. A list of vehicle trip generation rates for each building types is also provided in Appendix B-4.

All other MOVES input data were kept the same as in the baseline scenario, except for fuel properties and meteorological data. The fuel data used are based on the year 2012, given that no further information are available beyond 2012. Meteorological data used are 30 year averaged meteorological parameters. The developed data were input into the MOVES model and county total on-road mobile source emissions for the sprawl and compact scenarios were estimated.

6.3.1.1.2. Spatial Allocation of On-road Mobile Source Emissions

The estimated county total on-road mobile source emissions for all five pollutants were spatially allocated to emission grids as shown in Figure 6.2. The grid spacing is 1 km covering Hillsborough County, and 5 km elsewhere. The same grid network was used in the baseline scenario for 1,3-butadiene, benzene and NO_x. Spatial surrogates used to allocate on-road mobile source emissions were developed based on multiple linear regression using data in Hillsborough County from the baseline scenario.

In the baseline scenario, on-road mobile source emissions in Hillsborough County were estimated at each major roadway link, as well as at 1 km spacing grid cells covering

Hillsborough County. The estimated emissions from major roadway links were first distributed into the 1 km grid cells by:

$$E_{m,i} = \sum_{l=1}^{n} \frac{A_{l,i}}{A_l} E_l$$

where $E_{m,i}$ is the distributed emissions in grid cell i that are from major roadway links (tons per year); n is the number of major roadway links that are within grid cell i; $A_{l,i}$ is the area (m^2) of the area source for link l that is within grid cell i. Methods for generating the area sources are described in Chapter 4; A_l is the area (m^2) of the area source for link l; and E_l is pollutant emissions (tons per year) from link l;

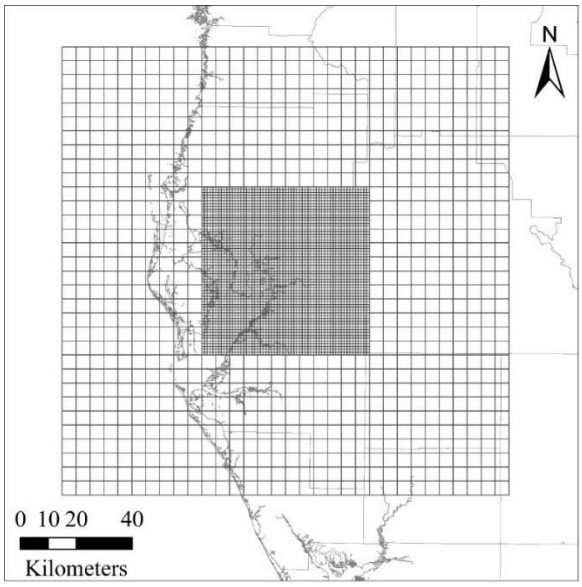

Figure 6.2 Grid network for allocating emissions from on-road mobile sources, non-road mobile sources, non-point sources and biogenic sources.

Total on-road mobile source emissions within all 1 km grid cells covering Hillsborough County were calculated, and the 1 km grid cells were re-grouped into three categories: all grid cells, the subset of the grid cells containing freeway links, and the subset not containing freeway links. Five regression equations (corresponding to five pollutants) were developed for each group of grid cells. The dependent variable used is

pollutant emissions (tons per year) in each grid cell, and candidate predictor variables are: major roadway length (km), minor roadway length (km), and area of seven aggregated land use types (km^2) (Table 6.2). These variables were selected as roadway length and land use types are correlated with air quality and have been frequently used in land use regression models related to air quality modeling (Hoek et al., 2008). Land use type classifications were chosen to be in consistent with the One Bay visioning data, and also accounted for limitations of the land use data in the baseline scenario.

Table 6.2 Seven land use types used in deriving multiple regression functions as in the One Bay visioning data

aggregated land use ID	land use type description
1	commercial, downtown center, office park, activity center, town center
2	medium density residential area, village center
3	downtown residential, development center, high density residential area
4	commerce park
5	public institutional
6	low density residential area
0	all other land use types

Land use data for 2000 in the seven counties were retrieved from the Southwest Florida Water Management District (SWFWMD). The land use type classifications used in the SWFWMD data are based on the Florida Land Use and Cover Classification System (FLUCCS) and they were mapped to the land use classification system used in the One Bay visioning data. Table 6.3 shows the mapping method used. The mapped land use data, together with roadway network data obtained from the Florida Department Of Transportation (2002), were spatially intersected with the 1 km grids as mentioned previously to calculate lengths of major and minor roadway, and areas of different land use types in each grid cell. The statistical computing package R (R Development Core Team, 2013) was then used to derive all multiple linear regression equations.

The developed equations were applied to predict the spatial surrogates for the allocation of on-road mobile source emissions for all counties in the future scenarios using the following:

$$S_{i,c} = \frac{E_{p,i}}{\sum_{i=1}^{q_c} E_{p,i}}$$

where $S_{i,c}$ is the calculated spatial surrogate for allocating on-road mobile source emissions in grid cell I and county c; q_c is the total number of grid cells that covers county c; $E_{p,i}$ is emissions in grid cell i as predicted by regression equations. Note that the predicted emissions in each grid cell are not actual emissions used in subsequent modeling, they are rather "relative" emissions used to derive spatial surrogates to allocate the previously estimated county total emissions. Different regression equations were used to calculate $E_{p,i}$ depending on grid cell location and whether the corresponding grid cell contained freeways. Specifically, for grid cells which are within Hillsborough County and also containing freeways, regression equations developed specifically for this group of grid cells were applied; for other grid cells within Hillsborough County but not containing freeways, another sets of regression equations developed for this group of grid cells were used. For the remaining grid cells, the last sets of regression equations, which were developed for all grid cells combined, were applied.

The county total on-road mobile source emissions estimated for all counties in the future scenarios were next allocated to the emission grids (Figure 6.2) using the developed surrogates. For grid cells located in Hillsborough County that contain freeways, emissions were further allocated to area sources of major roadways located within corresponding grid cells. Specifically, the predicted on-road mobile source emissions in grid cells that containing freeways were first divided into two parts:

emissions that come from major roadways and emissions that come from minor roadways. The proportion of emissions coming from major and minor roadways varied across grid cells and were assumed to be the same as in the baseline scenario. Then, emissions from major roadways were allocated to area sources of major roadways using area (m^2) of the area sources as surrogate.

Table 6.3 Seven land use types used in deriving multiple regression functions as in the FLUCCS data

Florida Land Use and Cover Classification System land use description	FLUCCS Code	aggregated land use ID
urban and built-up - commercial and services	1400	1
urban and built-up - residential, medium density	1200	2
urban and built-up - residential, high density	1300	3
urban and built-up - industrial	1500	4
urban and built-up - institutional	1700	5
urban and built-up - residential, low density	1100	6
all other land use types		0

6.3.1.2. Stationary Point Source Emissions

For NO_x, the same stationary point sources as modeled in the baseline scenario were used for the future scenarios. More point sources for acetaldehyde and formaldehyde were included in future scenarios than the baseline scenario due to larger emission estimation domain in the future scenarios. Point source emissions of NO_x, acetaldehyde and formaldehyde were included, however point source emissions for 1,3-butadiene and benzene were not included due to their small contributions to total emissions. Other source parameters such as stack height and exit velocity were assumed to be the same as in the baseline scenario.

In the baseline scenario, over 90% of the pollutant emissions from stationary point sources were emitted by electricity generation units. The California Emission Forecasting System (CEFS) contains projected point source emissions from electricity

generation units for future years, and the results were used in Hixson et al. (2010, 2012). In the California Emission Forecasting System, point source emissions were projected for each generation unit individually based on the types of boiler used in the corresponding unit, however this approach is not applicable in this study due to lack of data. A simplified alternative approach was developed and applied.

In this study, point source emissions in the future scenarios were extrapolated using increased electricity demand (incremental electricity demand compared with the baseline scenario) for the three future scenarios using:

$$E_{i,s} = D_s e$$

where $E_{i,s}$ is the increased total pollutant emissions (tons/year) due to increased electricity demand in the whole study domain; D_s is the increased electricity demands (GWh/year) in future scenarios in the study domain; and e is the estimated pollutant emission rates (tons/GWh) for point sources, which varies by pollutants. Methods for estimating the increased electricity demands and pollutant emission rates from point sources are provided below.

6.3.1.2.1. Increased Electricity Demand in Future Scenarios

Increased electricity demands for the sprawl and compact scenarios are available from the One Bay visioning data. Note that in the electric vehicle scenario, electricity demands will be further increased due to vehicle fleet electrification. The electricity demand for the electric vehicle scenario was estimated as:

$$D_e = D_c + \sum_{v=1}^{6} D_v M_v$$

where D_e is the increased electricity demand (Wh/year) in the electric vehicle scenario; D_c is the increased electricity demand (Wh/year) in the compact scenario (available from

the One Bay visioning data); v is the Highway Performance Monitoring System vehicle type as described in Chapter 3; D_v is the average electricity consumption for vehicle type v (Wh/mile); and M_v is total vehicle mileage travelled (miles/year) for vehicle type v.

Assumed electricity consumptions (D_v) for each vehicle type are shown in Table 6.4. The electricity consumptions were estimated as follows: First, for motorcycle and passenger cars, electricity consumptions were calculated based on technical specifications of available electric vehicles including Zero DS electricity motorcycle and Tesla Model S; For the rest vehicle types, average vehicle weights were first assigned to each MOVES vehicle type, and a 0.065 Wh/mile/lb electricity consumption factor was applied to calculate average electricity consumptions for each MOVES class. The vehicle weights were best estimates based on descriptions of vehicle types provided in the MOVES and MOBILE6.2 models (U.S. Environmental Protection Agency, 2004a, 2010b). The 0.065 Wh/mile/lb electricity consumption factor was calculated based on the electricity consumptions for passenger cars. Despite these simplified assumptions, the calculated electricity consumptions are equivalent or comparable to previous estimates (Alhajeri et al., 2011; Electric Power Research Institute, 2007). Finally, the estimated electricity consumptions were further aggregated to High Way Performance Monitoring System (HPMS) vehicle types, as the vehicle mileage travelled data are stratified by HPMS vehicle types.

6.3.1.2.2. Pollutant Emission Rates for Point Sources

Pollutant specific emission rates (e, tons/GWh) for point sources were estimated by:

$$e = \frac{\sum_{u=1}^{r}(E_u / G_u)}{r}$$

where u is an index for point source with data available, and r is the total number of point sources; G_u is the gross load of corresponding point sources (GWh/year); and E_u is pollutant emissions from corresponding point sources (tons/year). Information on gross loads were retrieved from the Environmental Protection Agency's air markets programs (http://ampd.epa.gov/ampd/), along with annual emissions of NO_x. Available information on annual emissions of acetaldehyde and formaldehyde from point sources with gross load information available were obtained by cross-referencing the gross load data with annual emission data from the 2002 National Emission Inventory, using the Facility Registry Identifier of each source.

Table 6.4 Assumed vehicle weights and electricity consumptions for each vehicle type

MOVES vehicle type ID	vehicle type description	Wh/mile	weight (lb)	HPMS vehicle type ID	Wh/mile
11	motorcycle	100	400	10	100
21	passenger car	300	4600	20	300
31	passenger truck	390	6000	30	460
32	light commercial truck	520	8000		
41	intercity bus	1300	20000	40	1300
42	transit bus	1300	20000		
43	school bus	1300	20000		
51	refuse truck	1300	20000	50	1700
52	single unit short-haul truck	1950	30000		
53	single unit long-haul truck	2275	35000		
54	motor home	1300	20000		
61	combination short-haul truck	3250	50000	60	3600
62	combination long-haul truck	3900	60000		

The estimated pollutant emission rates, together with increased electricity demands in the three future scenarios, were combined to calculate increased total pollutant emissions in the study domain. The calculated total emissions were then evenly distributed to all point sources that were included in the modeling.

6.3.1.2.3. Diurnal Vehicle Charging Profiles

Electric vehicles need to be charged frequently. When charging, electric vehicles draw electricity from the power grid, which impacts the load of electricity generation units and consequently impacts emissions from power plants, as well as the temporal distribution of emissions. To account for the impact of electric vehicle charging on the temporal distribution of emissions, temporal vehicle charging profiles were developed and applied. The profiles reflect temporal variations of the amount of electricity consumed by the charging of electric vehicles.

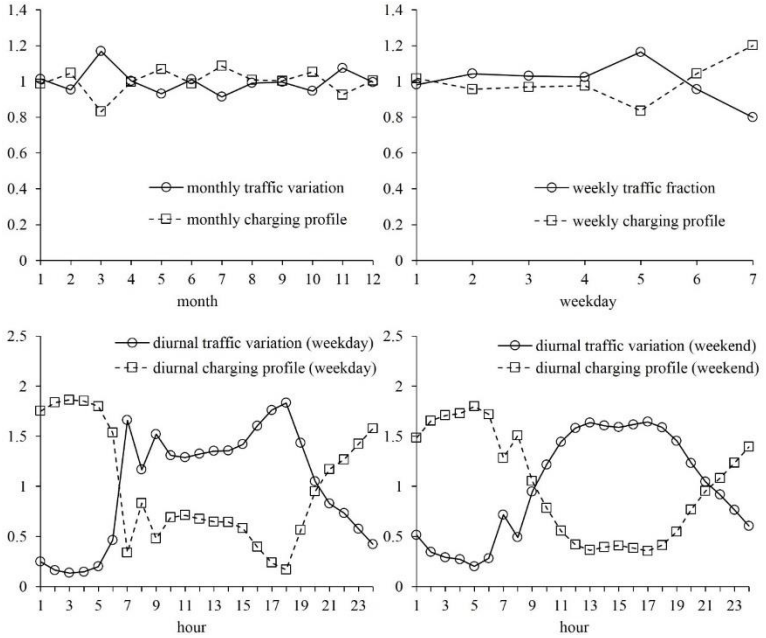

Figure 6.3 Developed temporal vehicle charging profiles and traffic volume variation profiles.

In earlier studies, charging of electric vehicles were assumed to occur from 10 pm to 6 am, or 10 pm to 10 am, or 10 pm to 8 am (Alhajeri et al., 2011; Electric Power Research Institute, 2007; Stephan & Sullivan, 2008), however these profiles may not be representative as they were arbitrarily determined. In this study, the temporal charging profiles of electric vehicles were assumed to be inversely correlated with the temporal

variations of traffic volume on roadway networks (see Chapter 4). Figure 6.3 shows the developed temporal vehicle charging profiles and traffic variation profiles.

For the sprawl and compact scenarios, hourly emission rates from stationary point sources were calculated using temporal allocation factors obtained from the Environmental Protection Agency (U.S. Environmental Protection Agency, 2007a). For the electric vehicle scenario, stationary point source emissions were divided into two parts: increased emissions due to vehicle fleet electrification and all other emissions. Hourly emission rates were estimated separately for the former and the latter by applying the developed vehicle charging profiles and temporal allocation factors from the Environmental Protection Agency, respectively. The calculated hourly emission rates were then combined afterward.

6.3.1.3. Non-Road, Non-Point and Biogenic Source Emissions

Non-road, non-point and biogenic source emissions were also projected to 2050 for the future scenarios (Table 6.1), and spatially allocated to the emission grids as shown in Figure 6.2. For the majority of non-road mobile sources, the NMIM (National Mobile Inventory Model) model was used to estimate pollutant emissions in the future scenarios, with default activity data applied. Non-road mobile source emissions from three specific categories were estimated separately: aircraft, commercial marine vessels and locomotives, as they were not included in NMIM model. Aircraft and locomotive emissions were extrapolated to 2050 based on population, and commercial marine vessel emissions were extrapolated using the predicted annual total cargo weights handled by the Port of Tampa, which is the largest marine port in the study domain. Cargo weights in 2002 were obtained from the Tampa Port Authority, and a 1.5% annual growth rate was

applied to cargo weights from 2010 to 2050. This growth rate was obtained from the strategic plan of the Tampa Port Authority (Norbridge Inc, 2011).

Annual total non-point source emissions in the baseline scenario were extrapolated to 2050 using 9 surrogates. Appendix B-5 provides a detailed list of the emissions and corresponding surrogate used. The surrogates were assigned based on the nature of the emission. Sources listed in Appendix B-5 account for over 98% of all non-point source emissions in the baseline scenario. Population was used to extrapolate the remaining 2% emissions.

Forest area was used to extrapolate biogenic emissions from the baseline scenario to the year 2050. Forest area in the future scenarios, as well as the other surrogates applied for non-point source emissions, were developed from the One Bay visioning data. Forest areas in the baseline scenario were calculated from land use data obtained from the Southwest Florida Water Management District.

In addition to total emissions, spatial distributions of pollutant emissions are also affected by urban growth. Similarly to the baseline scenario (see Chapter 4), spatial allocation surrogates were developed and applied for non-road, non-point and biogenic emissions. These surrogates were developed based upon the One Bay visioning data, as well as data for the baseline scenario. Appendix B-6 provides a list of the spatial surrogates developed for future scenarios and the corresponding method used to derive the surrogates. In each grid cell the surrogate value was calculated as surrogate metric/control total. The same method was applied for the sprawl and compact scenarios. The spatial surrogates used in the electric vehicle scenario are the same as in the compact

scenario. Regarding temporal distribution of the emissions, the same temporal profiles as used in the baseline scenario were used.

6.3.2. Results and Discussion of Emission Estimation for Future Scenarios

6.3.2.1. Estimated County Total On-road Mobile Source Emissions

Table 6.5 shows the estimated total on-road mobile source emissions in the sprawl and compact scenarios for all seven counties included in the One Bay visioning plan. Emissions in the baseline scenario were also included for comparison purposes. Detailed estimates for each county are listed in Appendix B-7. Compared to the baseline scenario, the estimated 1,3-butadiene, benzene and NO_x emissions in the future scenarios are substantially lower. Emissions of formaldehyde also decreased, but by a relatively smaller magnitude. Relative to the baseline scenario, while acetaldehyde emissions from the compact scenario show a 20% decrease, emissions from the sprawl scenario actually show a 2% increase, attributable to the higher vehicle mileage travelled in the sprawl scenario. Of the two future scenarios, the sprawl scenario consistently show higher on-road mobile source emissions than the compact scenario, especially for NO_x, for which emissions from the former are 40% higher than the latter. This observation is expected as the total vehicle mileage travelled in the sprawl scenario is 36% higher than the compact scenario (based on the One Bay visioning data). The estimated changes of on-road mobile source emissions from the baseline to the future scenarios are consistent with other studies where the MOVES model was used (Atlanta Regional Commission, 2010; Federal Highway Administration, 2012).

Figure 6.4 provides additional comparisons of the estimated county total on-road mobile source emissions between the sprawl and compact scenarios (county total

Table 6.5 Estimated total on-road mobile source emissions for baseline, sprawl and compact scenarios for all seven counties included in One Bay visioning plan

	annual emissions (metric tons)		
pollutant	baseline	sprawl	compact
NO_x	139635	51604	36646
1,3-butadiene	214.5	74.7	64.8
benzene	1845	452	394
acetaldehyde	302.5	308.9	241.0
formaldehyde	688.7	620.7	456.6

*In electric vehicle scenario, vehicle fleet are assumed to be 100% electric vehicles and hence there are no on-road mobile source emissions

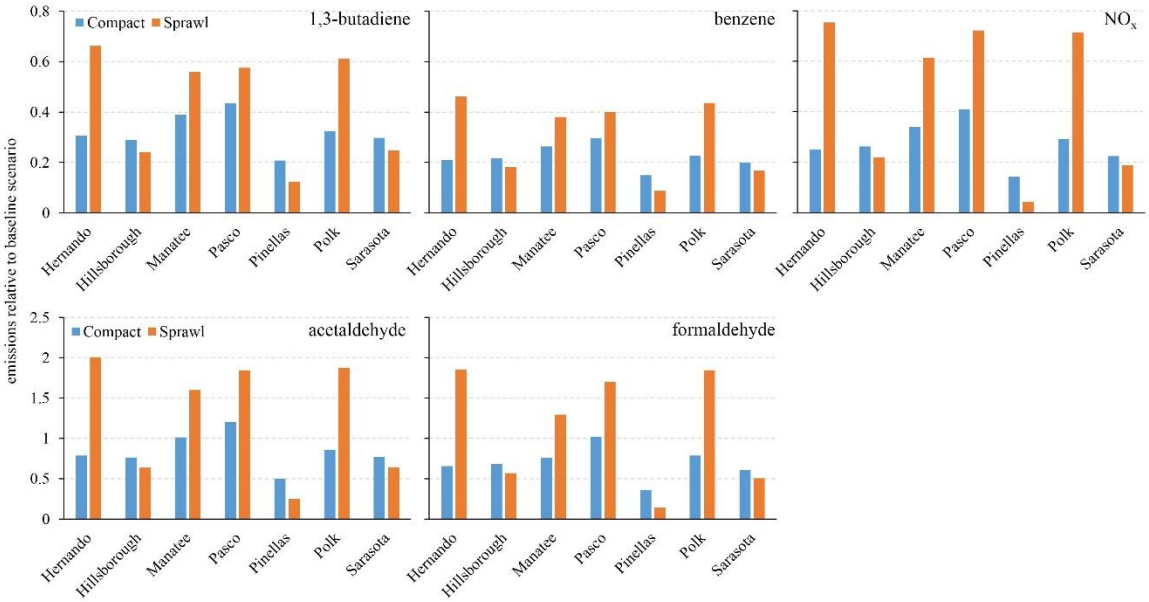

Figure 6.4 Comparison of county total on-road mobile source emissions in seven counties included in One Bay visioning plan. County total emissions in the baseline scenario were set to 1 for all pollutants.

emissions in the baseline scenario were set to 1 for all pollutants). On-road mobile source emissions of all pollutants from the compact scenario are consistently higher in extensively developed counties including Hillsborough, Pinellas and Sarasota County. Emissions from the sprawl scenario are higher in the relatively less developed counties including Hernando, Manatee, Pasco and Polk County. These results are also expected as in the compact scenario the majority of urban development occurs in areas which have

already been extensively developed, hence these areas are the ones which show an increase in emissions. On the other hand, in the sprawl scenario, urban development occurs more frequently in rural undeveloped areas, hence emissions from these rural areas will be the ones to increase.

6.3.2.2. Allocated On-road Mobile Source Emissions

The estimated county total on-road mobile source emissions were spatially allocated using spatial surrogates derived by multiple linear regression. The derived regression equations are shown in Table 6.6 through Table 6.8. All variables in the derived equations have significant p values of less than 0.05, as well as favorable adjusted R^2 values. Based on the derived equations, land use type 1 (see Table 6.2) is a strong predictor for on-road mobile source emissions.

Table 6.6 Parameters of the developed regression equations for grid cells within Hillsborough County and contains freeways

	major roadway length (km)	minor roadway length (km)	aggregated land use type ID		adjusted R^2
			0 (km^2)	1 (km^2)	
1,3-butadiene	2.45E-02†	6.12E-03†	1.82E-02*	7.69E-02*	0.75
benzene	2.11E-01†	5.23E-02†	1.56E-01*	6.69E-01*	0.75
NO_x	2.40E+01†	4.48E+00†	2.06E+01†	5.81E+01*	0.82
acetaldehyde	3.74E-02†	8.90E-03†	2.88E-02*	1.23E-01*	0.72
formaldehyde	8.56E-02†	2.04E-02†	6.59E-02*	2.81E-01*	0.72

$^{*}p < 0.05$; $^{\dagger}p < 0.001$

Table 6.7 Parameters of the developed regression equations for grid cells within Hillsborough County that do not contain freeways

	major roadway length (km)	minor roadway length (km)	aggregated land use type ID				adjusted R^2
			0 (km^2)	1 (km^2)	3 (km^2)	5 (km^2)	
1,3-butadiene	1.56E-02†	5.02E-03†	-7.30E-04†	2.99E-02†	3.36E-03†	4.43E-03*	0.97
benzene	1.34E-01†	4.31E-02†	-6.28E-03†	2.56E-01†	2.88E-02†	3.81E-02*	0.97
NO_x	1.53E+01†	2.89E+00†	-6.61E-01†	2.81E+01†	3.17E+00†	4.24E+00*	0.94
acetaldehyde	2.34E-02†	7.46E-03†	-1.07E-03†	4.43E-02†	4.92E-03†	6.62E-03*	0.97
formaldehyde	5.36E-02†	1.70E-02†	-2.46E-03†	1.01E-01†	1.13E-02†	1.52E-02*	0.97

$^{*}p < 0.05$; $^{\dagger}p < 0.001$

The allocated on-road mobile source emissions for NO_x in the sprawl and compact scenarios, as well as differences between the two scenarios, are shown in Figure 6.4. Spatial distributions of the allocated on-road mobile source emissions for the other pollutants are similar and hence are not shown here. Within Hillsborough County, in both sprawl and compact scenarios, emissions from the grid cells that containing freeways are clearly visible on the map, especially around major interstates such as I-275 and I-4. The spatial distributions of emission differences suggest generally higher emissions in Hillsborough, Pinellas and Sarasota County in compact scenario, and lower emissions in other counties. Such results are reasonable as the predicted populations in Hillsborough, Pinellas and Sarasota County are higher in the compact scenario, which lead to higher on-road mobile source emissions.

Table 6.8 Parameters of the developed regression equations for all emission grid cells

	major roadway length (km)	minor roadway length (km)	aggregated land use type ID	adjusted R^2
			1 (km^2)	
1,3-butadiene	2.88E-02†	5.08E-02†	2.20E-02†	0.82
benzene	2.47E-01†	4.36E-02†	1.90E-01†	0.82
NO_x	2.94E+01†	2.98E+00†	1.56E+01†	0.81
acetaldehyde	4.39E-02†	7.53E-+03†	3.26E-02†	0.80
formaldehyde	1.01E-01†	1.72E-02†	7.48E-02†	0.80

$^{*}p < 0.05$; $^{\dagger}p < 0.001$

6.3.2.3. Estimated Stationary Point Source Emissions

The estimated annual total pollutant emissions from stationary point sources for the three future scenarios, as well as for the baseline scenario, are shown in Table 6.9. Emissions in the future scenarios are substantially higher than in the baseline scenario. Compared to the sprawl scenario, total emissions for all three pollutants are smaller in the compact scenario, yet are approximately 35% higher in electric vehicle scenario. These

results again are expected as the projected electricity demand is higher in the sprawl scenario than the compact scenario, and is even higher in the electric vehicle scenario due to vehicle fleet electrification.

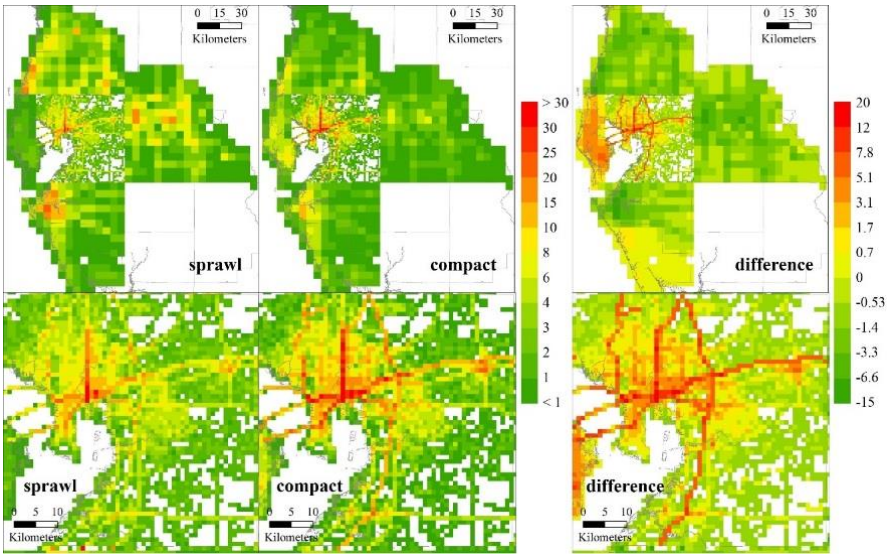

Figure 6.5 Spatial distributions of the allocated NO_x on-road mobile source emissions, and differences of the allocated emissions in seven counties for both sprawl and compact scenario. Unit of the values shown in the figure is metric tons/km^2. Upper figures show emissions in all counties, and lower figures show emissions in Hillsborough County. Differences were calculated by subtracting grid cell emissions of the sprawl scenario from the compact scenario (compact-sprawl). Spatial distributions of the allocated on-road mobile source emissions for other pollutants are similar and hence are not shown. NO on-road mobile source emissions in electric vehicle scenario.

Table 6.9 Stationary point source emissions in the baseline and three future scenarios

	annual stationary point source emissions (metric tons)			
	baseline	sprawl	compact	electric vehicle
NO_x	87100	200000	162000	268000
acetaldehyde	8.8	18	14	24
formaldehyde	22	42	35	56

*Note that fewer point sources were included in the baseline scenario for acetaldehyde and formaldehyde due to smaller emission estimation domain

Figure 6.6 shows spatial distributions of stationary point source emissions for NO_x, acetaldehyde and formaldehyde. Point sources with the highest NO_x emissions are found in Hillsborough County and are located around the Tampa Bay. For formaldehyde, most of the point sources are located within Hillsborough and Pinellas County. Point

sources for acetaldehyde are scattered and sources with the highest emissions are located in Polk, Manatee and Pasco County. The spatial distributions of stationary point source emissions do not vary substantially among three scenarios.

6.3.2.4. Estimated Non-Road, Non-Point and Biogenic Emissions

Table 6.10 provides the estimated total non-road, non-point and biogenic emissions in all counties included in the One Bay visioning plan for the future scenarios. Emissions from the electric vehicle scenario are very similar to those found in the compact scenario and hence are not shown here. Comparing the sprawl and compact scenarios, emissions of benzene and NO_x are higher in the former and emissions of the other three pollutants are, although very similar, slightly higher in the latter.

Further, Figure 6.7 provides comparisons of the total non-road mobile, non-point and biogenic emissions in the baseline, compact and sprawl scenario. For clarity, emissions of acetaldehyde and formaldehyde shown in the figure only included emissions from Hillsborough County due to different emission grids used in the baseline and the future scenarios. Note that non-road mobile source emissions were assumed to be the same for all three future scenarios hence the differences in emissions are affected by non-point and biogenic emissions.

Table 6.10 Non-road, non-point and biogenic emissions for the three future scenarios.

	aggregated annual non-road, non-point and biogenic emissions (metric tons)	
	sprawl	compact
1,3-butadiene	124	128
benzene	1640	1400
NO_x	51200	47000
acetaldehyde	2650	2740
formaldehyde	3230	3350

The estimated non-road, non-point and biogenic emissions for 1,3-butadiene, acetaldehyde and formaldehyde are lower in the future scenarios than in the baseline scenario. Benzene and NO_x emissions in some counties in the sprawl scenario are higher than the baseline. More specifically, benzene emissions from the sprawl scenario are higher in Hernando, Pasco and Polk County, and NO_x emissions are higher in Hernando and Manatee County. Closer examination of the data indicates that the higher non-point source emissions in these counties, the result of extensive development of industrial, commercial and commerce park land use, are responsible for the observed higher emissions in the sprawl scenario.

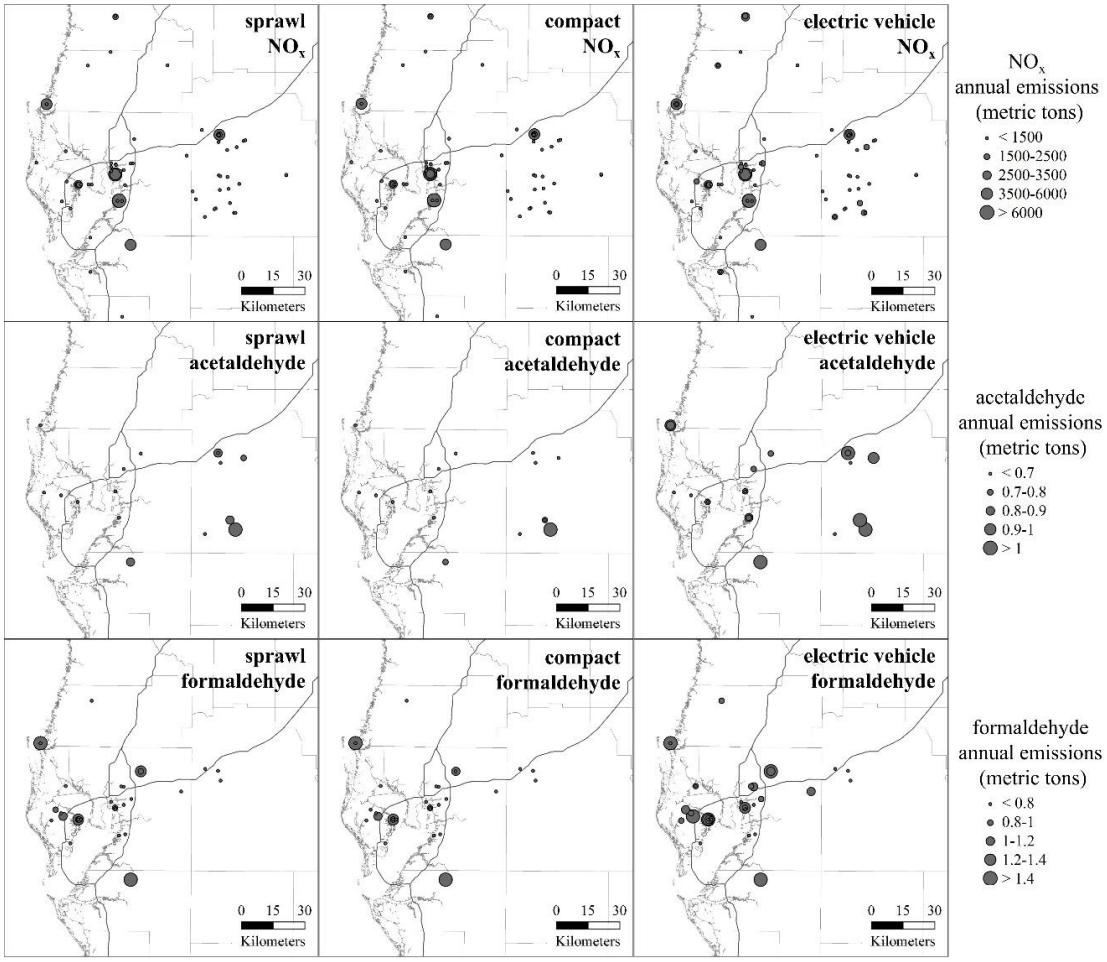

Figure 6.6 Spatial distribution of point source emissions of NO_x, acetaldehyde and formaldehyde for the three future scenarios. Stationary point sources for 1,3-butadiene and benzene were not included in the modeling.

Between the two future scenarios, emissions of 1,3-butadiene, acetaldehyde and formaldehyde are very similar, with generally slightly higher emissions in the compact scenario. Similarly to the baseline scenario, biogenic sources dominate acetaldehyde and formaldehyde emissions in the future scenarios. In the compact scenario, more vegetated land was conserved and hence biogenic emissions for acetaldehyde and formaldehyde are greater. For 1,3-butadiene, non-point source emissions from prescribed forest burning and managed logging debris burning are substantial. With more forested land area in the compact scenario, 1,3-butadiene emissions from these sources are expected to be higher.

Figure 6.8 shows spatial distributions of the estimated non-road, non-point and biogenic emissions of the five selected pollutants in the sprawl and compact scenarios. The spatial distribution patterns vary for different pollutants.

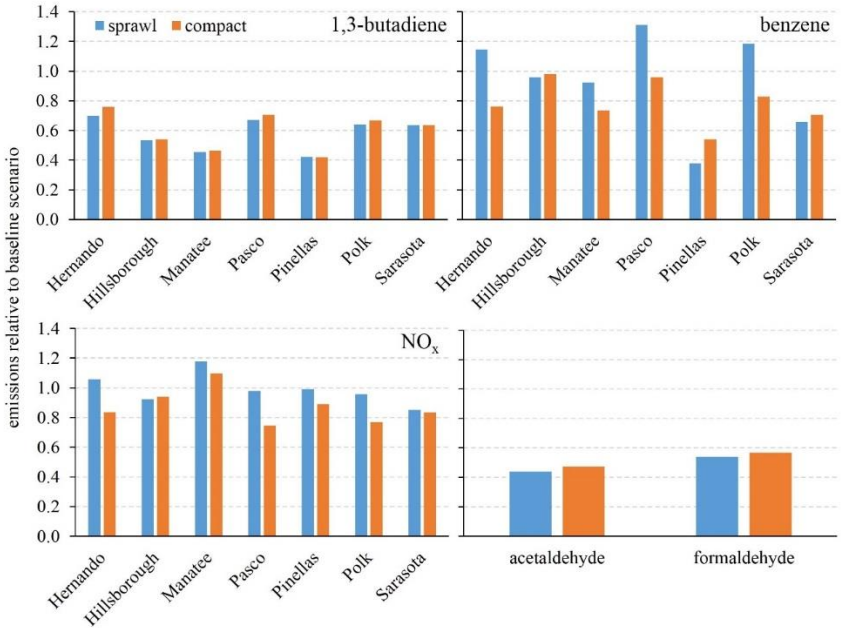

Figure 6.7 Comparison of total non-road mobile, non-point and biogenic emissions (normalized to emissions in baseline scenario) in the baseline, compact and sprawl scenario. Emissions in the baseline scenario were set to 1 for all pollutants. Acetaldehyde and formaldehyde emissions shown in the figure only included emissions from Hillsborough County.

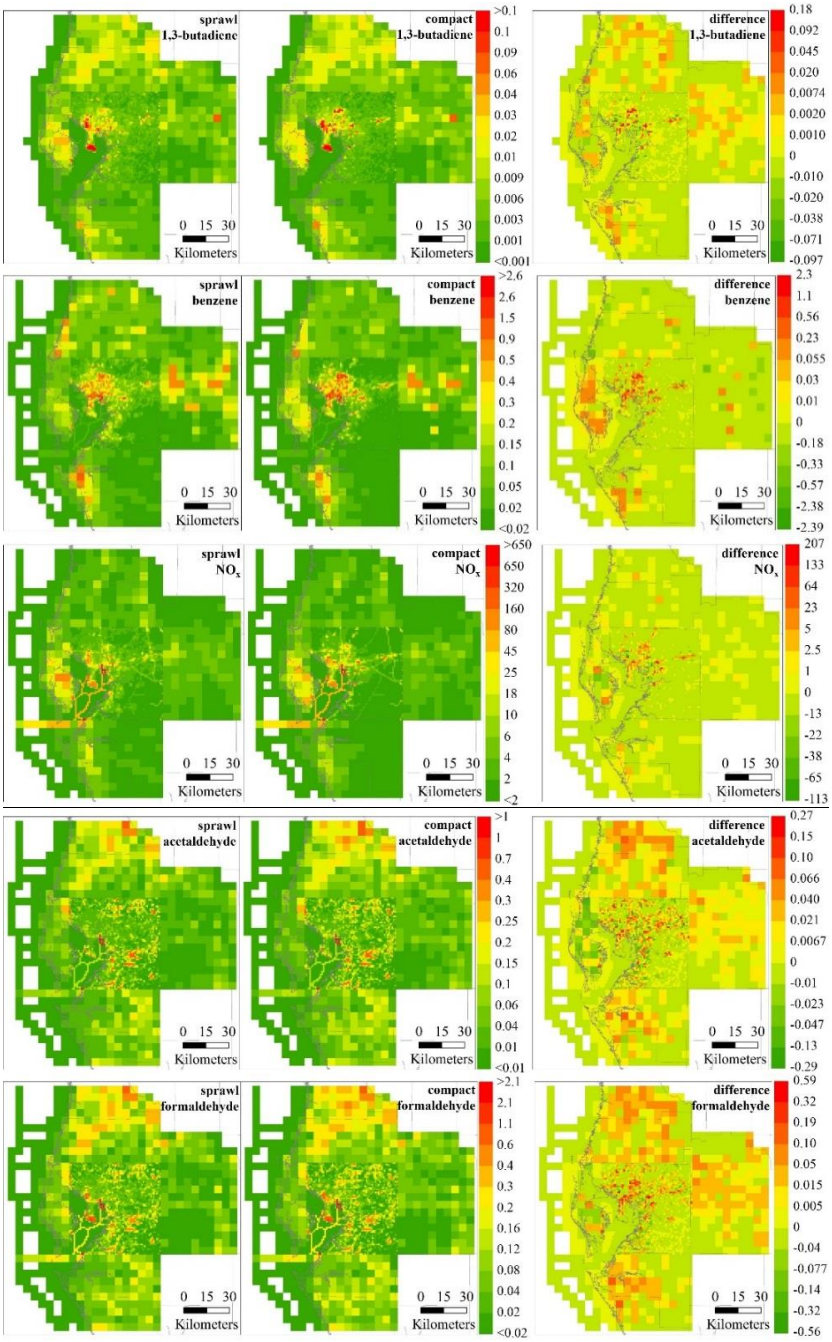

Figure 6.8 Spatial distributions of the allocated non-road, non-point and biogenic emissions, and differences in emissions between sprawl and compact scenarios. Unit of the values shown in the figure is metric tons/km^2. Differences were calculated by subtracting grid cell emissions of the sprawl scenario from the compact scenario (compact-sprawl).

In both sprawl and compact scenarios, the highest 1,3-butadiene emissions are found in the vicinity of airports: the Tampa International Airport and MacDill Air Force

Base. Emissions from commercial marine vessels are not visible on the map. Comparing the two future scenarios, spatial distributions of 1,3-butadiene emissions show slightly higher emissions in developed areas, such as areas near downtown Tampa.

For benzene, pollutant emissions are generally higher in urbanized areas for both scenarios, with more concentrated emissions in the compact scenario. Compared to the sprawl scenario, benzene emissions in the compact scenario are higher in urbanized area such as Tampa, Pinellas County and Bradenton, and slightly lower in other locations. Emissions from marine vessels are noticeable on the map, and emissions from airports are not as apparent as for 1,3-butadiene.

Airport emissions of NO_x are also visible on the map, but the highest NO_x emissions are found near major marine ports such as the Port of Tampa and the Port of Manatee, suggesting contributions from commercial marine vessels. Emissions from shipping lanes within Tampa Bay are also visible. Differences in emissions between the two scenarios show generally higher NO_x emissions in urbanized areas and along major interstates, and slightly lower emissions elsewhere.

The spatial distributions of acetaldehyde emissions are dominated by biogenic emissions: higher emissions are generally found in forested areas rather than urbanized areas. Within Hillsborough County, grid cells with the highest emission differences are scattered, rather than concentrated in urbanized areas as with benzene. NO_x emissions from marine ports and shipping lanes are also clearly visible on the map. Similarly to acetaldehyde, formaldehyde emissions are also dominated by biogenic sources, with greater proportions of airport emissions.

6.3.3. Discussion of Emissions Included in Dispersion Modeling

Emissions discussed above are total pollutant emissions estimated for all seven counties included in the One Bay visioning plan. Note that similarly to the baseline scenario, pollutant emissions within 50 km of the boundary of Hillsborough County were included in subsequent air quality modeling, and pollutant emitted beyond the 50 km limit were excluded as they are considered to not significantly impact pollutant concentrations within Hillsborough County. Table 6.11 provides summaries of the emissions that were included in dispersion modeling from different categories. Total pollutant emissions in Hillsborough County, and 1,3-butadiene, benzene and NO_x emissions in the baseline scenario were also listed for comparison purposes.

Table 6.11 Summary of the emissions included in dispersion modeling.

		annual emissions (metric tons)					
		on-road	stationary point	non-road	non-point	biogenic	total
NO_x	compact	34300	162000	28300	13100		237000
	sprawl	48100	200000	28100	16800		293000
	electric vehicle		268000	28300	13100		310000
	baseline	140000	87200	32800	9310		269000
1,3-butadiene	compact	60.4		46.5	40.7		148
	sprawl	69.5		46.1	36.3		152
	electric vehicle			46.5	40.7		87.2
	baseline	212		106	76.7		395
benzene	compact	368		328	775		1470
	sprawl	421		325	971		1720
	electric vehicle			328	775		1100
	baseline	1822		883	636		3340
acetaldehyde	compact	224	14.3	137	59.8	744.8	1180
	sprawl	286	17.8	135	58.7	645.5	1140
	electric vehicle		24.2	137	59.8	744.8	965
formaldehyde	compact	425	34.5	303	296	744.8	1800
	sprawl	575	42.2	300	276	645.5	1840
	electric vehicle		56	303	296	744.8	1400

*acetaldehyde and formaldehyde emissions in the baseline scenario were not listed due to different domain for emission estimation.

Compared to the baseline scenario, total 1,3-butadiene and benzene emissions in the future scenarios are lower, and NO_x emissions are higher. This observation is due to substantially increased point source emissions. As a result of increased electricity demand, point source emissions were approximately doubled in the compact and sprawl scenarios than the baseline scenario, and tripled in the electric vehicle scenario. For NO_x, emissions from stationary point sources accounted for 32% of the total emissions in the baseline scenario, and these respectively doubled or tripled stationary point source emissions lead to increased total emissions in the future scenarios. The impacts on acetaldehyde and formaldehyde are small, as emissions from stationary point sources only account for a small fraction (less than 5%) of their total emissions.

Between the compact and sprawl scenarios, total emissions of all pollutants except for acetaldehyde are higher in the latter. The implementation of vehicle fleet electrification reduces emissions for 1,3-butadiene, benzene, acetaldehyde and formaldehyde. Of all the scenarios, total NO_x emissions are the highest in the electric vehicle scenarios.

As discussed in Chapter 2, the vast majority of past studies regarding the impact of urban forms on air quality have found lower pollutant emissions in compact than sprawl urban form (Borrego et al., 2006; Ridder et al., 2008; Frank et al., 2000; Kahyaoğlu-Koračin et al., 2009; Liu, 2003; McDonald-Buller et al., 2010; Niemeier et al., 2011; Song et al., 2008; Stone et al., 2007, 2009). Similar findings were also found here, with the exception of acetaldehyde. Here discrepancy in the case of acetaldehyde is reasonable as biogenic sources dominate acetaldehyde emissions in the study area. In the compact scenario, more forested land area is conserved which consequently leads to

higher biogenic emissions. Biogenic emissions of formaldehyde are also higher in the compact scenario than the sprawl scenario, however the total emissions were ultimately lower as this increase was offset by reduced on-road mobile source emissions of formaldehyde. These findings suggest compact urban form may leads to lower anthropogenic pollutant emissions than sprawl urban form, but for pollutants with substantial biogenic source contributions, different results may be found.

Table 6.12 Summary of the emissions in Hillsborough County for three future scenarios.

		annual emissions (metric tons)					
		on-road	point	non-road	non-point	biogenic	total
NO_x	compact	11700	69700	7350	3960		92700
	sprawl	9780	79100	7350	3760		100000
	electric vehicle		95900	7350	3960		107000
	baseline	44400	50900	9290	1630		106000
1,3-butadiene	compact	18.0		16.2	1.7		35.9
	sprawl	15.0		16.2	1.5		32.8
	electric vehicle			16.2	1.7		17.9
	baseline	62.3		28.7	1.4		92.4
benzene	compact	116		108	247		471
	sprawl	96.5		108	238		443
	electric vehicle			108	247		355
	baseline	534		218	110		863
acetaldehyde	compact	71.0	4.3	73.5	8.5	145.6	303
	sprawl	59.3	5.7	73.5	11.7	126.4	277
	electric vehicle		8.1	73.5	8.5	145.6	238
	baseline	93.1	1.6	74.6	4.5	402.6	576
formaldehyde	compact	145	9.29	167	23.5	145.6	490
	sprawl	121	12.2	167	26.7	126.4	453
	electric vehicle		17.2	167	23.5	145.6	354
	baseline	213	3.6	175	14.4	402.6	809

In Hillsborough County alone (Table 6.12), for the compact scenario, total emissions are lower for NO_x and higher for the other pollutants. For all emissions included in dispersion modeling, again for the compact scenario, the total emissions are higher for acetaldehyde and lower for the other pollutants. These variations in emissions

are the results of spatial development differences between the sprawl and compact urban forms. More developments occur in Hillsborough County under compact urban form and hence lead to generally higher pollutant emissions within the county, although total emissions in the study area may be lower.

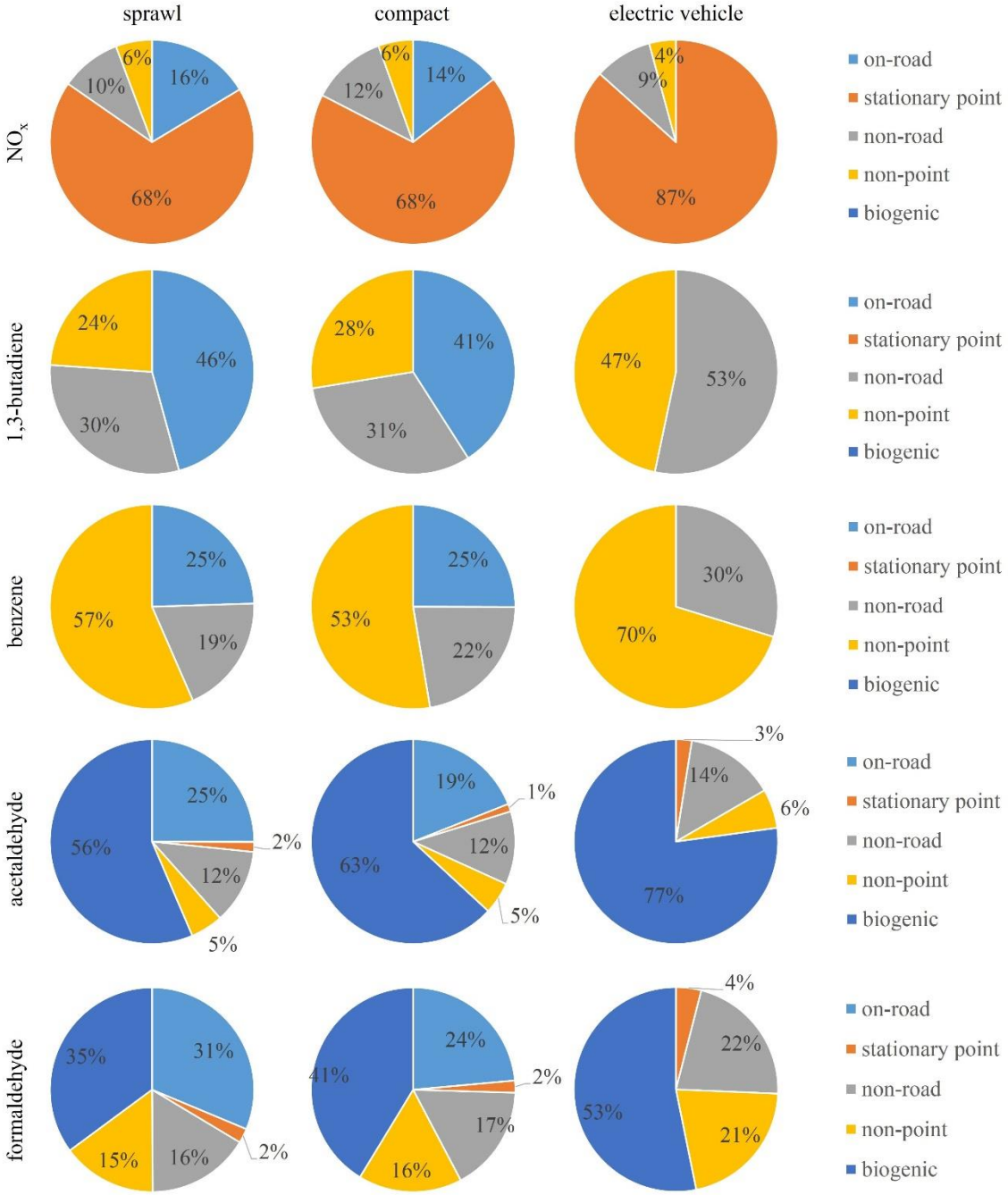

Figure 6.9 Fraction of emissions from different emission categories in the three scenario

Figure 6.9 provides fractions of emissions from different emission categories in the three scenarios. In the sprawl and compact scenarios, the fractions of emissions are similar for each category. On-road mobile sources dominate 1,3-butadiene emissions, accounting for over 40% of the total. For benzene on the other hand, over 50% of emissions were from non-point sources. Stationary point sources emitted the majority of NO_x, and for both acetaldehyde and formaldehyde, biogenic emissions dominate, with on-road mobile sources contributing the most to their anthropogenic emissions.

In the electric vehicle scenario, non-road, non-point and biogenic emissions remained the same as in the compact scenario, and on-road mobile sources emissions were completely eliminated due to vehicle fleet electrification. Fractions of emissions from the different emission categories thus changed accordingly. For 1,3-butadiene, non-road mobile source emissions now dominate, and for NO_x, stationary point sources now account for an even higher fraction of emissions (87%).

6.3.4. Limitations and Uncertainties in Emission Estimation

Emission estimates for stationary point sources may contain the largest uncertainties. In the future scenarios, point source emissions were estimated by extrapolating from the baseline scenario using the projected electricity demands. The average emission rates (tons of emissions per GWh of load) in the future scenarios were assumed to be the same as in the baseline scenario (2002). In practice, the emission rates in the future scenarios are expected to be lower due to improved technology and stringent regulations on power generation units. As an example, the California Emission Forecasting System predicts that NO_x emissions from stationary point sources would decrease from 2000 to 2020, despite that electricity demands may increase.

Uncertainties also exist in the estimated total on-road mobile source emissions, as well as the spatial distributions of these emissions. Total vehicle mileage travelled in the whole study domain were allocated to each county based on estimated vehicle trips generated in corresponding counties. Individual travel behaviors such as trip length and trip frequency may vary under different urban forms (Milakis et al., 2008), however such effects were not included in this study due to lack of information. Spatial distributions of on-road mobile source emissions were predicted to the future scenarios using multiple linear regression, and no travel demand analysis were performed. In addition, no roadway network expansions were included in the One Bay visioning plan, nor in the emission estimation.

In this study, non-road mobile source emissions were estimated using the NMIM model and default activity data were applied for both the compact and sprawl scenarios. The default data may not accurately reflect off-road motor-engine activities in each county, especially under different urban forms.

6.3.5. Summary and Conclusion of Emission Estimation

To summarize, on-road mobile, stationary point, non-road, non-point and biogenic emissions of five selected pollutants, 1,3-butadiene, benzene, NO_x, acetaldehyde and formaldehyde, were estimated for the three hypothetical future scenarios: sprawl, compact and an electric vehicle scenario. The MOVES model was applied to estimate future on-road mobile source emissions using extrapolated vehicle population and vehicle mileage travelled data. Spatial distributions of on-road mobile source emissions were estimated using multiple linear regressions. Pollutant emissions from stationary point sources were extrapolated to the future scenarios using predicted electricity demand data,

and temporal variations of point source emissions in the electric vehicle scenario were adjusted based on derived electric vehicle charging profiles. For non-point source emissions, 9 surrogates were used to extrapolate the baseline emissions to the year 2050. The NMIM model was used to calculate non-road mobile source emissions, and biogenic emissions were projected to the future scenarios based on forest area.

Compared to the baseline scenario (2002), the estimated on-road mobile source emissions in the future scenarios are substantially lower for 1,3-butadiene, benzene and NO_x. They are also slightly lower for formaldehyde, and acetaldehyde in the compact scenario, but slightly higher for acetaldehyde in the sprawl scenario. Between the two future scenarios, sprawl scenario consistently show higher on-road emissions due to higher predicted vehicle mileage travelled. Due to distinct development patterns, on-road emissions of all pollutants are higher in developed counties in the compact scenario, and higher in relatively less developed counties in the sprawl scenario.

The extrapolated stationary point source emissions are substantially higher in all three future scenarios than the baseline scenario. Point source emissions are the highest in the electric vehicle scenario due to vehicle fleet electrification, followed by sprawl, with the compact scenario show the lowest point source emissions. It does however needs to be noted that the predicted emissions from stationary sources are expected to be overestimated. The results for point sources represent what would happen if the emissions rates from power plants were not reduced.

Total emissions from non-road, non-point and biogenic sources are lower for 1,3-butadiene, acetaldehyde and formaldehyde in the future scenarios, due primarily to less forested areas. Emissions for benzene and NO_x are comparable with the baseline

scenario, and may even be higher in some counties. Industrial, commercial and residential stationary fuel combustions contribute to benzene and NO_x emissions.

Overall, the total amount of pollutant emissions included in dispersion modeling in the compact scenario are lower for 1,3-butadiene, benzene, NO_x and formaldehyde, but higher for acetaldehyde due to more forested land areas in the compact scenario. The findings suggest compact urban form may lead to less anthropogenic emissions, but contributions from biogenic sources may be substantial which could lead to higher total emissions. In Hillsborough County alone, total emissions in the compact scenario are lower for NO_x but higher for the other pollutants. The inconsistency in the direction of change in emissions may be caused by the different spatial development patterns in the two scenarios.

Regarding the fractions of emissions from each of the five emission categories, in the sprawl and compact scenarios, emissions were dominated by on-road, non-point and stationary point sources for 1,3-butadiene, benzene and NO_x, respectively. In addition, on-road mobile sources also contribute most significantly to anthropogenic emissions of acetaldehyde and formaldehyde. After eliminating on-road mobile source emissions in the electric vehicle scenario, non-road sources are responsible for the most 1,3-butadiene emissions. In all three scenarios, biogenic sources emitted the most acetaldehyde and formaldehyde emissions.

6.4. Concentration Estimation

Similarly to the baseline scenario, the non-steady-state Gaussian dispersion model CALPUFF was used to estimate concentrations of the five selected pollutants due to local emissions. However, no model output data from Eulerian grid models are available for

the future scenarios, hence no further concentration adjustments such as “blending” were performed for acetaldehyde and formaldehyde.

6.4.1. Methods of Concentration Estimation

The same meteorological data as used in the baseline scenario were used for the future scenarios. Model configurations including reaction parameters, dry and wet deposition parameters were also kept the same as in the baseline scenario. The three future scenarios were modeled separately. For computational tractability, the whole CALPUFF modeling was split into 867 cases with each case executed individually and the results were later aggregated.

6.4.2. Results and Discussion of Concentration Estimation

6.4.2.1. Modeled NOx Concentrations

Table 6.13 provides modeled concentration summaries for the highest 1 hour, 98th percentile of hourly and annual average NO_x concentrations for the sprawl, compact and electric vehicle scenarios. For comparison purposes, concentration summaries in the baseline scenario are also provided. Spatial distributions of the modeled NO_x concentrations are shown in Figure 6.9. Compared to the baseline scenario, the modeled NO_x concentrations are generally higher in the three future scenarios with the exception of the compact scenario at annual average scale. The modeled lower NO_x concentrations may be explained by the disproportionately small contributions of stationary point source emissions to NO_x concentrations (see section 5.5.2.1).

Among three scenarios, the electric vehicle scenario consistently shows the highest NO_x concentrations at all temporal metrics, followed by sprawl and then compact scenario with the lowest concentrations. The direction of concentration changes across

the three scenarios are consistent with the directions of emission changes as discussed previously.

Table 6.13 Concentration summaries for the modeled highest 1 hour, 98th percentile of hourly and annual average NO_x concentrations for the sprawl, compact, electric vehicle and the baseline scenarios

		concentrations ($\mu g/m^3$)			
		sprawl	compact	electric vehicle	baseline
highest 1 hour	range	95-45700	79-30800	144-122000	67-2740
	average	433	352	695	262
	std.	1200	812	2600	150
98th percentile	range	41-2800	33-1900	55-5340	25-524
	average	98	83	136	72
	std.	94	69	167	32
annual average	range	7-220	5-154	9-378	4-138
	average	17	14	21	14
	std.	12	9	17	7

*std.: standard deviation

Assuming standard ambient temperature and pressure, the National Ambient Air Quality Standard (NAAQS) standards for NO_2 are equivalent to 100 $\mu g/m^3$ and 188 $\mu g/m^3$, at annual and 98th percentile temporal scale. The modeled average NO_x concentrations are below the NO_2 standard at two temporal scales, but the modeled highest NO_x concentrations at some receptors exceeded the standard. For all three temporal metrics, the highest NO_x concentrations are found near Port of Tampa and above the intersections of I-4 and I-75, where a fugitive point source is located. The term "fugitive" refers to the unintended release of pollutants from non-designated release points (such as stacks), mainly from industrial processes. Fugitive emissions are normally released at near ground level and hence may impact air pollution concentrations at ground level. The Port of Tampa area has substantial NO_x emissions from commercial marine vessels, and also with a few major point sources located nearby. Regarding the

mentioned fugitive point source, although the amount of emissions from the specific point source is relatively small compared to other major sources (Figure 6.6), it still contributes to nearby NO_x concentrations due to its fugitive nature. The impacts of on-road mobile source emissions are not clearly observed from Figure 6.10, owing to significantly lower emissions in the future scenarios.

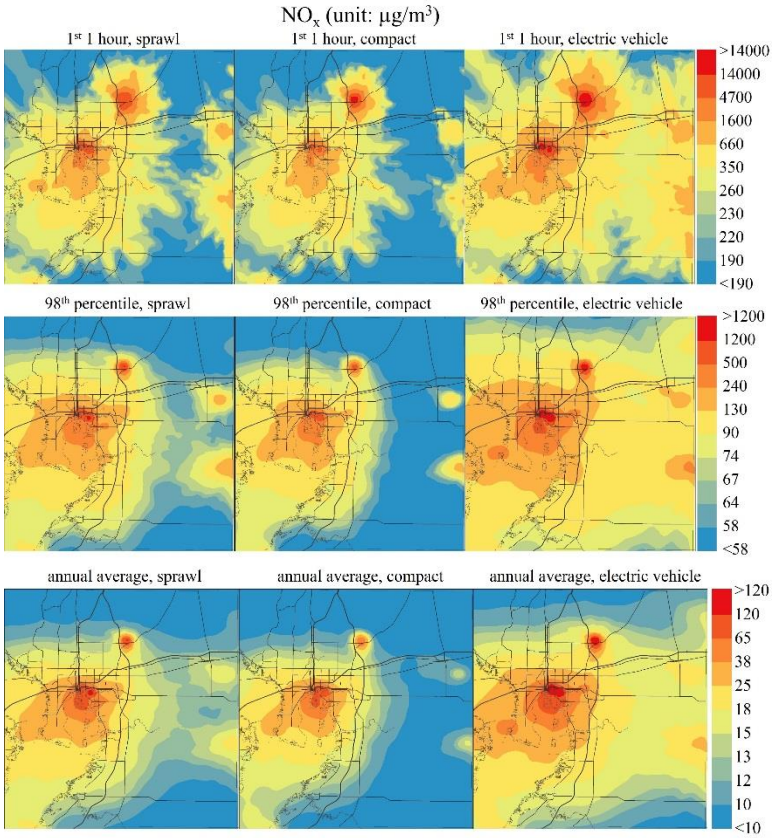

Figure 6.10 Modeled highest 1 hour (1st 1h), 98th percentile of hourly and annual average NO_x concentrations in the sprawl, compact and electric vehicle scenarios.

Comparing between scenarios (Figure 6.11), contributions of point sources to NO_x concentrations are apparent. Note that emissions from marine vessels were held constant in the three scenarios, hence they do not contribute to concentration changes among scenarios. Between the sprawl and the compact scenarios, NO_x concentrations are lower in the majority of the domain for all temporal metrics in the compact scenario than the sprawl scenario, and the largest concentration differences are found near Port of

Tampa, as well as near the fugitive point source mentioned previously. Between the electric vehicle and the compact scenarios, NO_x concentrations are higher in most areas of the study domain in the former, with the highest differences again found in the same areas as above.

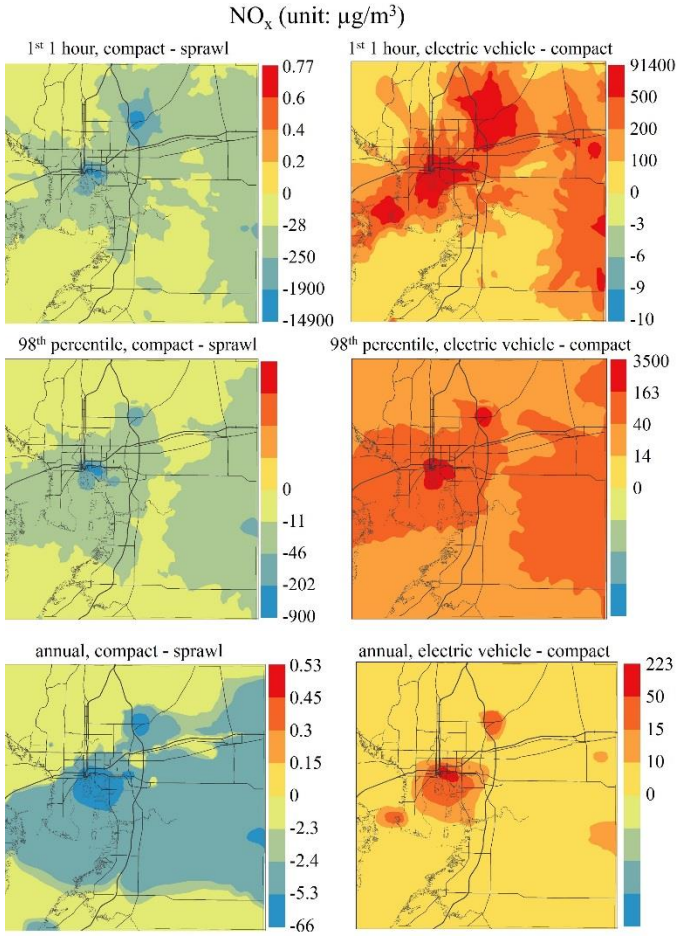

Figure 6.11 Concentration differences between the sprawl and compact, and between the compact and electric vehicle scenarios for highest 1 hour, 98th percentile and annual average NO_x concentrations.

Overall, the modeling results suggest that stationary point sources contribute substantially to the modeled NO_x concentrations, as well as the observed concentration differences between scenarios. Such results are expected as point sources dominate NOx emissions in all three scenarios (Figure 6.9). It is necessary to note that NO_x emissions from stationary point sources are likely to be overestimated. Considering NO_x alone, air

quality in Hillsborough County is better in the compact urban form than in the sprawl urban form, primarily due to the predicted lower electricity consumptions (which lead to lower point source emissions) in this County. However, air quality benefits arising from complete elimination of on-road mobile source NO_x emissions through vehicle fleet electrification are overcome by the substantially increased stationary point source emissions, and overall led to worse air quality in the electric vehicle scenario

6.4.2.2. Modeled 1,3-butadiene Concentrations

Table 6.14 provides concentration summaries for the modeled highest 1 hour and annual average 1,3-butadiene concentrations for three future scenarios and again for comparison, the baseline scenario. Compared to the baseline, the modeled 1,3-butadiene concentrations are substantially lower in the future scenarios, mainly due to reduced emissions (Table 6.11). Among the three future scenarios, 1,3-butadiene concentrations are slightly higher in the compact than sprawl scenarios at both temporal scales. Although total 1,3-butadiene emissions included in the whole modeling domain is 3% lower in the compact scenario (Table 6.11), emissions in Hillsborough County alone increased by approximately 10% (Table 6.12) which resulted in the observed concentration increase. Average 1,3-butadiene concentrations are the lowest in the electric vehicle scenario.

Figure 6.12 provides spatial distributions of the modeled highest 1 hour and annual average 1,3-butadiene concentrations in the three future scenarios. The highest 1,3-butadiene concentrations are generally found near airports such as Tampa International Airport and MacDill Air Force Base, suggesting concentration contributions from airport emissions. Although not as apparent, contributions from on-road mobile sources are also visible in annual average 1,3-butadiene concentration distributions for

the sprawl and compact scenarios, where increased concentrations can be found near major roadways. As shown in Table 6.11, on-road mobile sources emitted more 1,3-butadiene than non-road mobile sources (which include airport sources). Despite this, airport emissions are concentrated in certain locations, whereas on-road mobile sources are relatively sparsely distributed, hence the impact of airport emissions appear more prevalent in the results.

Table 6.14 Concentration summary for the modeled highest 1 hour and annual average 1,3-butadiene concentrations for sprawl, compact and electric vehicle scenario

		concentrations ($\mu g/m^3$)			
		sprawl	compact	electric vehicle	baseline
highest 1 hour	range	0.022-0.24	0.02-0.28	0.013-0.23	0.04-4.8
	average	0.076	0.089	0.049	0.24
	std.	0.038	0.049	0.031	0.18
annual average	range	0.0013-0.011	0.0012-0.013	0.0006-0.0091	0.003-0.21
	average	0.0041	0.0044	0.0021	0.012
	std.	0.0017	0.0022	0.0011	0.007

*std.: standard deviation

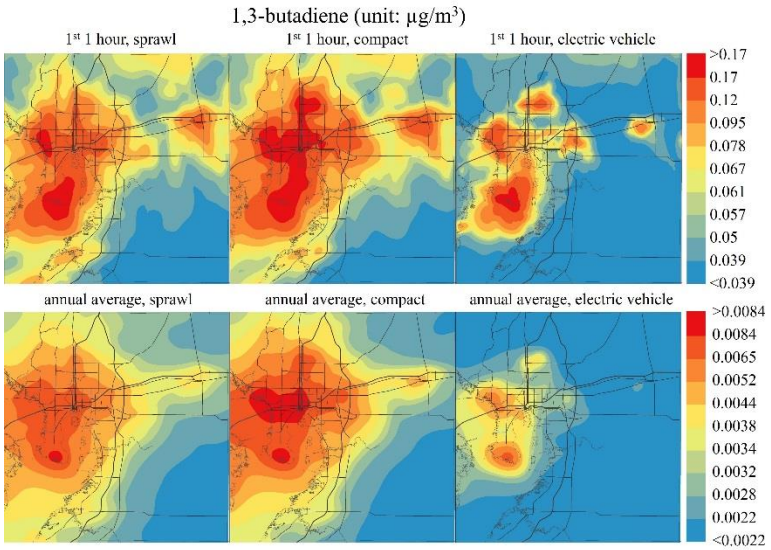

Figure 6.12 Modeled highest 1 hour (1st 1h) and annual average 1,3-butadiene concentrations in sprawl, compact and electric vehicle scenarios.

The modeled concentration differences for 1,3-butadiene between future scenarios are shown in Figure 6.13. Concentrations are higher in the majority of Hillsborough County in the compact scenario. The spatial patterns of the differences in 1,3-butadiene concentration essentially follow emission differences as shown in Figure 6.8, suggesting non-point sources contribute to the observed differences. Compared to the compact scenario, 1,3-butadiene concentrations are lower near major roadways, due to elimination of on-road mobile source emissions.

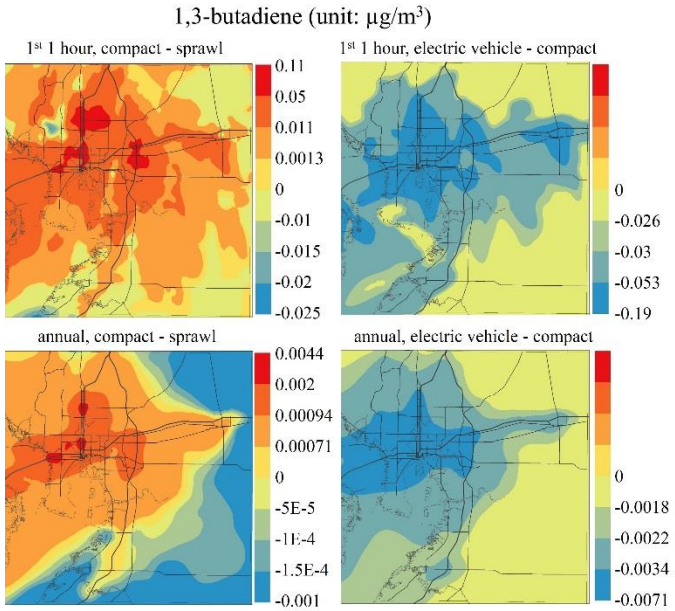

Figure 6.13 Concentration differences between sprawl and compact, and between compact and electric vehicle scenarios for highest 1 hour and annual average 1,3-butadiene concentrations.

For 1,3-butadiene, air quality in Hillsborough County is better in sprawl urban form than compact urban form, although the amount of total 1,3-butadiene emissions included in dispersion modeling is lower in the compact scenario. The spatial re-distribution of 1,3-butadiene emissions may be responsible for such observations. In addition, the modeling results show that through vehicle fleet electrification, air quality in Hillsborough County could be improved.

6.4.2.3. Modeled Benzene Concentrations

A summary of the modeled benzene concentrations in the baseline and three future scenarios are shown in Table 6.15. Generally, benzene concentrations are lower in future scenarios than in the baseline. Among the future scenarios, benzene concentrations are the highest in the sprawl scenario, followed by the compact scenario and finally are the lowest in the electric vehicle scenario. Total emissions of benzene included in dispersion modeling are also ranked in the same order (Table 6.11).

Table 6.15 Concentration summary for the modeled highest 1 hour and annual average benzene concentrations for the sprawl, compact and electric vehicle scenario

		concentrations ($\mu g/m^3$)			
		sprawl	compact	electric vehicle	baseline
highest 1 hour	range	0.69-5.6	0.50-6.23	0.40-5.17	1.1-4.5
	average	1.7	1.8	1.4	3.4
	std.	0.78	0.97	0.8	1.8
annual average	range	0.036-0.23	0.030-0.26	0.02-0.21	0.07-2.0
	average	0.094	0.091	0.066	0.19
	std.	0.033	0.041	0.031	0.085

*std.: standard deviation

Spatial distributions of the modeled benzene concentrations are shown in Figure 6.14, and concentration differences between scenarios are shown in Figure 6.15. Generally, benzene concentrations are higher near downtown and Port of Tampa in all scenarios. Compared to the sprawl scenario, the averaged benzene concentration across all receptors is lower in the compact scenario, but is higher in the left portion of Hillsborough County. The observed higher benzene concentrations in the compact scenario is contributed by higher benzene emissions in Hillsborough County (Table 6.12 and Figure 6.8). Comparing the electric vehicle and compact scenarios, benzene

concentrations are lower in all of Hillsborough County, due to elimination of on-road mobile source emissions.

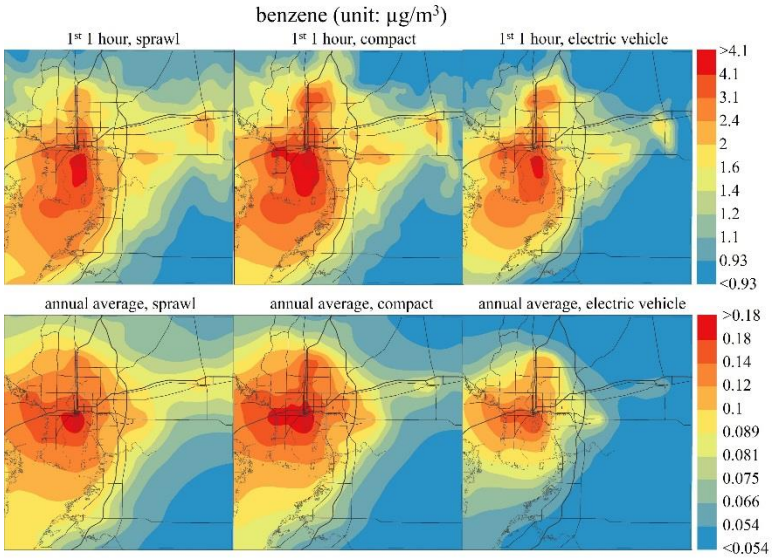

Figure 6.14 Modeled highest 1 hour (1st 1h) and annual average benzene concentrations in sprawl, compact and electric vehicle scenarios.

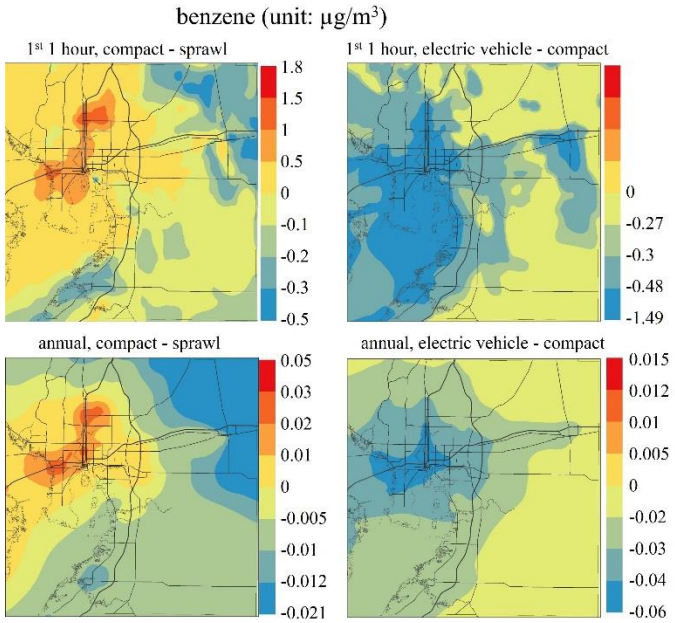

Figure 6.15 Concentration differences between sprawl and compact, and between compact and electric vehicle scenarios for highest 1 hour and annual average benzene concentrations.

Overall the average benzene concentration in Hillsborough County is lower in the compact scenario than the sprawl scenario, but this concentration is higher in some

regions of Hillsborough County. The observed higher benzene concentration areas are populated census block groups, which could result in higher human exposure to benzene in the compact scenario. In addition, vehicle fleet electrification would lead to lower average benzene concentration across the whole Hillsborough County region, and hence benzene exposure in the electric vehicle scenario is expected to be lower than in the compact scenario.

6.4.2.4. Modeled Acetaldehyde and Formaldehyde Concentrations

Both acetaldehyde and formaldehyde have substantial biogenic emissions. As shown in Table 6.11 and Table 6.12, the total acetaldehyde emission included in the modeling is slightly higher (3%) in the compact than the sprawl scenario, compared to slightly lower (-2%) for formaldehyde. In Hillsborough County alone, total acetaldehyde and formaldehyde emissions are 10% and 8% higher in the compact than sprawl scenario respectively. Regarding the modeled average pollutant concentration levels, results for both acetaldehyde and formaldehyde are higher in the compact scenario than the sprawl scenario (Table 6.16 and Table 6.17). The increased pollutant emissions in Hillsborough County in the compact scenario are responsible for these higher concentration levels. Due to elimination of on-road mobile source emissions, average acetaldehyde and formaldehyde concentrations in the electric vehicle scenario are found to be lower than in the compact scenario.

Figure 6.16 shows the modeled highest 1 hour and annual average acetaldehyde and formaldehyde concentrations in the three future scenarios, despite the fact that biogenic emissions dominate total emissions for the two pollutants, the highest pollutant concentrations are not found near forested areas. Specifically, highest acetaldehyde

concentrations are found near the Port of Tampa area, where marine vessel emissions are high (Figure 6.8). For formaldehyde, the highest concentrations are not only found near the same port area, but also are found near the locations of some point sources (Figure 6.5). Biogenic emissions are sparsely distributed across the whole modeling domain, and although the total amount of emissions are high, the per-area emission rates of biogenic sources are relatively low.

Table 6.16 Concentration summary for the modeled highest 1 hour and annual average acetaldehyde concentrations for sprawl, compact and electric vehicle scenario

		concentrations ($\mu g/m^3$)			
		sprawl	compact	electric vehicle	baseline
highest 1 hour	range	0.43-4.7	0.44-4.86	0.4-4.3	0.68-8.4
	average	0.87	0.94	0.8	1.6
	std.	0.42	0.42	0.38	0.48
annual average	range	0.021-0.15	0.02-0.15	0.016-0.14	0.02-0.4
	average	0.045	0.048	0.037	0.068
	std.	0.014	0.015	0.012	0.022

*std.: standard deviation. Baseline concentrations are those modeled directly by CALPUFF

Table 6.17 Concentration summary for the modeled highest 1 hour and annual average formaldehyde concentrations for sprawl, compact and electric vehicle scenario

		concentrations ($\mu g/m^3$)			
		sprawl	compact	electric vehicle	baseline
highest 1 hour	range	0.56-88	0.7-77	0.47-82	0.74-57
	average	1.6	1.8	1.4	2.1
	std.	2	1.8	2.3	1.1
annual average	range	0.03-0.56	0.047-0.55	0.021-0.54	0.03-0.9
	average	0.075	0.12	0.057	0.098
	std.	0.03	0.045	0.027	1

*std.: standard deviation. Baseline concentrations are those modeled directly by CALPUFF

The modeled concentration differences between the future scenarios for acetaldehyde and formaldehyde at two temporal scales are shown in Figure 6.17. Comparing the sprawl and compact scenarios, concentrations of both pollutants are higher in the majority of Hillsborough County in the latter. At the highest 1 hour temporal scale, the highest concentration differences are scattered and no apparent patterns can be observed between pollutants, although it is worth noting that some of the highest concentration differences correspond to low residential areas in the sprawl scenario (Figure 6.1). At the annual average temporal scale, the highest concentration changes can be observed near the downtown area, with some slightly less evident but still observable changes along major roadways, suggesting contributions from on-road mobile sources. Between the electric vehicle scenario and the compact scenario, acetaldehyde and formaldehyde concentrations are generally lowered across the whole County in the former. The increased point source emissions of acetaldehyde did not substantially impact acetaldehyde concentrations. At the highest 1 hour temporal scale, the impacts of point sources on concentrations of formaldehyde can be observed, however the impacts are mainly localized to a few point sources and are relatively small.

Overall, regarding acetaldehyde and formaldehyde, air quality in Hillsborough County is better in the sprawl than the compact scenario, due mainly to spatial re-distribution of pollutant emissions. With the elimination of on-road mobile source emissions, concentrations of acetaldehyde and formaldehyde were lowered in the electric vehicle scenario compared to the compact scenario, suggesting improved air quality with the implementation of vehicle fleet electrification.

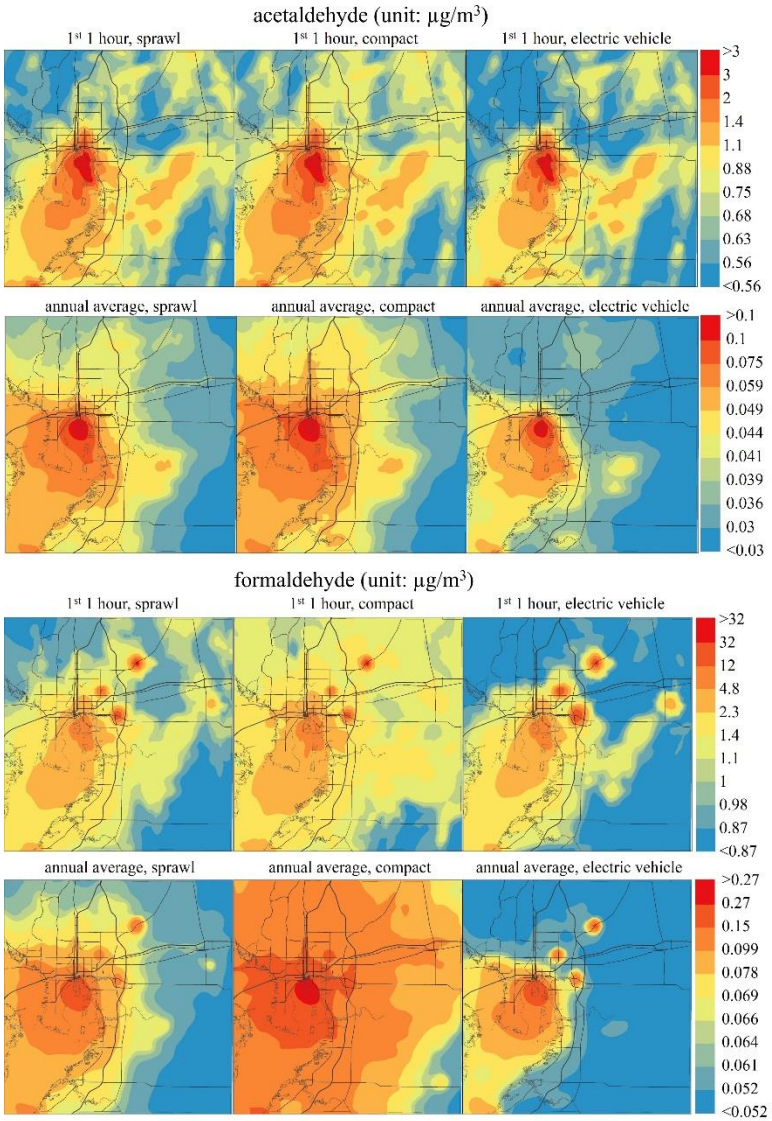

Figure 6.16 Modeled highest 1 hour (1st 1h) and annual average acetaldehyde and formaldehyde concentrations in sprawl, compact and electric vehicle scenarios.

6.4.3. Discussion of Concentration Estimation Findings

Using the CALPUFF model, the spatial distributions of pollutant concentrations in Hillsborough County were estimated for the three future scenarios. Restricted by the nature of the CALPUFF model, atmospheric formations of pollutants were not modeled, and as such the estimated pollutant concentrations are due to local emissions. Therefore, all pollutants are essentially modeled as primary pollutants in this study.

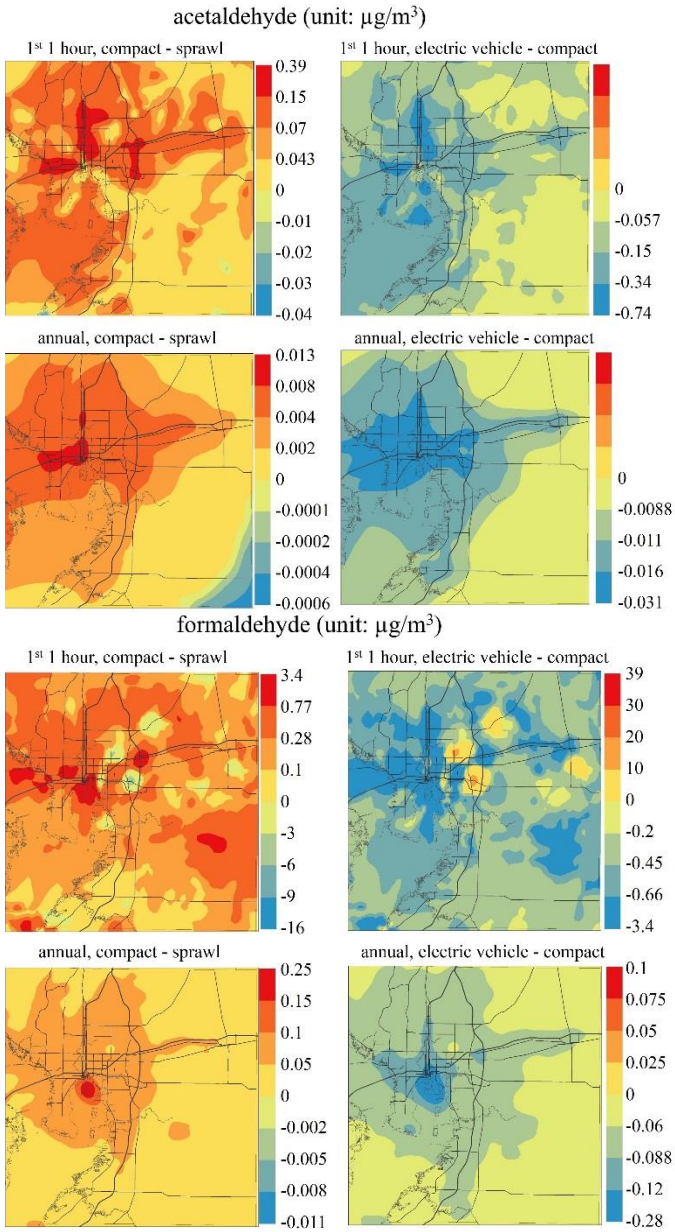

Figure 6.17 Concentration differences between sprawl and compact, and between compact and electric vehicle scenarios for highest 1 hour and annual average acetaldehyde and formaldehyde concentrations.

Most previous studies regarding the impact of urban forms on pollutant concentrations have found lower average pollutant concentrations in compact than sprawl urban form, for both primary pollutants and pollutants with substantial secondary contributions (Bechle et al., 2011; Ridder et al., 2008; Hixson. et al., 2012; Kahyaoğlu-Koračin et al., 2009; Martins, 2012; Schweitzer & Zhou, 2010). The findings are mainly

due to lower total pollutant emissions estimated in compact urban forms. For primary pollutants, urban centers were found to exhibit concentrated and increased emissions under compact urban form which consequently lead to higher concentrations in these urban centers (Hixson et al., 2010; Martins, 2012).

In this study, comparing the sprawl and compact scenarios, higher average pollutant concentrations were found in the compact scenario for 1,3-butadiene, acetaldehyde and formaldehyde. The findings are not contrary to but rather consistent with earlier literatures as pollutant concentrations were estimated for Hillsborough County only, which is a one of the most urbanized regions of all seven counties included in the One Bay visioning plan. As mentioned previously, concentration levels of primary pollutants were also found to be higher in urban centers in compact urban form.

Regarding NO_x and benzene, average pollutant concentrations are lower in the compact than sprawl scenario. Spatially, benzene concentrations in urbanized areas in Hillsborough County are generally higher in the compact than sprawl scenario (Figure 6.15), while concentrations in the remaining regions are generally lower. Despite this, for NO_x, pollutant concentrations are consistently lower across the whole county in the compact than sprawl scenario (Figure 6.11), particularly near downtown Tampa area, where the largest concentration differences were found.

The results for NO_x adds to the present range of knowledge in the field by demonstrating that concentrations of primary pollutants are not guaranteed to be higher in urban centers in the compact urban form. Rather, these pollutant concentrations may depend on the type of dominant emissions sources, as well as the locations of these emission sources.

In this study, the majority of NO_x emissions were from point sources, and some of the point sources with the highest emissions were located near downtown Tampa area. Due to the predicted lower electricity consumptions, point source emissions are lower in the compact scenario, which in turn lead to lower NO_x concentrations nearby. For other pollutants, on-road, non-road or non-point source emissions contribute most to pollutant concentrations. Since emissions from these sources tend to be greater and concentrated around urban centers in compact urban form, higher pollutant concentrations are expected in the compact than sprawl scenario around these urban centers. Again, it needs to be noted that the estimated NO_x emissions from stationary point sources may be overestimated.

The modeling results suggest that with vehicle fleet electrification, concentration levels of 1,3-butadiene, benzene, acetaldehyde and formaldehyde could be lowered, whereas concentrations of NO_x may be increased due to increased point source emissions. Hence, the impacts of vehicle fleet electrification on air quality are rather pollutant specific, and may not be always beneficial.

6.4.4. Limitations and Uncertainties in Concentration Estimation

There are several important limitations to the modeling of pollutant concentrations for the future scenarios. First, due to data availability, the CALPUFF modeled acetaldehyde and formaldehyde concentrations were not combined with any Eulerian model outputs as in the baseline scenario. A substantial amount of acetaldehyde and formaldehyde are formed in the atmosphere rather than directly emitted (Finlayson-Pitts & Pitts, 1999), but these concentrations cannot be captured by the CALPUFF model.

A second limitation is the less explicit representation of major roadways. In the baseline scenario, all major roadways were modeled on a link by link basis. However in future scenarios only freeways were modeled link by link and all other major roadways were modeled as area sources. Hence, the near road impact of those links not modeled explicitly may not be accurately captured.

6.4.5. Summary and Conclusions

Using dispersion modeling, concentrations of five selected pollutants (NO_x, 1,3-butadiene, benzene, acetaldehyde and formaldehyde) were estimated for three future scenarios (sprawl, compact and electric vehicle scenario) at multiple temporal scales. Average concentrations and the spatial distribution of concentrations were compared to evaluate the impact of different urban forms and vehicle fleet electrification on air quality.

The modeling results show lower average pollutant concentrations of NO_x and benzene, and higher average concentrations of the other three pollutants in the compact than the sprawl scenario. Spatially, 1,3-butadiene, acetaldehyde and formaldehyde concentrations in the compact scenario are higher in the majority of Hillsborough County; benzene concentrations are higher in urbanized areas and NO_x concentrations are consistently lower across the whole county.

The findings for 1,3-butadiene, benzene, acetaldehyde and formaldehyde are consistent with past studies. Findings for NO_x suggest that concentration levels of primary pollutants may not necessarily be higher in urban centers in compact urban form, and they rather these concentrations depend on the dominant emissions sources and their locations.

In addition, vehicle fleet electrification was found to result in lower concentration levels of 1,3-butadiene, benzene, acetaldehyde and formaldehyde, but higher concentration levels of NO_x in the whole county. The increased point source emissions of NO_x are responsible for these observed concentration increases. Overall, the impacts of vehicle fleet electrification on air quality are pollutant specific, and may not always be beneficial.

6.5. Exposure Estimation in Future Scenario

The CALPUFF modeled pollutant concentrations in the three future scenarios were combined with projected population data to estimate human exposures to air pollution in future scenarios. Results for the different scenarios were compared to evaluate the impact of urban form and vehicle fleet electrification on air pollution exposure.

6.5.1. Methods of Exposure Estimation

First, block group level population distributions in the future scenarios were estimated. Population weighted exposures were then calculated for three scenarios and comparisons were performed.

Block group populations in the future scenarios were estimated by combining populations in the baseline scenario with estimated population changes in the corresponding block group, which were calculated in a similar way to the calculation for county total populations described in section 5.3.1.1.1:

$$P_{b,s} = p_H \sum_{k=1}^{15} \left(L_{b,k,s,u} H_{k,u} + L_{b,k,s,d} H_{k,d} \right)$$

where $P_{b,s}$ is the population change in block group b for scenario s; p_H is average person per household (2.46 person per household); k is land use types as defined in the One Bay

visioning plan; $L_{b,k,s,u}$ is the total land area (acres) of land use type *k* in block group *b* in scenario *s* that is already developed to some extent in the baseline scenario, but with no further development in future scenarios; $H_{k,u}$ is the household density (households per acre) for land use type *k* that is already developed to some extent but with no further development in future scenarios; $L_{b,k,s,d}$ is the total land area (acres) of land use type *k* in block group *b* of scenario *s* that is newly or re-developed in the future scenario; and $H_{k,d}$ is the household density (households per acre) for land use type *k* that is re-developed in the future scenario.

6.5.2. Results and Discussion of Exposure Estimation

Table 6.18 provides the estimated population exposures to the five selected pollutants in the three future scenarios. The county average human exposures are higher in the sprawl than compact scenarios for NO_x, but are lower for the other four pollutants. The findings for 1,3-butadiene, benzene, acetaldehyde and formaldehyde are consistent with previous studies, where higher human exposures to primary pollutants are found in compact urban form (Hixson et al., 2010; Martins, 2012). This is mainly due to the co-location of populated areas and areas with higher pollutant concentrations.

Table 6.18 Estimated population weighted exposure to the five chosen pollutants in the future scenarios.

	population weighted exposure (μg/m^3)								
	highest 1 hour			annual average			98th percentile		
	spr	com	elec	spr	com	elec	spr	com	elec
NOx	547	457	991	19	18	27	116	109	186
1,3-butadiene	0.085	0.12	0.064	0.0046	0.006	0.0028			
benzene	1.9	2.3	1.8	0.11	0.12	0.089			
acetaldehyde	0.89	1	0.79	0.047	0.054	0.039			
formaldehyde	1.7	2.1	1.6	0.08	0.14	0.064			

*spr: sprawl scenario; com: compact scenario; elec: electric vehicle scenario

As discussed in Section 5.4.2.1, the modeled NO_x concentrations in urbanized areas are lower in the compact than sprawl scenario due to lower NO_x emissions from point sources. These urbanized areas have densely distributed populations in the compact scenario, and hence human populations are co-located with lower NO_x concentrations. Consequently, human exposures to NO_x are lower in the compact than sprawl scenario, suggesting compact urban form may not necessarily always have higher human exposures to primary pollutants than sprawl urban form.

Comparing the compact and electric vehicle scenarios, county average exposures are higher in the latter for NO_x, but lower for other pollutants. For 1,3-butadiene, benzene, acetaldehyde and formaldehyde, ambient concentration levels are largely contributed by other emissions sources besides point sources. By eliminating on-road mobile sources emissions, their ambient concentrations will be lowered. Regarding NO_x, point sources dominate emissions and contribute to NO_x concentrations. Through vehicle fleet electrification point source emissions of NO_x were significantly increased, which in turn leads to higher ambient NO_x concentration in Hillsborough County and hence higher NO_x exposures. Therefore, the implementation of vehicle fleet electrification as a potential strategy for the alleviation of air pollution exposures in compact urban form may be favorable for some pollutants, but not all.

6.5.3. Limitations and Uncertainties of Exposure Estimation

Block group population projections may contains significant uncertainties. More comprehensive and rigorous models are available, such as UrbanSim (The UrbanSim Project, 2011) and MoSeS (Townend et al., 2009), which are suggested for future studies.

Similar with exposure estimation for the baseline scenario, there are overlapping in the category definition for race/ethnicity groups. Human activity patterns, as well as pollutant concentration variations at micro-environments were not included in the exposure estimation. Additional analysis are suggested.

6.5.4. Summary and Conclusion of Exposure Estimation

The modeled pollutant concentrations of NO_x, 1,3-butadiene, benzene, acetaldehyde and formaldehyde are combined with the projected population in the future scenarios to estimate human exposures to air pollution. Results for different scenarios were compared to investigate the impact of urban form on air pollution exposure.

Past literatures consistently show that human exposures to air pollution may be higher in compact urban form for primary pollutants. Consistent findings were found for 1,3-butadiene, benzene, acetaldehyde and formaldehyde, however for NO_x the current results suggest the possibility of a reversed relationship: air pollution exposure to NO_x is in fact higher in the sprawl than in compact urban form. The type of emission source that contributes to the ambient pollutant concentrations, and the locations of these emission sources are important.

6.6. Explore Exposure Inequalities in Future Scenarios

To explore the potential impact of urban form on exposure inequalities among population subgroups, demographic data at block group level were projected to the future scenarios and combined with the modeled pollutant concentrations to estimate air pollution exposures among chosen race/ethnicity, age and income subgroups.

6.6.1. Methods for Exposure Inequalities Estimation

Demographic data used in the baseline scenarios were extrapolated to the year 2050. First, projected total populations of race/ethnicity (black, Hispanic, white) and age (age < 5, between 5 and 65 and age > 65) subgroups in Hillsborough County for the year 2030 were obtained from the Bureau of Economic and Business Research (BEBR). Population fractions of each chosen subgroup were calculated and further extrapolated linearly to the year 2050. The total populations of each chosen subgroup were then estimated by multiplying the extrapolated fractions with county total population for Hillsborough County in future scenarios (see section 5.3.1.1.1). Total population changes for each specific subgroup were obtained by subtracting the baseline population of each subgroup from the predicted populations of the corresponding subgroup in the future scenarios. The calculated subgroup population changes were then spatially distributed to each census block group proportional to the total population changes in the corresponding block group. Finally, subgroup populations in each census block group for race/ethnicity and age groups were estimated by summing the baseline population with the distributed population changes for the corresponding subgroup.

Regarding income subgroups, it was assumed that the proportions of each income groups in each block group in the future scenarios are the same as in the baseline scenario. The estimated subgroup populations were then combined with modeled pollutant concentrations to estimate exposure inequalities. Population weighted exposures and subgroup inequality index were used to quantify exposure distribution among subgroups.

6.6.2. Results and Discussion for Exposure Inequalities Estimation

Table 6.19 through Table 6.23 show the estimated population weighted exposures for all five pollutants in the three future scenarios, and the estimated inequality indices are provided in Appendix B-8 through Appendix B-22.

Among race/ethnicity subgroups, in the compact and electric vehicle scenarios, black and Hispanic subgroups consistently experience higher than county average population-weighted exposures, while white subgroup experiences lower than county average exposures. However in the sprawl scenario for 1,3-butadiene and benzene, as well as acetaldehyde and formaldehyde at annual average scale, the directions of change in exposure for white and Hispanic subgroups are reversed. The white subgroup now experiences higher exposure levels whereas the Hispanic subgroup experiences lower than county average exposure. For NO_x, acetaldehyde and formaldehyde at the highest 1 hour temporal scale, the reverse patterns are not observed. This finding suggests that urban forms do have impact inequalities regarding air pollution exposures, but the impacts differ by pollutants and temporal scales. Similar reversed exposure patterns are also observed for age subgroups.

Among income subgroup, the lowest income subgroup consistently experiences the highest exposures, and the population weighted exposure levels generally decreases with the increase of income. The only exception to this pattern is for the highest income subgroup (> 100K). This observation suggests that exposures tend to be inversely correlated with annual household income.

Appendix B-8 through Appendix B-22 provide detailed population distributions and estimated inequality indices for each population subgroup in the three scenarios for

Table 6.19 Population weighted exposures for NO_x at three future scenarios. Exposure values larger than county average are shaded.

		population weighted exposure (μg/m^3)								
		highest 1 hour			98th percentile			annual average		
		spr	com	elec	spr	com	elec	spr	com	elec
race/ethnicity	white	403	346	639	108	92	146	18.5	15.5	22.5
	black	660	527	1186	127	119	208	20.4	19.3	29.5
	Hispanic	629	503	1142	122	118	207	19.5	19.1	29.2
age	< 5	519	440	940	114	105	179	18.7	17.3	26.1
	between 5 and 65	519	440	938	114	106	180	18.9	17.5	26.3
	> 65	627	502	1139	120	117	203	19.4	19.0	29.0
annual household income	< 20K	771	582	1376	140	124	223	22.1	19.9	30.9
	between 20K to 40K	544	462	971	116	111	187	19.1	18.2	27.3
	between 40K to 60K	492	412	842	110	104	174	18.1	17.1	25.4
	between 60K to 100K	409	350	657	97	92	148	16.6	15.5	22.7
	> 100k	407	349	676	99	94	150	17.1	16.0	23.2
county average		547	457	991	116	109	186	19.0	17.9	27.0

*spr: sprawl scenario; com: compact scenario; elec: electric vehicle scenario

Table 6.20 Population weighted exposures for 1,3-butadiene at three future scenarios. Exposure values larger than county average are shaded.

		population weighted exposure (μg/m^3)					
		highest 1 hour			annual average		
		spr	com	elec	spr	com	elec
race/ethnicity	white	0.091	0.110	0.058	0.0050	0.0056	0.0026
	black	0.090	0.134	0.068	0.0048	0.0065	0.0030
	Hispanic	0.081	0.127	0.067	0.0044	0.0063	0.0029
age	< 5	0.088	0.121	0.063	0.0048	0.0060	0.0027
	between 5 and 65	0.087	0.121	0.063	0.0048	0.0060	0.0028
	> 65	0.079	0.125	0.065	0.0043	0.0062	0.0028
annual household income	< 20K	0.094	0.137	0.069	0.0050	0.0066	0.0030
	between 20K to 40K	0.087	0.125	0.065	0.0047	0.0062	0.0028
	between 40K to 60K	0.083	0.119	0.063	0.0045	0.0059	0.0027
	between 60K to 100K	0.078	0.108	0.057	0.0043	0.0055	0.0025
	> 100k	0.078	0.107	0.059	0.0044	0.0056	0.0026
county average		0.085	0.122	0.064	0.0046	0.0060	0.0028

*spr: sprawl scenario; com: compact scenario; elec: electric vehicle scenario

Table 6.21 Population weighted exposures for benzene at three future scenarios. Exposure values larger than county average are shaded.

		population weighted exposure (μg/m^3)					
		highest 1 hour			annual average		
		spr	com	elec	spr	com	elec
race/ethnicity	white	1.96	2.129	1.69	0.115	0.11	0.083
	black	1.97	2.503	1.98	0.110	0.13	0.096
	Hispanic	1.82	2.391	1.89	0.102	0.13	0.092
age	< 5	1.90	2.292	1.81	0.109	0.12	0.088
	between 5 and 65	1.90	2.299	1.82	0.109	0.12	0.089
	> 65	1.82	2.392	1.89	0.100	0.12	0.091
annual household income	< 20K	2.06	2.582	2.04	0.114	0.13	0.097
	between 20K to 40K	1.93	2.386	1.89	0.108	0.12	0.091
	between 40K to 60K	1.82	2.239	1.77	0.104	0.12	0.087
	between 60K to 100K	1.73	2.075	1.64	0.100	0.11	0.081
	> 100k	1.76	2.151	1.71	0.103	0.11	0.083
county average		1.88	2.323	1.84	0.107	0.12	0.089

*spr: sprawl scenario; com: compact scenario; elec: electric vehicle scenario

Table 6.22 Population weighted exposures for acetaldehyde at three future scenarios. Exposure values larger than county average are shaded.

		population weighted exposure (μg/m3)					
		highest 1 hour			annual average		
		spr	com	elec	spr	com	elec
race/ethnicity	white	0.829	0.911	0.733	0.048	0.052	0.037
	black	0.957	1.069	0.833	0.047	0.055	0.039
	Hispanic	0.905	1.019	0.804	0.046	0.055	0.039
age	< 5	0.868	0.979	0.774	0.046	0.053	0.038
	between 5 and 65	0.873	0.983	0.780	0.047	0.054	0.038
	> 65	0.923	1.033	0.817	0.046	0.055	0.040
annual household income	< 20K	0.977	1.091	0.851	0.048	0.056	0.040
	between 20K to 40K	0.903	1.019	0.801	0.047	0.055	0.039
	between 40K to 60K	0.848	0.952	0.753	0.046	0.053	0.038
	between 60K to 100K	0.822	0.913	0.732	0.045	0.051	0.037
	> 100k	0.839	0.925	0.755	0.046	0.054	0.039
county average		0.886	0.996	0.789	0.047	0.054	0.039

*spr: sprawl scenario; com: compact scenario; elec: electric vehicle scenario

Table 6.23 Population weighted exposures for formaldehyde at three future scenarios. Exposure values larger than county average are shaded.

		population weighted exposure (μg/m3)					
		highest 1 hour			annual average		
		spr	com	elec	spr	com	elec
race/ethnicity	white	1.49	1.83	1.29	0.082	0.136	0.0597
	black	1.93	2.33	1.85	0.081	0.149	0.0660
	Hispanic	1.83	2.24	1.77	0.078	0.148	0.0657
age	< 5	1.66	2.07	1.56	0.079	0.142	0.0623
	between 5 and 65	1.68	2.08	1.59	0.080	0.143	0.0631
	> 65	1.85	2.26	1.79	0.079	0.148	0.0661
annual household income	< 20K	1.85	2.28	1.62	0.084	0.150	0.0658
	between 20K to 40K	1.70	2.11	1.50	0.080	0.145	0.0641
	between 40K to 60K	1.53	1.95	1.37	0.077	0.140	0.0615
	between 60K to 100K	1.52	1.85	1.37	0.075	0.136	0.0595
	> 100k	1.44	1.85	1.29	0.078	0.142	0.0634
county average		1.72	2.13	1.64	0.080	0.144	0.0639

*spr: sprawl scenario; com: compact scenario; elec: electric vehicle scenario

all pollutants at multiple temporal scales. Overall, the findings correspond well with findings for population weighted exposures among subgroups.

Among race/ethnicity subgroups, the estimated indices for the black subgroup show a consistently increasing trend for all pollutants in the compact scenario, suggesting larger inequalities at higher concentrations levels. In the sprawl and electric vehicle scenarios, the indices for the black subgroup are generally positive, but the trend varies. In the compact and electric vehicle scenarios, inequality indices for the Hispanic subgroup are generally positive (disproportionately exposed), and indices for white subgroup are generally negative (disproportionately not exposed). The magnitude of the indices for the Hispanic subgroup is generally smaller than those for the black subgroup.

Comparing the sprawl and compact scenarios, the impacts of urban form on air pollution exposure inequalities can also be seen. For example, positive indices were

estimated for the white subgroup whereas negative indices were estimated for the Hispanic subgroup in sprawl scenario, compared to the opposite compact scenario. This patterns however is not consistent for the other pollutants.

The estimated inequality indices for the age subgroups are relatively small, with more fluctuations. Slightly positive indices were calculated for the older age subgroup (age > 65) in the compact and electric vehicle scenarios. The impact of urban form on inequalities can also be observed for this subgroup, especially for 1,3-butadiene and benzene.

With the increase of annual household income, the estimated inequality indices generally decrease for all pollutants in all scenarios, with some fluctuations. This finding suggests that with the increase of income, the corresponding subgroup are more likely to live in areas with lower pollutant concentrations and hence are less likely to be disproportionately exposed to air pollution. The population distributions among income subgroups also show similar patterns: the population fractions of lower income subgroups seems to be greater in areas with higher pollutant concentrations. This pattern is reversed for higher income subgroups.

Overall, these findings suggest urban forms do impact exposure inequalities among different subgroups, but the impact seems to differ by pollutant and temporal scale. Further, previous studies suggest on-road mobile sources may contribute significantly to inequalities related to air pollution exposure (Chakraborty, 2009). However when on-road mobile source emissions were eliminated, inequalities still exist.

Past literatures regarding the impact of urban forms on air pollution exposure inequalities are limited (Ridder et al., 2008). These findings contribute to current

knowledge. However, evidences shown here are rather exploratory. Mechanisms regarding how urban forms impact exposure inequalities are still largely unknown. Future studies on this subject are needed to better understand this relationship.

6.6.3. Limitation and Uncertainties for Exposure Inequalities Estimation

The attempt to estimate exposure inequalities in future scenarios is exploratory in nature. Many assumptions were applied and lead to substantial uncertainties. The method used to predict subgroup populations at each census block group may contain the largest uncertainties. Some models, such as the previous mentioned UrbanSim (The UrbanSim Project, 2011) and MoSeS (Townend et al., 2009) model, are suggested for future work.

6.7. Overall Summary and Conclusion

In this chapter, the impacts of urban form on pollutant emissions, concentrations and pollution exposures were investigated. Five pollutants: NO_x, 1,3-butadiene, benzene, acetaldehyde and formaldehyde were chosen. Emissions of these pollutants were projected to the year 2050 for three future scenarios: sprawl, compact and electric vehicle scenario. Concentration distributions of the pollutants were modeled using CALPUFF model. The modeled concentrations were then combined with projected demographic data to estimate human exposures to air pollution in the three scenarios, as well as exposure among chosen population subgroups.

Emission estimation results show that emissions of NO_x, 1,3-butadiene, benzene and formaldehyde are lower in the compact than sprawl scenario, while emissions of acetaldehyde are higher due to more forested land areas in compact urban form. With vehicle fleet electrification, emissions of 1,3-butadiene, benzene, acetaldehyde and formaldehyde are lowered but emissions of NO_x were substantially increased as a result

of increased electricity demand. However it needs to be noted that the predicted emissions from stationary sources are expected to be overestimated, if new technologies that reduce NO_x emissions are implemented.

Concentration estimation results show that domain averaged concentrations of NO_x and benzene are lower in the compact than sprawl scenario, and the averaged concentrations of the other pollutants are higher. Comparing the compact and electric vehicle scenarios, average pollutant concentrations are higher in the latter for NO_x, due to substantially increased point source emissions, and are lower for other pollutants. In urbanized areas, a comparison of the spatial distribution of concentrations between the sprawl and compact scenarios show higher 1,3-butadiene and benzene concentrations, and higher annual average acetaldehyde and formaldehyde concentrations in the compact scenario. Concentrations of NO_x are lower in the majority of Hillsborough County in the compact scenario, with the biggest concentration differences found near downtown Tampa and near a major fugitive point source. Between the compact and electric vehicle scenario, pollutant concentrations are higher in the majority of Hillsborough County for NO_x, and are lower for other pollutants in the latter.

Much previous studies suggest higher pollutant concentrations near urban centers in compact urban form when compared to sprawl urban form. Results of concentration estimation show the possibility of the opposite. Whether compact urban form leads to higher pollutant concentrations may be dependent on the emission sources that contribute to ambient pollutant concentrations, and the locations of those emission sources. In addition, vehicle fleet electrification was found to lead to generally worse air quality regarding NO_x, but better air quality regarding the other four pollutants.

Overall population exposure estimations show that compact urban form may not necessarily lead to higher human exposure to air pollution, again the emission sources that contribute to the pollutant concentrations and the locations of these emission sources are important. Furthermore, exploratory estimations for exposure inequalities in future scenarios suggest that urban forms do impact inequalities regarding air pollution exposures, although the impacts differ by pollutants and temporal scales.

CHAPTER 7

SUMMARY AND CONCLUSIONS

7.1. Introduction

Rapid urban growth and motor-vehicle dependency lead to drastically increased vehicle miles travelled. This results in substantial mobile source pollutant emissions, contributing to the deterioration of urban air quality, and human exposure to air pollution. Additionally, mobile source emissions also contribute to inequalities in air pollution exposure, which is a well-recognized issue in air quality management.

This work investigated urban air pollution and exposure inequality by characterizing the complex relationship of urban form, pollutant emission, pollutant concentration, exposure to air pollution, and exposure inequalities. First, we investigated the impact of a small-scale transportation management project, specifically the '95 Express' high occupancy toll lane project, on pollutant emissions and air quality in the surrounding area. Second, we modeled the spatiotemporal concentration distributions of selected pollutants in the Tampa, FL area. We estimated residential human exposure to these pollutants, as well as exposure inequalities for selected race/ethnicity, age and income subgroups. Third, we investigated the impact of sprawl and compact urban forms, as well as vehicle fleet electrification, on pollutant emissions, spatiotemporal concentration distributions, air pollution exposure, and related exposure inequalities. Summaries from the three components are provided.

7.2. Impact of Transportation Infrastructure Improvements on Air Quality

To investigate the air quality impact of the '95 Express' high occupancy toll lane project (Phase 1A and 1B), baseline air quality was assessed by analyzing historical regulatory monitoring data. Next, on-road mobile source emissions from the study corridor were estimated. Ambient pollutant concentration levels were then determined using AERMOD model for areas surrounding the corridor.

Baseline air quality data show that concentration levels of chosen criteria air pollutants including CO, NO2, O3, PM10 and PM2.5 are generally below corresponding standards established in the National Ambient Air Quality Standards. However, concentrations of NO2 (highest 1 hour), O3 (fourth highest 8 hour), and PM2.5 (98th percentile of 24 hour) exceeded corresponding standards in certain years. From 2000 - 2009, concentrations of CO, NO2, and 1,3-butadiene in Broward and Miami-Dade counties, and benzene in Broward County show a declining trend. No apparent trend was observed for other pollutants. Air quality index in the two counties suggest a slightly better air quality in Miami-Dade County.

On-road mobile source emissions from the study corridor were calculated by combining emission factors estimated from MOBILE6.2 model with traffic characteristics calculated by CORSIM model. Results show that implementation of the high occupancy toll lane project will slightly increase total emissions for CO, NOx, PM10, and benzene, and slightly decrease emissions of HC. Emissions from buses show a consistent decrease for all pollutants. The observed changes in emissions can be attributed to the changes in vehicle mileage travelled and emission factors, due to improved corridor performance.

The increase in on-road mobile source emissions for CO, NOx and benzene led to slightly elevated ambient concentration levels of these pollutants in the majority of the study domain. The northern end of the corridor experienced decreased concentrations due to spatially re-distributed vehicle mileage travelled as a result of the implementation of the high occupancy toll lane project.

Results of the investigation contribute to the field by demonstrating performance improvements of transportation infrastructure do not equal a reduction in on-road mobile source emissions. It is rather determined by vehicle mileage travelled and the relationships between vehicle speed and pollutant emissions. Finally, the findings from this study could help better understanding the impact of transportation management choices on air quality, and could also be utilized to assist the designing of transportation infrastructure.

7.3. Human Exposure and Exposure Inequalities to Selected Pollutant in the Tampa, FL area

To appropriately characterize air pollution exposure and exposure inequalities in the Tampa, FL area, stationary point, on-road, non-road, non-point and biogenic emissions of NOx, 1,3-butadiene, benzene, acetaldehyde and formaldehyde were estimated for the study area and surrounding counties. Ambient concentration levels of the five pollutants were then estimated through either direct dispersion modeling using the CALPUFF model, or combining CMAQ data with CALPUFF modeling results. The estimated pollutant concentrations were spatially combined with census demographic data to estimate air pollution exposure and exposure inequalities among chosen population subgroups.

An improved modeling method was developed here. Hourly average traveling speed on each major roadway link were characterized and applied in emission estimation. A simplified chemistry algorithm was developed and applied in dispersion modeling. Finally, a full set of tools were developed that could be applied to automate modeling processes for the CALPUFF model.

The results of emission estimation indicate a significant contribution of on-road mobile sources to total emissions. Spatial distribution of emissions show generally higher pollutant emissions in urbanized areas.

Estimated spatiotemporal pollutant concentrations show different spatial patterns at multiple temporal scales, suggesting the necessity of exposure assessment at multiple temporal scales. Processes that cannot be cannot be captured by CALPUFF model, such as atmospheric formation of pollutants, were found to contribute substantially to concentrations of acetaldehyde and formaldehyde. Additionally, on-road mobile sources were found to contribute disproportionately to ground level pollutant concentrations. This suggests the potential influence of urban form on air quality, since on-road mobile source emissions are directly impacted by urban form.

The results of exposure assessment indicate different exposure distributions for different pollutants. For NO_x, 1,3-butadiene and benzene, black, Hispanic, and low income (annual household income less than $20,000) subgroups were disproportionately exposed, white and higher income subgroups were disproportionately less exposed to these pollutants. For acetaldehyde and formaldehyde, complex, and sometimes even reversed exposure patterns (at certain temporal scales) were observed.

The details emission estimation and modeling methods developed here can be readily applied in other regions for air quality and exposure assessment purposes. The findings help better understanding environmental inequalities related to air pollution exposure, and may be used to assist urban planning toward the direction of sustainable and equitable.

7.4. Impact of Urban Form on Air Quality, Pollution Exposure and Exposure Inequalities

Emissions of five chosen pollutants were projected to 2050 for the sprawl, compact, and electric vehicle scenarios. The CALPUFF model was used to estimate the spatiotemporal distributions of pollutant concentrations, which were combined with projected demographic data to estimate air pollution exposure, and explore exposure inequalities among chosen population subgroups in different scenarios.

Results of emission estimation show higher NOx emissions in the future scenarios, due to increased emissions from stationary point sources, and lower emissions for other pollutants. The compact scenario has lower emissions of NOx, 1,3-butadiene, benzene, and formaldehyde, but higher emissions of acetaldehyde when compared to sprawl scenario. The electric vehicle scenario showed higher NOx emissions, but lower emissions for all other pollutants, due to increased electricity demand from vehicle fleet electrification.

CALPUFF modeled pollutant concentrations show lower average concentrations for NOx and benzene in the compact than the sprawl scenario, and higher concentrations for the other pollutants. The electric vehicle scenario has higher average NOx concentration than the compact scenario, but lower average concentrations for other

pollutants. Spatial distributions of the modeled pollutant concentrations show generally consistent patterns, with higher concentrations found in urbanized areas.

Overall population exposure to air pollution is higher in the compact than the sprawl scenario for all pollutants except NOx. With vehicle fleet electrification, county average exposure levels were reduced for all pollutants except NOx. In addition, by exploring exposure inequalities under different scenarios, evidence was found suggesting different urban forms lead to different exposure inequalities.

Although there are substantial uncertainties in the estimation of pollutant emissions, especially for stationary point source emissions, results still suggest that the compact urban form does not necessarily lead to higher exposure for primary pollutants. Exposures are dependent on the types of emission sources that contribute to pollutant concentrations, as well as locations of those emissions sources.

The findings here contribute to our understandings of the impacts of urban forms and transportation management choices on pollutant emissions, concentrations, exposures, as well as exposure inequalities among different population subgroups. These findings could also be used for better urban planning to improve air quality, and to reduce pollution exposure and exposure inequalities.

APPENDIX A

SUPPLEMENT MATERIALS FOR CHAPTER 5

Appendix A- 1 List of the Tampa Bay regional planning model (TBRPM) area types

TBRPM area type ID	area type description
11	urbanized area (population over 500,000), primary city CBD*
12	urbanized area (population under 500,000), CBD
13	other urbanized area, CBD and small city downtown
14	non-urbanized area, small city downtown
21	all CBD fringe areas
31	developed portions of urbanized areas
32	undeveloped portions of urbanized areas
33	transitioning areas/urban areas over 5,000 population
34	residential beach area
41	major outlying business districts
42	other outlying business districts
43	beach outlying business districts
51	developed rural areas/small cities under 5,000 population
52	undeveloped rural areas

*CBD: Central business district.

Appendix A- 2 List of the Tampa Bay regional planning model (TBRPM) roadway types

TBRPM roadway type ID	roadway type description
11	urban freeway group 1 (cities with population 500,000 or more)
12	other urban freeway
15	collector/distributor freeway lanes/facilities
16	controlled access expressways
17	controlled access parkways
21	divided arterial unsignalized (55 mph)
22	divided arterial unsignalized (45 mph)

[a]Class I roadways: density of signalized intersections less than or equals to 2.49/mile (urban area), or 1.50/mile (rural area); [b]Class II roadways: density of signalized intersections from 2.5 to 4.5/mile (urban area), or more than 1.50/mile (rural area); [c]Class III/IV roadways: density of signalized intersections more than 4.5/mile.

Appendix A- 2 (Continued) List of the Tampa Bay regional planning model (TBRPM) roadway types

TBRPM roadway type ID	roadway type description
23	divided arterial class I[a]
24	divided arterial class II[b]
25	divided arterial class III/IV[c]
31	undivided arterial unsignalized with turn bays
32	undivided arterial class I with turn bays
33	undivided arterial class II with turn bays
34	undivided arterial class III/IV with turn bays
35	undivided arterial unsignalized without turn bays
36	undivided arterial class I without turn bays
37	undivided arterial class II without turn bays
38	undivided arterial class III/IV without turn bays
41	major local divided roadway
42	major local undivided roadway with turn bays
43	major local undivided roadway without turn bays
44	other local divided roadway
45	other local undivided roadway with turn bays
46	other local divided roadway without turn bays
47	low speed local collector
48	very low speed local collector
49	truck restricted facilities
51	basic centroid connector
52	external station centroid connector
53	dummy zone centroid connectors
61	one-way facilities unsignalized
62	one-way facilities class I
63	one-way facilities class II
64	one-way facilities class III/IV
65	frontage road unsignalized
66	frontage road class I
67	frontage road class II
68	frontage road class III/IV
71	freeway on/off ramp

[a]Class I roadways: density of signalized intersections less than or equals to 2.49/mile (urban area), or 1.50/mile (rural area); [b]Class II roadways: density of signalized intersections from 2.5 to 4.5/mile (urban area), or more than 1.50/mile (rural area); [c]Class III/IV roadways: density of signalized intersections more than 4.5/mile.

Appendix A- 2 (Continued) List of the Tampa Bay regional planning model (TBRPM) roadway types

TBRPM roadway type ID	roadway type description
72	freeway on/off loop ramp
73	other on/off ramp
74	other on/off loop ramp
75	freeway-freeway ramp
76	truck-only ramp
81	freeway group 1 HOV lane (barrier separated)
82	other freeway HOV lane (barrier separated)
83	freeway group 1 HOV lane (non-barrier separated)
84	other freeway HOV lane (non-barrier separated)
85	non freeway HOV lane
86	am & pm peak HOV ramp
87	am peak only HOV ramp
88	pm peak only HOV ramp
89	all day HOV ramp
91	freeway group 1 toll facility
92	other freeway toll facility
93	expressway/parkway toll facility
94	divided arterial toll facility
95	undivided arterial toll facility
96	freeway group 1 reversible elevated lanes toll facility
97	other freeway reversible elevated lanes toll facility
98	acceleration/deceleration lanes - toll facility
99	toll plaza - toll facility

[a]Class I roadways: density of signalized intersections less than or equals to 2.49/mile (urban area), or 1.50/mile (rural area); [b]Class II roadways: density of signalized intersections from 2.5 to 4.5/mile (urban area), or more than 1.50/mile (rural area); [c]Class III/IV roadways: density of signalized intersections more than 4.5/mile.

Appendix A- 3 Free flow speed (mph) look-up table from the Tampa Bay regional planning model (TBRPM)

TBRPM roadway type	TBRPM Area Type ID														
	11	12	13	14	21	31	32	33	34	41	42	43	51	52
11	45				50	50				50				
12						50	65	60		50	50		65	70
15					45	47								
16						52					45			
17						50	55				47			

Appendix A- 3 (Continued) Free flow speed (mph) look-up table from the Tampa Bay regional planning model (TBRPM)

TBRPM roadway type	TBRPM Area Type ID													
	11	12	13	14	21	31	32	33	34	41	42	43	51	52
21						42		43		41	42	42		55
22						40		40			39		45	45
23				42	37	38	39	39	38	35	38		42	
24		31		36	33	34				33	36	36		
25	28	28	30		31	33				30	33			
31						38		42			37		45	46
32					33	36	36	36	36		34		40	41
33				35	25	27					32	33	36	
34						31					31			
35						37					36		42	
36					32	33							39	
37					29	30		30						
38	24	24			26	28								
41					30	32					32			43
42	28		29		29	31	31	31	30		30		37	
43	26				28	30	30	30			30		36	39
44					27	28	28	28		28	29			
45	25				24	27		27			27	27	30	33
46	22	25	26		24	25		25		25	25		29	30
47			22	25	21	24	24	24			24			25
48	21					24		24			24			
49	22													
51	10	10	12.5	16	12.5	16	16	24	16	15	16	16	25	25
52						50		50					65	65
61						40					40			
62	29				32	33					33			
63	27			35	30	32					30	30		
64	23	23			25	30					27			
66					33					40				
67					30	25					35			
71	27				28	30	30	30		28	28			40
72	22				23	25	25	25		23	23			35
73						29			29					

Appendix A- 3 (Continued) Free flow speed (mph) look-up table from the Tampa Bay regional planning model (TBRPM)

TBRPM roadway type	TBRPM Area Type ID													
	11	12	13	14	21	31	32	33	34	41	42	43	51	52
74						24								
75					40	45	45			40	40			55
91	54				54	55								
92						55	65	65						
93						50	65			45				
96					54									
97						55								
98					40	42								
99					17.5	20		23	20	19				

Appendix A- 4 Bureau of Public Roads (BPR) function parameter look-up table from the Tampa Bay regional planning model (TBRPM)

TBRPM roadway type	σ	β	TBRPM roadway type	σ	β	TBRPM roadway type	σ	β
10	0.15	4	40	0.15	4	70	0.15	4
11	0.283	3.018	41	0.25	3.5	71	0.25	3.5
12	0.283	3.018	42	0.25	3.5	72	0.25	3.5
13	0.15	4	43	0.25	3.5	73	0.25	3.5
14	0.15	4	44	0.25	3.5	74	0.25	3.5
15	0.15	4	45	0.25	3.5	75	0.25	3.5
16	0.283	3.018	46	0.25	3.5	76	0.15	4
17	0.283	3.018	47	0.25	3.5	77	0.15	4
18	0.15	4	48	0.25	3.5	78	0.15	4
19	0.15	4	49	0.15	4	79	0.15	4
20	0.15	4	50	0.15	4	80	0.15	4
21	0.15	4	51	0.15	4	81	0.2	5
22	0.15	4	52	0.15	4	82	0.2	5
23	0.136	1.234	53	0.15	4	83	0.2	5
24	0.073	3.14	54	0.15	4	84	0.2	5
25	0.195	1.105	55	0.15	4	85	0.2	5
26	0.15	4	56	0.15	4	86	0.2	5
27	0.15	4	57	0.15	4	87	0.2	5
28	0.15	4	58	0.15	4	88	0.2	5
29	0.15	4	59	0.15	4	89	0.2	5
30	0.15	4	60	0.15	4	90	0.15	4
31	0.15	4	61	0.15	4	91	0.283	3.018

Appendix A- 4 (Continued) Bureau of Public Roads (BPR) function parameter look-up table from the Tampa Bay regional planning model (TBRPM)

TBRPM roadway type	σ	β	TBRPM roadway type	σ	β	TBRPM roadway type	σ	β
32	0.136	1.234	62	0.136	1.234	92	0.283	3.018
33	0.073	3.14	63	0.073	3.14	93	0.283	3.018
34	0.195	1.105	64	0.195	1.105	94	0.2	5
35	0.15	4	65	0.15	4	95	0.2	5
36	0.136	1.234	66	0.136	1.234	96	0.283	3.018
37	0.073	3.14	67	0.073	3.14	97	0.283	3.018
38	0.195	1.105	68	0.195	1.105	98	0.2	5
39	0.15	4	69	0.15	4	99	0.2	5

Appendix A- 5 List of the FDOT Quality/Level of Service Handbook area types

LOS area type ID*	area type description
201	urban
202	transition
203	rural undeveloped
204	rural developed with pop < 5000

*LOS area type IDs are self-coded for convenience purposes

Appendix A- 6 List of the FDOT Quality/Level of Service Handbook roadway types

LOS handbook roadway types	capacity class ID*
Freeway	101
uninterrupted highway - divided	102
uninterrupted highway - undivided	103
class I signalized arterials - divided	104
class I signalized arterials - undivided	105
class II signalized arterials - divided	106
class II signalized arterials - undivided	107
class III/IV signalized arterials - divided	108
class III/IV signalized arterials - undivided	109
non-arterial roads - divided	108

*capacity classes are self-coded for convenience purposes

Appendix A- 7 Mapping method from Tampa Bay regional planning model area type to FDOT Quality/Level of Service Handbook area types

TBRPM area type ID	LOS area type ID
11,12,13,14,21,31,34,41,42,43	201
32,33	202
51	204
52	203

Appendix A- 8 Mapping method from Tampa Bay regional planning model roadway type to FDOT Quality/Level of Service Handbook roadway types. Associated capacity adjustment factors are also listed.

TBRPM roadway type ID	LOS roadway type ID	capacity adjustment factor	TBRPM roadway type ID	LOS roadway type ID	capacity adjustment factor
11	101	1	62	105	0.6
12	101	1	63	107	0.6
15	101	1	64	109	0.6
16	101	1	65	103	0.6
17	101	1	66	105	0.6
21	102	1	67	107	0.6
22	102	1	68	109	0.6
23	104	1	71	101	1
24	106	1	72	101	1
25	108	1	73	101	1
31	103	1	74	101	1
32	105	1	75	101	1
33	107	1	76	101	1
34	109	1	81	101	1
35	103	0.75	82	101	1
36	105	0.75	83	101	1
37	107	0.75	84	101	1
38	109	0.75	85	101	1
41	108	0.9	86	101	1
42	109	0.9	87	101	1
43	109	0.9	88	101	1
44	108	0.65	89	101	1
45	109	0.65	91	101	1
46	108	0.65	92	101	1
47	109	0.65	93	101	1
48	109	0.65	94	104	1
49	109	0.65	95	105	1
51	109	0.65	96	101	1

Appendix A- 8 (Continued) Mapping method from Tampa Bay regional planning model roadway type to FDOT Quality/Level of Service Handbook roadway types. Associated capacity adjustment factors are also listed.

TBRPM roadway type ID	LOS roadway type ID	capacity adjustment factor	TBRPM roadway type ID	LOS roadway type ID	capacity adjustment factor
52	109	0.65	97	101	1
53	109	0.65	98	103	1
61	103	0.6	99	109	1

Appendix A- 9 Roadway capacity look-up table

LOS area type ID	capacity class ID	number of lanes	capacity	LOS area type ID	capacity class ID	number of lanes	capacity
201	101	4	5500	203	104	2	460
201	101	6	8320	203	104	4	1000
201	101	8	11050	203	104	6	1550
201	101	10	13960	203	105	2	460
201	101	12	18600	203	105	4	1000
201	103	2	1460	203	105	6	1550
201	102	4	4660	203	106	2	460
201	102	6	6990	203	106	4	1000
201	105	2	1500	203	106	6	1550
201	104	4	3440	203	107	2	460
201	104	6	5200	203	107	4	1000
201	104	8	6970	203	107	6	1550
201	107	2	1020	203	108	2	460
201	106	4	2420	203	108	4	1000
201	106	6	3790	203	108	6	1550
201	106	8	5150	203	109	2	460
201	109	2	500	203	109	4	1000
201	108	4	1220	203	109	6	1550
201	108	6	1910	204	101	4	5140
201	108	8	2620	204	101	6	7690
202	101	4	5410	204	101	8	10320
202	101	6	8140	204	103	2	1420
202	101	8	10870	204	102	4	3710
202	101	10	13690	204	102	6	5570
202	103	2	1460	204	104	2	950
202	102	4	4400	204	104	4	2260
202	102	6	6600	204	104	6	3530
202	105	2	1370	204	105	2	950
202	104	4	3110	204	105	4	2260
202	104	6	4710	204	105	6	3530

Appendix A- 9 (Continued) Roadway capacity look-up table

LOS area type ID	capacity class ID	number of lanes	capacity	LOS area type ID	capacity class ID	number of lanes	capacity
202	107	2	910	204	106	2	950
202	106	4	2200	204	106	4	2260
202	106	6	3460	204	106	6	3530
202	109	2	460	204	107	2	950
202	108	4	1110	204	107	4	2260
202	108	6	1750	204	107	6	3530
203	101	4	5230	204	108	2	950
203	101	6	7870	204	108	4	2260
203	101	8	10410	204	108	6	3530
203	103	2	790	204	109	2	950
203	102	4	4020	204	109	4	2260
203	102	6	6040	204	109	6	3530

Appendix A- 10 Vehicle classification system in MOVES model

MOVES vehicle type ID	description
11	Motorcycle
21	Passenger Car
31	Passenger Truck
32	Light Commercial Truck
41	Intercity Bus
42	Transit Bus
43	School Bus
51	Refuse Truck
52	Single Unit Short-haul Truck
53	Single Unit Long-haul Truck
54	Motor Home
61	Combination Short-haul Truck
62	Combination Long-haul Truck

Appendix A- 11 List of MOVES roadway types

MOVES roadway type ID	description
1	off-network
2	rural restricted access
3	rural unrestricted access
4	urban restricted access
5	urban unrestricted access

Appendix A- 12 Mapping method from Tampa Bay Regional Planning Model (TBRPM) area and roadway types to MOVES roadway types

TBRPM		MOVES	TBRPM		MOVES	TBRPM		MOVES
area* type	roadway type	roadway type	area type	roadway type	roadway type	area type	roadway type	roadway type
10X	11	4	20X	75	4	40X	45	5
10X	12	4	20X	76	4	40X	46	5
10X	15	4	20X	81	4	40X	47	5
10X	16	4	20X	82	4	40X	48	5
10X	17	4	20X	83	4	40X	49	5
10X	21	5	20X	84	4	40X	51	5
10X	22	5	20X	85	4	40X	52	5
10X	23	5	20X	86	4	40X	53	5
10X	24	5	20X	87	4	40X	61	5
10X	25	5	20X	88	4	40X	62	5
10X	31	5	20X	89	4	40X	63	5
10X	32	5	20X	91	4	40X	64	5
10X	33	5	20X	92	4	40X	65	5
10X	34	5	20X	93	4	40X	66	5
10X	35	5	20X	94	5	40X	67	5
10X	36	5	20X	95	4	40X	68	5
10X	37	5	20X	96	4	40X	71	4
10X	38	5	20X	97	4	40X	72	4
10X	41	5	20X	98	4	40X	73	4
10X	42	5	20X	99	5	40X	74	4
10X	43	5	30X	11	4	40X	75	4
10X	44	5	30X	12	4	40X	76	4
10X	45	5	30X	15	4	40X	81	4
10X	46	5	30X	16	4	40X	82	4
10X	47	5	30X	17	4	40X	83	4
10X	48	5	30X	21	5	40X	84	4
10X	49	5	30X	22	5	40X	85	4
10X	51	5	30X	23	5	40X	86	4
10X	52	5	30X	24	5	40X	87	4
10X	53	5	30X	25	5	40X	88	4
10X	61	5	30X	31	5	40X	89	4
10X	62	5	30X	32	5	40X	91	4
10X	63	5	30X	33	5	40X	92	4
10X	64	5	30X	34	5	40X	93	4
10X	65	5	30X	35	5	40X	94	5

*Here 10X refers to TBRPM area type 11, 12, 13, 14; 20X refers to TBRPM area type 21; 30X refers to TBRPM area type 31, 32, 33, 34; 40X refers to TBRPM area type 41, 42, 43; 50X refers to TBRPM area type 51, 52.

Appendix A- 12 (Continued) Mapping method from Tampa Bay Regional Planning Model (TBRPM) area and roadway types to MOVES roadway types

TBRPM		MOVES	TBRPM		MOVES	TBRPM		MOVES
area* type	roadway type	roadway type	area type	roadway type	roadway type	area type	roadway type	roadway type
10X	66	5	30X	36	5	40X	95	4
10X	67	5	30X	37	5	40X	96	4
10X	68	5	30X	38	5	40X	97	4
10X	71	4	30X	41	5	40X	98	4
10X	72	4	30X	42	5	40X	99	5
10X	73	4	30X	43	5	50X	11	2
10X	74	4	30X	44	5	50X	12	2
10X	75	4	30X	45	5	50X	15	2
10X	76	4	30X	46	5	50X	16	2
10X	81	4	30X	47	5	50X	17	2
10X	82	4	30X	48	5	50X	21	3
10X	83	4	30X	49	5	50X	22	3
10X	84	4	30X	51	5	50X	23	3
10X	85	4	30X	52	5	50X	24	3
10X	86	4	30X	53	5	50X	25	3
10X	87	4	30X	61	5	50X	31	3
10X	88	4	30X	62	5	50X	32	3
10X	89	4	30X	63	5	50X	33	3
10X	91	4	30X	64	5	50X	34	3
10X	92	4	30X	65	5	50X	35	3
10X	93	4	30X	66	5	50X	36	3
10X	94	5	30X	67	5	50X	37	3
10X	95	4	30X	68	5	50X	38	3
10X	96	4	30X	71	4	50X	41	3
10X	97	4	30X	72	4	50X	42	3
10X	98	4	30X	73	4	50X	43	3
10X	99	5	30X	74	4	50X	44	3
20X	11	4	30X	75	4	50X	45	3
20X	12	4	30X	76	4	50X	46	3
20X	15	4	30X	81	4	50X	47	3
20X	16	4	30X	82	4	50X	48	3
20X	17	4	30X	83	4	50X	49	3
20X	21	5	30X	84	4	50X	51	3
20X	22	5	30X	85	4	50X	52	3
20X	23	5	30X	86	4	50X	53	3

*Here 10X refers to TBRPM area type 11, 12, 13, 14; 20X refers to TBRPM area type 21; 30X refers to TBRPM area type 31, 32, 33, 34; 40X refers to TBRPM area type 41, 42, 43; 50X refers to TBRPM area type 51, 52.

Appendix A- 12 (Continued) Mapping method from Tampa Bay Regional Planning Model (TBRPM) area and roadway types to MOVES roadway types

TBRPM		MOVES	TBRPM		MOVES	TBRPM		MOVES
area* type	roadway type	roadway type	area type	roadway type	roadway type	area type	roadway type	roadway type
20X	24	5	30X	87	4	50X	61	3
20X	25	5	30X	88	4	50X	62	3
20X	31	5	30X	89	4	50X	63	3
20X	32	5	30X	91	4	50X	64	3
20X	33	5	30X	92	4	50X	65	3
20X	34	5	30X	93	4	50X	66	3
20X	35	5	30X	94	5	50X	67	3
20X	36	5	30X	95	4	50X	68	3
20X	37	5	30X	96	4	50X	71	2
20X	38	5	30X	97	4	50X	72	2
20X	41	5	30X	98	4	50X	73	2
20X	42	5	30X	99	5	50X	74	2
20X	43	5	40X	11	4	50X	75	2
20X	44	5	40X	12	4	50X	76	2
20X	45	5	40X	15	4	50X	81	2
20X	46	5	40X	16	4	50X	82	2
20X	47	5	40X	17	4	50X	83	2
20X	48	5	40X	21	5	50X	84	2
20X	49	5	40X	22	5	50X	85	2
20X	51	5	40X	23	5	50X	86	2
20X	52	5	40X	24	5	50X	87	2
20X	53	5	40X	25	5	50X	88	2
20X	61	5	40X	31	5	50X	89	2
20X	62	5	40X	32	5	50X	91	2
20X	63	5	40X	33	5	50X	92	2
20X	64	5	40X	34	5	50X	93	2
20X	65	5	40X	35	5	50X	94	3
20X	66	5	40X	36	5	50X	95	2
20X	67	5	40X	37	5	50X	96	2
20X	68	5	40X	38	5	50X	97	2
20X	71	4	40X	41	5	50X	98	2
20X	72	4	40X	42	5	50X	99	3
20X	73	4	40X	43	5			
20X	74	4	40X	44	5			

*Here 10X refers to TBRPM area type 11, 12, 13, 14; 20X refers to TBRPM area type 21; 30X refers to TBRPM area type 31, 32, 33, 34; 40X refers to TBRPM area type 41, 42, 43; 50X refers to TBRPM area type 51, 52.

APPENDIX B

SUPPLEMENT MATERIALS FOR CHAPTER 6

Appendix B- 1. List of 15 land use types in One Bay visioning plan

land use type ID	description
1	low density residential 1
2	low density residential 2
3	medium density residential 1
4	medium density residential 2
5	high density residential
6	commercial
7	office Park
8	commerce Park
9	public institutional
10	regional activity center
11	town center
12	village center
13	regional transit oriented development center
14	downtown residential
15	downtown center

Appendix B- 2 List of 32 building types in One Bay visioning plan

building type category	building type ID*	description
mixed land use	1	downtown (office/retail/residential)
	2	downtown residential (residential/retail)
	3	city center (office/residential)
	4	city center (retail/residential)
	5	district center (retail/residential)
	6	corridor (office/retail)
	7	corridor (retail/residential)
residential	8	high density apartment/condo
	9	medium density apartment/condo
	10	low density apartment/condo
	11	townhome
	12	mobile home
	13	residential zero lot
	14	residential small lot
	15	residential medium lot
	16	residential large lot
	17	rural residential
employment	19	downtown office
	20	downtown mall
	21	city center office
	22	district center office
	23	regional mall
	24	lifestyle center
	25	office park
	26	light industrial
	27	heavy industrial
	28	urban corridor commercial
	29	urban neighborhood commercial
	30	strip commercial
institutional	31	university campus

*As defined in One Bay visioning data, building type ID 18 and 32 refer to “services” and “institutional”, however they were never used, hence they were excluded here.

Appendix B- 3 List of lane use type, associated building types and assumed building type fractions in One Bay visioning plan

	land use type ID														
building type ID	1	2	3	4	5	6	7	8	9	10	11	12	13	14	15
1					0.1									0.1	0.1
2					0.1								0.1	0.7	0.2
3				0.2						0.2	0.1		0.1	0.1	
4				0.2						0.1			0.3	0.1	
5			0.1					0.1			0.2		0.1		
6												0.2			
7												0.1			
8					0.4								0.2	0.1	
9			0.2	0.4	0.2						0.1	0.1	0.1	0.1	
10			0.1	0.1			0.1	0.1			0.1	0.2	0.1		
11			0.2	0.2			0.1					0.1	0.1		
12															
13		0.2	0.2									0.2			
14		0.2	0.1									0.1			
15	0.2	0.3													
16	0.6	0.3													
17	0.2														
19					0.1					0.2					0.4
20															
21										0.1	0.2				0.4
22			0.1			0.1									
23						0.7				0.3					
24															
25							0.8	0.2							
26								0.4							
27								0.2							
28															
29											0.2				
30	0.1	0.1	0.1		0.1	0.2	0.1	0.1		0.2	0.1	0.1			
31					0.1				1	0.1	0.1	0.1			

Appendix B- 4 List of vehicle trip generation rates and electricity demand for each building type in One Bay visioning plan

building type ID	vehicle trips generated (trips per acre)	electricity demand (annual KWh)
1	2219	4287264
2	1621	3453786
3	599	1376840
4	1473	1369000
5	1241	952004
6	1223	956669
7	1070	735284
8	1990	1487012
9	306	566498
10	132	216852
11	70	156060
12	75	118490
13	104	185130
14	77	150000
15	48	102500
16	25	66650
17	4	10740
19	2916	4700560
20	3765	1552644
21	1458	2350280
22	413	784080
23	654	379625
24	970	568693
25	195	313632
26	52	353182
27	7	352850
28	185	327203
29	677	348443
30	430	298345
31	382	280657

Appendix B- 5 List of non-point source emissions and corresponding surrogate used

source classification code	description	surrogate
2102004000	stationary fuel combustion /industrial /distillate oil /total: boilers and internal combustion engines	total industrial land area
2102005000	stationary fuel combustion /industrial /residual oil /total: all boiler types	total industrial land area
2102006000	stationary fuel combustion /industrial /natural gas /total: boilers and internal combustion engines	total industrial land area
2102007000	stationary fuel combustion /industrial /liquefied petroleum gas /total: all boiler types	total industrial land area
2102011000	stationary fuel combustion /industrial /kerosene /total: all boiler types	population
2102012000	stationary fuel combustion /industrial /waste oil /total	population
2103001000	stationary fuel combustion /commercial/institutional /anthracite coal /total: all boiler types	population
2103002000	stationary fuel combustion /commercial/institutional /bituminous/subbituminous coal /total: all boiler types	population
2103004000	stationary fuel combustion /commercial/institutional /distillate oil /total: boilers and internal combustion engines	total commercial plus institutional land area
2103005000	stationary fuel combustion /commercial/institutional /residual oil /total: all boiler types	total commercial plus institutional land area
2103006000	stationary fuel combustion /commercial/institutional /natural gas /total: boilers and internal combustion engines	total commercial plus institutional land area
2103007000	stationary fuel combustion /commercial/institutional /liquefied petroleum gas /total: all combustor types	total commercial plus institutional land area
2103010000	stationary fuel combustion /commercial/institutional /process gas /POTW digester gas-fired boilers	population
2103011000	stationary fuel combustion /commercial/institutional /kerosene /total: all combustor types	population
2104004000	stationary fuel combustion /residential /distillate oil /total: all combustor types	population
2104006000	stationary fuel combustion /residential /natural gas /total: all combustor types	population
2104007000	stationary fuel combustion /residential /liquefied petroleum gas /total: all combustor types	population
2104008001	stationary fuel combustion /residential /wood /fireplaces: general	population
2104008002	stationary fuel combustion /residential /wood /fireplaces: insert; non-EPA certified	population
2104008004	stationary fuel combustion /residential /wood /fireplaces: insert; EPA certified; catalytic	population
2104008010	stationary fuel combustion /residential /wood /woodstoves: general	population
2104008030	stationary fuel combustion /residential /wood /catalytic woodstoves: general	population
2104011000	stationary fuel combustion /residential /kerosene /total: all heater types	population
2199004000	stationary fuel combustion /total area source /distillate oil /total: boilers and internal combustion engines	total industrial plus institutional land area
2199005000	stationary fuel combustion /total area source /residual oil /total: all boiler types	total industrial plus institutional land area
2199006000	stationary fuel combustion /total area source /natural gas /total: boilers and internal combustion engines	total industrial plus institutional land area
2199007000	stationary fuel combustion /total area source /liquefied petroleum gas /total: all boiler types	total industrial plus institutional land area
2199011000	stationary fuel combustion /total area source /kerosene /total: all heater types	population
2302002100	food & kindred products /commercial cooking - charbroiling /conveyorized charbroiling	population

Appendix B- 5 (Continued) List of non-point source emissions and corresponding surrogate used

source classification code	description	surrogate
2302002200	food & kindred products /commercial cooking - charbroiling /under-fired charbroiling	population
2305070000	mineral processes /concrete, gypsum, plaster products /total	population
2306010000	petroleum refining /asphalt paving/roofing materials /total	population
2310000000	oil & gas exploration & production /all processes /total: all processes	population
2310020000	oil & gas exploration & production /natural gas /total: all processes	population
2399000000	industrial processes: NEC /industrial processes: NEC /total	population
2401002000	surface coating /architectural coatings - solvent-based /total: all solvent types	population
2401003000	surface coating /architectural coatings - water-based /total: all solvent types	population
2430000000	rubber/plastics /all processes /total: all solvent types	population
2461800000	misc. non-industrial: commercial /pesticide application: all processes /total: all solvent types	total commercial plus institutional land area
2501011011	residential portable gas cans /permeation	population
2501011012	residential portable gas cans /evaporation (includes diurnal losses)	population
2501011013	residential portable gas cans /spillage during transport	population
2501011014	residential portable gas cans /refilling at the pump - vapor displacement	population
2501011015	residential portable gas cans /refilling at the pump - spillage	population
2501012011	commercial portable gas cans /permeation	population
2501012012	commercial portable gas cans /evaporation (includes diurnal losses)	population
2501012013	commercial portable gas cans /spillage during transport	population
2501012014	commercial portable gas cans /refilling at the pump - vapor displacement	population
2501012015	commercial portable gas cans /refilling at the pump - spillage	population
2501050120	petrol & petrol product storage /bulk terminals: all evaporative losses /gasoline	total vehicle mileage travelled
2501055120	petrol & petrol product storage /bulk plants: all evaporative losses /gasoline	population
2501060052	gasoline service stations /stage 1: splash filling	total vehicle mileage travelled
2501060100	gasoline service stations /stage 2: total	total vehicle mileage travelled
2501060201	gasoline service stations /underground tank: breathing and emptying	total vehicle mileage travelled
2501080050	petrol & petrol product storage /airports : aviation gasoline /stage 1: total	population
2501080100	petrol & petrol product storage /airports : aviation gasoline /stage 2: total	population
2505020090	petrol & petrol product transport /marine vessel /distillate oil	population
2505020120	petrol & petrol product transport /marine vessel /gasoline	total vehicle mileage travelled
2505020150	petrol & petrol product transport /marine vessel /jet naphtha	population
2505020180	petrol & petrol product transport /marine vessel /kerosene	population
2505030120	petrol & petrol product transport /truck /gasoline	population

Appendix B- 5 (Continued) List of non-point source emissions and corresponding surrogate used

source classification code	description	surrogate
2505040120	petrol & petrol product transport /pipeline /gasoline	total vehicle mileage travelled
2601010000	on-site incineration /industrial /total	population
2601020000	on-site incineration /commercial/institutional /total	population
2610000300	open burning /all categories /yard waste - weed species unspecified (include grass)	population
2610000500	open burning /all categories /land clearing debris (use 28-10-005-000 for logging debris burning)	developed land area
2610030000	open burning /residential /household waste (use 26-10-000-xxx for yard wastes)	total low residential area
2620000000	landfills /all categories /total	population
2630020000	wastewater treatment /public owned /total processed	population
2801500100	agriculture - crops /field burning - whole field set on fire /crops unspecified	population
2801500170	agriculture - crops /field burning - whole field set on fire /crop is grasses: burning techniques not important	population
2801500360	agriculture - crops /field burning - whole field set on fire /orchard crop is citrus (orange, lemon)	population
2810001000	forest wildfires - wildfires - unspecified	forest area
2810005000	managed burning, slash (logging debris) /unspecified burn method (use 2610000500 for non-logging debris)	forest area
2810015000	prescribed forest burning /unspecified	forest area
2810030000	structure fires /unspecified	population
2810050000	motor vehicle fires /unspecified	population
2810060100	cremation /humans	population
2810060200	cremation /animals	population

Appendix B- 6 List of spatial surrogates used to allocate non-road, non-point and biogenic emissions, and method for deriving the surrogates.

ID	surrogate description	deriving surrogates	
		Surrogate metric	control total
100	population	baseline population + number of increased household * average household size	county total population
140	housing change and population	number of increased household	county total number of increased household
240	total road miles	same as baseline	
250	urban primary plus rural primary roads		
260	total railroad miles		
270	class 1 railroad miles		
280	class 2 and 3 railroad miles		
300	low intensity residential	baseline low intensity residential area + redeveloped low density residential area	county total low intensity residential area
310	total agriculture	baseline grid agriculture area - grid total redeveloped area	county total agriculture land area
311	total agriculture without orchards/vineyards	baseline grid agriculture area excluding orchards & vineyards - grid total redeveloped area	county total agriculture area excluding orchards & vineyards
312	orchards/vineyards	baseline grid orchards & vineyards area - grid total redeveloped area	county total orchards & vineyards land area
320	forest land	baseline grid forest land area - grid total redeveloped area	county total forest land area
350	water	baseline grid water area - grid total redeveloped area	county total water area
400	rural land area	baseline rural land area - grid total redeveloped area	county total rural land area
505	industrial land	baseline industrial land area + new commerce park land area * 0.6	county total industrial land area
510	commercial plus industrial land use	baseline commercial & industrial land area + new commerce park area * 0.6 + commercial land area	county total commercial & industrial land area

*in each grid cell, surrogate value is calculated by: surrogate metric/control total

Appendix B- 6 (Continued) List of spatial surrogates used to allocate non-road, non-point and biogenic emissions, and method for deriving the surrogates.

ID	surrogate description	deriving surrogates	
		Surrogate metric	control total
515	commercial plus institutional land use	baseline commercial & institutional land area + new commercial + new public institutional land area	county total commercial & institutional land area
520	commercial plus industrial plus institutional land use	baseline commercial & industrial & institutional land area + new commercial + new commerce park * 0.6 + new public institutional land area	county total commercial & industrial & institutional land area
525	golf courses plus institutional plus industrial plus commercial land use	baseline number of golf courses, and baseline commercial & industrial & institutional land area + new commercial + new commerce park * 0.6 + new public institutional land area	baseline county total number of golf courses and updated county total commercial & industrial & institutional land area
535	residential + commercial + industrial + institutional + government land use	baseline residential & commercial & industrial & institutional & government land area + new commercial + new commerce park * 0.6 + new public institutional land area	county total residential + commercial + industrial + institutional + government land area
580	food, drug, chemical industrial land use	same as baseline	
585	metals and minerals industrial land use		
590	heavy industrial land use	baseline heavy industry land area + new commerce park * 0.2	county total heavy industry land type area
596	industrial plus institutional plus hospitals land use	baseline industrial & institutional & hospitals land area + new commerce park * 0.6 + new public institutional land area	county total industrial plus institutional plus hospitals land area

*in each grid cell, surrogate value is calculated by: surrogate metric/control total

Appendix B- 6 (Continued) List of spatial surrogates used to allocate non-road, non-point and biogenic emissions, and method for deriving the surrogates.

ID	surrogate description	deriving surrogates	
		Surrogate metric	control total
600	gas stations		
650	refineries and tank farms		
700	airport areas		
720	military airports		
800	marine ports	same as baseline	
810	navigable waterway activity		
850	golf courses		
870	wastewater treatment facilities		
890	commercial timber	baseline commercial timber site numbers, grids with redeveloped land are removed	county total commercial timber site number

*in each grid cell, surrogate value is calculated by: surrogate metric/control total

Appendix B- 7 Estimated on-road mobile source emissions for seven counties included in the study domain

scenario	county	county ID	pollutant	annual emission (metric tons)
sprawl	Hernando	12053	1,3-butadiene	5.2
			acetaldehyde	23.5
			benzene	30.9
			formaldehyde	49.0
			NO_x	4396.4
	Hillsborough	12057	1,3-butadiene	15.0
			acetaldehyde	59.3
			benzene	96.5
			formaldehyde	120.8
			NO_x	9783.4
	Manatee	12081	1,3-butadiene	15.7
			acetaldehyde	57.9
			benzene	91.4
			formaldehyde	106.0
			NO_x	8985.2
	Pasco	12101	1,3-butadiene	11.3
			acetaldehyde	51.4
			benzene	67.5
			formaldehyde	107.3
			NO_x	9336.9
	Pinellas	12103	1,3-butadiene	6.1
			acetaldehyde	15.0
			benzene	37.9
			formaldehyde	19.8
			NO_x	1186.9
	Polk	12105	1,3-butadiene	16.3
			acetaldehyde	83.8
			benzene	98.3
			formaldehyde	185.5
			NO_x	15389.9
	Sarasota	12115	1,3-butadiene	5.0
			acetaldehyde	18.1
			benzene	29.2
			formaldehyde	32.4
			NO_x	2525.4

Appendix B- 7 (Continued) Estimated on-road mobile source emissions for seven counties included in the study domain

scenario	county	county ID	pollutant	annual emission (metric tons)
compact	Hernando	12053	1,3-butadiene	2.4
			acetaldehyde	9.2
			benzene	14.1
			formaldehyde	17.3
			NO_x	1457.6
	Hillsborough	12057	1,3-butadiene	18.0
			acetaldehyde	71.0
			benzene	115.8
			formaldehyde	144.5
			NO_x	11699.3
	Manatee	12081	1,3-butadiene	10.9
			acetaldehyde	36.7
			benzene	63.2
			formaldehyde	62.3
			NO_x	4969.6
	Pasco	12101	1,3-butadiene	8.5
			acetaldehyde	33.6
			benzene	50.0
			formaldehyde	64.3
			NO_x	5302.1
	Pinellas	12103	1,3-butadiene	10.3
			acetaldehyde	30.5
			benzene	64.9
			formaldehyde	50.2
			NO_x	3870.0
	Polk	12105	1,3-butadiene	8.6
			acetaldehyde	38.3
			benzene	51.1
			formaldehyde	79.1
			NO_x	6312.2
	Sarasota	12115	1,3-butadiene	6.0
			acetaldehyde	21.7
			benzene	35.1
			formaldehyde	38.9
			NO_x	3034.9

Appendix B- 8 Population distributions and estimated subgroup inequality indices for race/ethnicity subgroups regarding NO_x exposures in three future scenarios.

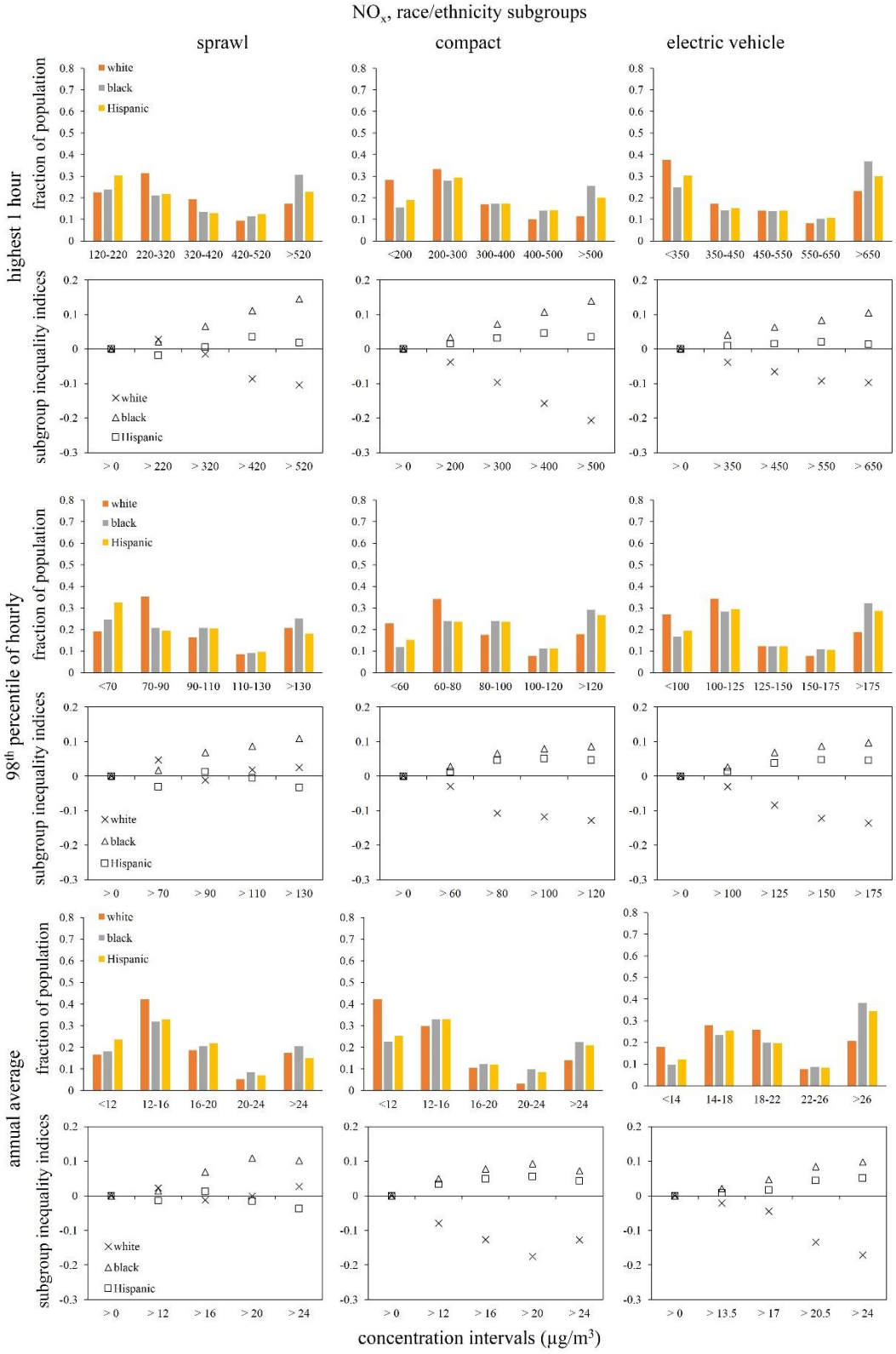

Appendix B- 9 Population distributions and estimated subgroup inequality indices for age subgroups regarding NO_x exposures in three future scenarios.

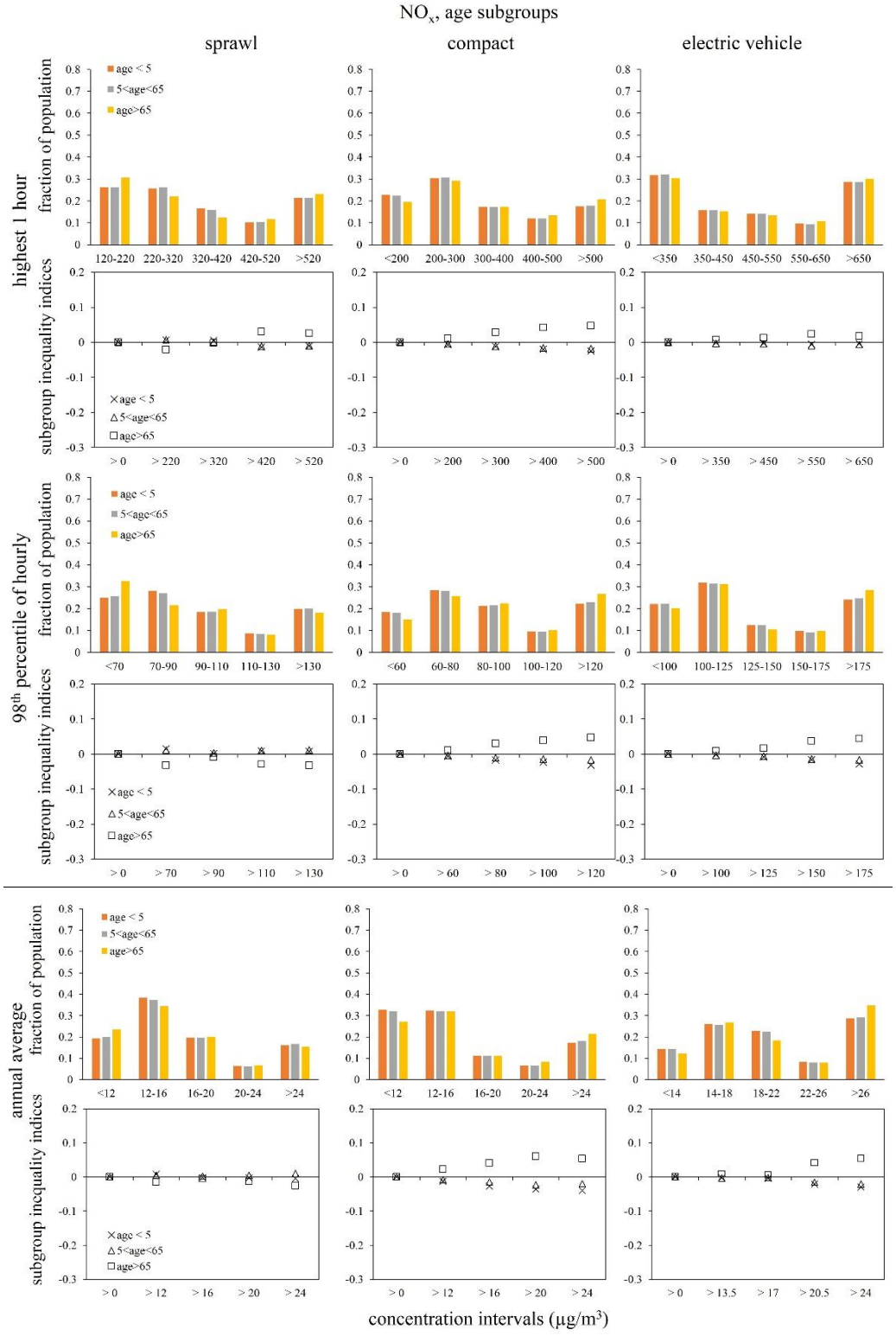

Appendix B- 10 Population distributions and estimated subgroup inequality indices for income subgroups regarding NO_x exposures in three future scenarios.

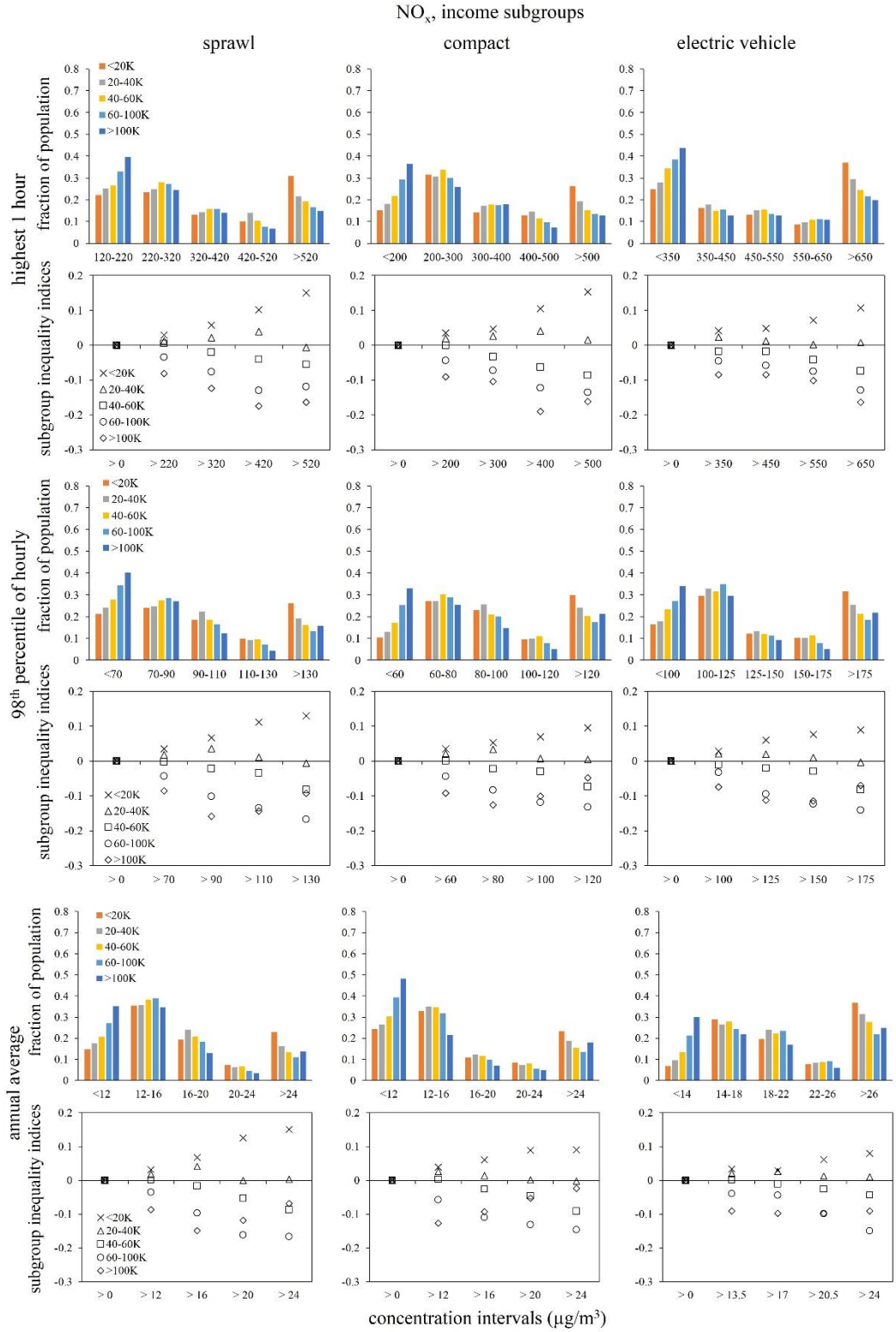

Appendix B- 11 Population distributions and estimated subgroup inequality indices for race/ethnicity subgroups regarding 1,3-butadiene exposures in three future scenarios.

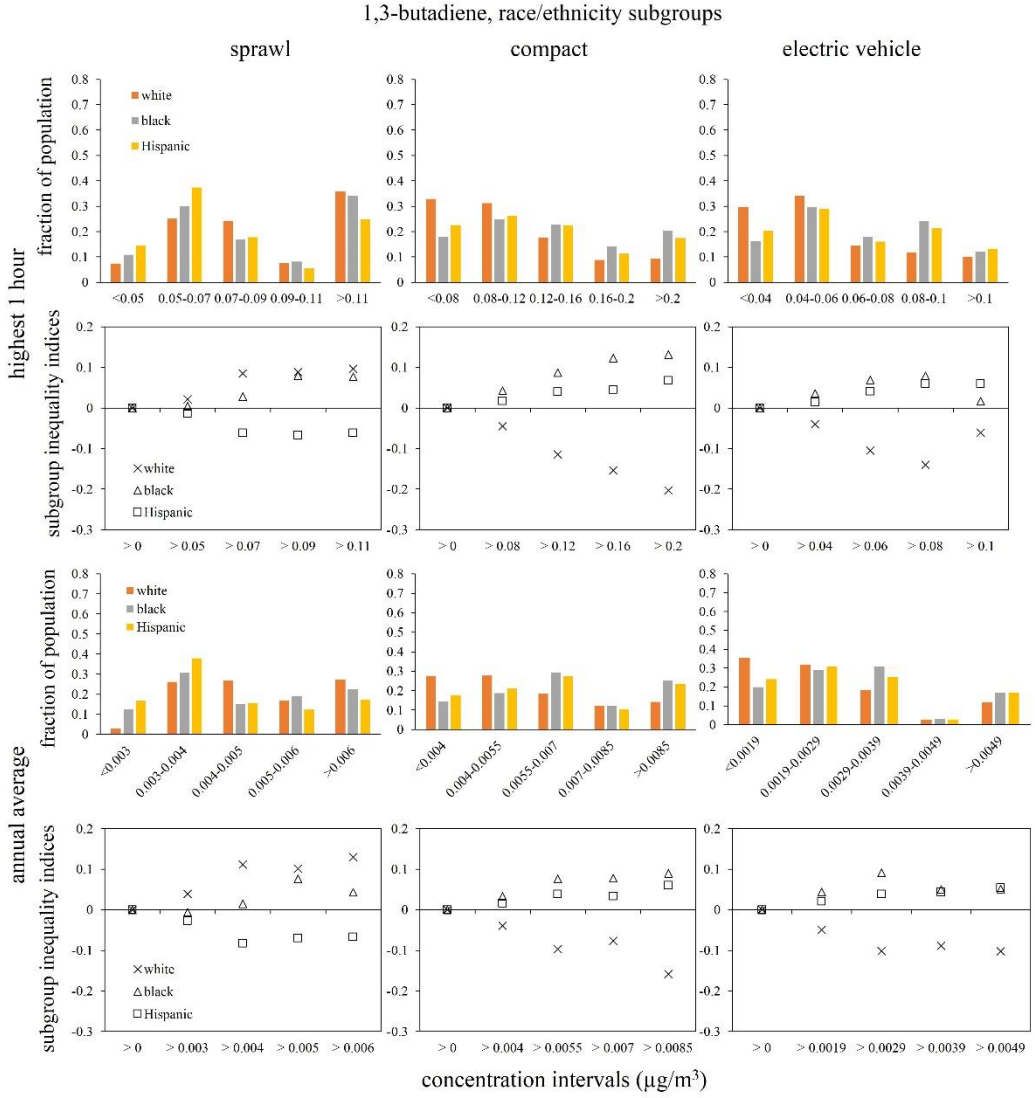

Appendix B- 12 Population distributions and estimated subgroup inequality indices for age subgroups regarding 1,3-butadiene exposures in three future scenarios.

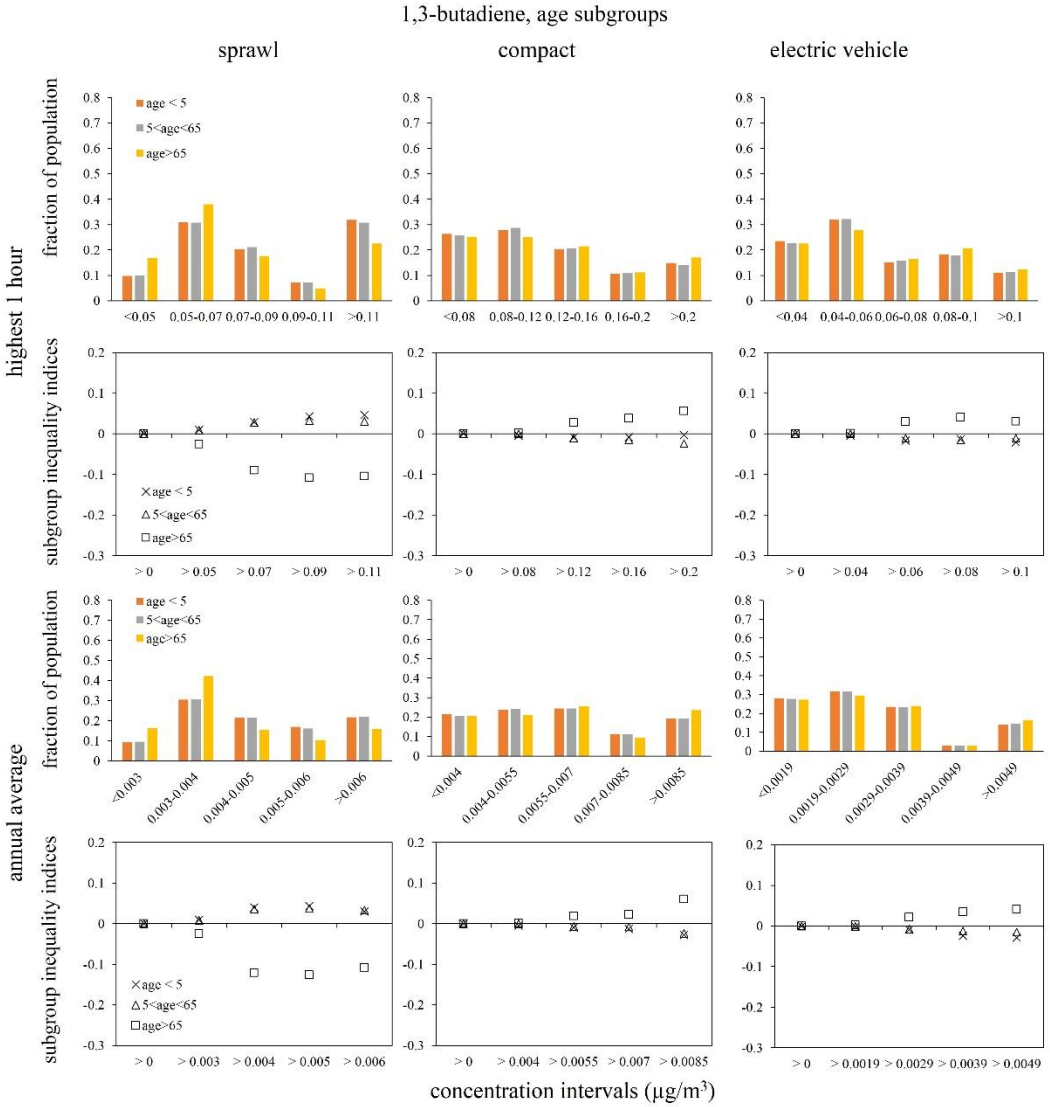

Appendix B- 13 Population distributions and estimated subgroup inequality indices for income subgroups regarding 1,3-butadiene exposures in three future scenarios.

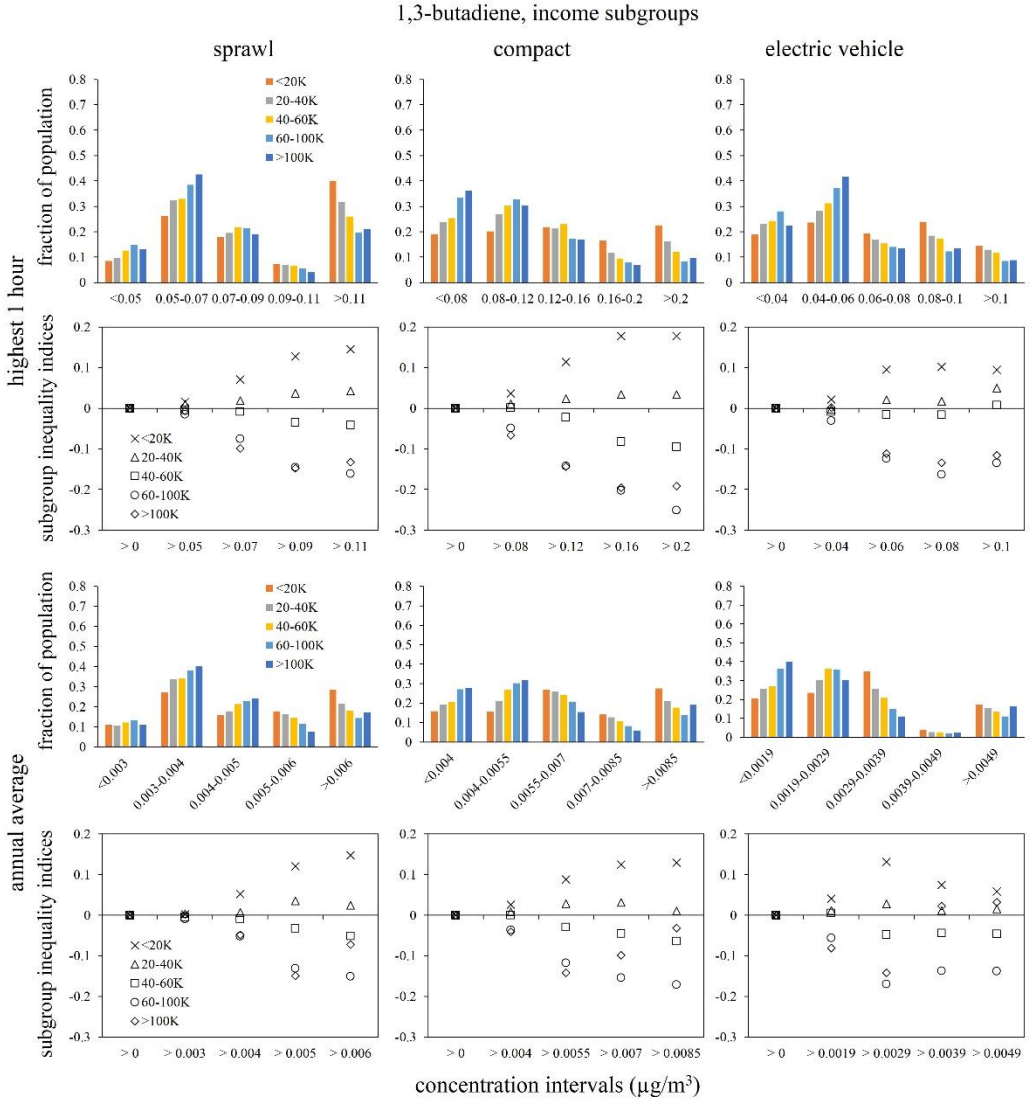

Appendix B- 14 Population distributions and estimated subgroup inequality indices for race/ethnicity subgroups regarding benzene exposures in three future scenarios.

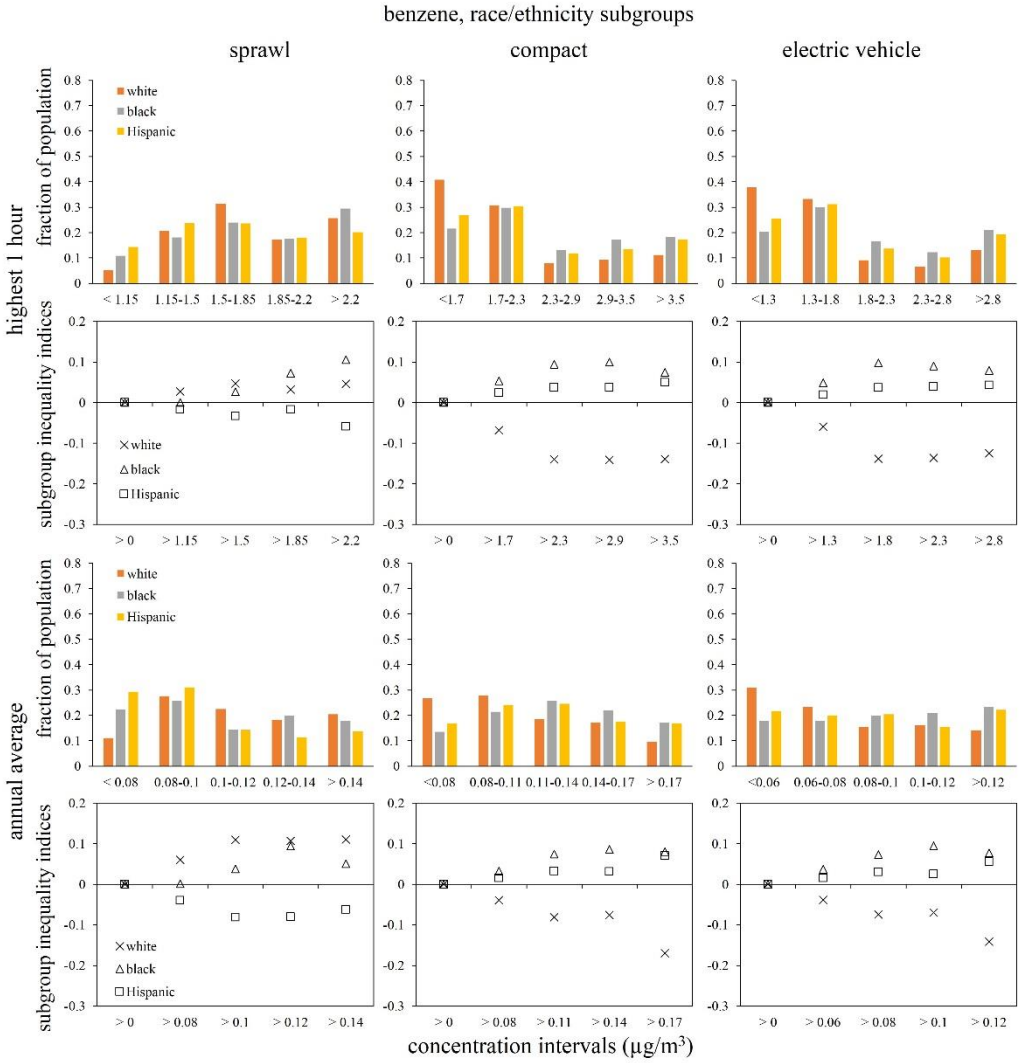

Appendix B- 15 Population distributions and estimated subgroup inequality indices for age subgroups regarding benzene exposures in three future scenarios.

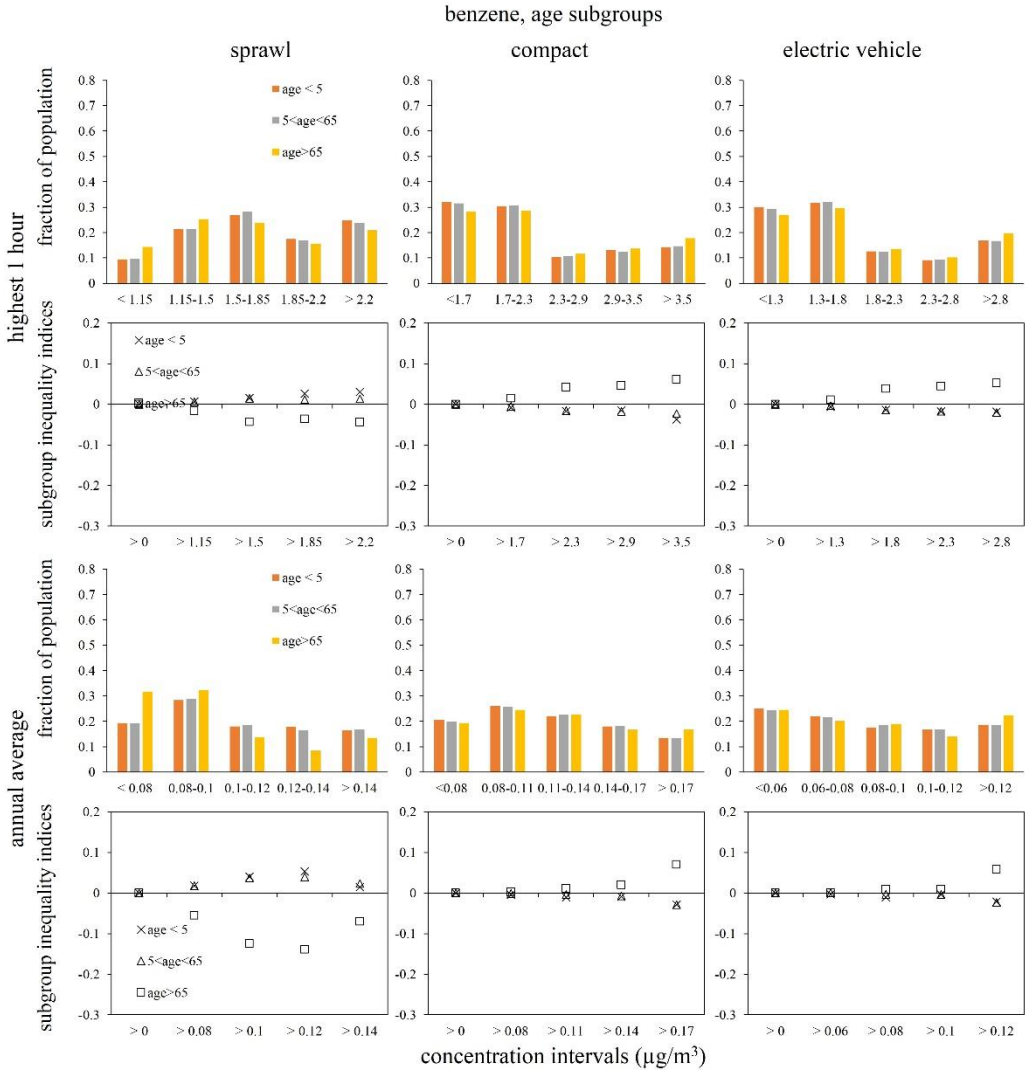

Appendix B- 16 Population distributions and estimated subgroup inequality indices for income subgroups regarding benzene exposures in three future scenarios.

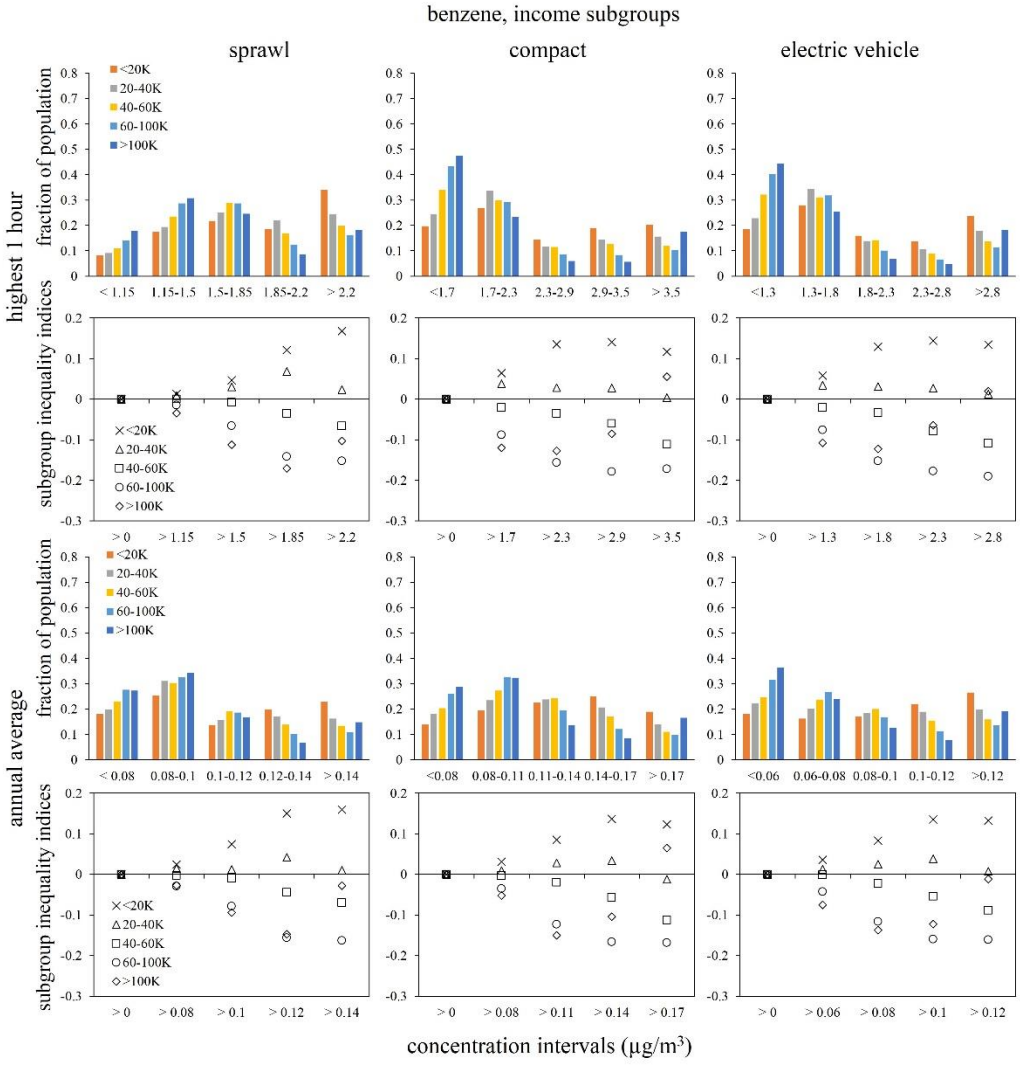

Appendix B- 17 Population distributions and estimated subgroup inequality indices for race/ethnicity subgroups regarding acetaldehyde exposures in three future scenarios.

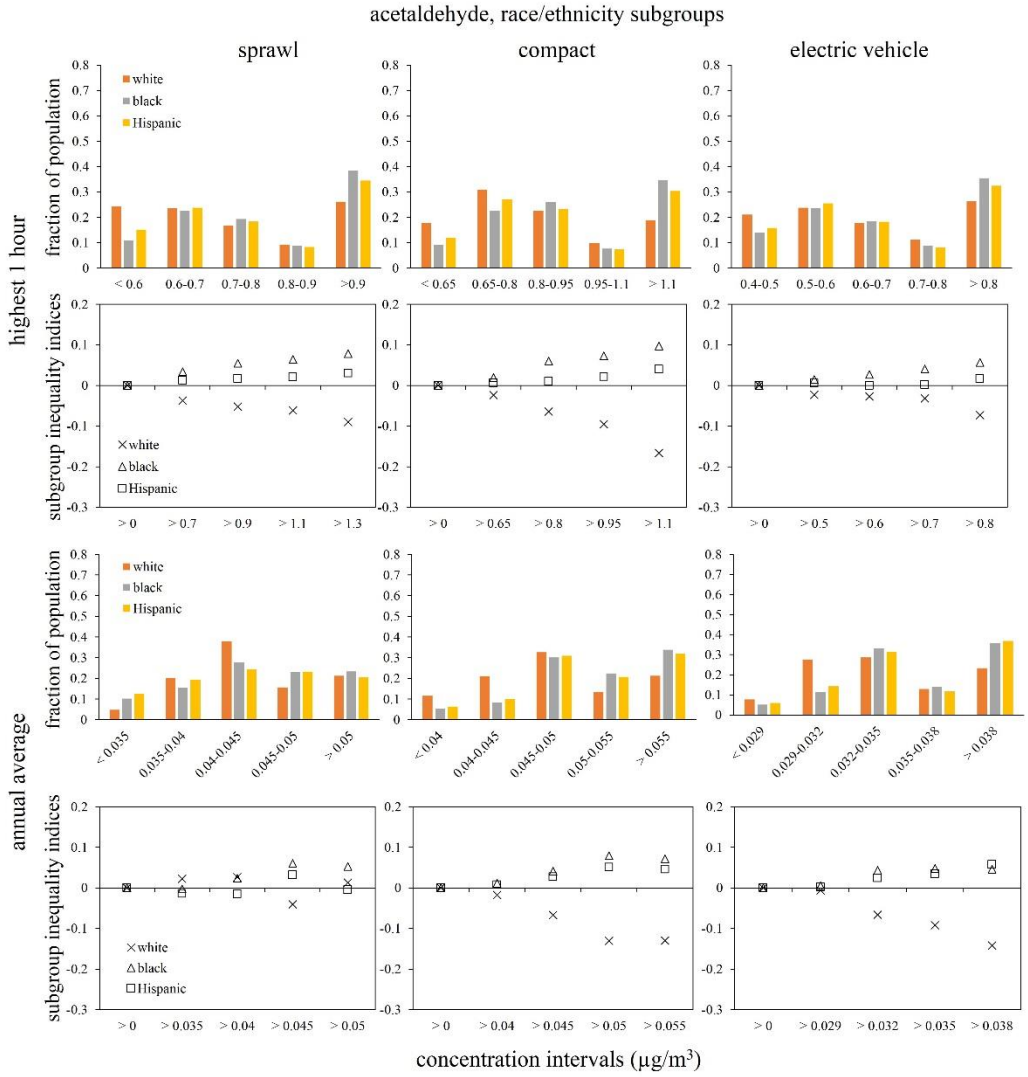

Appendix B- 18 Population distributions and estimated subgroup inequality indices for age subgroups regarding acetaldehyde exposures in three future scenarios.

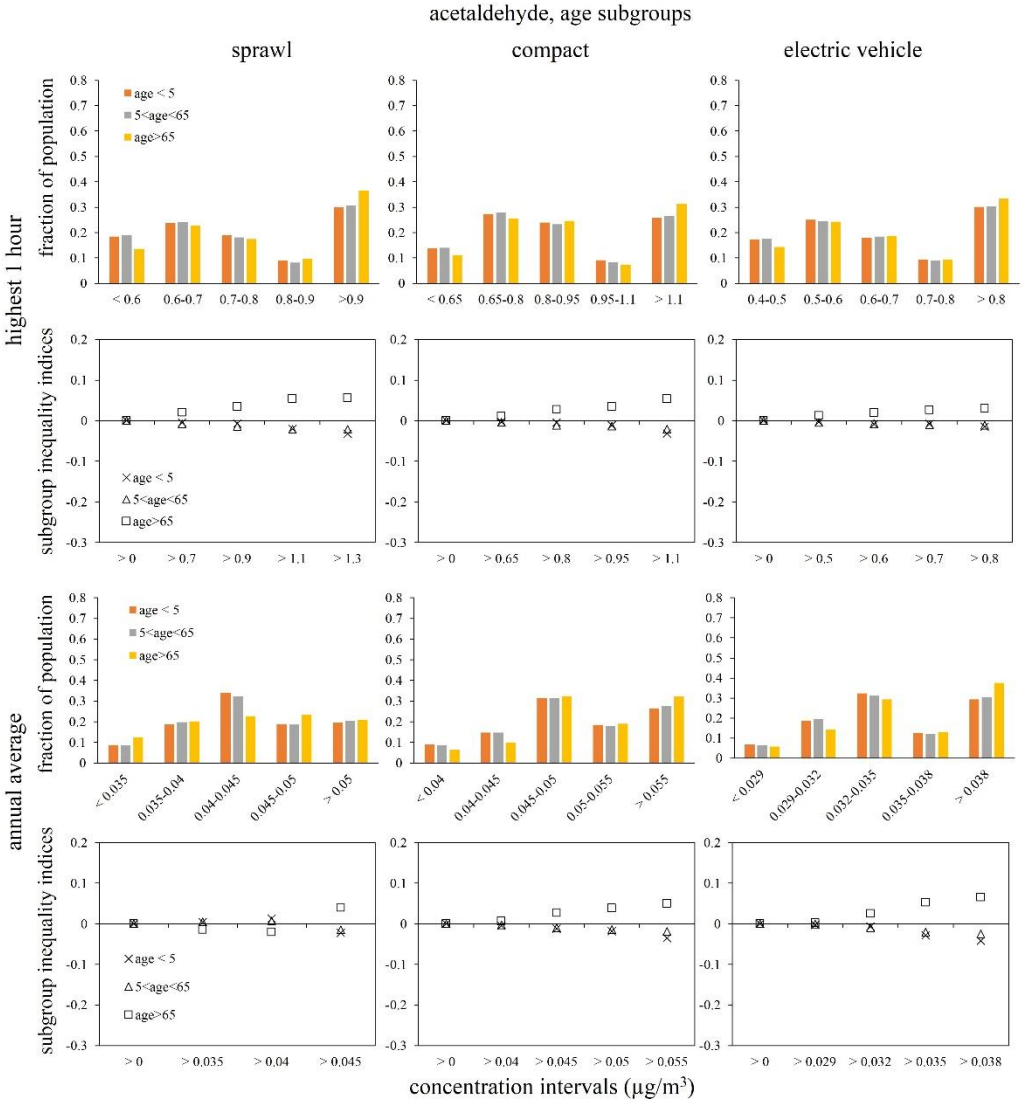

Appendix B- 19 Population distributions and estimated subgroup inequality indices for income subgroups regarding acetaldehyde exposures in three future scenarios.

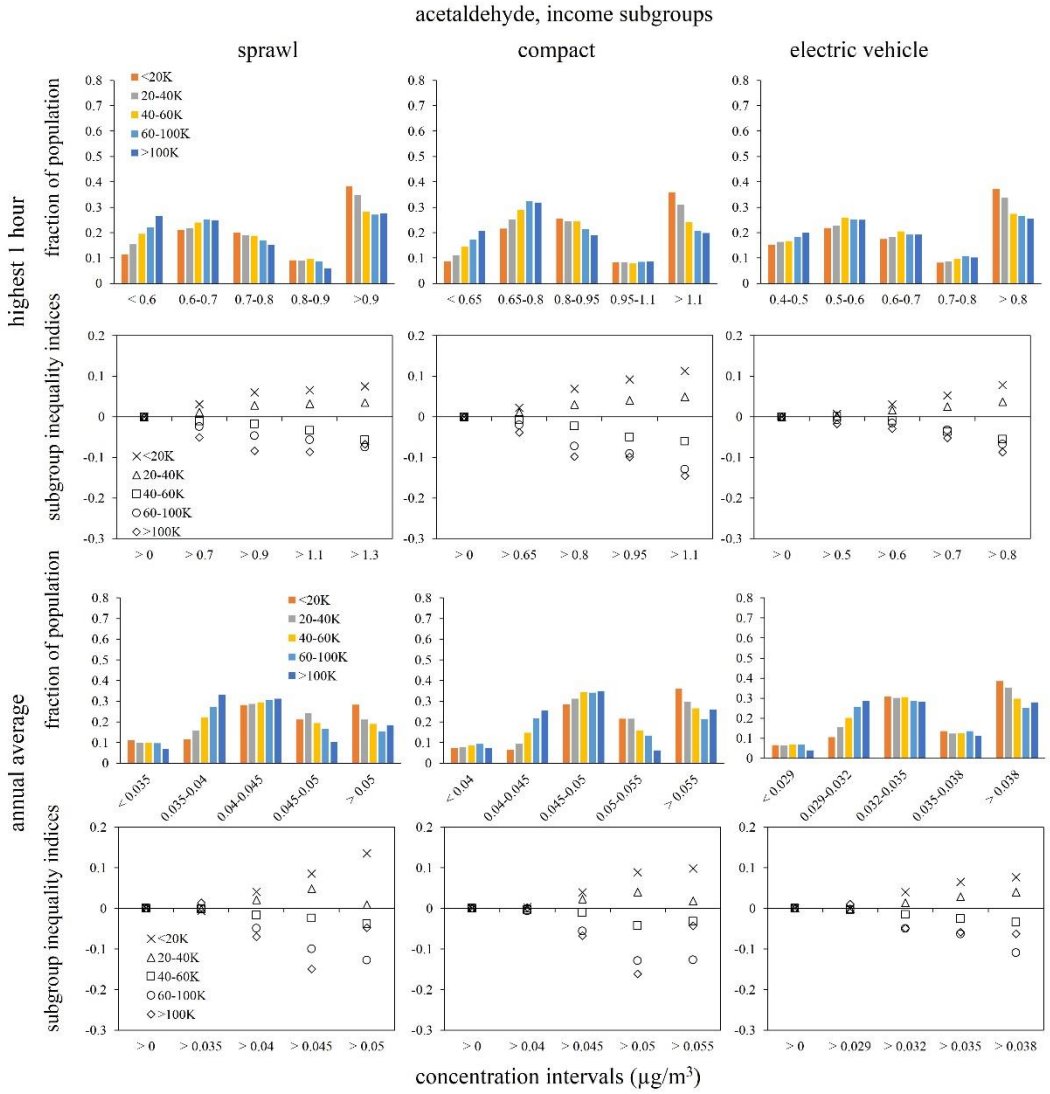

Appendix B- 20 Population distributions and estimated subgroup inequality indices for race/ethnicity subgroups regarding formaldehyde exposures in three future scenarios.

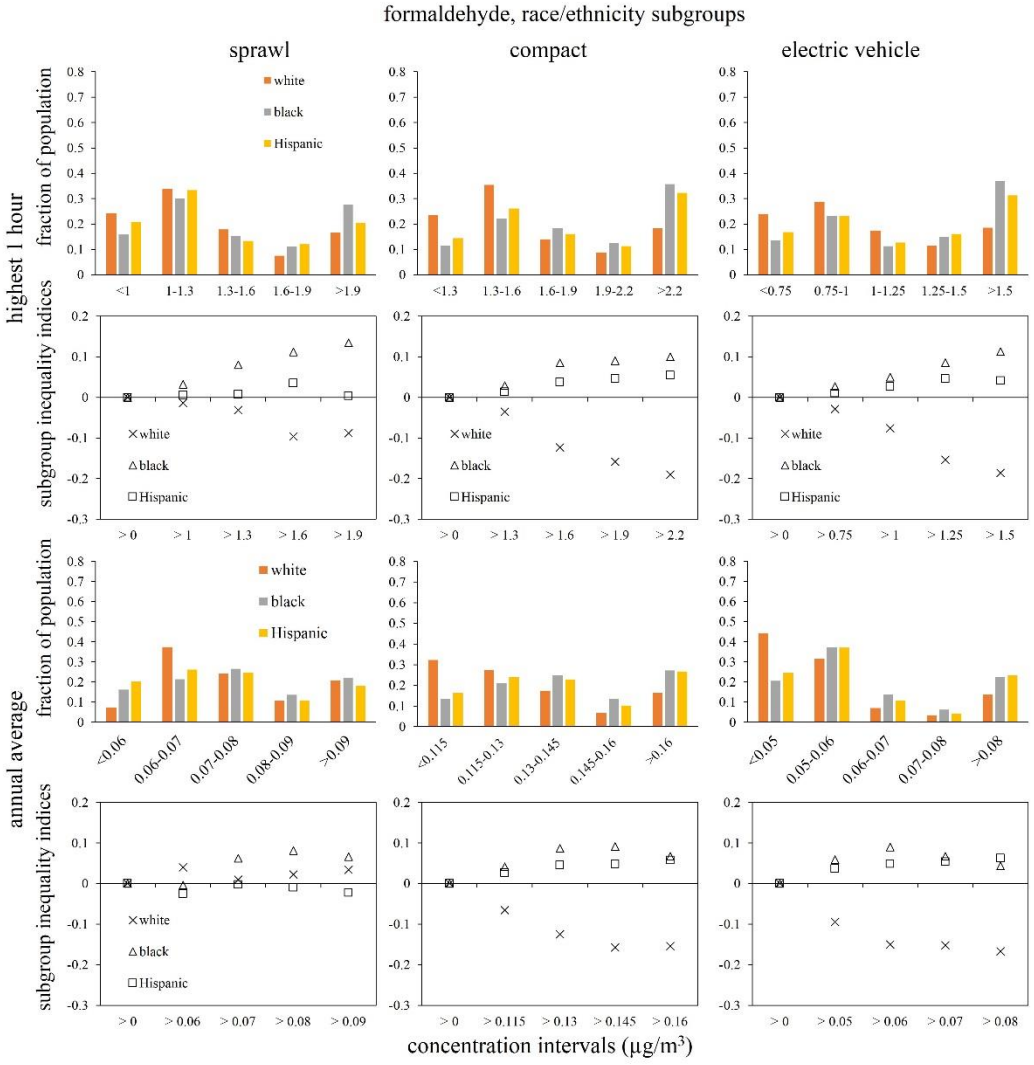

Appendix B- 21 Population distributions and estimated subgroup inequality indices for age subgroups regarding formaldehyde exposures in three future scenarios.

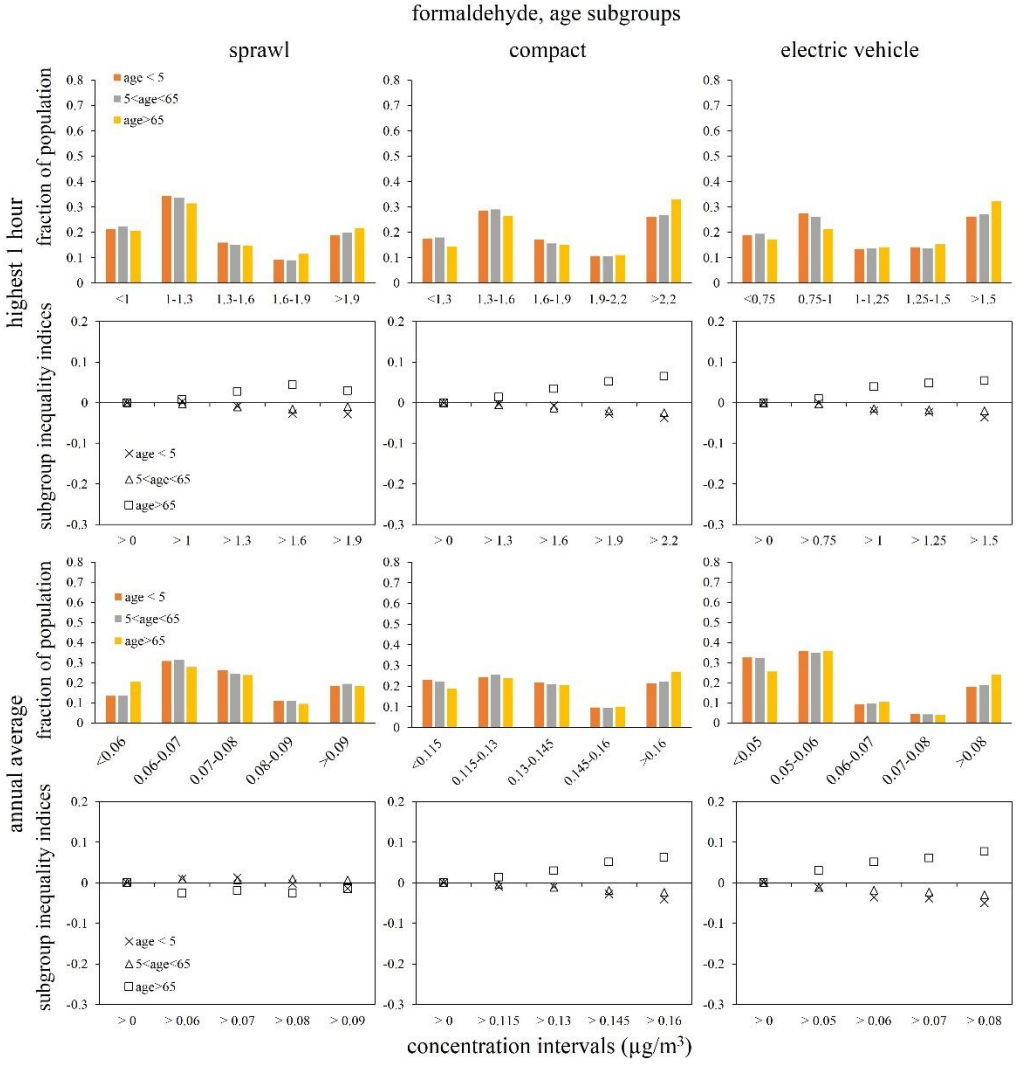

Appendix B- 22 Population distributions and estimated subgroup inequality indices for income subgroups regarding formaldehyde exposures in three future scenarios.

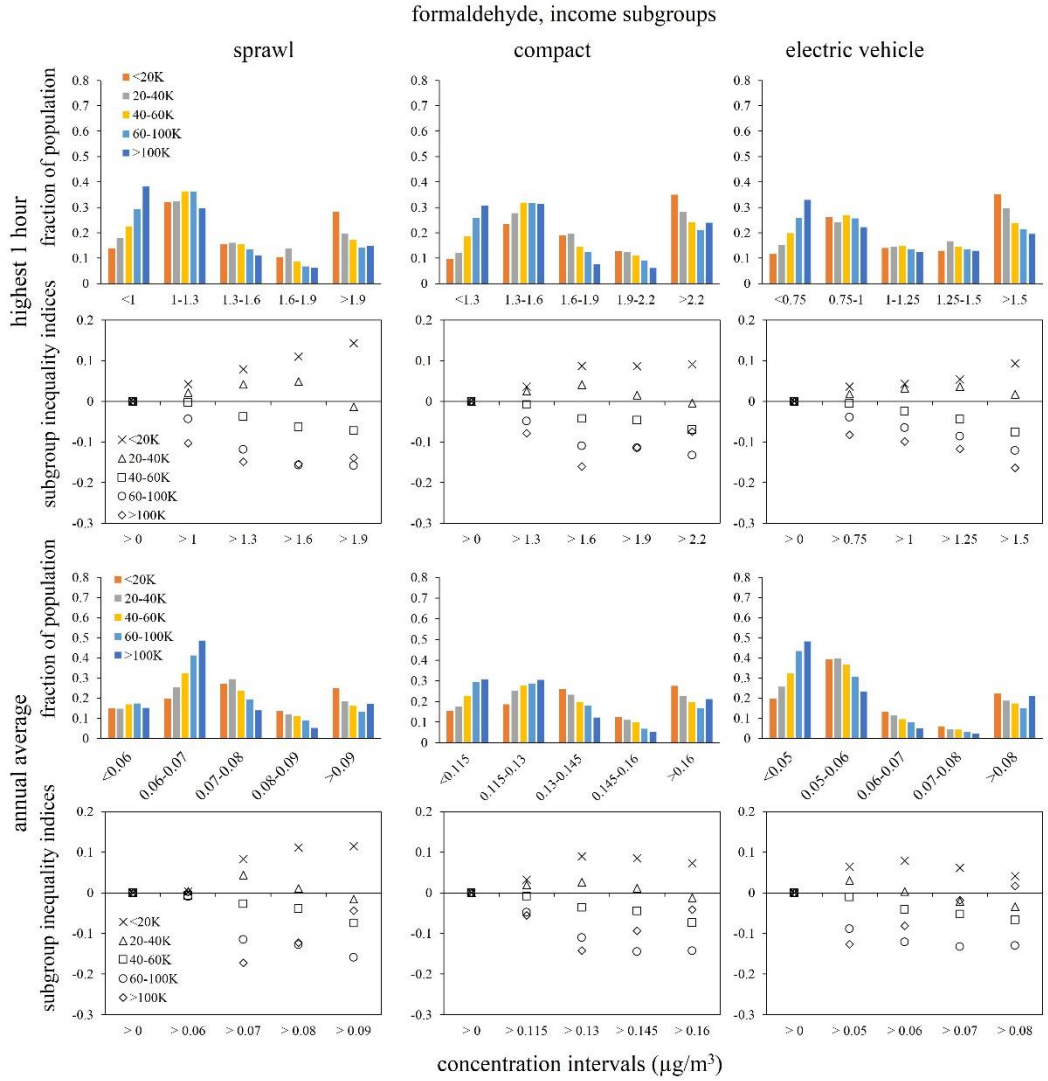

REFERENCES

Agency for Toxic Substances and Disease Registry. (2007). *Toxicological Profile for Benzene*. Atlanta, Georgia 30333.

Agency for Toxic Substances and Disease Registry. (2009). *Toxicological Profile for 1,3 - Butadiene*. Atlanta, Georgia 30333.

Alhajeri, N. S., McDonald-Buller, E. C., & Allen, D. T. (2011). Comparisons of air quality impacts of fleet electrification and increased use of biofuels. *Environmental Research Letters, 6*(2), 1-11.

Allen, R. W., Criqui, M. H., Roux, A. V. D., Allison, M., Shea, S., Detrano, R., . . . Kaufman, J. D. (2009). Fine Particulate Matter Air Pollution, Proximity to Traffic, and Aortic Atherosclerosis. [Article]. *Epidemiology, 20*(2), 254-264. doi: 10.1097/EDE.0b013e31819644cc

Allred, E. N., Bleecker, E. R., Chaitman, B. R., Dahms, T. E., Gottlieb, S. O., Hackney, J. D., . . . Warren, J. (1989). Short-term effects of carbon monoxide exposure on the exercise performance of subjects with coronary artery disease. *The New England journal of medicine, 321*(21), 1426-1432.

American Academy of Pediatrics Committee on Environmental Health. (2004). Ambient air pollution: health hazards to children. *Pediatrics, 114*(6), 1699-1707.

Andersen, Z. J., Bønnelykke, K., Hvidberg, M., Jensen, S. S., Ketzel, M., Loft, S., Raaschou-Nielsen, O. (2012). Long-term exposure to air pollution and asthma hospitalisations in older adults: a cohort study. *Thorax, 67*(1), 6-11. doi: 10.1136/thoraxjnl-2011-200711

Arain, M. A., Blair, R., Finkelstein, N., Brook, J. R., Sahsuvaroglu, T., Beckerman, B., . . . Jerrett, M. (2007). The use of wind fields in a land use regression model to predict air pollution concentrations for health exposure studies. *Atmospheric Environment, 41*(16), 3453-3464. doi: http://dx.doi.org/10.1016/j.atmosenv.2006.11.063

Atlanta Regional Commission. (2010). MOVES Based Mobile Source Emissions Modeling for the Atlanta Nonattainment Area. Atlanta, GA: Atlanta Regional Commission.

Bai, S., Nie, Y., & Niemeier, D. A. (2007). The impact of speed post-processing methods on regional mobile emissions estimation. *Transportation Research Part D: Transport and Environment, 12*(5), 307-324. doi: 10.1016/j.trd.2007.03.005

Batterman, S. A., Zhang, K., & Kononowech, R. (2010). Prediction and analysis of near-road concentrations using a reduced-form emission/dispersion model. [Article]. *Environmental Health, 9*. doi: 10.1186/1476-069x-9-29

Bechle, M. J., Millet, D. B., & Marshall, J. D. (2011). Effects of Income and Urban Form on Urban NO2: Global Evidence from Satellites. *Environmental Science & Technology, 45*(11), 4914-4919. doi: 10.1021/es103866b

Beevers, S. D., Kitwiroon, N., Williams, M. L., & Carslaw, D. C. (2012). One way coupling of CMAQ and a road source dispersion model for fine scale air pollution predictions. [Article]. *Atmospheric Environment, 59*, 47-58. doi: 10.1016/j.atmosenv.2012.05.034

Benson, P., Pinkerman, K., Brown, G., Connally, P., Cramer, R., Edwards, G., . . . Robertson, K. (1989). CALINE4 - A Dispersion Model for Predicting Air Pollution Concentrations Near Roadways. Sacramento, California: California Department of Transportation.

Berkowicz, R. (2000). OSPM - A Parameterised Street Pollution Model. *Environmental Monitoring and Assessment, 65*(1-2), 323-331. doi: 10.1023/a:1006448321977

Boarnet, M. G., & Crane, R. (2001). *Travel by Design: The Influence of Urban Form on Travel* New York: Oxford University Press.

Boriboonsomsin, K., & Barth, M. (2008). Impacts of freeway high-occupancy vehicle lane configuration on vehicle emissions. *Transportation Research Part D: Transport and Environment, 13*(2), 112-125. doi: http://dx.doi.org/10.1016/j.trd.2008.01.001

Borrego, C., Martins, H., Tchepel, O., Salmim, L., Monteiro, A., & Miranda, A. I. (2006). How urban structure can affect city sustainability from an air quality perspective. *Environmental Modelling & Software, 21*(4), 461-467. doi: http://dx.doi.org/10.1016/j.envsoft.2004.07.009

Brauer, M. (2008). A cohort study of traffic related air-pollution impacts on birth outcomes. [Correction]. *Environmental Health Perspectives, 116*(12), A519-A519.

Breheny, M. (1996). Centrists, Decentrists and Compromisers: Views on the Future of Urban Form *The Compact City: A sustainable urban form?* Oxford, UK: Oxford Brookes University.

Brook, R. D., Rajagopalan, S., Pope, C. A., Brook, J. R., Bhatnagar, A., Diez-Roux, A. V., . . . Metabolism. (2010). Particulate Matter Air Pollution and Cardiovascular Disease: An Update to the Scientific Statement From the American Heart Association. *Circulation, 121*(21), 2331-2378. doi: 10.1161/CIR.0b013e3181dbece1

Brzezinski, D., Hart, C., & Enns, P. (2001). *Final Facility Specific Speed Correction Factors*. (EPA420-R-01-060). Ann Arbor, MI: Retrieved from http://www.epa.gov/oms/models/mobile6/r01060.pdf.

Buzzelli, M., & Jerrett, M. (2007). Geographies of Susceptibility and Exposure in the City: Environmental Inequity of Traffic-Related Air Pollution in Toronto. *Canadian Journal of Regional Science, 30*, 195-210.

Byun, D., & Schere, K. L. (2006). Review of the governing equations, computational algorithms, and other components of the models-3 Community Multiscale Air Quality (CMAQ) modeling system. [Review]. *Applied Mechanics Reviews, 59*(1-6), 51-77. doi: 10.1115/1.2128636

Cambridge Environmental Research Consultants. (2010). ADMS-Urban. An Urban Air Quality Management System User's Guide Version 3.0. Cambridge, UK.

Chakraborty, J. (2009). Automobiles, Air Toxics, and Adverse Health Risks: Environmental Inequities in Tampa Bay, Florida. *Annals of the Association of American Geographers, 99*(4), 674-697.

Chakraborty, J., & Bosman, M. M. (2010). *Spatial and Environmental Injustice in an American Metropolis: A Study of Tampa Bay, Florida*. Amherst, New York 14228: Cambria Press.

Chang, H., Parandvash, G., & Shandas, V. (2010). Spatial Variations of Single-Family Residential Water Consumption in Portland, Oregon. *Urban Geography, 31*(7), 953-972. doi: 10.2747/0272-3638.31.7.953

Clark, L. P., Millet, D. B., & Marshall, J. D. (2011). Air Quality and Urban Form in U.S. Urban Areas: Evidence from Regulatory Monitors. *Environmental Science & Technology, 45*(16), 7028-7035. doi: 10.1021/es2006786

Cohen, A. J., Anderson, H. R., Ostro, B., Pandey, K. D., Krzyzanowski, M., Künzli, N., . . . Smith, K. R. (2004). Urban Air Pollution *Comparative Quantification of Health Risks. Global and Regional Burden of Disease Attribution to Selected Major Risk Factors* (Vol. 2, pp. 1353-1433). Geneva, Switzerland: World Health Organization.

Cohen, B. (2004). Urban Growth in Developing Countries: A Review of Current Trends and a Caution Regarding Existing Forecasts. *World Development, 32*(1), 23-51. doi: DOI: 10.1016/j.worlddev.2003.04.008

Colvile, R. N., Hutchinson, E. J., Mindell, J. S., & Warren, R. F. (2001). The transport sector as a source of air pollution. *Atmospheric Environment, 35*(9), 1537-1565. doi: http://dx.doi.org/10.1016/S1352-2310(00)00551-3

Committee to Review EPA's Mobile Source Emissions Factor (MOBILE) Model. (2000). Modeling Mobile-Source Emissions. Washington, D.C.

Community Modeling and Analysis System. (2010). Operational Guidance for the Community Multiscale Air Quality (CMAQ) Modeling System: Community Modeling and Analysis System, Institute for the Environment, University of North Carolina at Chapel Hill, Chapel Hill, NC 27599.

Cook, R., Isakov, V., Touma, J. S., Benjey, W., Thurman, J., Kinnee, E., & Ensley, D. (2008). Resolving Local-Scale Emissions for Modeling Air Quality near Roadways. *Journal of the Air & Waste Management Association, 58*, 451-461.

Cook, R., Touma, J. S., Beidler, A., & Strum, M. (2006). Preparing highway emissions inventories for urban scale modeling: A case study in Philadelphia. *Transportation Research Part D: Transport and Environment, 11*(6), 396-407. doi: DOI: 10.1016/j.trd.2006.08.001

Cressie, N., Calder, C. A., Clark, J. S., Hoef, J. M. V., & Wikle, C. K. (2009). Accounting for uncertainty in ecological analysis: the strengths and limitations of hierarchical statistical modeling. *Ecological Applications, 19*(3), 553-570. doi: 10.1890/07-0744.1

Davidson, K., Hallberg, A., McCubbin, D., & Hubbell, B. (2007). Analysis of PM2.5 Using the Environmental Benefits Mapping and Analysis Program (BenMAP)∗. *Journal of Toxicology and Environmental Health, Part A, 70*(3-4), 332-346. doi: 10.1080/15287390600884982

De Ridder, K., Lefebre, F., Adriaensen, S., Arnold, U., Beckroege, W., Bronner, C., . . . Weber, C. (2008). Simulating the impact of urban sprawl on air quality and population exposure in the German Ruhr area. Part II: Development and evaluation of an urban growth scenario. *Atmospheric Environment, 42*(30), 7070-7077. doi: DOI: 10.1016/j.atmosenv.2008.06.044

Denby, B., Cassiani, M., de Smet, P., de Leeuw, F., & Horálek, J. (2011). Sub-grid variability and its impact on European wide air quality exposure assessment. *Atmospheric Environment, 45*(25), 4220-4229. doi: http://dx.doi.org/10.1016/j.atmosenv.2011.05.007

Department of Transportation (DOT) Order To Address Environmental Justice in Minority Populations and Low-Income Populations, OST Docket No. OST-95-141 (50125) C.F.R. (1997).

Denison. (2000). Health Effects of Five Common Air Contaminants and Recommended Protective Ranges: Ministry for the Environment, New Zealand.

Dollard, G. J., C. J. Dore, et al. (2001). "Ambient concentrations of 1,3-butadiene in the UK." Chemico-Biological Interactions 135–136(0): 177-206.

Dowling, R., Ireson, R., Skabardonis, A., Gillen, D., & Stopher, P. (2005). Predicting Air Quality Effects of Traffic Flow Improvements. NCHRP Report 535. Washington D.C: Transportation Research Board.

Draxler, R., Stunder, B., Rolph, G., Stein, A., & Taylor, A. (2012). *HYSPLIT4 USER's GUIDE*. Silver Spring, MD: Retrieved from http://www.arl.noaa.gov/documents/reports/hysplit_user_guide.pdf.

Dudhia, J., Gill, D., Manning, K., Wang, W., Bruyere, C., Kelly, S., & Lackey, K. (2005). PSU/NCAR Mesoscale Modeling System Tutorial Class Notes and User's Guide: MM5 Modeling System Version 3: National Center for Atmospheric Research.

Electric Power Research Institute. (2007). Environmental Assessment of Plug-In Hybrid Electric Vehicles Volume 1: Nationwide Greenhouse Gas Emissions. Palo Alto, CA: Electric Power Research Institute

ENVIRON International Corporation. (2006). Expanding and Updating the Master List of Compounds Emitted by Mobile Sources - Phase III Final Report: Washington, DC.

ENVIRON International Corporation. (2011). CAMx User's Guide. Comprehensive Air Quality Model with Extensions Version 5.4. Novato, California: ENVIRON International Corporation.

Escobedo, J. F., Gomes, E. N., Oliveira, A. P., & Soares, J. (2009). Modeling hourly and daily fractions of UV, PAR and NIR to global solar radiation under various sky conditions at Botucatu, Brazil. *Applied Energy, 86*(3), 299-309. doi: http://dx.doi.org/10.1016/j.apenergy.2008.04.013

Evans, A. M., & Stuart, A. L. (2009). *An Investigation of Small-scale Spatial Variability in Aldehyde Concentrations through Passive Sampling and Analysis*. Paper presented at the Air Pollution and Health: Bridging the Gap from Sources to Health Outcomes, San Diego, California.

Ewing, R. (1997). Is Los Angeles-Style Sprawl Desirable? *Journal of the American Planning Association, 63*(1), 107-126. doi: 10.1080/01944369708975728

Ewing, R., & Cervero, R. (2001). Travel and the Built Environment: A Synthesis. *Transportation Research Record: Journal of the Transportation Research Board, 1780*(-1), 87-114. doi: 10.3141/1780-10

Ewing, R., & Cervero, R. (2010). Travel and the Built Environment. *Journal of the American Planning Association, 76*(3), 265-294. doi: 10.1080/01944361003766766

Ewing, R., Pendall, R., & Chen, D. (2002). Measuring Sprawl and Its Impact. Smart Growth Smaerican. Washington, DC.

Ewing, R., & Rong, F. (2008). The impact of urban form on U.S. residential energy use. *Housing Policy Debate, 19*(1), 1-30. doi: 10.1080/10511482.2008.9521624

Fan, Y., & Song, Y. (2009). Is Sprawl Associated with a Widening Urban–Suburban Mortality Gap? *Journal of Urban Health, 86*(5), 708-728. doi: 10.1007/s11524-009-9382-3

Federal Highway Administration. (2012). Interim Guidance Update on Mobile Source Air Toxic Analysis in NEPA. Washington, DC: Federal Highway Administration.

Federal Highway Administration. (2013). Highway Statistics 2010 Retrieved March 25, 2013, from http://www.fhwa.dot.gov/policyinformation/statistics/2010/

Finlayson-Pitts, B., & James Pitts, J. (1999). *Chemistry of the Upper and Lower Atmosphere - Theory, Experiments, and Applications*: Academic Press

Florida Department of Highway Safety and Motor Vehicles. (2002). *Revenue Report: July 1, 2001 - June 30, 2002*. Retrieved from http://flhsmv.gov/html/revpub/2002revpub.pdf.

Florida Department of Highway Safety and Motor Vehicles. (2003). *Revenue Report: July 1, 2002 - June 30, 2003*. Retrieved from http://flhsmv.gov/html/revpub/revpub2003.pdf.

Florida Department Of Transportation. (2002). 2002 Florida Traffic Information DVD. Tallahassee, FL: Transportation Statistics Office, Florida Department Of Transportation.

Florida Department of Transportation. (2003). *Florida Highway Mileage Reports - Public Roads*. Retrieved from http://www.dot.state.fl.us/planning/statistics/mileage-rpts/public02.pdf.

Florida Department of Transportation. (2009). 2009 Quality/Level of Service Handbook. Tallahassee, FL: Florida Department of Transportation.

Florida Geographic Data Library. (2012). Florida Geographic Data Library (FGDL). from GeoPlan Center, University of Florida http://www.fgdl.org/

Frank, L. D., & Engelke, P. (2005). Multiple Impacts of the Built Environment on Public Health: Walkable Places and the Exposure to Air Pollution. *International Regional Science Review, 28*(2), 193-216.

Frank, L. D., Stone Jr, B., & Bachman, W. (2000). Linking land use with household vehicle emissions in the central puget sound: methodological framework and findings. *Transportation Research Part D: Transport and Environment, 5*(3), 173-196. doi: http://dx.doi.org/10.1016/S1361-9209(99)00032-2

Fridh, S., & Stuart, A. L. (2012). Spatial variation in ambient benzene concentration over a city park. *Journal of Environmental Health, Accepted May*.

Frumkin, H., Frank, L., & Jackson, R. J. (2004). *Urban Sprawl and Public Health. Designing, planning, and building for healthy communities*. Washington: Island Press.

Fujita, E. M., Campbell, D. E., Zielinska, B., Chow, J. C., Lindhjem, C. E., DenBleyker, A., . . . Lawson, D. R. (2012). Comparison of the MOVES2010a, MOBILE6.2, and EMFAC2007 mobile source emission models with on-road traffic tunnel and remote sensing measurements. *Journal of the Air & Waste Management Association, 62*(10), 1134-1149. doi: 10.1080/10962247.2012.699016

Fujita, E. M., Campbell, D. E., Zielinska, B., Sagebiel, J. C., Bowen, J. L., Goliff, W. S., . . . Lawson, D. R. (2003). Diurnal and Weekday Variations in the Source Contributions of Ozone Precursors in California's South Coast Air Basin. *Journal of the Air & Waste Management Association, 53*(7), 844-863. doi: 10.1080/10473289.2003.10466226

Gannett Fleming Inc. (2010). Technical Report 2 - Tampa Bay Regional Planning Model (TBRPM) Version 7.0 Procedural Guide. Tampa, FL: Gannett Fleming, Inc.

Geurs, K. T., & van Wee, B. (2006). Ex-post Evaluation of Thirty Years of Compact Urban Development in the Netherlands. *Urban Studies, 43*(1), 139-160. doi: 10.1080/00420980500409318

Ghannam, K., & El-Fadel, M. (2013). Emissions characterization and regulatory compliance at an industrial complex: An integrated MM5/CALPUFF approach. *Atmospheric Environment, 69*(0), 156-169. doi: http://dx.doi.org/10.1016/j.atmosenv.2012.12.022

Ghosh, J. K. C., Wilhelm, M., Su, J., Goldberg, D., Cockburn, M., Jerrett, M., & Ritz, B. (2012). Assessing the Influence of Traffic-related Air Pollution on Risk of Term Low Birth Weight on the Basis of Land-Use-based Regression Models and Measures of Air Toxics. *American Journal of Epidemiology, 175*(12), 1262-1274. doi: 10.1093/aje/kwr469

Glaeser, E. L., Kahn, M., & Chu, C. (2001). *Job Sprawl: Employment Location in U.S. Metropolitan Areas*. Washington,DC: Center on Urban & Metropolitan Policy, The Brookings Institution.

Godish, T. (2004). *Air Quality - 4th Edition*: Lewis Publishers.

Grabow, M. L., Spak, S. N., Holloway, T., Stone, B., Mednick, A. C., & Patz, J. A. (2012). Air Quality and Exercise-Related Health Benefits from Reduced Car Travel in the Midwestern United States. [Article]. *Environmental Health Perspectives, 120*(1), 68-76. doi: 10.1289/ehp.1103440

Green, R. S., Smorodinsky, S., Kim, J. J., McLaughlin, R., & Ostro, B. (2003). Proximity of California Public Schools to Busy Roads. *Environ Health Perspect, 112*(1).

Grineski, S., Bolin, B., & Boone, C. (2007). Criteria Air Pollution and Marginalized Populations: Environmental Inequity in Metropolitan Phoenix, Arizona*. *Social Science Quarterly, 88*(2), 535-554. doi: 10.1111/j.1540-6237.2007.00470.x

Gurram, S., Stuart, A. L., & Pinjari, A. R. (2012). *Characterization of exposures to ambient NOx levels in the Tampa area considering spatiotemporal travel activity data*. Paper presented at the Air & Waste Management Association Annual Conference & Exposition, San Antonio, TX.

Halse, A. K., Eckhardt, S., Schlabach, M., Stohl, A., & Breivik, K. (2013). Forecasting long-range atmospheric transport episodes of polychlorinated biphenyls using FLEXPART. *Atmospheric Environment, 71*(0), 335-339. doi: http://dx.doi.org/10.1016/j.atmosenv.2013.02.022

Handy, S. (2005). Smart Growth and the Transportation-Land Use Connection: What Does the Research Tell Us? *International Regional Science Review, 28*(2), 146-167. doi: 10.1177/0160017604273626

Hatzopoulou, M. (2008). *An integrated multi-model approach for predicting the impact of household travel on urban air quality and simulating population exposure.* Ph.D., University of Toronto, Toronto.

Hatzopoulou, M., & Miller, E. J. (2010). Linking an activity-based travel demand model with traffic emission and dispersion models: Transport's contribution to air pollution in Toronto. *Transportation Research Part D: Transport and Environment, 15*(6), 315-325. doi: 10.1016/j.trd.2010.03.007

HEI Panel on the Health Effects of Traffic-Related Air Pollution. (2010). Traffic-Related Air Pollution: A Critical Review of the Literature on Emissions, Exposure, and Health Effects. HEI Special Report 17. Boston, MA: Health Effects Institute.

Held, T., Ying, Q., Kleeman, M. J., Schauer, J. J., & Fraser, M. P. (2005). A comparison of the UCD/CIT air quality model and the CMB source–receptor model for primary airborne particulate matter. *Atmospheric Environment, 39*(12), 2281-2297. doi: http://dx.doi.org/10.1016/j.atmosenv.2004.12.034

Henderson, S. B., Beckerman, B., Jerrett, M., & Brauer, M. (2007). Application of Land Use Regression to Estimate Long-Term Concentrations of Traffic-Related Nitrogen Oxides and Fine Particulate Matter. *Environmental Science & Technology, 41*(7), 2422-2428. doi: 10.1021/es0606780

Hinds, W. C. (1999). *Aerosol Technology: Properties, Behavior, and Measurement of Airborne Particles. Second Edition*: John Wiley & Sons, Inc.

Hixson, M., Mahmud, A., Hu, J., Bai, S., Niemeier, D. A., Handy, S. L., . . . Kleeman, M. J. (2010). Influence of regional development policies and clean technology adoption on future air pollution exposure. *Atmospheric Environment, 44*(4), 552-562. doi: DOI: 10.1016/j.atmosenv.2009.10.041

Hixson., M., Mahmud, A., Hu, J. L., & Kleeman, M. J. (2012). Resolving the interactions between population density and air pollution emissions controls in the San Joaquin Valley, USA. [Article]. *Journal of the Air & Waste Management Association, 62*(5), 566-575. doi: 10.1080/10962247.2012.663325

Hoek, G., Beelen, R., de Hoogh, K., Vienneau, D., Gulliver, J., Fischer, P., & Briggs, D. (2008). A review of land-use regression models to assess spatial variation of outdoor air pollution. *Atmospheric Environment, 42*(33), 7561-7578. doi: 10.1016/j.atmosenv.2008.05.057

Hoek, G., Brunekreef, B., Goldbohm, S., Fischer, P., & van den Brandt, P. A. (2002). Association between mortality and indicators of traffic-related air pollution in the Netherlands: a cohort study. [Article]. *Lancet, 360*(9341), 1203-1209. doi: 10.1016/s0140-6736(02)11280-3

Huo, H., Zhang, Q., Wang, M. Q., Streets, D. G., & He, K. (2010). Environmental Implication of Electric Vehicles in China. *Environmental Science & Technology, 44*(13), 4856-4861. doi: 10.1021/es100520c

Indiana Department of Environmental Management. (2012). Onroad Emissions MOBILE6.2 to MOVES Replacement Submittal: Indiana Department of Environmental Management.

Irwin, J. S., & Brown, T. M. (1985). A SENSITIVITY ANALYSIS OF THE TREATMENT OF AREA SOURCES BY THE CLIMATOLOGICAL DISPERSION MODEL. [Article]. *Journal of the Air Pollution Control Association, 35*(4), 359-364.

Isakov, V., Irwin, J. S., & Ching, J. (2007). Using CMAQ for Exposure Modeling and Characterizing the Subgrid Variability for Exposure Estimates. *Journal of Applied Meteorology and Climatology, 46*(9), 1354-1371. doi: doi:10.1175/JAM2538.1

Isakov, V., Touma, J. S., Burke, J., Lobdell, D. T., Palma, T., Rosenbaum, A., & Ozkaynak, H. (2009). Combining Regional- and Local-Scale Air Quality Models with Exposure Models for Use in Environmental Health Studies. [Article]. *Journal of the Air & Waste Management Association, 59*(4), 461-472. doi: 10.3155/1047-3289.59.4.461

Isakov, V., & Venkatram, A. (2006). Resolving Neighborhood Scale in Air Toxics Modeling: A Case Study in Wilmington, CA. *Journal of Air & Waste Management Association, 56*, 559-568.

Jacobson, M. Z. (2005). *Fundamentals of Atmospheric Modeling. Second Edition*: Cambridge University Press, NY.

Jacobson, M. Z. (2012). History of, Processes in, and Numerical Techniques in GATOR-GCMOM. Retrived from: http://www.stanford.edu/group/efmh/jacobson/GATOR/GATOR-GCMOMHist.pdf

Jensen, S. S., Larson, T., Deepti, K. C., & Kaufman, J. D. (2009). Modeling traffic air pollution in street canyons in New York City for intra-urban exposure assessment in the US Multi-Ethnic Study of atherosclerosis and air pollution. *Atmospheric Environment, 43*(30), 4544-4556. doi: http://dx.doi.org/10.1016/j.atmosenv.2009.06.042

Jerrett, M., Arain, A., Kanaroglou, P., Beckerman, B., Potoglou, D., Sahsuvaroglu, T., . . . Giovis, C. (2005). A Review and Evaluation of Intraurban Air Pollution Exposure Models. *Journal of Exposure Analysis and Environmental Epidemiology, 15*, 185 - 204.

Jerrett, M., Burnett, R. T., III, A. P., Krewski, D., Thurston, G., Christakos, G., . . . Lee, S.-J. (2012). Spatiotemporal Analysis of Air Pollution and Mortality in California Based on the American Cancer Society Cohort: Final Report. Sacramento CA.

Jungers, B. D., Niemeier, D., Kear, T., & Eisinger, D. (2006). A Survey of Air Quality Dispersion Models for Project Level Conformity Analysis (D. o. C. a. E. Engineering, Trans.): University of California, Davis.

Kahyaoğlu-Koračin, J., Bassett, S. D., Mouat, D. A., & Gertler, A. W. (2009). Application of a scenario-based modeling system to evaluate the air quality impacts of future growth. *Atmospheric Environment, 43*(5), 1021-1028. doi: 10.1016/j.atmosenv.2008.04.004

Kall, D., Guensler, R., Rodgers, M., & Pandey, V. (2009). Effect of High-Occupancy Toll Lanes on Mass Vehicle Emissions. *Transportation Research Record: Journal of the Transportation Research Board, 2123*(-1), 88-96. doi: 10.3141/2123-10

Kalthoff, N., Bäumer, D., Corsmeier, U., Kohler, M., & Vogel, B. (2005). Vehicle-induced turbulence near a motorway. *Atmospheric Environment, 39*(31), 5737-5749. doi: 10.1016/j.atmosenv.2004.06.048

Karamchandani, P., Zhang, Y., & Chen, S.-Y. (2012). Development and initial application of a sub-grid scale plume treatment in a state-of-the-art online Multi-scale Air Quality and Weather Prediction Model. *Atmospheric Environment, 63*(0), 125-134. doi: http://dx.doi.org/10.1016/j.atmosenv.2012.09.014

Kassteele, J., Stein, A., Dekkers, A. M., & Velders, G. M. (2009). External drift kriging of NOx concentrations with dispersion model output in a reduced air quality monitoring network. *Environmental and Ecological Statistics, 16*(3), 321-339. doi: 10.1007/s10651-007-0052-x

Keating, M. (2004). Air of Injustice: How Air Pollution Affects the Health of Hispanics and Latinos. Washington, D.C.: League of United Latin American Citizens.

Kingham, S., & Dorset, W. (2011). Assessment of exposure approaches in air pollution and health research in Australia and New Zealand. *Air Quality and Climate Change, 45*(2), 28-38.

Kinnee, E. J., Touma, J. S., Mason, R., Thurman, J., Beidler, A., Bailey, C., & Cook, R. (2004). Allocation of onroad mobile emissions to road segments for air toxics modeling in an urban area. *Transportation Research Part D: Transport and Environment, 9*(2), 139-150. doi: DOI: 10.1016/j.trd.2003.09.003

Kwak, K.-H., & Baik, J.-J. (2012). A CFD modeling study of the impacts of NOx and VOC emissions on reactive pollutant dispersion in and above a street canyon. *Atmospheric Environment, 46*(0), 71-80. doi: http://dx.doi.org/10.1016/j.atmosenv.2011.10.024

Lee, G., You, S., Ritchie, S., Saphores, J.-D., Sangkapichai, M., & Jayakrishnan, R. (2009). Environmental Impacts of a Major Freight Corridor. *Transportation Research Record: Journal of the Transportation Research Board, 2123*(-1), 119-128. doi: 10.3141/2123-13

Leksmono, N. S., Longhurst, J. W. S., Ling, K. A., Chatterton, T. J., Fisher, B. E. A., & Irwin, J. G. (2006). Assessment of the relationship between industrial and traffic sources contributing to air quality objective exceedences: a theoretical modelling exercise. *Environmental Modelling & Software, 21*(4), 494-500. doi: 10.1016/j.envsoft.2004.07.012

Levy, J. I., Chemerynski, S. M., & Tuchmann, J. L. (2006). Incorporating concepts of inequality and inequity into health benefits analysis. *International Journal for Equity in Health, 5*(2).

Li, L., Wu, J., Ghosh, J. K., & Ritz, B. (2013). Estimating spatiotemporal variability of ambient air pollutant concentrations with a hierarchical model. *Atmospheric Environment, 71*(0), 54-63. doi: http://dx.doi.org/10.1016/j.atmosenv.2013.01.038

Lin, M., Fiore, A. M., Horowitz, L. W., Cooper, O. R., Naik, V., Holloway, J., . . . Wyman, B. (2012). Transport of Asian ozone pollution into surface air over the western United States in spring. *Journal of Geophysical Research: Atmospheres, 117*(D4), D00V07. doi: 10.1029/2011jd016961

Lindhjem, C. E., Pollack, A. K., DenBleyker, A., & Shaw, S. L. (2012). Effects of improved spatial and temporal modeling of on-road vehicle emissions. *Journal of the Air & Waste Management Association, 62*(4), 471-484. doi: 10.1080/10962247.2012.658955

Litman, T. (2013). Evaluating Public Transit Benefits and Costs. Best Practices Guidebook. Victoria, BC, Canada: Victoria Transport Policy Institute.

Liu, F. (2003). Quantifying Travel and Air-Quality Benefits of Smart Growth in Maryland's State Implementation Plan. *Transportation Research Record: Journal of the Transportation Research Board, 1858*(-1), 80-88. doi: 10.3141/1858-11

Liu, X., Jeffries, H. E., & Sexton, K. G. (1999). Hydroxyl radical and ozone initiated photochemical reactions of 1,3-butadiene. *Atmospheric Environment, 33*(18), 3005-3022. doi: 10.1016/s1352-2310(99)00078-3

Lobdell, D. T., Isakov, V., Baxter, L., Touma, J. S., Smuts, M. B., & Ozkaynak, H. (2011). Feasibility of Assessing Public Health Impacts of Air Pollution Reduction Programs on a Local Scale: New Haven Case Study. [Article]. *Environmental Health Perspectives, 119*(4), 487-493. doi: 10.1289/ehp.1002636

Lowe, D. C. and U. Schmidt (1983). Formaldehyde (HCHO) measurements in the nonurban atmosphere. Journal of Geophysical Research: Oceans 88(C15): 10844-10858.

Lyman W., Rosenblatt D., Reehl W. (1990). Handbook of Chemical Property Estimation Methods: Environmental Behavior of Organic Compounds. pp.15-9 – 15-13, pp.17-8 – 17-17.

MacIntosh, D. L., Stewart, J. H., Myatt, T. A., Sabato, J. E., Flowers, G. C., Brown, K. W., . . . Sullivan, D. A. (2010). Use of CALPUFF for exposure assessment in a near-field, complex terrain setting. *Atmospheric Environment, 44*(2), 262-270. doi: http://dx.doi.org/10.1016/j.atmosenv.2009.09.023

Mage, D., Ozolins, G., Peterson, P., Webster, A., Orthofer, R., Vandeweerd, V., & Gwynne, M. (1996). Urban air pollution in megacities of the world. *Atmospheric Environment, 30*(5), 681-686. doi: Doi: 10.1016/1352-2310(95)00219-7

Marshall, J. D. (2008). Environmental inequality: Air pollution exposures in California's South Coast Air Basin. [Article]. *Atmospheric Environment, 42*(21), 5499-5503. doi: 10.1016/j.atmosenv.2008.02.005

Marshall, J. D., McKone, T. E., Deakin, E., & Nazaroff, W. W. (2005). Inhalation of motor vehicle emissions: effects of urban population and land area. *Atmospheric Environment, 39*(2), 283-295. doi: DOI: 10.1016/j.atmosenv.2004.09.059

Martins, H. (2012). Urban compaction or dispersion? An air quality modelling study. *Atmospheric Environment, 54*(0), 60-72. doi: http://dx.doi.org/10.1016/j.atmosenv.2012.02.075

McConnell, R., Islam, T., Shankardass, K., Jerrett, M., Lurmann, F., Gilliland, F., . . . Berhane, K. (2010). Childhood Incident Asthma and Traffic-Related Air Pollution at Home and School. [Article]. *Environmental Health Perspectives, 118*(7), 1021-1026. doi: 10.1289/ehp.0901232

McDonald-Buller, E., Webb, A., Kockelman, K., & Zhou, B. (2010). Effects of Transportation and Land Use Policies on Air Quality. *Transportation Research Record: Journal of the Transportation Research Board, 2158*(-1), 28-35. doi: 10.3141/2158-04

McTrans. (2008). CORSIM Reference Manual. In U. o. Florida (Ed.). Gainesville, FL.

Mennis, J. L., & Jordan, L. (2005). The Distribution of Environmental Equity: Exploring Spatial Nonstationarity in Multivariate Models of Air Toxic Releases. *Annals of the Association of American Geographers, 95*(2), 249-268.

Mensink, C., & Cosemans, G. (2008). From traffic flow simulations to pollutant concentrations in street canyons and backyards. *Environmental Modelling & Software, 23*(3), 288-295. doi: http://dx.doi.org/10.1016/j.envsoft.2007.06.005

Mensink, C., & Lewyckyj, N. (2001). A simple model for the assessment of air quality in streets. *International Journal of Vehicle Design, 27*(1), 242-250.

Mercer, L. D., Szpiro, A. A., Sheppard, L., Lindström, J., Adar, S. D., Allen, R. W., . . . Kaufman, J. D. (2011). Comparing universal kriging and land-use regression for predicting concentrations of gaseous oxides of nitrogen (NOx) for the Multi-Ethnic Study of Atherosclerosis and Air Pollution (MESA Air). *Atmospheric Environment, 45*(26), 4412-4420. doi: http://dx.doi.org/10.1016/j.atmosenv.2011.05.043

Milakis, D., Vlastos, T., & Barbopoulos, N. (2008). Relationships between Urban Form and Travel Behaviour in Athens, Greece. A Comparison with Western European and North American Results. [Article]. *European Journal of Transport and Infrastructure Research, 8*(3), 201-215.

Millet, D. B., A. Guenther, et al. (2010). "Global atmospheric budget of acetaldehyde: 3-D model analysis and constraints from in-situ and satellite observations." Atmos. Chem. Phys. 10(7): 3405-3425.

Milionis, A. E., & Davies, T. D. (1994). Regression and stochastic models for air pollution—I. Review, comments and suggestions. *Atmospheric Environment, 28*(17), 2801-2810. doi: http://dx.doi.org/10.1016/1352-2310(94)90083-3

Miranda, A. I., Borrego, C., & Martins, H. (2008). Linking Urban Structure and Air Quality *Transportation Land Use, Planning, and Air Quality* (pp. 219-227): American Society of Civil Engineers.

Mölter, A., Lindley, S., de Vocht, F., Simpson, A., & Agius, R. (2010). Modelling air pollution for epidemiologic research--Part I: A novel approach combining land use regression and air dispersion. *The Science of the total environment, 408*(23), 5862-5869.

Morgenstern, V., Zutavern, A., Cyrys, J., Brockow, I., Koletzko, S., Krämer, U., . . . Group, a. t. L. S. (2008). Atopic Diseases, Allergic Sensitization, and Exposure to Traffic-related Air Pollution in Children. *American Journal of Respiratory and Critical Care Medicine, 177*(12), 1331-1337. doi: 10.1164/rccm.200701-036OC

Morris, R. E., Koo, B., Wang, B., Stella, G., McNally, D., Loomis, C., . . . Tonnesen, G. (2007). Draft Final Report. Technical Support Document for VISTAS Emissions and Air Quality Modeling to Support Regional Haze State Implementation Plans.

National Renewable Energy Laboratory. (2007). National Solar Radiation Database 1991–2005 Update: User's Manual. Oak Ridge, TN: National Renewable Energy Laboratory.

National Research Council. (2004). Air Quality Management in the United States. Washington, DC.

National Toxicological Program. (2010). Report on Carcinogens, Twelfth Edition, Formaldehyde.: Department of Health and Human Services, National Toxicology Program.

National Toxicological Program. (2011). Report on Carcinogens, Twelfth Edition, Acetaldehyde.: Department of Health and Human Services, National Toxicology Program.

Niemeier, D., Bai, S., & Handy, S. (2011). The impact of residential growth patterns on vehicle travel and pollutant emissions. *The Journal of Transport and Land Use, 4*(3), 65-80.

Norbridge Inc. (2011). 2010 Strategic Plan Update. Reston, VA: Norbridge Inc.

O'Neill, M. S., Jerrett, M., Kawachi, I., Levy, J. I., Cohen, A. J., Gouveia, N., . . . Conditions, W. o. A. P. a. S. (2003). Health, wealth, and air pollution: advancing theory and methods. *Environ Health Perspect, 111*(16), 1861-1870.

One Bay. (2010). Voice It. My say for tomorrow's community. My One Bay. In O. Bay (Ed.).

Papathanassiou, A., Douros, I., & Moussiopoulos, N. (2008). A simplified three-dimensional approach to street canyon modelling using SEP-SCAM. [Article]. *Environmental Modelling & Software, 23*(3), 304-313. doi: 10.1016/j.envsoft.2007.05.015

Payne-Sturges, D., & Gee, G. C. (2006). National environmental health measures for minority and low-income populations: Tracking social disparities in environmental health. *Environmental Research, 102*(2), 154-171. doi: 10.1016/j.envres.2006.05.014

Peckham, S., Grell, G. A., McKeen, S. A., Barth, M., Pfister, G., Wiedinmyer, C., . . . Freitas, S. (2011). WRF/Chem Version 3.3 User's Guide. NOAA Technical Memo.

Pénard-Morand, C., Raherison, C., Charpin, D., Kopferschmitt, C., Lavaud, F., Caillaud, D., & Annesi-Maesano, I. (2010). Long-term exposure to close-proximity air pollution and asthma and allergies in urban children. *European Respiratory Journal, 36*(1), 33-40. doi: 10.1183/09031936.00116109

Pennsylvania Department of Environmental Protection. (2013). *State Implementation Plan Revision: NOx Motor Vehicle Emission Budget Revisions Based on the MOVES2010a Model*. Harrisburg, PA.

Perlin, S. A., Sexton, K., & Wong, D. W. S. (1999). An examination of race and poverty for populations living near industrial sources of air pollution. *Journal of Exposure Analysis and Environmental Epidemiology, 9*, 29-48.

Poor, N. D. (2008). Nitrogen Emission/Deposition Ratios for Air Pollution Sources That Contribute to the Nitrogen Loading of Tampa Bay: Mid-Term Progress Report.: Environmental Protection Commission of Hillsborough County.

R Development Core Team. (2013). R: A language and environment for statistical computing. R Foundation for Statistical Computing Vienna, Austria.

Rasmussen, R. A. and M. A. K. Khalil (1983). Atmospheric benzene and toluene. Geophysical Research Letters 10(11): 1096-1099.

Revision to the Guideline on air quality models: adoption of a Preferred General Purpose (Flat and complex terrain) dispersion model and other Revisions; Final Rule., 70 No. 216 C.F.R. (2005b).

Rose, N., Cowie, C., Gillett, R., & Marks, G. B. (2010). Validation of a Spatiotemporal Land Use Regression Model Incorporating Fixed Site Monitors. *Environmental Science & Technology, 45*(1), 294-299. doi: 10.1021/es100683t

Ryan, P. H., & LeMasters, G. K. (2007). A Review of Land-use Regression Models for Characterizing Intraurban Air Pollution Exposure. *Inhalation Toxicology, 19*(s1), 127-133. doi: 10.1080/08958370701495998

Sacks, J. D., Stanek, L. W., Luben, T. J., Johns, D. O., Buckley, B. J., Brown, J. S., & Ross, M. (2011). Particulate Matter–Induced Health Effects: Who Is Susceptible? *Environmental Health Perspectives, 119*(4), 446-454.

Saide, P., Zah, R., Osses, M., & Ossés de Eicker, M. (2009). Spatial disaggregation of traffic emission inventories in large cities using simplified top-down methods. *Atmospheric Environment, 43*(32), 4914-4923. doi: DOI: 10.1016/j.atmosenv.2009.07.013

Salon, D., Boarnet, M. G., Handy, S., Spears, S., & Tal, G. (2012). How do local actions affect VMT? A critical review of the empirical evidence. *Transportation Research Part D: Transport and Environment, 17*(7), 495-508. doi: http://dx.doi.org/10.1016/j.trd.2012.05.006

Sander, R. (1999). Compilation of Henry's Law Constants for Inorganic and Organic Species of Potential Importance in Environmental Chemistry. Mainz, Germany: Max-Planck Institute of Chemistry.

Sander, S. P., Friedl, R. R., Abbatt, J. P. D., Barker, J. R., Burkholder, J. B., Golden, D. M., . . . Orkin, V. L. (2011). Chemical Kinetics and Photochemical Data for Use in Atmospheric Studies Evaluation Number 17 Pasadena, California Jet Propulsion Laboratory, California Institute of Technology

Saori, K., Takashi, Y., Toshihide, T., & Hiroyuki, D. (2009). *Application of land use regression to regulatory air quality data in Japan* (Vol. 407). Kidlington, ROYAUME-UNI: Elsevier.

SAS Institute Inc. (2011). SAS/STAT® 9.3 User's Guide. Cary, NC: SAS Institute Inc.

Schultz, E. S., Gruzieva, O., Bellander, T., Bottai, M., Hallberg, J., Kull, I., . . . Pershagen, G. (2012). Traffic-related Air Pollution and Lung Function in Children at 8 Years of Age: A Birth Cohort Study. *American Journal of Respiratory and Critical Care Medicine, 186*(12), 1286-1291. doi: 10.1164/rccm.201206-1045OC

Schwanen, T., Dieleman, F. M., & Dijst, M. (2001). Travel behaviour in Dutch monocentric and policentric urban systems. *Journal of Transport Geography, 9*(3), 173-186. doi: http://dx.doi.org/10.1016/S0966-6923(01)00009-6

Schwanen, T., Dijst, M., & Dieleman, F. M. (2004). Policies for Urban Form and their Impact on Travel: The Netherlands Experience. *Urban Studies, 41*(3), 579-603. doi: 10.1080/0042098042000178690

Schweitzer, L., & Zhou, J. (2010). Neighborhood Air Quality, Respiratory Health, and Vulnerable Populations in Compact and Sprawled Regions. *Journal of the American Planning Association, 76*(3), 363-371. doi: 10.1080/01944363.2010.486623

Scire, J. S., Strimaitis, D. G., & Yamartini, R. J. (2000). A User's Guide for the CALPUFF Dispersion Model. Concord, MA 01742: Earth Tech. Inc.

Seinfeld, J. H., & Pandis, S. N. (1997). *Atmospheric Chemistry and Physics: From Air Pollution to Climate Change*: Wiley-Interscience.

Shewmake, S. (2012). Can Carpooling Clear the Road and Clean the Air? Evidence from the Literature on the Impact of HOV Lanes on VMT and Air Pollution. *Journal of Planning Literature*. doi: 10.1177/0885412212451028

Song, J., Webb, A., Parmenter, B., Allen, D. T., & McDonald-Buller, E. (2008). The Impacts of Urbanization on Emissions and Air Quality: Comparison of Four Visions of Austin, Texas. *Environmental Science & Technology, 42*(19), 7294-7300. doi: 10.1021/es800645j

Stein, A. F., Isakov, V., Godowitch, J., & Draxler, R. R. (2007). A hybrid modeling approach to resolve pollutant concentrations in an urban area. *Atmospheric Environment, 41*(40), 9410-9426. doi: DOI: 10.1016/j.atmosenv.2007.09.004

Steinle, S., Reis, S., & Sabel, C. E. (2013). Quantifying human exposure to air pollution—Moving from static monitoring to spatio-temporally resolved personal exposure assessment. *Science of The Total Environment, 443*(0), 184-193.

Stephan, C. H., & Sullivan, J. (2008). Environmental and Energy Implications of Plug-In Hybrid-Electric Vehicles. *Environmental Science & Technology, 42*(4), 1185-1190. doi: 10.1021/es062314d

Stohl, A., Sodemann, H., Eckhardt, S., Frank, A., Seibert, P., & Wotawa, G. (2011). The Lagrangian particle dispersion model FLEXPART version 8.2. Kjeller, Norway: Norwegian Institute for Air Research.

Stone, B., Mednick, A. C., Holloway, T., & Spak, S. N. (2007). Is Compact Growth Good for Air Quality? *Journal of the American Planning Association, 73*(4), 404-418.

Stone, B., Mednick, A. C., Holloway, T., & Spak, S. N. (2009). Mobile Source CO2 Mitigation through Smart Growth Development and Vehicle Fleet Hybridization. *Environmental Science & Technology, 43*(6), 1704-1710. doi: 10.1021/es8021655

Stuart, A. L., Lin, P.-S., Lee, C., Yu, H., & Chen, H. (2010). Assessing Air Quality Impacts of Managed Lanes. Tampa, FL: National Center for Transit Research.

Stuart, A. L., Mudhasakul, S., & Sriwatanapongse, W. (2009). The Social Distribution of Neighborhood-Scale Air Pollution and Monitoring Protection. *Journal of Air & Waste Management Association, 59*, 591-602.

Stuart, A. L., & Zeager, M. (2011). An inequality study of ambient nitrogen dioxide and traffic levels near elementary schools in the Tampa area. *Journal of Environmental Management, 92*(8), 1923-1930. doi: 10.1016/j.jenvman.2011.03.003

The American Lung Association. (2001). Urban Air Pollution and Health Inequities: A Workshop Report. *Environmental Health Perspectives, 109*(ArticleType: research-article / Issue Title: Supplement 3 / Full publication date: Jun., 2001 / Copyright © 2001 The National Institute of Environmental Health Sciences (NIEHS)), 357-374.

The UrbanSim Project. (2011). The Open Platform for Urban Simulation and UrbanSim Version 4.3. Users Guide and Reference Manual. Berkeley, CA: University of California Berkeley, and University of Washington.

Tong, Z., Wang, Y. J., Patel, M., Kinney, P., Chrillrud, S., & Zhang, K. M. (2011). Modeling Spatial Variations of Black Carbon Particles in an Urban Highway-Building Environment. *Environmental Science & Technology, 46*(1), 312-319. doi: 10.1021/es201938v

Touma, J. S., Isakov, V., Ching, J., & Seigneur, C. (2006). Air Quality Modeling of Hazardous Pollutants: Current Status and Future Directions. *Journal of the Air & Waste Management Association, 56*, 547-558.

Townend, P., Xu, J., Birkin, M., Turner, A., & Wu, B. (2009). MoSeS: Modelling and Simulation for e-Social Science. *Philosophical Transactions of the Royal Society A: Mathematical, Physical and Engineering Sciences, 367*(1898), 2781-2792. doi: 10.1098/rsta.2009.0041

Traisantikul, W. (2008). Air Pollution Dispersion Modeling for Localized Exposure in Tampa: King Mongkut's University of Technology Thonburi, Thailand.

TRC Environmental. (2007). Modeling Support to VISTAS State Agencies in Analyses of Best Available Retrofit Technology (BART).

Trivikrama Rao, S., Sedefian, L., & Czapski, U. H. (1979). Characteristics of Turbulence and Dispersion of Pollutants Near Major Highways. *Journal of Applied Meteorology, 18*(3), 283-293. doi: 10.1175/1520-0450(1979)018<0283:cotado>2.0.co;2

U.S. Census Bureau. (1983). *1980 Census of Population. Characteristics of the Population. Number of Inhabitants. United States Summary*. Washington, D.C.:

U.S. Census Bureau. (2010). TIGER®, TIGER/Line® and TIGER®-Related Products Retrieved January 20, 2010, from http://www.census.gov/geo/www/tiger/

U.S. Census Bureau. (2013). *United States Summary: 2010. Population and Housing Unit Counts. 2010 Census of Population and Housing*. Washington, DC: Retrieved from http://www.census.gov/prod/cen2010/cph-1-1.pdf.

U.S. Environmental Protection Agency. (1998). *Transportation control measures: high occupancy vehicle lanes*. (EPA420-S-98-006). Washington, DC.

U.S. Environmental Protection Agency. (1999). *Meteorological Processor for Regulatory Models (MPRM) User's Guide*. (EPA-454/B-96-002).

U.S. Environmental Protection Agency. (2001). *Fleet Characterization Data for MOBILE6: Development and Use of Age Distributions, Average Annual Mileage Accumulation Rates, and Projected Vehicle Counts for Use in MOBILE6*. Retrieved from http://www.epa.gov/oms/models/mobile6/r01047.pdf.

U.S. Environmental Protection Agency. (2004a). *Technical Guidance on the Use of MOBILE6.2 for Emission Inventory Preparation*. Retrieved from http://www.epa.gov/otaq/models/mobile6/420r04013.pdf.

U.S. Environmental Protection Agency. (2004b). *User's Guide for the AMS/EPA Regulatory Model – AERMOD*. Retrieved from http://www.epa.gov/scram001/7thconf/aermod/aermodugb.pdf.

U.S. Environmental Protection Agency. (2005a). *EPA's National Inventory Model (NMIM), A Consolidated Emissions Modeling System for MOBILE6 and NONROAD*. (EPA420-R-05-024).

U.S. Environmental Protection Agency. (2006). 2002 National Emissions Inventory Data & Documentation Retrieved March 10, 2011

U.S. Environmental Protection Agency. (2007a). Emissions Modeling Clearinghouse Temporal Allocation Retrieved January 11th, 2011, from http://www.epa.gov/ttn/chief/emch/temporal/index.html

U.S. Environmental Protection Agency. (2007b). Emissions Modeling Clearinghouse, Related Spatial Allocation Files - "New" Surrogates Retrieved March 1, 2012, from http://www.epa.gov/ttn/chief/emch/spatial/newsurrogate.html

U.S. Environmental Protection Agency. (2008a). *Integrated Science Assessment for Oxides of Nitrogen - Health Criteria (Final Report)*. Research Triangle Park, NC: Retrieved from http://ofmpub.epa.gov/eims/eimscomm.getfile?p_download_id=475020.

U.S. Environmental Protection Agency. (2008b). List of the 33 Urban Air Toxics Retrieved October 12, 2011, from http://www.epa.gov/ttn/atw/urban/list33.html

U.S. Environmental Protection Agency. (2009). *Reassessment of the Interagency Workgroup on Air Quality Modeling (IWAQM) Phase 2 Summary Report: Revisions to Phase 2 Recommendations*. Research Triangle Park, North Carolina 27711 Retrieved from http://www.epa.gov/scram001/guidance/reports/Draft_IWAQM_Reassessment_052709.pdf.

U.S. Environmental Protection Agency. (2010a). Biogenic Emissions Inventory System (BEIS) Modeling Retrieved March 1, 2012, from http://www.epa.gov/AMD/biogen.html

U.S. environmental Protection Agency. (2010b). *Motor Vehicle Emission Simulator (MOVES) User Guide for MOVES2010a*. (EPA-420-B-10-036). Retrieved from http://www.epa.gov/oms/models/moves/MOVES2010a/420b10036.pdf.

U.S. Environmental Protection Agency. (2012a). 1970 - 2012 Average annual emissions, all criteria pollutants in MS Excel, from http://www.epa.gov/ttn/chief/trends/index.html

U.S. Environmental Protection Agency. (2012b). National Ambient Air Quality Standards (NAAQS) Retrieved April 26, 2012, from http://www.epa.gov/air/criteria.html

U.S. environmental Protection Agency. (2012c). *Using MOVES to Prepare Emission Inventories in State Implementation Plans and Transportation Conformity: Technical Guidance for MOVES2010, 2010a and 2010b*. (EPA-420-B-12-028). Retrieved from http://www.epa.gov/otaq/models/moves/documents/420b12028.pdf.

U.S. Environmental Protection Agency. (2013). 2008 National Emissions Inventory Retrieved March 4, 2013, from http://www.epa.gov/ttn/chief/net/2008inventory.html

United Nations. (2008). World Urbanization Prospects: The 2007 Revision Population Database. from New York: United Nations

University of North Carolina at Chapel Hill. (2010). SMOKE v2.7 User's Manual. Chapel Hill, NC: The institute for the Environment, University of North Carolina at Chapel Hill,.

US Department of Health and Human Services. (2000). *Healthy People 2010: Understanding and Improving Health. 2nd ed.* Washington D.C.: US Government Printing Office.

Vardoulakis, S., Fisher, B. E. A., Pericleous, K., & Gonzalez-Flesca, N. (2003). Modelling air quality in street canyons: a review. *Atmospheric Environment, 37*(2), 155-182. doi: http://dx.doi.org/10.1016/S1352-2310(02)00857-9

Venkatram, A., Isakov, V., Seila, R., & Baldauf, R. (2009). Modeling the impacts of traffic emissions on air toxics concentrations near roadways. *Atmospheric Environment, 43*(20), 3191-3199. doi: DOI: 10.1016/j.atmosenv.2009.03.046

Vineis, P., & Husgafvel-Pursiainen, K. (2005). Air pollution and cancer: biomarker studies in human populations. *Carcinogenesis, 26*(11), 1846-1855. doi: 10.1093/carcin/bgi216

Wang, G., Bai, S., & Ogden, J. M. (2009). Identifying contributions of on-road motor vehicles to urban air pollution using travel demand model data. *Transportation Research Part D: Transport and Environment, 14*(3), 168-179.

Wang, Y. J., Nguyen, M. T., Steffens, J. T., Tong, Z., Wang, Y., Hopke, P. K., & Zhang, K. M. (2013). Modeling multi-scale aerosol dynamics and micro-environmental air quality near a large highway intersection using the CTAG model. *Science of The Total Environment, 443*(0), 375-386. doi: http://dx.doi.org/10.1016/j.scitotenv.2012.10.102

Wang, Y. J., & Zhang, K. M. (2009). Modeling Near-Road Air Quality Using a Computational Fluid Dynamics Model, CFD-VIT-RIT. *Environmental Science & Technology, 43*(20), 7778-7783. doi: 10.1021/es9014844

Weber, S., Kordowski, K., & Kuttler, W. (2013). Variability of particle number concentration and particle size dynamics in an urban street canyon under different meteorological conditions. *Science of The Total Environment, 449*(0), 102-114. doi: http://dx.doi.org/10.1016/j.scitotenv.2013.01.044

Wesely, M. L. (1989). "Parameterization of surface resistances to gaseous dry deposition in regional-scale numerical models." Atmospheric Environment (1967) 23(6): 1293-1304.

Westerink, J., Haase, D., Bauer, A., Ravetz, J., Jarrige, F., & Aalbers, C. B. E. M. (2012). Dealing with Sustainability Trade-Offs of the Compact City in Peri-Urban Planning Across European City Regions. *European Planning Studies*, 1-25. doi: 10.1080/09654313.2012.722927

Whitworth, K. W., Symanski, E., Lai, D., & Coker, A. L. (2011). Kriged and modeled ambient air levels of benzene in an urban environment: an exposure assessment study. [Article]. *Environmental Health, 10*. doi: 10.1186/1476-069x-10-21

Williams, M., & Wright, M. (2007). The Impact of the Built Environment on the Health of the Population: A Review of the Review Literature. Barrie, Ontario: Simcoe Muskoka District Health Unit

Wilton, D. C. (2011). *Modelling Nitrogen Oxides in Los Angeles Using a Hybrid Dispersion/Land Use Regression Model.* Ph.D., University of Washington, Washington DC.

Wong, D. W., Yuan, L., & Perlin, S. A. (2003). Comparison of spatial interpolation methods for the estimation of air quality data. *J Expo Anal Environ Epidemiol, 14*(5), 404-415.

Wu, J., Wilhelm, M., Chung, J., & Ritz, B. (2011). Comparing exposure assessment methods for traffic-related air pollution in an adverse pregnancy outcome study. *Environmental Research, 111*(5), 685-692. doi: http://dx.doi.org/10.1016/j.envres.2011.03.008

Yantosca, B., Long, M., Payer, M., & Cooper, M. (2012). GEOS–Chem v9–01–03 Online User's Guide. Cambridge, MA: Harvard University.

Yim, S. H. L., Fung, J. C. H., & Lau, A. K. H. (2010). Use of high-resolution MM5/CALMET/CALPUFF system: SO2 apportionment to air quality in Hong Kong. *Atmospheric Environment, 44*(38), 4850-4858. doi: http://dx.doi.org/10.1016/j.atmosenv.2010.08.037

You, S., Lee, G., Ritchie, S., Saphores, J.-D., Sangkapichai, M., & Ayala, R. (2010). Air Pollution Impacts of Shifting Freight from Truck to Rail at California's San Pedro Bay Ports. *Transportation Research Record: Journal of the Transportation Research Board, 2162*(-1), 25-34. doi: 10.3141/2162-04

Yu, H. L., Chen, J. C., Christakos, G., & Jerrett, M. (2009). BME Estimation of Residential Exposure to Ambient PM10 and Ozone at Multiple Time Scales. [Article]. *Environmental Health Perspectives, 117*(4), 537-544. doi: 10.1289/ehp.0800089

Yvon, S. A., Plane, J. M. C., Nien, C. F., Cooper, D. J., & Saltzman, E. S. (1996). Interaction between nitrogen and sulfur cycles in the polluted marine boundary layer. *J. Geophys. Res., 101*(D1), 1379-1386. doi: 10.1029/95jd02905

Zou, B., Wilson, J. G., Zhan, F. B., & Zeng, Y. (2009). Air pollution exposure assessment methods utilized in epidemiological studies. *J Environ Monit, 11*(1464-0325). doi: 10.1074/jbc.M202849200

Zou, B., Wilson, J. G., Zhan, F. B., & Zeng, Y. (2009). Spatially differentiated and source-specific population exposure to ambient urban air pollution. *Atmospheric Environment, 43*(26), 3981-3988. doi: http://dx.doi.org/10.1016/j.atmosenv.2009.05.022